



Some pages of this thesis may have been removed for copyright restrictions.

If you have discovered material in Aston Research Explorer which is unlawful e.g. breaches copyright, (either yours or that of a third party) or any other law, including but not limited to those relating to patent, trademark, confidentiality, data protection, obscenity, defamation, libel, then please read our [Takedown policy](#) and contact the service immediately (openaccess@aston.ac.uk)

Novel Collagen-Based Biomaterials For Bone Regeneration

Haris Ahmad Choudhery

Doctor of Philosophy

October 2018

©Haris Ahmad Choudhery, 2018 asserts his moral right to be identified as the author of this thesis. This copy of the thesis has been supplied on condition that anyone who consults it is understood to recognise that its copyright belongs to its author and that no quotation from the thesis and no information derived from it may be published without appropriate permission or acknowledgement.

Novel collagen- based biomaterials for bone regeneration

Haris Ahmad Choudhery

Doctor of Philosophy

October 2018

Bone is primarily made of type I collagen, which is a highly abundant natural protein. Collagen can be crosslinked through several methods including chemical agents, physical heating and UV radiation. The result is enhanced physical characteristics such as thermal stability, resistance to proteolytic breakdown, mechanical strength and increased overall biocompatibility. However, with these methods there are drawbacks; including toxicity of residual cross-linking agents, or difficulties with scaling. In recent years, collagen has been cross-linked by a safer, efficient and more practical means by using enzymes as biological catalysts.

We demonstrate that crosslinking native collagen with both tissue transglutaminase (TG2) and microbial transglutaminase (mTG- from *Streptomyces mobaraense*) leads to an increase in the proliferation of human osteoblasts (HOB) and an increase in integrins on their cell surface compared to culture on native collagen. These integrins include αV , $\alpha 5$, $\beta 1$ and $\beta 3$ which are all important for the ability of HOBs to mature and differentiate. In addition to this, the HOBs were shown to mineralise at a faster rate than on native collagen. Moreover, it was demonstrated that integrin expression and mineralisation rates are further increased in HOBs on crosslinked collagen by incorporating 45S5 bioglass particles.

Investigations here show distinct differences between the micro-structure of the scaffolds and the mean pore size between fibrils in native and crosslinked collagen. These results suggest that the crosslinked collagen changes the behaviour of HOBs when seeded, such that through the Wnt canonical pathway there is an overall increased drive towards mineralisation and deposition of collagen by the HOBs.

This work shows that crosslinked collagen scaffolds with 45S5 bioglass have the potential to be used as biomaterials for bone regeneration and may eventually replace allografts and titanium plates.

Dedication

For my mother who has always nourished my soul with her unconditional love. I hope to always make you proud because I take so much pride in having you as my mum

For my naani, Farhat Arif, every day you have lived with us has been a true blessing.

For my Fiancé, who has given me unwavering support like no other. With you by my side I will never want for more

Acknowledgements

I would like to thank Dr Russell Collighan for all of his kind advice and support for helping me through the most turbulent times of my PhD and for helping me reach the finish line. His patience and guidance will always be remembered and I will always be grateful for his help. Likewise I would also like to thank Dr Richard Martin for helping me to learn about materials science and how I could integrate this knowledge into my PhD. I also acknowledge inputs from Prof Martin Griffin and Dr Zhuo Wang.

A big thank you to Prof Andrew Devitt for standing up for what is right and helping myself and others in my lab group. Without your help we would all be worse off. Of course I could never get through the day to day grind without my fellow “lab rats”; Dr Oluseyi Ayinde, Shaun Fell and James Gavin and Dr Chathyan Pararasa. Thank you all for keeping the lab a fun place and for helping me every time something went wrong.

Of course none of this would never have happened without my loving parents, sisters and my grandmother. Your support (and home cooked meals) were what allowed me to start this PhD in the first place. For listening to me endlessly complain, I have to also thank my girlfriend Amy Walsh. Your unwavering support is what helped me focus towards the end goal in my darkest days.

There are many friends and who helped get me to the end. You all know who you are and I thank you from the bottom of my heart. Last but not least, thank you to Dr Pavel and Dr Hellfern.

Contents

List of Tables.....	10
List of Figures	11
List of abbreviations.....	15
Chapter 1 – Introduction.....	16
1.1 Type I Collagen	17
1.2 Transglutaminases	18
1.3 Microbial transglutaminase (mTG)	22
1.3.1 Enzymatic properties of mTG.....	22
1.3.2 Structure of mTG.....	23
1.3.3 Production of mTG	26
1.4 Transglutaminase 2	27
1.4.1 Transamidating and deamidation ability of TG2.....	27
1.4.2 More enzymatic functions of TG2.....	29
1.4.3 Structure and conformation of TG2	29
1.4.4 Regulation of TG2 gene expression	35
1.4.5 The role of TG2 in cell adhesion and signalling.....	37
1.4.6 The role of TG2 in wound healing.....	40
1.4.7 The involvement of TG2 in pathological conditions	41
1.5 Involvement of TG2 in physiological bone development	42
1.5.1 TG2 and its involvement in matrix maturation	44
1.5.2 Transamidating independent pathway	44
1.6 Bone regeneration and biomaterials for tissue repair.....	48
1.6.1 Tissue engineering	48
1.6.2 Bone tissue engineering.....	49
1.6.3 The biology of bone.....	50
1.6.4 Bone development.....	55
1.6.5 Healing from bone fracture.....	56
1.6.6 Biomaterials and current options for clinical regeneration.....	57
1.7 45S5 bioglass	60
Chapter 2: Materials and Methods.....	63
2.1 Materials	64
2.1.1 General chemicals	64

2.1.2 Cell culture	64
2.1.3 Immunochemicals	65
2.1.4 Western blot chemicals.....	65
2.1.5 Mineralisation and collagen staining kits.....	65
2.1.6 Sub cellular fractionation	65
2.2 Methods	65
2.2.1 Cell culture	65
2.2.2 Passaging cells	66
2.2.3 Cryopreservation.....	66
2.2.4 Retrieving cells from storage	67
2.2.5 Differentiation of HOBs.....	67
2.3 Protein expression assays	67
2.3.1 Protein concentration	67
2.3.2 Lysing and collecting whole cell lysates	68
2.3.3 Transglutaminase activity assay.....	69
2.4 Collagen purification and assays.....	70
2.4.1 Isolation and purification	70
2.4.2 Collagen concentration assay	70
2.4.3 Modification of collagen by transglutaminase.....	71
2.4.4 Coomassie blue staining of collagen	71
2.4.5 Coomassie blue degradation assay	72
2.4.6 Collagen sedimentation	72
2.5 Analysis of cell proteins.....	73
2.5.1 Sodium dodecyl sulphate polyacrylamide gel electrophoresis (SDS-PAGE)	73
2.5.2 Western blotting	74
2.5.3 Membrane stripping	75
2.6 Determination of cell behaviour	75
2.6.1 Cell proliferation	75
2.6.2 Mineralisation of HOB cultures.....	76
2.7 Using SEM to analyse crosslinked surface topography.....	76
2.8 Collagen staining assay	77
2.9 Sub cellular fractionation protocol	78
2.10 Amino acid analysis of crosslink proteolytic digestion for crosslink analysis	79
2.10.1 Ammonia analysis	80
2.11 Statistical analysis	81
Chapter 3: Characterisation of novel type I collagen scaffolds generated using transglutaminases	82

3.1 Introduction	83
3.2 Characterisation of transglutaminase inhibitors, type 1 collagen and optimisation of collagen crosslinking.....	84
3.2.1 Assessment of type I collagen purity	84
3.2.2 Assessing the concentration of 1-155 required to inhibit TG2	86
3.2.3 Assessing the concentration of R281 required to inhibit mTG	88
3.2.4 Dependence of TG2 activity on reduction by DTT	90
3.2.5 The effect of collagen pH on TG2 activity	92
3.3 Effect of transglutaminase cross-linking on collagen properties.....	94
3.3.1 Observing the macromolecular effects of mTG and TG2 crosslinked collagen	94
3.3.2 Observing the macromolecular effects of TG2 crosslinked collagen without calcium and DTT	96
3.3.3 SEM imaging of collagen scaffolds	98
3.3.4 SDS PAGE of native mTG and TG2 crosslinked collagen	101
3.3.5 Determination of the $\epsilon(\gamma\text{-glutamyl})\text{lysine}$ content of TG cross-linked collagen	103
3.4 Cellular response of HOB cells to native and crosslinked collagen.....	107
3.4.1 Proliferation of human osteoblasts on native and crosslinked collagen	107
3.4.2 Observing the macromolecular effects of mTG and TG2 crosslinked collagen with 45S5 bioglass particles	109
3.4.3 Proliferation of human osteoblasts on native and crosslinked collagen containing 45S5 bioglass particles	111
3.4.4 Stability of crosslinked collagen matrices	113
3.4.5 Proliferation of human osteoblasts on native and crosslinked collagen containing cobalt bioglass.....	115
3.5 Discussion.....	117
Chapter 4: Mineralisation of human osteoblasts in novel collagen scaffolds	121
4.1 Introduction	122
4.2 Characterising the mineralisation of collagen scaffolds with mTG and TG2	124
4.2.1 Mineralisation of HOBs	124
4.2.2 Effect of mTG and TG2 on mineralisation in HOBs	126
4.2.3 Mineralisation of HOBs when seeded on mTG and TG2 crosslinked collagen	128
4.2.4 Mineralisation of HOBs when seeded onto TG2 crosslinked collagen without DTT.....	130
4.2.5 Mineralisation of HOBs when seeded onto TG2 crosslinked collagen without calcium	132
4.2.6 Mineralisation of HOBs when seeded onto TG2 crosslinked collagen without calcium and DTT	134
4.3 Characterising the mineralisation of collagen scaffolds with transglutaminases and transglutaminase inhibitors	136

4.3.1 Optimising the use of 1-155 inhibitor when cells are seeded onto TG2 crosslinked collagen	136
4.3.2 Optimising the use of R281 inhibitor when cells are seeded onto mTG crosslinked collagen	139
4.3.3 Assessing the mineralisation effect of 1-155 on HOBs	142
4.3.4 Assessing the effect of R281 on mineralisation of HOBs	145
4.3.5 Mineralisation of HOBs on mTG crosslinked collagen with 1-155	148
4.4 Assessing the mineralisation of HOBs on crosslinked collagen and crosslinked collagen mixed with glass.....	150
4.4.1 Comparing the mineralisation rates between collagen scaffolds with transglutaminases and 45S5 bioglass particles	150
4.4.2 Assessing the mineralisation rates between collagen scaffolds with transglutaminases and 45S5 bioglass particles at earlier time points	153
4.5 Crosslinked collagen deposition by human osteoblasts	156
4.5.1 Quantification of crosslinked collagen when transglutaminases are added to HOBs on plastic tissue	156
4.6 Discussion.....	158
Chapter 5: Intracellular effects of seeding HOBs on novel crosslinked collagen scaffolds.....	162
5.1 Introduction	163
5.2 Integrin expression of HOBs on collagen scaffolds	164
5.2.1 Expression of $\beta 3$ integrin on human osteoblasts over 3 days	164
5.2.2 Expression of αV integrin on human osteoblasts over 3 days	166
5.2.3 Expression of LRP5 on human osteoblasts with transglutaminases added	168
5.3 Characterisation of integrin expression on human osteoblasts when seeded onto collagen scaffolds with transglutaminase	170
5.3.1 $\beta 3$ integrin expression in HOBs grown on collagen scaffolds	170
5.3.2 αV integrin expression for HOBs grown on collagen scaffolds	172
5.3.3 $\beta 1$ integrin expression for HOBs grown on collagen scaffolds	174
5.3.4 $\alpha 5$ integrin expression for HOBs grown on collagen scaffolds	176
5.3.5 $\alpha 1$ integrin expression for HOBs grown on collagen scaffolds	178
5.3.6 $\alpha 2$ integrin expression for HOBs grown on collagen scaffolds	180
5.3.7 LRP5 integrin expression for HOBs grown on collagen scaffolds.....	182
5.4 Characterisation of integrin expression on human osteoblasts when seeded onto collagen scaffolds with transglutaminase and 45S5 bioglass.....	184
5.4.1 $\beta 3$ integrin expression for HOBs grown on collagen scaffolds mixed with 45S5 bioglass ..	184
5.4.2 αV integrin expression for HOBs grown on collagen scaffolds mixed with 45S5 bioglass ..	186
5.4.3 $\beta 1$ integrin expression for HOBs grown on collagen scaffolds mixed with 45S5 bioglass ..	188

5.4.4 α 5 integrin expression for HOBs grown on collagen scaffolds mixed with 45S5 bioglass..	190
5.4.5 β -catenin expression in HOBs	193
5.4.6 β -catenin expression in HOBs grown on collagen scaffolds	196
5.5 Discussion.....	200
Chapter 6- General discussion	204
6.1 Background	205
6.2 How novel collagen scaffolds effect the behaviour of human osteoblasts	206
6.3 Conclusions	210
References.....	212
End of thesis.....	227

List of Tables

Table 1.1: A summary of transglutaminases and their basic properties.	20
Table 1.2: Exogenous and endogenous binding partners of TG2	
Table 2.1: The recipes for different concentrations of acrylamide in separating gels	73
Table 2.2: A series of lithium buffers used during the amino acid separation phase.....	80
Table 5.1: A summary of integrin expression seen on HOBs when seeded on various collagen scaffolds.....	192

List of Figures

Figure 1.1: Schematic ribbon structure of mTG	24
Figure 1.2: A series of post-translational reactions which are catalysed by the transamidase activity of TG2.	28
Figure 1.3: Schematic representation of the functional domains of TG2	31
Figure 1.4: Representative models of TG2 derived through x-ray crystallography	34
Figure 1.5: Diagram of the TG2 promoter	36
Figure 1.6 Scheme of Wnt signalling and its antagonists	47
Figure 1.7: Hierarchical structure of bone from macrostructure through to sub-nanostructure	51
Figure 1.8: The three main stages of osteoblast differentiation	54
Figure 1.9: SEM images of the HCA layer bonding to bone	61
Figure 3.1: Coomassie blue stain for type 1 collagen following separation by SDS PAGE	85
Figure 3.2: TG2 inhibition activity assay	87
Figure 3.3: R281 inhibition activity assay	89
Figure 3.4: DTT activity assay	89
Figure 3.5: TG2 pH activity assay	93
Figure 3.6: Image of centrifuged collagen samples	95
Figure 3.7: Image of centrifuged collagen samples	97

Figure 3.8: SEM images of native and crosslinked collagen	100
Figure 3.9: Observation and quantification of native and crosslinked collagen bands	102
Figure 3.10: Amino acid analyser crosslink assay	104
Figure 3.11: Observation of different pH level collagen scaffolds and deamidation assay for collagen scaffolds	106
Figure 3.12: XTT proliferation assay for native and crosslinked collagen	108
Figure 3.13: Image of centrifuged collagen samples with 45S5 bioglass	110
Figure 3.14: XTT proliferation assay for native and crosslinked collagen mixed with 45S5 bioglass glass	112
Figure 3.15: Collagen digestion assay	114
Figure 3.16: XTT proliferation assay for native and collagen admixed with cobalt bioglass glass	116
Figure 4.1: Mineralisation of HOBs cultured over 10 days on native and crosslinked collagen	125
Figure 4.2: Mineralisation of HOBs with mTG and TG2 added	127
Figure 4.3: Mineralisation of HOBs when seeded onto mTG and TG2 crosslinked collagen	129
Figure 4.4: Mineralisation when HOBs were seeded onto TG2 crosslinked collagen without DTT	131
Figure 4.5: Mineralisation of HOBs when HOBs were seeded onto TG2	

crosslinked collagen without calcium	133
Figure 4.6: Mineralisation when HOBs were seeded onto TG2 crosslinked	
collagen without calcium and DTT	135
Figure 4.7: Mineralisation of HOBs when 1-155 was added to collagen	138
Figure 4.8: Mineralisation of HOBs when R281 was added to collagen	141
Figure 4.9: Mineralisation of HOBs when 1-155 was added	144
Figure 4.10: Mineralisation of HOBs when R281 was added	147
Figure 4.11: Mineralisation of HOBs when 1-155 was added to mTG crosslinked	
collagen	149
Figure 4.12: Mineralisation of HOBs when seeded onto native and crosslinked	
collagen with 45S5 bioglass particles	152
Figure 4.13: Mineralisation of HOBs when seeded onto native and crosslinked	
collagen with 45S5 bioglass particles over 5 days	155
Figure 4.14: HOBs production of crosslinked collagen in extracellular matrix	157
Figure 5.1: Expression of $\beta 3$ integrin in whole cell lysate	165
Figure 5.2: Expression of αV integrin in whole cell lysate	
1657	
Figure 5.3: Expression of LRP5 integrin in whole cell lysate	169
Figure 5.4: Expression of $\beta 3$ integrin in HOBs seeded onto collagen scaffolds	171
Figure 5.5: Expression of αV integrin in HOBs seeded onto collagen scaffolds	173
Figure 5.6: Expression of $\beta 1$ integrin in HOBs seeded onto collagen scaffolds	175
Figure 5.7: Expression of $\alpha 5$ integrin in HOBs seeded onto collagen scaffolds	177
Figure 5.8: Expression of $\alpha 1$ integrin in HOBs seeded onto collagen scaffolds	179
Figure 5.9: Expression of $\alpha 2$ integrin in HOBs seeded onto collagen scaffolds	181

Figure 5.10: Expression of LRP5 integrin in HOBs seeded onto collagen scaffolds	183
Figure 5.11: Expression of $\beta 3$ integrin in HOBs seeded onto collagen scaffolds with 45S5 bioglass	185
Figure 5.12: Expression of αV integrin in HOBs seeded onto collagen scaffolds with 45S5 bioglass	187
Figure 5.13: Expression of $\beta 1$ integrin in HOBs seeded onto collagen scaffolds with 45S5 bioglass	189
Figure 5.14: Expression of $\alpha 5$ integrin in HOBs seeded onto collagen scaffolds with 45S5 bioglass	191
Figure 5.15: Expression of β -catenin in HOB cell fractions	195
Figure 5.16: Expression of β -catenin in HOB cell fractions seeded on collagen scaffolds	199

List of abbreviations

BSA	bovine serum albumin
Ca ²⁺	free calcium ion
CO ₂	carbon dioxide
Cys	cysteine
DMEM	Dulbecco's Modified Eagle's Medium
DMSO	dimethyl sulphoxide
DTT	dithiothreitol
ECL	enhanced chemiluminescence
ECM	extracellular matrix
EDTA	ethylene diamine tetraacetic acid
FAK	focal adhesion kinase
FBS	foetal bovine serum
FN	fibronectin
FXIII	factor XIII
Gly	glycine
His	histidine
HRP	horseradish peroxidase
HOB	human osteoblast cells
HYP	hydroxyproline
IL-6	interleukin- 6
kDa	kilodaltons
M	molar
ml	milliliters
mM	millimolar
MMP	matrix metalloproteinase
µl	microliter
µM	micromolar
mTG	microbial transglutaminase
PAGE	polyacrylamide gel electrophoresis
PBS	phosphate buffered saline
pH	negative log of hydrogen ion concentration
PMSF	phenyl methyl sulfonyl fluoride
Pro	proline
R281	N-benzyloxycarbonyl-L-phenylalanyl-6-dimethylsulfonium-5-oxo-L-norleucine
RGD	arginine-glycine-aspartic acid
SD	standard deviation
SDS	sodium dodecyl sulphate
TEMED	N,N,N,N'-tetramethylene diamine
TG	transglutaminase
TGF	transforming growth factor
TG2	tissue transglutaminase
Tris	tris(hydroxymethyl)-aminoethane
Triton X-100	t-octylphenoxypolyethoxyethanol
UV	ultra violet
XTT	(2,3-bis[methoxy-4-nitro-5-sulphophenyl]-2H-tetrazolium-5-carboxanilide)

Chapter 1 – Introduction

1.1 Type I collagen

Regenerative medicine focuses on the idea of, not just healing tissue after traumatic injury, but restoring the tissue's native function. In the beginning biomaterials were designed to be inert and elicited no response from the immune system (Hench & Polak, 2002). However through molecular and cellular biology advances a new ideal for medical materials has emerged: creating materials which can stimulate native tissue regeneration and restore the original functionality. One way to communicate to cells during the healing process is through the diverse cues provided by porous biomaterial scaffolds (Hench & Polak, 2002). The interconnected pores of scaffolds not only support and direct cellular growth, but can also be used as a part of drug and growth factor release. (Mullen *et al.* 2010).

One promising approach has been to utilise natural biological polymers, which already have innate chemistry to communicate to cells built into the molecule. Of these polymers, type I collagen is the most widely used, as it is the major structural component of extra cellular matrix (ECM) in living tissue. Type I collagen is the first in a superfamily comprised of 28 different types, all of which fall under fibrillar (type I falls under this category) or non-fibrillar (such as type IV). The versatility of collagen scaffolds is due, in part, to the diverse ways in which the structures can be modified. The pore architecture can be designed to mimic the anisotropic ECM of native tissues, which is important for tissues such as tendon and meniscus (Pawelec *et al.* 2014 & Davidenko *et al.* 2010). As a further modifier of biological activity, collagen can also be combined with other polymers, such as chitosan or elastin, which influences chemical and mechanical properties (Martinez *et al.* 2015 & Grover *et al.* 2012).

Cellular response to biomaterials is dictated by a combination of mechanical, architectural and chemical cues from the scaffold. Sensing cues from the environment is a complex and dynamic process (Shiller *et al.* 2013). The mechanism used by cells, notably a class of trans-membrane receptors known as integrins, can control many functions, including differentiation (Huebsch *et al.* 2010). For tissue engineering scaffolds, tailoring biological response is linked

to controlling the ligands, or cell signalling moieties, which are presented to cells and react with receptors.

Throughout decades of research, it has been determined that collagen is not a single molecule, but a large family of molecules. The defining feature of a collagen is a protein composed of three polypeptide chains incorporating at least one region with a repeating amino acid sequence (Fratzl *et al.* 2008). Collagen Type I, for example, has a repeating sequence of glycine-X-Y which forms a right-handed triple helix. At least 28 different types of collagen have been found thus far, even excluding the proteins with collagenous regions which have not been called collagen for historical reasons (Fratzl *et al.* 2008). Within the collagen superfamily, members are further classified based on their structure and distribution.

The most widespread collagens are the fibrillar collagens, composed primarily of a triple-helical region with a characteristic repeating band where fibers connect, known as D-banding (Fratzl *et al.* 2008). Collagen types I, II and III all belong to the fibrillary group of collagens and vary in amino acid composition and distribution within the body (Friess, 1998). Collagen type I is the most common, constituting the major structural protein for skin, tendon and bone. For this reason and the ones outlined above, collagen has been investigated as a scaffold to be used in bone regeneration.

1.2 Transglutaminases

Transglutaminases (EC 2.3.2.13, henceforth TGs) are a group of ubiquitous enzymes that are found throughout many mammals, plants, invertebrates and the human body. They catalyse post-translation modifications of proteins by the formation of isopeptide bonds (Griffin *et al.*, 2002). This is carried out in one of two ways: either through protein crosslinking via ϵ -(γ -glutamyl) lysine bonds or via a calcium-dependent reaction. Here, transglutaminases form a covalent bond between the γ -carboxamide group of peptide-bound glutamine and the ϵ -amino group of a peptide-bound lysine (or primary amine). Clarke *et al.* were the first group to derive

mammalian transglutaminase from the guinea pig liver in 1959. Key stages of a cell's life cycle, including its reproduction, growth and even death, are influenced by the presence of transglutaminases. These enzymes are able to affect the proliferation and differentiation of several types of cells (Beninati and Piacentini, 2004), hence why so many researchers are now looking into these molecules.

By cross-linking and forming these isopeptide bonds, proteins become highly resistant to mechanical forces and proteolytic degradation. This type of cross-linking in humans is carried out by, but not limited to, type 2 tissue transglutaminase (TG2), primarily expressed in skin, hair, blood clotting and in wound healing (Lorand and Conrad, 1984). It has been found that TG2 amino acid and cDNA sequences are highly conserved between most species including guinea pig (liver), bovine, mice, chickens and humans (Ikura *et al.*, 1988, Nakanishi *et al.*, 1991, Gentile *et al.*, 1991, Weraarchakulboonmark *et al.*, 1992). TG2 is a monomer that is composed of 685-691 amino acids and has a molecular weight of approximately 77-85kDa. When compared to mouse and guinea pigs, human TG2 has nearly 80% homology between the amino acid sequences. Of this sequence, 49 out of 51 residues in the active site region are identical (Gentile *et al.*, 1991).

To date there are nine different transglutaminase isoenzymes that have been identified in mammals, however, only six have been isolated and characterised at the protein level. The nine transglutaminases and their characteristics are summarised below.

Table 1.1: A summary of transglutaminases and their basic properties.

Mammalian Transglutaminase family	Molecular mass (kDa)	Regulation and GTP activity	Description and use
Factor XIII	83	Activated by thrombin and Ca^{2+} ; also requires reducing agent	Perhaps the most well-known of all TGs is Factor XIII, which is a key zymogen in the blood clotting network. It is converted via proteolysis into active Factor XIIIa during wound healing when fibrin clots are formed (Griffin <i>et al.</i> , 2002)
Keratinocyte /Type 1 transglutaminase (TG1)	90	Protease and Ca^{2+} required for activation, reducing agent required	TG1 is a keratinocyte which exists in both membrane-bound and soluble forms. Its main purpose is to be activated via proteolysis and plays a key role in the terminal differentiation of keratinocytes (Griffin <i>et al.</i> , 2002)
Tissue/ Type 2 transglutaminase (TG2)	78	Ca^{2+} required for activation, reducing agent also required	The most ubiquitous transglutaminase seen in the body. This multifunctional protein governs cell-matrix interactions, tissue repair and a variety of other cell functions (Aeschlimann and Thomazy, 2000 & Fesus and Piacentini, 2002)
Epidermal/ Type 3 transglutaminase (TG3)	77	Latent (protease activated); Ca^{2+} activated, reducing agent required	Epidermal transglutaminase is similar to TG1 in that it also undergoes proteolysis in order to become active. It is also involved in the terminal differentiation of keratinocytes (Eckert <i>et al.</i> , 2005).
Prostate/ Type 4 transglutaminase (TG4)	77	Ca^{2+} activated, reducing agent required	A prostatic secretory transglutaminase that is essential for fertility in rodents and potentially in humans (Iismaa, 2016)
TG5	80	Ca^{2+} activated	Is seen to cross-link keratins as well as many other differentiation-specific structural proteins, including involucrin, loricrin, filaggrin and small proline-rich proteins, in the formation of the cornified cell envelope of the stratum

			corneum the outermost “dead” layer of the epidermis (Kalinin <i>et al.</i> , 2002)
TG6	70	Ca ²⁺ activated	Catalyses cross-linking between proteins and the conjugation of polyamines to proteins. Mutations in this gene are linked to spinocerebellar ataxia type 35 (SCA35) (Wang <i>et al.</i> , 2010a)
TGM7	80	Ca ²⁺ activated	Possible biomarker for neurodegenerative disease
Band 4.2	72	No enzyme activity	Membrane; structural protein, membrane skeletal component in erythrocyte (Yawata, 1994)
Microbial Transglutaminase / mTG	39	No Ca ²⁺ required for activation	This transglutaminase is not found in mammals. Is found instead in <i>Streptomyces mobaraensis</i> . Unlike many other transglutaminases mTG is calcium-independent and has a lower molecular weight (Yokoyama <i>et al.</i> , 2004)

1.3 Microbial transglutaminase (mTG)

Other than the transglutaminases that have been found in mammals, there have been discoveries of transglutaminases in other organisms. One of the first non-mammalian sourced transglutaminases was sourced from a culture of *Streptomyces mobaraensis* (formerly known as *Streptoverticillium mobaraense*) and commonly known as microbial transglutaminase or mTG (Ando *et al.*, 1989). Since then this transglutaminase has been found in other species of *Streptomyces*, where it is secreted as a zymogen from the cytoplasm membrane and activated through proteolytic cleavage (Pasternack *et al.*, 1989). *Streptomyces mobaraensis* was found to secrete the enzyme into the culture medium, and thus its purification was relatively simple, which led to its rapid commercialisation. Microbial transglutaminase was first commercially described by researchers at Ajinomoto Co., Inc. in 1989. Since then, it has become one of the most widely used enzymes for the cross-linking of proteins and peptides in many food and biotechnological applications (Steffen *et al.*, 2017). In mammals, “side-chain to side-chain” isopeptide bonds confer mechanical strength and increase resistance to degradation, much like TG2. However, in *Bacillus subtilis* (when heat treated), the enzymatic activity of mTG causes crosslinking of GerQ in spores, which leads to increased spore formation and stability (Kuwana *et al.*, 2006)

1.3.1 Enzymatic properties of mTG

There are major differences between the mammalian sourced TG2 and mTG. The former is far larger, measuring 78kDa. The latter is only 38 kDa and consists of 331 amino acids (Kanaji *et al.*, 1993). Moreover, there is very little amino acid sequence homology between mammalian transglutaminases (Duran *et al.*, 1998). The active site on TG2 is made up of three crucial amino acids: cysteine 277 (Cys 277), histidine 335 (His 335) and aspartic acid 358 (Asp 358). In contrast to this, only the cysteine (Cys 64) has been identified as the sole catalytic residue in mTG’s sequence, it has recently been proposed that mTG uses a cysteine protease-like mechanism in which Asp 255 plays the role of the histidine residue

(normally seen in animal transglutaminases) (Rachel and Pelletier, 2013). Interestingly, unlike animal-based transglutaminases (including TG2) mTG activity is not dependent on the presence of GTP or Ca^{2+} . This property has made it very useful in the modification of food proteins since caseins, soybean globulins, myosins and many more, are sensitive to Ca^{2+} ions and are easily precipitated by them. On the other hand, it has since been discovered that, in the absence of reducing agents, Cu^{2+} , Zn^{2+} , Pb^{2+} and Li^+ are found to be strongly inhibitory to mTG activity. This is because heavy metals are thought to bind the thiol group of the single cysteine residue which strongly supports the idea that this particular residue forms part of the active site of mTG (Yokoyama *et al.*, 2004).

mTG is a simple monomeric protein with just a single domain, unlike TG2, and has a higher optimum temperature of 55°C and a lower optimum pH of 5.5 (Ho *et al.*, 2000). Moreover mTG has shown activity at a pH as low as 4 and as high as 9 (Ando *et al.*, 1989). It has even been reported to retain some activity between 10°C and near freezing temperatures. Looking at specificity, it has been shown that mTG is able to crosslink a wide array of proteins including wheat glutens, egg yolk, albumin proteins, myosins, fibrins, collagen, caseins as well as many others (Nonaka *et al.*, 1992, Nonaka *et al.*, 1997).

1.3.2 Structure of mTG

mTG has no detectable sequence homology to TG2, apart from the transglutaminase fold, and exhibits a different structure compared to it as well (Strop, 2014, Makarova *et al.*, 1999). The crystal structure of mTG was determined at 2.4Å resolution (Kashiwagi *et al.*, 2002). The monomeric molecule forms a single, compact disc-shaped domain (overall dimensions 65 x 59 x 41Å), which folds to form a deep cleft at the edge of the molecule. The catalytic Cys 64 residue is located at the bottom of a 16Å deep cleft. It is produced as a zymogen, whereby the N-terminus folds into a helical structure that occupies the active site and blocks substrate access (Yang *et al.*, 2012). Dissociation of the N-terminus helical

structure by endogenous metalloprotease and tripeptidyl aminopeptidase activates the zymogen.

As seen in Figure 1.1A) the overall structure contains 11 α -helices and 8 β -strands; one of the β -sheets is surrounded by α -helices, which are clustered into three regions. The central β -sheet forms a seven-stranded anti-parallel structure which is severely twisted between β_5 and β_6 strands. Here, there is only one hydrogen bond present between the main chains of these strands (Trp 258 and Thr 237). In Figure 1.1, the first cluster of α -helices is composed of the α_1 , α_2 and α_3 helices and the key Cys 64 residue is in the loop between α_2 and α_3 helices. The second cluster comprises of α_4 , α_5 and α_{10} . Finally, the third cluster is made up of α_6 , α_7 α_8 and α_9 .

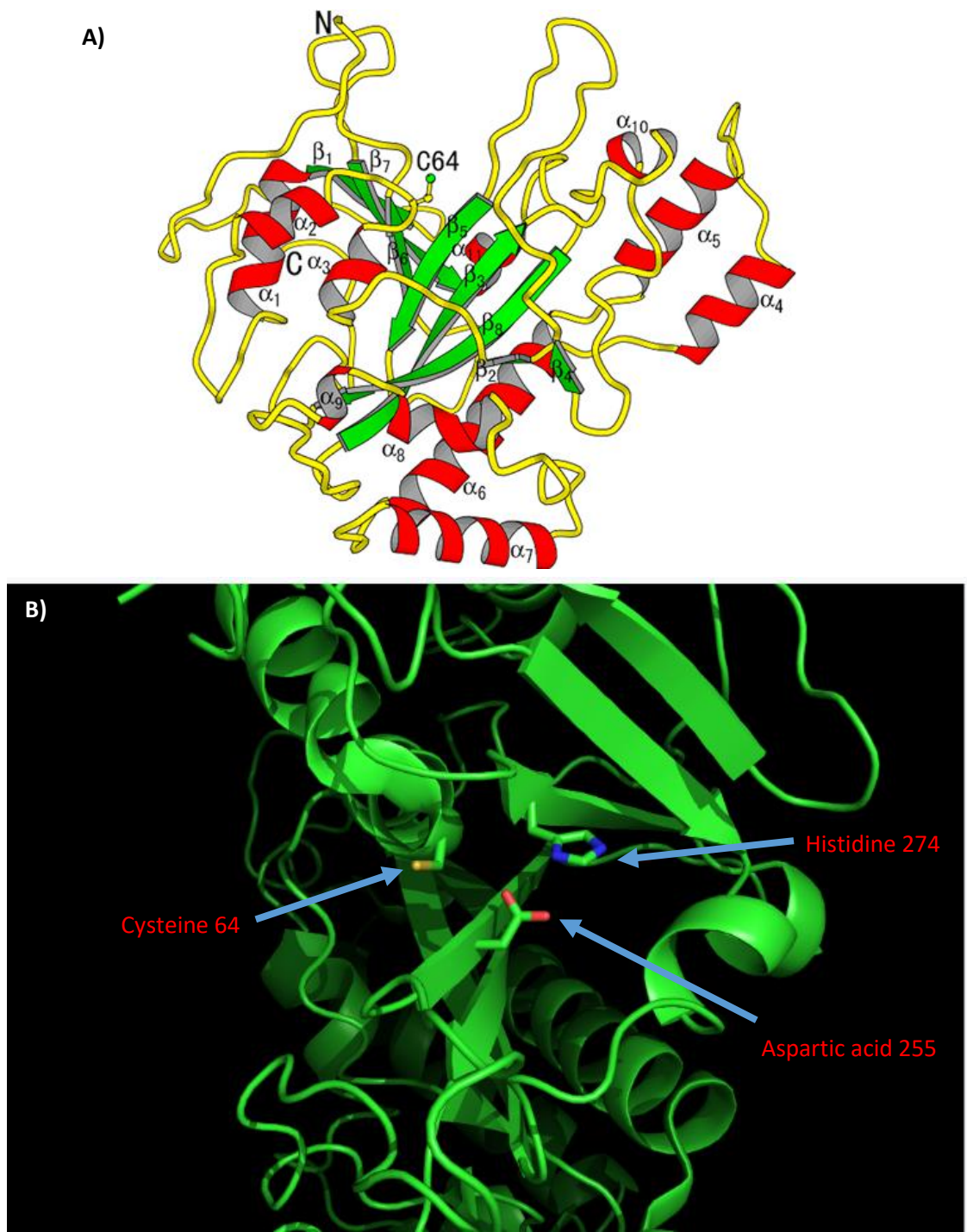


Figure 1: A) Schematic ribbon structure of mTG. The secondary structure is numbered for clarity. The side chain of cysteine 64 is represented as a “ball and stick model”. Adapted from Yokoyama et al. 2004. **B) A top down view of a ribbon model of mTG depicting the active site triad.**

Both TG2 and mTG contain a Cys-His-Asp catalytic triad, however, there are differences in the structural orientation between the two. For instance, relative to the active site cysteine, the position of His and Asp are reversed in the two enzymes (Strop, 2014). It has been proposed that Asp 255 plays a similar role to the catalytic triad histidine in TG2. Alanine mutagenesis confirmed the critical role of Asp 255 in mTG, whereby the activity of Ala 255 mutant was reduced to background levels. This is further supported by mutagenesis of His 274, here the catalytic activity was reduced by approximately 50%, suggesting that while it has a role it does not play a critical one in mTG (Kashiwagi *et al.*, 2002).

1.3.3 Production of mTG

The gene that codes for mTG contains a 1,221 nucleotide open reading frame that encodes a 407 amino acid protein. This corresponds to a predicted pre-region of 31 amino acids, the pro-region of 45 amino acids and the mature region of 331 amino acids. Proteases in the culture medium of *S. mobaraensis* process the pro-region, which inhibits enzyme activity and increases enzyme thermostability (Pasternack *et al.*, 1998). In the past, mTG was produced from *S. mobaraensis* by conventional fermentation. Recently though, more efficient systems have been described that produce mTG in host-vector systems such as *S. lividans* and *E. coli*. In the latter system, Salis *et al.* yielded a very high amount of mTG; over 6 g/l LacZ₁₋₈PNP₁₋₂₀Met-MTGase fusion protein per batch-fed fermentation process (Salis *et al.*, 2015).

The characteristics of mTG outlined above, i.e Ca²⁺ independence, smaller molecular weight and size, higher reaction rate are all more advantageous compared to TG2 when it comes to commercial meat processing (increasing its gelation, water-binding, emulsion stability). It is because of these properties that mTG is so widely used in the food industry to improve the physical properties of meat, fish and other protein-rich foods (Nonaka *et al.*, 1997).

1.4 Transglutaminase 2

TG2 has many different names: the official name is TGM2, but more common terms include tissue transglutaminase (tTG), cytosolic transglutaminase (cTG) and erythrocyte transglutaminase. Many different types of cells in the body express TG2 to varying degrees, which is why it has been described as the most ubiquitous of all the transglutaminases. The transamidating activity of TG2 is regulated by Ca^{2+} and GTP/GDP binding, where binding of Ca^{2+} results in active TG2 and binding of GTP/GDP results in inactivated TG2 (Smethurst and Griffin, 1996).

1.4.1 Transamidating and deamidation ability of TG2

In 1959, Clarke *et al.* were the first to reveal transamidation activity carried out by TG2 and this discovery sparked further interest in TG2 for the next two decades by researchers across the globe (Folk, 1983). Two important steps make up the biochemical mechanism that underlies the enzyme's reaction. The first step is a rate limiting one that involves the formation of the thioester bond between the cysteine in the active site of TG2 and the substrate. During this step, the sulphur on the Cys 277 carries out a nucleophilic attack on the γ -carboxamide group of a glutamine residue, thereby releasing ammonia as a by-product, as shown in Figure 1.2. During the second step, the acyl intermediate is attacked by the nucleophilic substrate; here, if the attacking nucleophile is primary amine (a small amine group or ε -amino group of a peptide-bound lysine residue), the reaction is called transamidation. However if a water molecule, acts as a nucleophile then it is called deamidation.

The results of TG2 transamidation are two-fold: the modification of the substrate protein with small amines or the formation of an isopeptide bond between acyl-acceptor and acyl-donor proteins. If the nucleophilic substrate is a small primary amine, then the result of the transamidation reaction ends with the addition of a small amine group to the substrate protein, which can then change its biological properties. N,N-bis(γ -glutamyl)polyamine formation is the

result of polyamine incorporation into a protein followed by another transamidation with another protein.

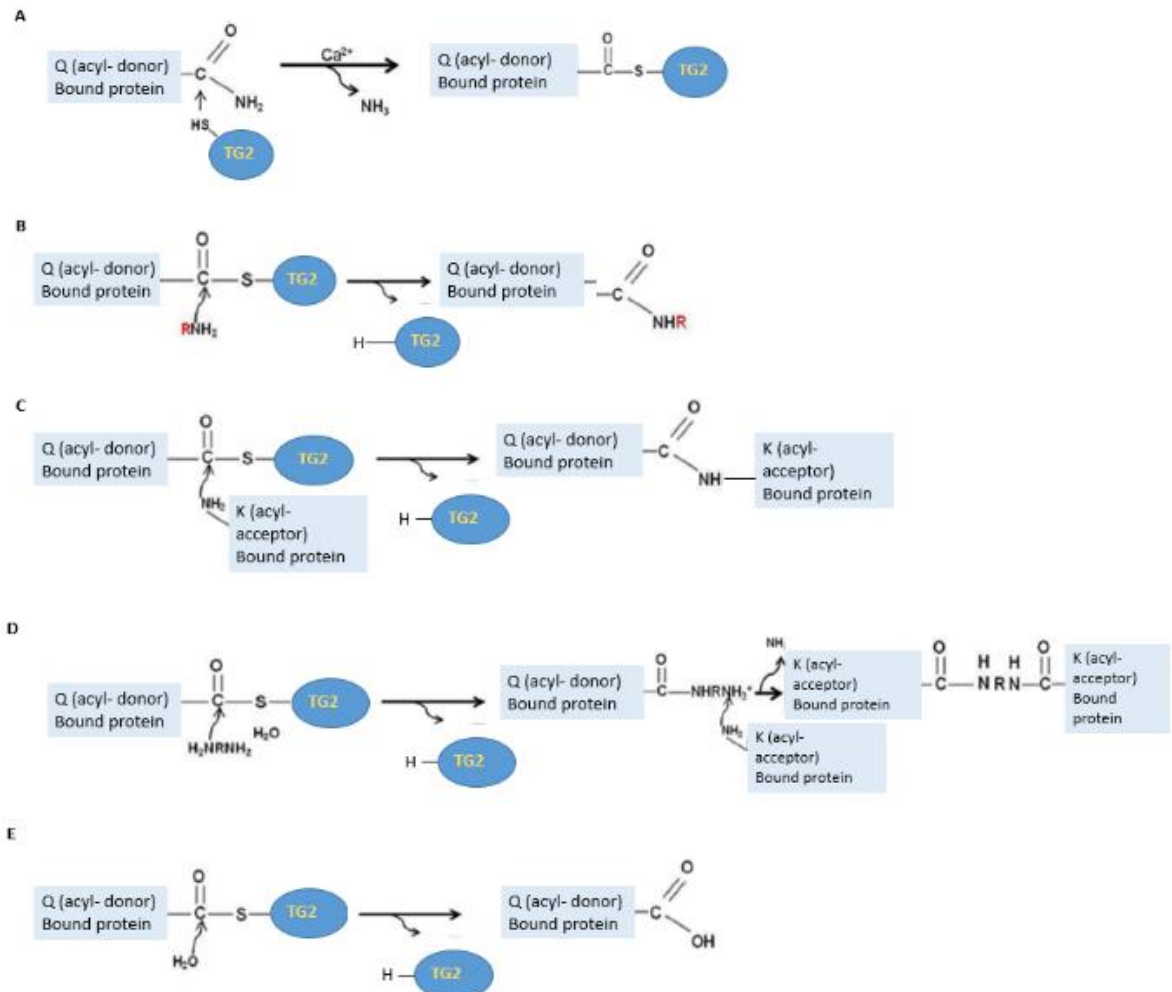


Figure 1.2: A series of post-translational reactions which are catalysed by the transamidase activity of TG2. A-B) Represent the two step catalysis reaction carried out by TG2. C) Represents the path taken when TG2 carries out a crosslinking reaction. D) Represents the polyamine incorporation reaction. E) Shows how deamidation is carried out by TG2

Deamidation results in the conversion of an acyl-donor glutamine residue into a glutamate residue, and was first thought to occur only under specific conditions. For example, a limited number of primary amines acting as acyl-acceptors would mean that water would act as an attacking group. It has also been reported that deamidation is favoured in a low pH environment (Fleckenstein *et al.*, 2002). A study conducting the crosslinking of small heat-shock proteins (sHsps) by TG2 showed that only one glutamine residue goes deamidation

while the rest underwent transamidation (Boros *et al.*, 2006). Furthermore, it has also been observed that the capacity for deamidation by TG2 is both dependent on structure and perhaps by pathological conditions (Stamnaes *et al.*, 2008).

1.4.2 More enzymatic functions of TG2

Regarding location, TG2 is predominantly a cytosolic protein, but is also seen in the nucleus and associated with both the inner and outer sides of the cell membrane. It is becoming clear that the different activities and conformations are key when discussing the role of TG2 in physiological and pathological processes. This versatile protein also carries out disulphide isomerase and guanine/adenine nucleotide binding and has hydrolysing abilities (Gundemir *et al.*, 2012). It should be noted that ATP/ADP binding has no effect on its transamidating activity (Lai *et al.*, 1998). However, the binding of calcium or GTP/GDP will inversely regulate the transamidating activity. Put simply, TG2 is only active when bound to calcium (open conformation) and inactive (closed conformation) when bound to GTP/GDP (Begg *et al.*, 2006, Chen and Mehta, 1999). What makes TG2 so unusual is that it has recently been reported to function as a protein disulphide isomerase (PDI), a protein kinase and as a DNA hydrolase (Hasegawa *et al.*, 2003, Mishra and Murphy, 2004, Akimov and Belkin, 2001).

1.4.3 Structure and conformation of TG2

The TG2 enzyme is made up of four domains: an N-terminal β -sandwich domain, the catalytic core and two C-terminal β -barrel domains (Figure 1.3). A catalytic triad for transamidating activity has been eluded that consists of Cys 277, His 335 and Asp 358 (Liu *et al.*, 2002). It was found that when the cysteine was mutated into serine at position 277, the transamidating and GTP/GDP binding capability of TG2 was completely abolished, In addition to this there are two more tryptophan residues (Trp 241 and Trp 332) that have been identified as critical for TG2 crosslinking activity. Trp 241 and Trp 332 are thought to be necessary to

stabilise the enzyme-thioester intermediate that forms during the first step of catalysis (Murthy *et al.*, 2002). Mutating tryptophan 241 to alanine abolished transamidating activity but didn't affect GTPase activity. However, swapping tryptophan 332 for phenylalanine resulted in the loss of GTP/GDP binding ability. Pinkas *et al.* discovered that a tyrosine (Tyr 516) seated within the catalytic pocket was crucial for crosslinking activity. In the inactive TG2 form, a hydrogen bond between Cys 227 and Tyr 516 is formed, which favours the inactive state of the enzyme (Gundemir *et al.*, 2012). Figure 1.3 below shows the four domains of TG2 as a linear diagram and which residues are seen in the binding sites.

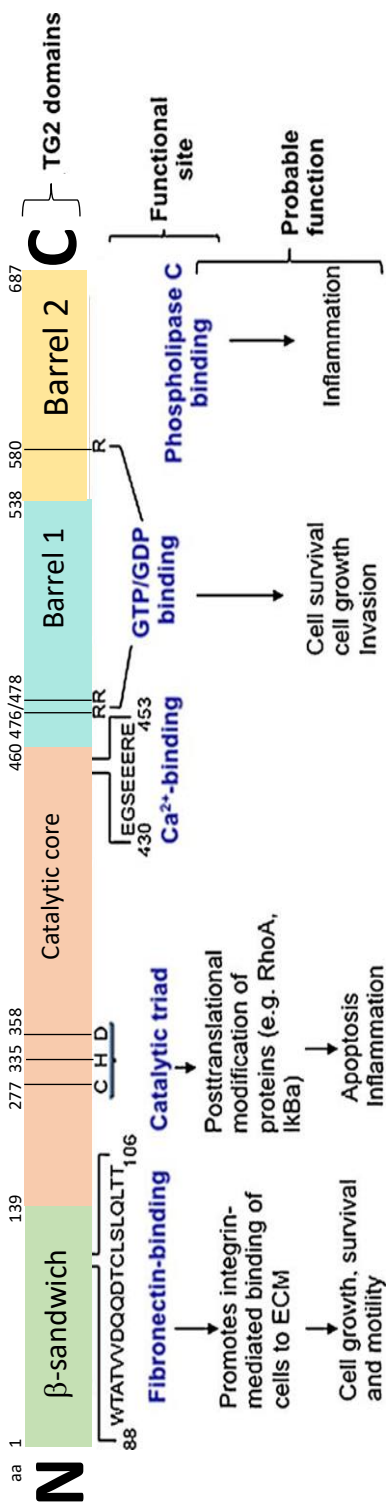
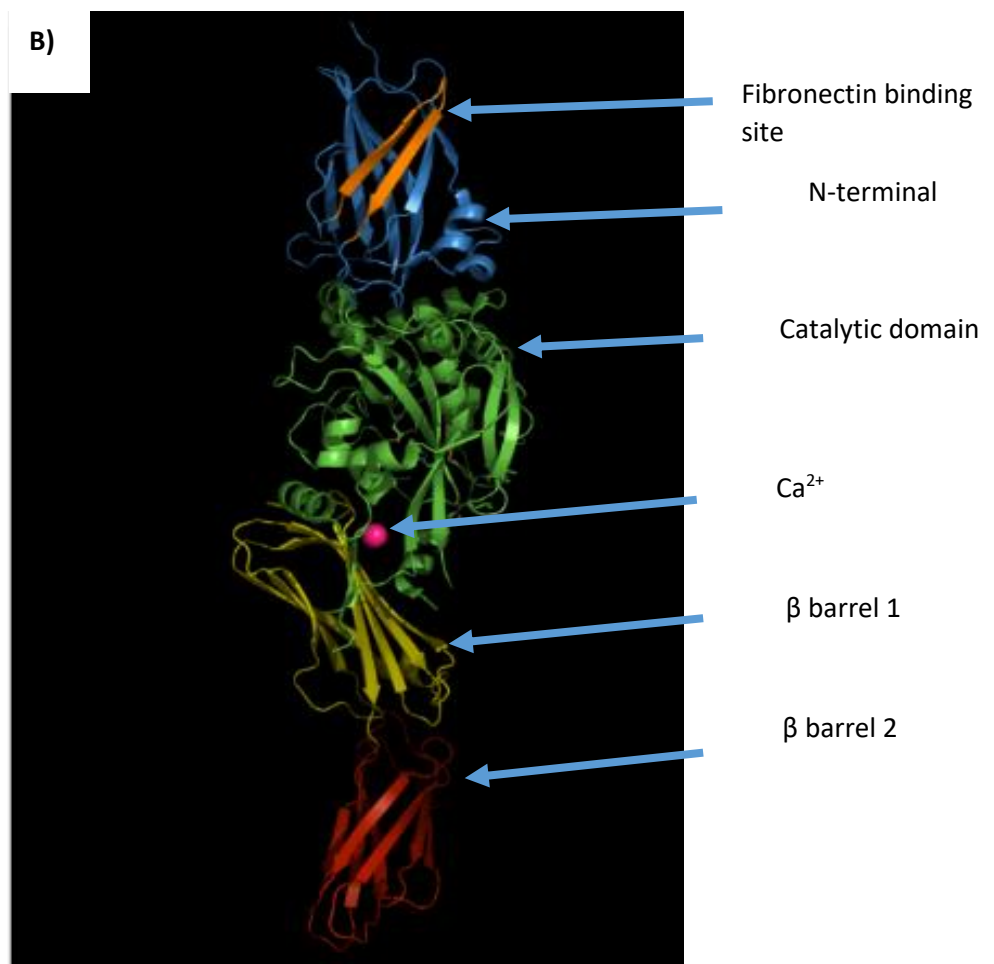
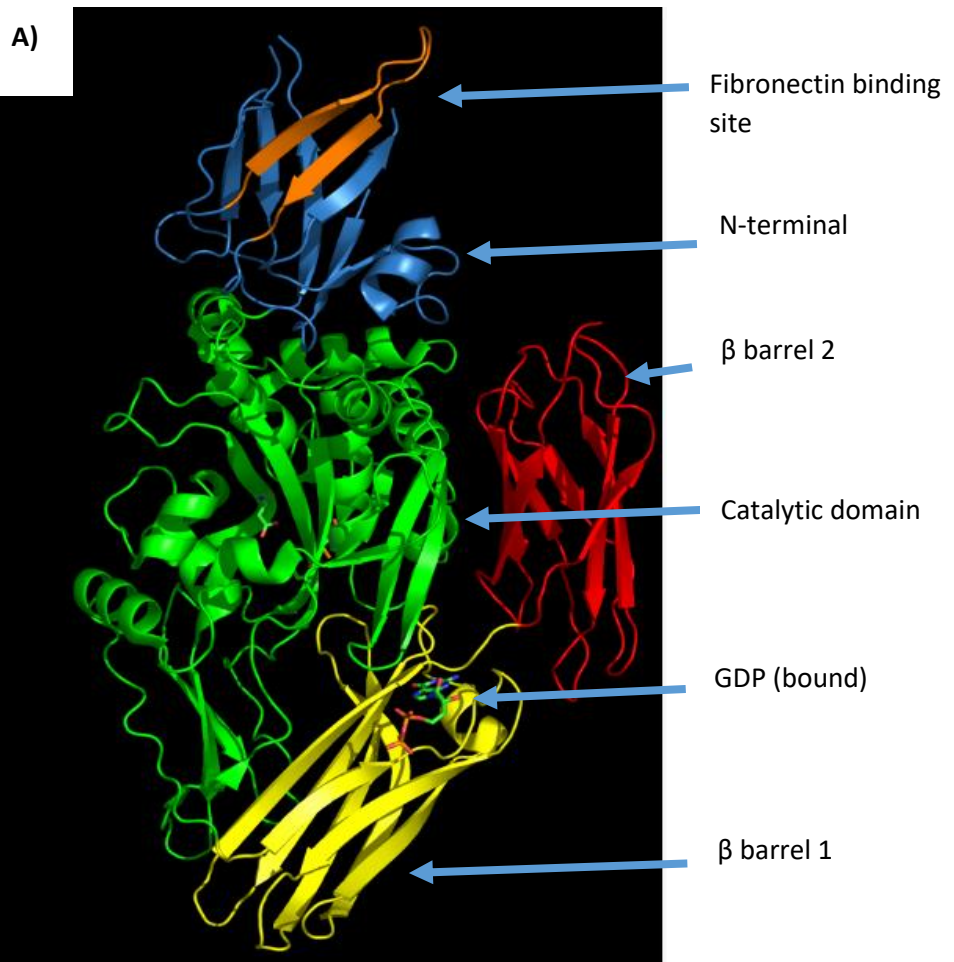


Figure 1.3: Schematic representation of the functional domains of TG2. Four distinct domains make up the protein. The N-terminal β-sandwich domain contains a high-affinity binding site for fibronectin and promotes direct or indirect attachment of cells to the ECM. When calcium is present, the conformation of the protein is open, so the catalytic core domain of TG2 is exposed and is responsible for cross-linking various cellular proteins by establishing highly stable isopeptide bonds. Barrel 1 domain contains a GTP/ATP-binding site that plays an important role in TG2-mediated signalling pathways. The C-terminal barrel 2 domain under certain conditions (e.g., in GTP-bound form) can contribute to pro-inflammatory responses. Adapted from Mehta *et al.* 2010.

The main GTP/ATP binding site has been found to be in a cleft between the catalytic core and the first β -barrel. TG2 interacts with GTP in the absence of Mg^{2+} (Jang *et al.*, 2014). Later, in 2010, Han *et al.* observed that less hydrogen bonding occurred between ATP and the binding pocket compared to the GTP complex structure. Furthermore, the residues S482 and R580 were shown to participate in GTP binding. Point mutation of R580 led to loss of GTP/GDP binding activity and inhibition of transamidase activity (Han *et al.*, 2010).

As previously stated, the ubiquitous TG2 is an enzyme that plays a part in many cell processes and thus has been studied heavily in order to elucidate how it functions within the body. In order to achieve this its structure has been described and studied by many. In 2007 the two major conformations of TG2 were solved with the aid of x-ray crystallography. Liu *et al.* discovered the (inactive) GDP-bound, compact form and the active site covalent inhibitor bound, open form (active). The catalytic domain of the GDP-bound crystal structure was inaccessible due to the two β -barrel domains preventing binding of the substrate to the enzyme. However, the Ac-P(DON)LPF-NH₂ inhibitor was used with TG2 to form a stable extended conformation or “open form” (Begg *et al.*, 2006, Mariani *et al.*, 2000). In this open form, the transamidating active sites were exposed to substrates, and it was believed that a disulphide bond between Cys 370 and Cys 371 was the key to stabilising this extended open form. The two major conformations of TG2 that were solved using x-ray crystallography are shown in Figure 1.4 below.



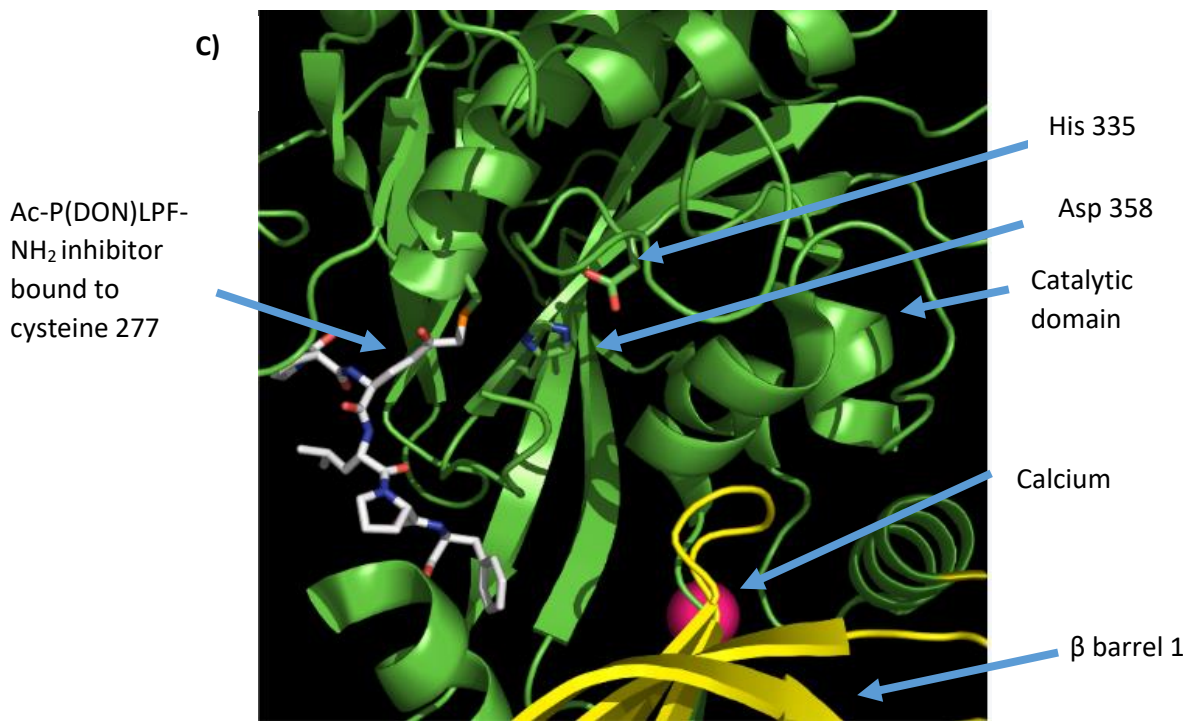


Figure 1.4: Representative models of TG2 derived through x-ray crystallography. Conformations of TG2 are represented as ribbon models. For each conformation blue represents the N-terminal, orange the fibronectin domain, green represents the catalytic domain, yellow and red represent the first and second β -barrels respectively. **A)** Represents the GDP bound closed conformation of TG2. **B)** The conformation when TG2 is open with calcium bound to it (represented as a pink ball). **C)** Conformation of TG2 when Cys 277 is bound to Ac-P(DON)LPF-NH₂ inhibitor.

1.4.4 Regulation of TG2 gene expression

At first it was thought that the expression of human TG2 (by the gene *TGM2*) occurred via several activators. As shown in the Figure 1.5, there are four Sp1 binding sites that have been revealed within TG2 and numerous activator regulating sites. These regulator sites include: nuclear factor κβ (NFκβ), interleukin-6 response element (IL-6), tumour growth factor-β1 (TGFβ1) response element, retinoic acid response elements (RRE1 and RRE2) and a glucocorticoid response element (GRE). Of all the activators of TG2, the most studied is retinoic acid (RA), which activates the retinoid response elements roughly 1.7kb upstream of the transcription start site (Nagy *et al.*, 1996). This reaction occurs as a tripartite response: Firstly the ligand activates either retinoic acid receptors (RAR) or retinoid x receptor heterodimers (RXR) or RAR/RXR homodimers. Following on from this, the RRE binds to the RAR/RXR heterodimers via three hexanucleotide half-sites (two canonical and one non-canonical). Finally, the complex binds to the Sp1 binding site with the help of other co-activators (Griffin *et al.*, 2002).

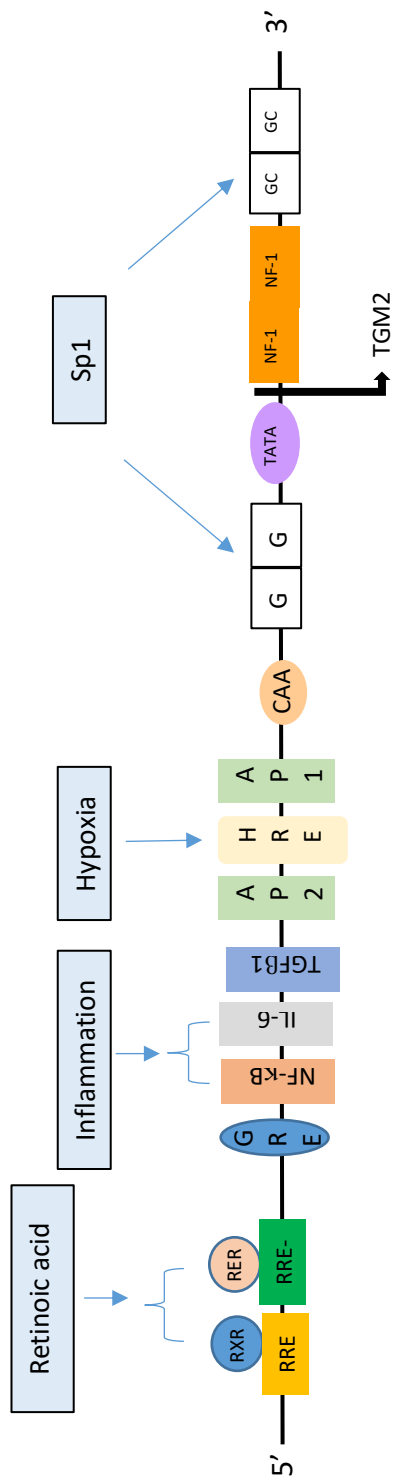


Figure 1.5: **Diagram of the *TG2* promoter.** *TGM2* gene expression is primarily regulated by RA, inflammation and stress factors. Acronyms: RXR: retinoid x receptor heterodimers, RRE: retinoic acid response elements, GRE: glucocorticoid response element, NF κ K

1.4.5 The role of TG2 in cell adhesion and signalling

Although the majority of cellular TG2 is found in the cytosol, the role of TG2 is dependent on the location of the enzyme itself (Bruce and Peters, 1983). TG2 is also located on the plasma membrane (Begg *et al.*, 2006), in the mitochondria (Rodolfo *et al.*, 2004) and the nucleus (Bruce and Peters, 1983, Lesort *et al.*, 1998). Furthermore, there are studies showing that TG2 is present in the extracellular matrix (ECM) (Zemskov *et al.*, 2006, Upchurch *et al.*, 1991). Although TG2 is considered as a stress-related protein whose expression radically increases upon stress or injury (see Figure 1.5), it is also expressed continuously in several cells including endothelial cells, fibroblasts, and smooth muscle cells (Jones *et al.*, 1997, Ou *et al.*, 2000).

TG2 interacts with many different proteins and enzymes in the body. It has been well-established to promote cell-ECM adhesion and cell migration (Belkin, 2011). Table 1.2 lists the endogenous and exogenous substrates and binding partners of TG2.

Table 1.2: Exogenous and endogenous substrates and binding partners of TG2 (Griffin et al., 2002, Esposito and Caputo, 2005)

ECM and cell surface	Cytosol	Organelle Proteins	Nucleus	Others
β -casein	Actin	α -oxoglutarate	Calbindin	<i>Candida albicans</i> surface proteins
Collagen	Aldolase A	Acetylcholine esterase	Core histones	glycoproteins gp120 and gp41
Fibronectin	β -crystallin	band III	Importin- α 3	Hepatitis C virus core protein
Fibronogen	β -tubulin	CD38	pRB	HIV aspartyl proteinase
IGFBP-1	C-CAM	Cytochromes		Pea legumin
Laminin	GADPH	Erythrocyte (band 3)		Soy protein
LTBP-1	Glucagon	Histone H2B		Wheat gliadin
Midkine	GST			Whey proteins
Osteocalcin	Lipocortin I			
Osteonectin	Melittin			
Osteopontin	Myosin			

Phospholipase A2	Phosphorylase kinase			
Substance P	RhoA			
Vitronectin	Secretory vesicle IV			
	Tau protein			
	Thymosin β			

In addition to this, it triggers the organisation of extracellular matrix proteins through two different pathways: The first is integrin-TG2 interaction and syndecan-4-TG2 complexes (Belkin, 2011). The second is through an RGD-ligand independent manner, TG2 was also found to associate with the membrane protein heparan sulphate proteoglycan (HSPG) syndecan-4 to promote cell-ECM adhesion (Telci *et al.*, 2008). This adhesion pathway is hypothesised to be crucial for cell survival during injury/tissue remodelling. This is because TG2/fibronectin (FN)/syndecan-4 complexes activate PKC α , leading to the activation of $\beta 1$ integrins even when they are blocked by RGD peptides. These FN/TG2/syndecan-4 complexes can also be activated by proteins including syndecan-2 via PKC α (Wang *et al.*, 2010b). Some of the most important integrin subunits that TG2 non-covalently interacts with include $\beta 1$, $\beta 3$, $\beta 5$, αV , and $\alpha 5$ on cells. It should be noted that the binding sites for TG2 and integrins do not overlap on fibronectin. This means that the affinities of TG2 with these two proteins on the cell surface significantly enhance the interaction of cells with finbronectin (FN) and further promote cell adhesion and ECM-triggered signalling (Akimov and Belkin, 2000, Akimov and Belkin, 2001). In the absence of integrin-ligand interactions, TG2 may also be able to induce integrin clustering (Janiak *et al.*, 2006). These TG2/integrin complexes have been found to decrease the activity of the Src-p190RhoGAP regulatory pathway, thus increasing the

activation levels of RhoA GTPase and its downstream signalling target, ROCK (Janiak *et al.*, 2006).

In summary, the association of TG2 with cell membrane integrins and ECM proteins can be considered an amplifier of outside-in adhesion signalling.

1.4.6 The role of TG2 in wound healing

TG2 is active in different stages of the wound healing process via both transamidation-dependent and independent mechanisms. Soon after mechanical or chemical injury of fibroblasts, it has been observed that TG2 is secreted into the ECM and co-localises with ECM proteins (Upchurch *et al.*, 1991). It has been established that TG2 crosslinking activity is found in every layer of skin, as shown in a rat dermal skin wound model (Bowness *et al.*, 1988). Moreover, within wound areas, TG2 expression and activity in vascular endothelial cells and erythrocytes were suggested to support and amplify FXIIIa-mediated blood clot formation (Murthy *et al.*, 1991, Barsigian *et al.*, 1991, Auld *et al.*, 2001). Recently, it has been theorised that TG2-promoted cell adhesion is crucial in the wound healing process. Here, TG2/FN complexes can interact with cell membrane syndecan receptors and enhance cell adhesion and survival when cells undergo anoikis (Telci *et al.* 2005; Verdario *et al.*, 2003). Furthermore, an increase in TG2 mRNA expression is also linked to collagen-producing phenotypes during matrix remodelling stages (Schnabel *et al.*, 2004, Klingberg *et al.*, 2013). It is important to note that these two opposite actions may occur distinctly depending on different cell types, the type of stimulus and the intracellular localisation of TG2. In situations where myofibroblasts persist in the extracellular matrix, a fibrotic phenotype develops. In wounds, this is manifested as hypertrophic scar or keloid (Sayah *et al.*, 1999; Kothari *et al.* 2014). In conclusion, in order to determine whether normal wound healing or abnormal scar tissue formation will take place, there has to be a balance struck within cells regarding the pro-apoptotic (see 1.3.7 below) and anti-apoptotic abilities of TG2.

1.4.7 The involvement of TG2 in pathological conditions

TG2 is now known to have numerous roles in multiple diseases and disorders such as coeliac disease, cancer and fibrosis. Specifically, it was found by Fesus *et al.* that TG2 is involved in apoptosis. Here, levels of enzyme expression correlated with the cellular regression found in livers of rats after the induction of hyperplasia (Fesus *et al.*, 1987). Following on from this, it was discovered that TG2 stabilises apoptotic cells via intracellular cross-linking in order to prevent loss of intracellular components before clearance by phagocytosis (Melino & Piacentini., 1998).

TG2 has also been found to have physiological roles. When cells respond to stress or are damaged, TG2 is up-regulated and externalised into the matrix. Once externalised, TG2 contributes to a chronic inflammatory response through excessive matrix deposition, ECM crosslinking and tissue fibrosis. Chronic inflammation and near constant TGF- β activation are observed in several fibrotic disease models including pulmonary (Richards *et al.*, 1991), renal (Johnson *et al.*, 1997, Johnson *et al.*, 1999, Johnson *et al.*, 2007) and liver fibrosis (Skill *et al.*, 2001). TG2 crosslinks large pools of latent TGF- β binding protein-1 (LTBP-1) in the ECM, which in turn makes the extracellular matrix resistant to degradation (Johnson *et al.*, 2007).

TG2 also plays a role in coeliac disease in that deamidation of glutamine residues in gliadin results in their increased binding affinity to the disease-predisposing human leukocyte antigen (HLA) DQ2 and DQ8 molecules. Thus causing a strong immune response to be launched via the activation of T-lymphocytes (Lindfors *et al.*, 2011). Similarly, a high activity of TG2 is seen in Alzheimer's disease due to the polymerisation of proteins such as beta-amyloid precursor protein and Ab peptides in affected brains (Benilova *et al.*, 2012).

Recently, it has been shown that S100A4 (a biomarker for highly metastatic cancer) is a substrate for TG2. Crosslinking of S100A4 by TG2 can be inhibited by the TG2 specific inhibitor R294, leading to the abolishment of S100A4-enhanced cell migration. The mechanism for this

S100A4/TG2-related cell migration involves the activation of the syndecan-4 and $\alpha 5\beta 1$ integrin co-signalling pathway linked by PKC α (Wang and Griffin, 2013). Furthermore, tumour cells have been found to contain modified forms of TG2 that are inactive even when secreted into the ECM (Beninati, 1995).

1.5 Involvement of TG2 in physiological bone development

Transglutaminases have been associated with the promotion of chondrocyte and osteoblast differentiation as well as matrix mineralisation (Yin *et al.*, 2012a). Through recent studies, it has been theorised that one or more transglutaminases involved in the processes mentioned above might be mediated by the protein crosslinking activity of transglutaminases. Either by the GTPase activity of TG2 or through non-catalytic signalling effects (Nurminskaya and Kaartinen, 2006).

Bone development starts during embryogenesis, continues postnatally and further continues to be remodelled throughout a lifetime. It is a complex process that is controlled locally as well as systematically by growth factors, hormones and extracellular molecules such as bone morphogenic proteins (BMPs) 2, 4 and 7. Of the nine members of the TG family, only two have been discovered in cartilage and osseous tissue, these are TG2 and FXIIIa. Through immunohistochemistry, it was first demonstrated that TG2 is upregulated in the hypertrophic zone of the growth plate in juvenile rats (Aeschlimann *et al.*, 1993). Following this, a significant increase in FXIIIa expression was discovered in the hypertrophic zone of the avian embryonic growth plate (Nurminskaya and Linsenmayer, 1996).

TGs are very important in early bone formation; this was shown through the expression patterns of TG2 and FXIIIa in early embryonic limb development (using a chicken model) that were analysed to understand their potential roles. As early as 4 days into development, the formation of the tibia begins in the regions of mesenchymal condensation. By 6.5 days, both TG2 and FXIIIa are present throughout the areas of chondrocyte condensation. There were

higher levels of both transglutaminases in the hypertrophic zone and epiphyseal regions of the long bone. Towards the end of embryonic development, the expression of both enzymes is more restricted and only expressed in the superficial layers of cells (Pechak *et al.*, 1986, Nurminskaya and Linsenmayer, 1996). These results suggest that there is an early activation of TG2 and FXIIIa in the mesenchymal condensation phase, but then later on during development, the expression of these enzymes is restricted to proliferative chondroblasts close to the epiphyses.

Further study in the expression of transglutaminases in the perichondrium/ periosteum region revealed more clues of their role in osteoblasts. Through immunohistochemistry, it was shown that by day 6 of development, there was an absence of transglutaminase 2 and FXIII expression in the perichondrium during the mesenchymal condensation phase. However, by day 9 when ossification has taken place in the periosteum, expression of transglutaminase and FXIII was detected (Nurminskaya and Kaartinen, 2006). This suggests that TG2 and FXIII are expressed in the cells undergoing differentiation into osteoblasts. This study suggests that the initiation of TG2 and FXIII synthesis by osteoblasts correlates with the deposition of the mineral matrix (Nurminskaya and Linsenmayer, 1996).

The transamidating activity of TG2 has been shown to be crucial in bone development, and TG2 induces mineralisation. It has been shown that, when TG2 is blocked with inhibitors, the outcome was impaired mineralisation occurs in MC3T3-E1 pre-osteoblast cultures (Al-Jallad *et al.*, 2006). This work lead other research groups to theorise that TG2 could be playing different roles in mineralisation. These include potentially inducing mineralisation through its ATPase activity (Nakano *et al.*, 2007, Nakano *et al.*, 2010) or by activating the Wnt pathway by activating LRP5/β-catenin (Faverman *et al.*, 2008, Beazley *et al.*, 2012).

1.5.1 TG2 and its involvement in matrix maturation

Transglutaminases are well-established as matrix stabilisers and several substrates (bone matrix proteins) that they affect including collagen I, osteopontin, bone sialoprotein and FN (Kaartinen *et al.*, 1999; Kaartinen *et al.*, 1997; Forsprecher *et al.*, 2011). Of all the transglutaminases, TG2 has been related to secretion and deposition of ECM proteins the most. In addition to this, TG2 crosslinking of ECM proteins has been shown to improve cell adhesion, proliferation and differentiation (Png and Tong, 2013, Nadalutti *et al.*, 2011).

The organic bone matrix is mostly comprised of type I collagen (~90%) and, as stated previously, is a well-known TG2 substrate in mineralised tissue. Upregulation of TG2 has been observed to increase deposition of collagen I in many fibrotic conditions such as lung fibrosis (Jones *et al.*, 2005 & Shweke *et al.*, 2008) kidney fibrosis (Johnson *et al.*, 2007) and cardiac fibrosis (Wang *et al.*, 2018). Regarding extracellular collagen, polymerisation could take place via intermolecular crosslinking (Chau *et al.*, 2005) or between non-collagenous bone matrix proteins and collagen. A well-organised fibrillar collagen network forms the foundation of mineralisation and transglutaminases are suggested to play a role in fibre organisation through their crosslinking ability (Pawelec *et al.*, 2016). Evidence has also shown that transglutaminases can promote collagen synthesis and assembly which leads to the promotion of cell differentiation (Al-Jallad *et al.*, 2006). On the whole, TG2 promotes mineralisation in osteoblasts, promotes matrix protein secretion, deposition and maturation through crosslinking-mediated modification of ECM which further enhances cell attachment.

1.5.2 Transamidating independent pathway

At this time there are several theories regarding TG2-containing adhesive/signalling pathways which have been proposed. One of the most studied is the involvement of TG2 in RGD dependent integrin signalling. Akimov *et al.* first showed in 2000 that TG2 non-covalently interacts with $\beta 1$ and $\beta 3$ integrins (located on the cell surface) and regulates the interaction

between FN and the integrins. It was theorised that TG2 acts as an integrin-associated coreceptor to improve cell adhesion and spreading. This interaction between extracellular TG2 and integrins leads to integrin clustering on the cell surface, FN deposition and finally mineralisation (Akimov *et al.*, 2000, Zemskov *et al.*, 2006).

Telci *et al.* also reported on another important TG2 adhesion pathway, here TG2 and FN bound to syndecan-4 could associate with β 1 integrin. This triggers an outside-in signal through PKC α and triggers an RGD-independent cell adhesion process. These complexes also trigger an inside-out response from syndecan-2, which then modulates cytoskeletal organisation through the ROCK pathway to maintain the RGD- independent adhesion of osteoblasts (Wang *et al.*, 2011).

Nurminskaya *et al.* revealed in several cell cultures that the addition of exogenous TG2 promotes pre osteoblast differentiation, chondrocyte maturation and calcification of vascular smooth muscle cells (VSMCs) (Faverman *et al.*, 2008, Nurminskaya *et al.*, 2003). These experiments showed a correlation between extracellular TG2 and the mineralisation process in several cell lines. The following theories were put forward by these researchers:

The first is that exogenous TG2 promotes pre-osteoblast differentiation and matrix mineralisation in a crosslinking activity independent mechanism (Yin *et al.*, 2012a). This is supported by the revelation that there are no changes in the pattern of protein crosslinking after pre-osteoblasts were treated with chondrocyte-derived TG2. Cells that were transfected with mutant inactive TG2 were still able to develop hypertrophic differentiation. However, extracellular TG2 induced hypertrophy was not affected by the use of GTP-bound, transamidase inactive TG2 (Johnson and Terkeltaub, 2005).

Secondly, TG2 bound to GTP acts as a molecular switch for hypertrophic differentiation and calcification of chondrocytes, in which its transamidase and GTPase activities are not required. Johnson and Terkeltaub (2005) suggest this might be down to the nucleotide-bound form of TG2 being in a conformation that is ideal for triggering collagen expression and

calcification of chondrocytes in response to specific agonists (such as BMP2 and other wnt ligands). It should be noted that transamidating activity inhibitors are reported to change conformation of TG2 (Pinkas *et al.*, 2007).

The third and final theory is that direct binding of TG2 to cell surface proteins in pre-osteoblasts, without the formation of cross-links has been demonstrated. This cell surface receptor superfamily that directly interacts with TG2 has been identified as low density lipoprotein receptor related-protein (LRP). The interaction with this group of proteins and TG2 leads to internalisation and degradation of surface TG2 and further regulates cell adhesion and signalling. Using immunoprecipitation, it has been shown that LRP5 interacts with TG2 and is involved in pathological calcification of VSMCs (Faverman *et al.*, 2008). For over a decade now, LRP5 has been implicated in bone formation, as mutants with loss-of-function of LRP5 present a severe osteoporosis phenotype (Gong *et al.*, 2001). Moreover, gain of function mutant studies with LRP5 showed a high bone mass phenotype (Boyden *et al.*, 2002). It has now been asserted that β -catenin singalling, a major component of the canonical Wnt pathway, directly regulates osteoblast maturation via interaction with LRP5. Although there is contention regarding whether crosslinking activity is essential for exogenous TG2-induced mineralisation (Beazley *et al.*, 2012), the interaction between LRP5 and TG2 as well as the downstream activation of β -catenin pathway might play a common role in calcified tissue. Figure 1.6 shows the Wnt signalling pathways and their antagonists.



Figure 1.6 **Scheme of Wnt signalling and its antagonists.** **(A)** Binding of Wnt to Frizzled and co-receptors, LRP5/6, activates the canonical pathway. Axin is recruited to LRP5/6 and subsequently degraded. The disruption of the link between β -catenin and glycogen synthase kinase 3 beta (GSK-3 β) causes β -catenin to be released. Intracellular β -catenin is stabilised due to free from phosphorylation. **(B)** Presence of Wnt signalling antagonists, such as secreted Frizzled-related protein (sFRP), Wnt inhibitory factor-1 (WIF-1) and Cerberus (CER), block both the canonical and non-canonical pathways. Bone morphogenetic protein (BMP) and Nodal are two subsets of transforming growth factor beta (TGF- β) superfamily. **(C)** Interaction among antagonist Dickkopf-1 (Dkk-1) and LRP5/6 and the co-receptor Kremen 1/2 (Krm, green) triggers LRP5/6 endocytosis. The canonical pathway is inactive due to absence of LRP5/6–Wnt–Frizzled complex. β -catenin is phosphorylated by GSK-3 β and thereby undergoes degradation. However, the non-canonical pathway remains active via interaction of Wnt with Frizzled without LRP5/6. (Kawano and Kypta, 2003).

1.6 Bone regeneration and biomaterials for tissue repair

Due to the ubiquitous expression of TG2 throughout the body and its involvement in various tissue developmental and wound healing processes, it is possible that TG2-based biomaterials could be beneficial for wound healing. Below, the advantages and potential uses of TG2 crosslinked biomaterials for soft and hard tissue repair are summarised below.

1.6.1 Tissue engineering

It was in 1988 that Robert Nerem first coined the term “tissue engineering” at a National Science Foundation workshop. This term was further extended and formalised in a review paper in *Science* by Langer and Vacanti. Here, the modern day definition was given:

“Tissue engineering is an interdisciplinary field that applies the principles of engineering and the life sciences toward the development of biological substitutes that restore, maintain or improve tissue function” (Langer and Vacanti, 1993).

In short, tissue engineering introduces a great promise and potential for producing engineered replacements as alternatives therapies for human disease and injury.

The first step is understanding cell-cell interactions, then choosing the appropriate matrices based on cell-matrix interaction and finally to supplement with extra biochemical signalling or growth factors. Thus, it is clear that cell sources, biomaterials and growth factors are the three fundamental elements in tissue engineering. Furthermore, there is a need for vascularisation to occur to provide blood and nutrients to engineered tissues. This need has recently been drawing more attention, especially within the field of bioengineered tissue reconstruction (Naderi *et al.*, 2011). Following this approach, some achievement has been made in basic research and in a clinical setting including skin, bone, heart valves, cartilage, esophagus, blood vessels, liver, pancreas, nerves and tracheal constructs (Horch, 2006).

Of all the tissue engineering subdivisions, bioengineered bone substrates are considered as one of the most studied and successful. At present, there is a demand for bone substitutes to repair and replace diseased or damaged tissue, degenerative disease and cancer. Moreover, due to the increasing aging population, there is a surging demand for substitutes to replace, restore or regenerate bone. This is a major clinical need in the fields of spinal, dental, cranial, orthopaedic and maxillofacial surgery. After transfused blood products, bone implants are the second most implanted materials and yet the availability and quality of bone substitutes fall short of the current requirement (Wang and Yeung, 2017). Thus, developing appropriate bone constructs to meet these growing needs is vital. However, due to the complexities of regenerating complex tissues and organs such as heart, muscle, kidney, liver and lung, there are still major milestones to be reached in tissue engineering. However, whilst growing relatively “simple” tissue such as cornea is becoming a reality (Ruberti and Zieske, 2008), the quality and quantity of artificial grafts is far below the clinical demand for more complex tissues (Lash *et al.*, 2015).

1.6.2 Bone tissue engineering

During 2015 in the US the annual medication and treatment costs for hip fractures alone was estimated to be between 10.3 and 15.2 billion dollars (Dy *et al.*, 2011). Furthermore, 5% of the 1.2 million cases of overall fractures showed non-union or delayed healing after surgery (Leighton *et al.*, 2017). In 2010, it was estimated that worldwide there were 4 million operations that involved bone grafting or bone substitutes (Brydone *et al.*, 2010). The aging society has meant that the number of joint replacement operations has increased greatly which further highlights the requirement of bioengineered bone tissue. To illustrate this point, during 2011-2012, it was estimated that 180,000 cases of primary knee and hip replacement procedures were entered into the National Joint Registry in the UK. Of this total, around 9% of primary joint replacements underwent revision surgery (NJR, 2011). It is clear, therefore, that the need to continue research in bone engineering is urgent. The sections below summarise

the biology of bone as well as current options of bone grafting and recent developments in cell engineering.

1.6.3 The biology of bone

Bone is described as a rigid organ that provides mechanical support for anchoring muscles, confers protection to organs and facilitates movement. Bones also produce red and white blood cells and store minerals. Bones come in many different shapes and sizes and have a complex internal and external structure. They are lightweight yet strong and hard, and serve multiple functions as listed above. Bone is a unique organ in that its complex cellular composition is made up of both organic and inorganic architecture which is classified as micro and macro composite tissue. The mineralised matrix consists of an organic phase (collagen, 35% dry weight) which is responsible for its rigidity, viscoelasticity and a mineral phase. The latter is made of up of carbonated apatite (65% dry weight) for structural reinforcement, stiffness and mineral homeostasis. Finally, there are also non-collagenous proteins present that form a microenvironment that is stimulatory towards cellular functions (Hutmacher, 2013).

Looking at the morphology of bone, there can be two categories in which bone can fall under: cortical (or compact) bone and trabecular bone (cancellous or spongy). Cortical bone is formed of a condensed layer that consists of densely packed collagen fibrils in concentric lamellae. It has a low porosity when compared to other bone tissues, ranging from 5-30%. This type of bone is responsible for the mechanical strength and rigidity in the skeleton and contributes to 80% of the total bone mass in adults. Trabecular bone, on the other hand, is composed of a porous latticework of matrix and primarily functions to store minerals in the body (Deakin, 2006). Bone tissue can be categorised through the hierarchical organisation of its constituents at the macrostructure (cancellous and cortical bone), the microstructure (Haversian systems, osteons), sub-microstructure (lamellae), nanostructure (fibrillar collagen

and embedded minerals) and finally the sub-nanostructure (minerals, collagen and non-collagenous proteins) (Rho *et al.*, 1998). This macroscopic hierarchy of structure is summarised in Figure 1.7.

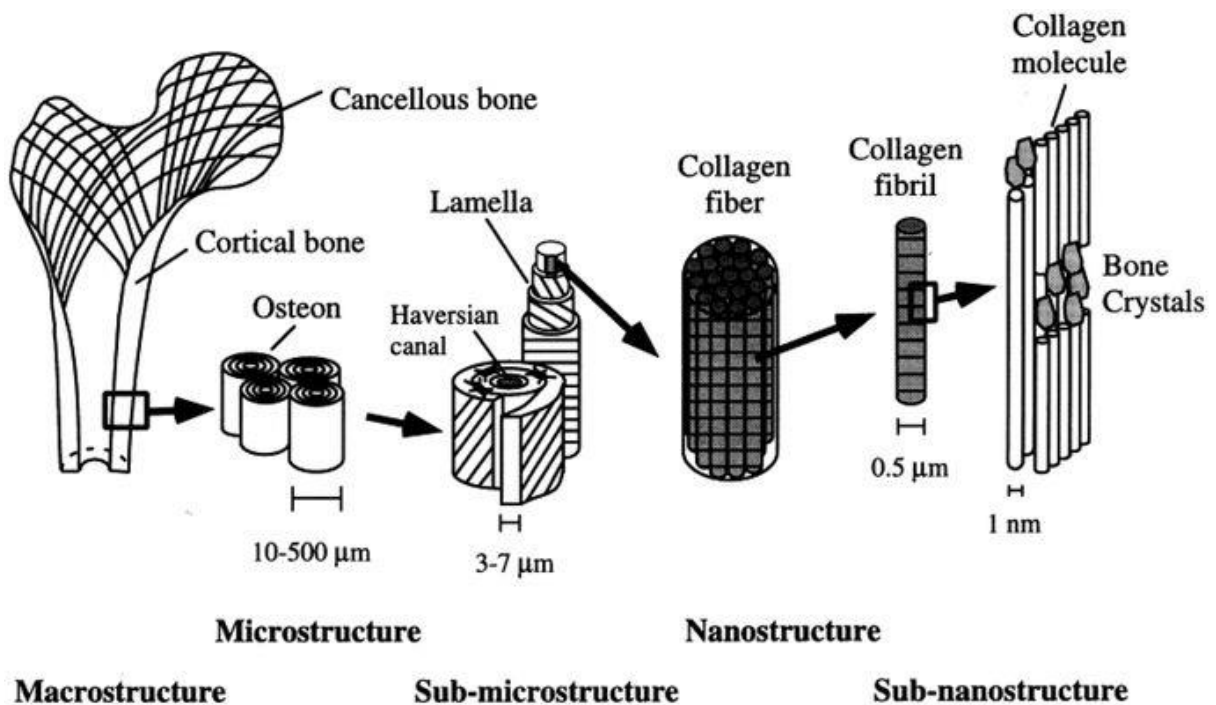


Figure 1.7: **Hierarchical structure of bone from macrostructure through to sub-nanostructure.** Adapted from (Rho *et al.*, 1998).

Macroscopically, bone is seen as a hard dense cylindrical shell of cortical bone, along the shaft of which the bone becomes thinner with greater distance from the ends. At these proximal and distal ends of the bone, cortical bone encompasses the porous trabecular bone to optimise articular load transfer (Webster and Ahn, 2007). When comparing densities, trabecular bone has a porosity of 50%-90% with an average spacing of around 1 mm and average density of $0.2\text{g}/\text{cm}^3$ (Barrere *et al.*, 2008). Whereas cortical bone is much denser with a porosity of 3-12% and an average density of $1.8\text{g}/\text{cm}^3$ (Cooper *et al.*, 2004).

Looking at the microscopic scale, both trabecular struts and cortical bone are composed of mineralised collagen fibres, which are stacked parallel to form layers. These are

called lamellae (3-7 μ m thick) (Webster and Ahn, 2007). In mature bone these lamellae wrap in concentric layers around a canal which is called the Haversian canal. This contains the nerve and blood vessels to form an osteon. This is a cylindrical structure that runs parallel to the axis of the bone. On the nanostructure level, collagen fibres are surrounded by mineral.

Several types of bone cells and bone extracellular matrix form the mineralised bone matrix. Regarding bone cells, there are four types: osteoclasts, osteocytes, bone lining cells and osteoblasts. In addition to these four integral types there are also more cell types that are contained within the bone marrow within the central intramedullary canal of the bone shaft (Marks and Popoff, 1988). Part of the organ's purpose is to serve as a place to store minerals that are used by the body's endocrine system in order to regulate phosphate and calcium homeostasis. Recent studies have shown that bone exerts an endocrine function itself. It is thought that this is because the bones themselves are producing hormones that regulate phosphate and glucose homeostasis (DiGirolamo *et al.*, 2012).

Bone is a connective tissue that is highly dynamic. It undergoes continuous remodelling via a removal of bone through osteoclasts and formation of new bone by osteoblasts. This well-orchestrated relationship of removal and formation shifts to adapt the bone's structure and functional demands such as mechanical loading and nutritional needs (Hutmacher, 2013). The mechanical properties of bone depends on its composition (mineralisation and porosity etc.) as well as the structural organisation (trabecular or cortical bone architecture, collagen fibre orientation etc. (Martin, 1991).

Osteoprogenitor cells differentiate to osteoblasts, which go on to synthesise bone matrix which is composed of mostly type I collagen. It is thought that flattened bone lining cells (FBLs) are quiescent osteoblasts which line non-remodelling bone surfaces. These FBLs are thought to be important in the maintenance of mineral homeostasis and regulate remodelling signals (Miller *et al.*, 1989). Osteoblasts secrete matrix and become trapped inside it as they transition to osteocytes (which are shaped like stars as opposed to the triangular shaped osteoblasts). Osteocytes reside and network inside lacunae, similar to the way the nervous

system works, via long cytoplasmic extensions in tiny canals called canaliculi. Even though osteocytes have a low synthetic activity, there have been studies that showed they are actively involved in turnover of bony matrix via numerous mechanisms (Schaffler *et al.*, 2014).

Mesenchymal stem cells (MSCs) are multipotent cells that are able to differentiate into different lineages of mesenchymal tissue, including cartilage, fat, bone and various connective tissues (Phinney & Prockop, 2007). These cells have been now isolated from adult blood, tooth pulp and bone marrow. One of the master modulators in the differentiation of MSCs into Osteoprogenitor cells is the canonical Wnt/ β -catenin pathway (Logan and Nusse, 2004). Studies have also shown that high and low bone mass phenotypes are associated with activation of LRP5 (a co-receptor of Wnt protein receptor) (Gong *et al.*, 2001, Boyden *et al.*, 2002). It has even been shown that myogenic cells can give rise to osteoprogenitor de-differentiation under certain circumstances (Doherty *et al.*, 1998). Here blood vessel pericytes could undergo de-differentiation and develop into osteoblasts, chondrocytes fibroblasts and adipocytes (Mills *et al.* 2013).

There is a significant morphology shift seen in osteoblast precursors as they are seen to transition from spindle-like cells to a large cuboidal shape when they are fully differentiated into mature osteoblasts. Functioning and mature osteoblasts are also seen to be surrounded by alkaline phosphatase (ALP) positive osteoprogenitor cells in bone remodelling nodules. After decades of research, it has now been established that there are three major stages of osteoblast differentiation and mineralisation which are summarised in the Figure 1.8 (Stein *et al.*, 1990).

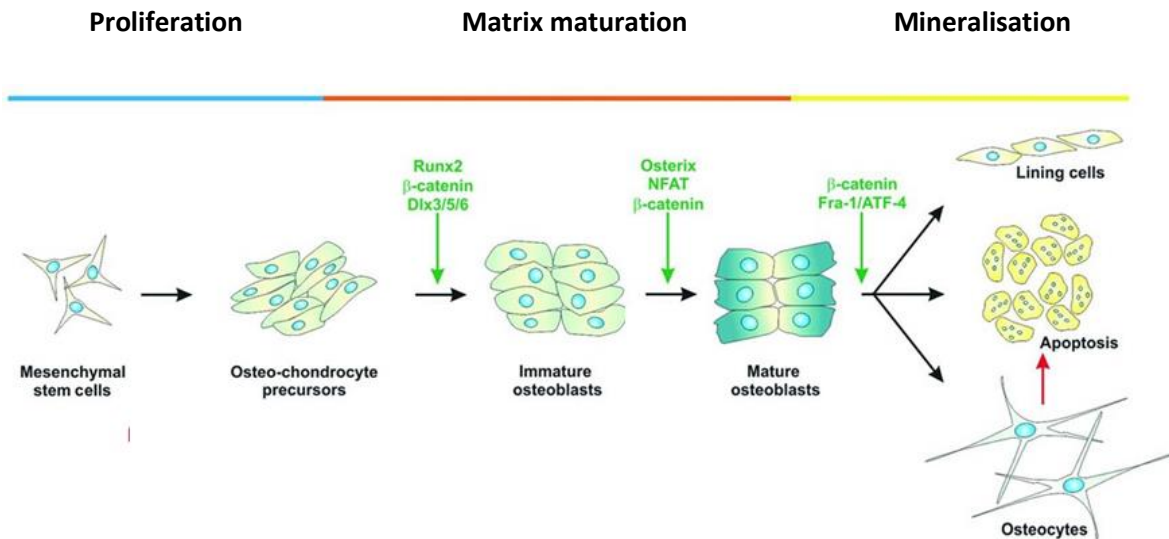


Figure 1.8: The three main stages of osteoblast differentiation. 1- Proliferation, where cells are rapidly dividing and starting to secrete ECM proteins such as fibronectin and type I collagen. 2- Matrix maturation, here there is an increased release of ALP and secretion of bone matrix proteins (BMPs) like osteopontin and osteonectin. 3- Mineralisation, secretion of osteocalcin, deposition of Ca^{2+} into bone matrix and decline in ALP activity.

Osteoclasts are generally believed to be derived from mononuclear precursor cells of monocyte-macrophage lineage in bone marrow (Nijweide *et al.*, 1986). Regarding osteoclast formation, there are two key cytokines; receptor activator of nuclear factor κB ligand (RANKL) and macrophage colony-stimulating factor (M-CSF). Both stromal cells and osteoblasts are needed in osteoclastogenesis. This process is regulated by soluble and membrane bound RANKL and M-CSF that are regulated by the stromal cells and osteoblasts (Teitelbaum and Ross, 2003). On osteoclast precursor cells, RANKL signals through receptor activator of nuclear factor κB (RANK) to mediate osteoclast differentiation, activation and survival during normal bone modelling and remodelling processes. However, osteoprotegerin (OPG) can bind to RANKL and prevent RANK binding to it (Boyce and Xing, 2007). M-CSF, on the other hand, promotes survival, proliferation and differentiation of osteoclast precursors and regulates the cytoskeleton of cells. Osteoclasts are known to be responsible for resorbing bone mineral into the blood stream during bone remodelling. Cell integrins are crucial for the interaction between osteoclasts and bone matrix and bone matrix peptides. One of the key integrins is $\beta 1$, which is

anchored and expressed in osteoclasts, which binds to collagen, fibronectin and laminin (Pawelec *et al.*, 2016).

1.6.4 Bone development

The first stage in the development of mesenchymal tissues is called condensation, here previously dispersed populations of MSCs gather together and differentiate into a single type of tissue such as cartilage, bone, tendon, muscle, etc. There are two mechanisms that are involved in skeletal development: endochondral ossification and intramembranous development which occur after MSC condensation. The majority of the skeleton, including all long bones, are formed through endochondral ossification, whereas the development of the skull and mandible would be formed through intramembranous ossification (Scotti *et al.*, 2013, Opperman, 2000).

Endochondral ossification starts with precursor cells differentiating into pre-chondrocytes and forming the cartilage scaffold. Following this, the chondrocytes are then replaced with mineralised bone matrix. This primary ossification occurs at the centre of the long bone, where the chondrocytes have stopped proliferating and have become hypertrophic. They will also mineralise the matrix and secrete vascular endothelial growth factor (VEGF) to promote vascular invasion and attract chondroclasts. Hypertrophic chondrocytes cause adjacent perichondral cells to differentiate into osteoblasts, which in turn secrete collagen type 1-rich matrix that results in the formation of the bone collar. The hypertrophic chondrocytes then undergo apoptosis leaving behind the cartilage matrix behind as a scaffold for osteoblast mineralisation (Majidinia *et al.*, 2018). Growth plates are zones of proliferating chondrocytes, which lengthen the long bones that are in between primary and secondary ossification centres (Kronenberg, 2003).

As stated above, flat bone growth and bone widening of long bones occurs through intramembranous ossification. In this process, MSCs are directly differentiated into pre-

osteoblasts and then osteoblasts. However, this is not a process that is well characterised at time of writing.

1.6.5 Healing from bone fracture

Today, bone fracture repair is considered to be a regenerative process. Fracture healing is a fascinating process whereby the formation of new bone tissue is indiscernible from uninjured bone (Fazzalari, 2011). This feature of bone regeneration is very different from soft tissues, whereby a fibrous scar is produced at the site of injury. Bone repair after a fracture is made up of two mechanisms: direct remodelling with minimal callus formation and indirect remodelling with callus formation through a combination of both intra-membranous and endochondral ossification, the latter is more prominent in fracture healing. In general, the process consists of three overlapping phases: inflammation, renewal and remodelling (Wang *et al.*, 2013).

After a bone becomes fractured, just like in other tissue injuries, there is an inflammatory response that peaks after 24 hours after initiation (Marsell and Einhorn, 2011). During this phase, there is an intricate network of pro-inflammatory signals and growth factors at play. This results in the expression of several inflammatory molecules, including tumour necrosis factor α (TNF α) and interleukins (IL-1, IL-6, IL-11, IL-8) (Fazzalari, 2011, Rundle *et al.*, 2006). After this, polymorphonuclear neutrophils (PMNs) and macrophages are recruited so that the fracture derived-microdebris and micro-organisms can be endocytosed (Schett, 2011). Soon after this, platelets are induced as a consequence of injury to blood vessels, which produce platelet-derived growth factor (PDGF), transforming growth factor- β 1 (TGF- β 1), tumour derived growth factor- β (TGF- β), insulin-like growth factors (IGFs) and fibroblast growth factor-2 (FGF-2). These are all released by macrophages in order to form the initial hematoma (Cho *et al.*, 2002, Lieberman *et al.*, 2002). In addition, at the fracture site, BMPs will also be expressed by osteoprogenitor cells. All these factors culminate in the recruitment of MSCs.

In the renewal phase, the recruited MSCs present at the fracture site proliferate and differentiate into osteoblasts to form bone through intramembranous ossification, around 7-10 days after the fracture. Following on from this is the start of chondrogenesis in the injured tissue (Cho *et al.*, 2002). It is important to note that, at this point there is an absence of inflammatory mediators. BMPs and TGF- β 2 signalling induces endochondral bone formation in the cartilaginous callus (Cho *et al.*, 2002, Gerstenfeld *et al.*, 2003). At the end of this phase the cartilage that has been formed calcifies and is then replaced with woven bone (Fayaz *et al.*, 2011). When the remodelling phase commences osteoprogenitor cells then differentiate into osteoblasts and osteoclasts. Both osteoblasts and osteoclasts mediate the replacement of the woven bone with lamellar bone through their reforming and resorbing actions (Mountziaris and Mikos, 2008). Furthermore, it is thought that (human) growth hormone and parathyroid hormone also play a part of the remodelling phase and contribute to the healing speed and strengthens the fracture callus (Nakajima *et al.*, 2002). In addition to the signalling pathways that are involved in MSC differentiation, chondrocyte maturation, angiogenesis and ossification seem to all have similar events occurring during foetal skeletal development (Mountziaris and Mikos, 2008). Nevertheless, the absence of inflammatory response in embryonic development (as well as the involvement of embryonic stem cells) is the key difference between fracture healing and foetal skeletogenesis (Hall and Miyake, 2000).

1.6.6 Biomaterials and current options for clinical regeneration

When certain pathological fractures or when large bone defects occur and bone repair fails, clinical intervention is required (Dimitriou *et al.*, 2011). Furthermore, the capacity of bone to repair itself can also be diminished by numerous conditions such as bone infection, infection in the periphery tissues, insufficient blood supply and systemic diseases (Dimitriou *et al.*, 2011). This is where bone grafts are utilised. In general bone grafts are an implanted material which induces bone repair through osteogenesis, osteoconduction and osteoinduction either

in combination with other materials or alone (Bauer and Muschler, 2000). The decision of which appropriate type of bone graft to use depends on graft size, tissue viability, defect size, shape and volume to name a few (Sheikh *et al.*, 2015). There are four main categories that materials used in bone grafts can be separated into to repair bone defects: autografts, allografts, xenografts and bone graft substitute (Sheikh *et al.*, 2015). In order for a bone graft material to be successful in regenerating bone there are four major characteristics that they have to demonstrate

- Osteogenesis: The capacity to generate bone tissue via the differentiation of osteoblasts from osteoprogenitors (Greenwald *et al.*, 2001)
- Osteoinductivity: The capacity for the bone graft materials to be able to promote the production of bone-forming cells.
- Osteoconductivity: Where the graft material is able to be reabsorbed into the body after serving as a scaffold for new bone growth.
- Osseointegration: The capacity for the graft materials to bind with periphery bone tissues without generating any intervening layer of fibrous tissue.

These are the qualities that are necessary for an ideal bone graft material in successful bone regeneration.

Autografting (autologous or autogenous) are the current gold standard of bone grafting material and is defined as transplantation of a cancellous or cortical bone tissue from one part of the body to another within the same individual (Zimmermann and Moghaddam, 2011). Autografts are comprised of surviving cells which include osteoinductive factors such as BMP-2, BMP-7, FGF, IGF and PDGF (Bauer and Muschler, 2000). They will also lack immunogenicity as well as retain immediate viability after transplantation (Janicki and Schmidmaier, 2011). All of these factors are what make autografts the best bone grafting material available. However, due to the additional surgery that is required for the harvesting of grafts from another site on the body, there is an increased risk of donor pain, infection, complications and morbidity. In addition, there is only a finite amount of autograft material

available from the donor. These limitations may be overcome by introducing other graft materials (Janicki and Schmidmaier, 2011).

A common substitute for autografts are allografts, which are obtained from one individual and implanted into another individual of the same species (Ehrler and Vaccaro, 2000). Either cortical, cancellous or even a combination of both materials can be used as either intact or divided forms (Parikh, 2002). Allografts can be harvested from either living donors or cadavers, as it is possible for the latter to retain their cellular and organic content (Zimmermann and Moghaddam, 2011). The disadvantages mentioned above for autografts do not apply to allografts. In fact, unlike autografts, there is a broad range of shapes and sizes of allograft materials and a higher availability of them too. However, allografts are not perfect, as there can be a lack of viable cells and thus a lower osteogenic potential. Moreover there is a risk of transmitting bacterial infections and viral diseases. These can include but are not limited to HIV, hepatitis B and C. It has been found that, due to the low osteogenic potential, there is a lower rate of healing and that the grafts can also trigger immunological reactions in the host body (Gomes *et al.*, 2008, Oryan *et al.*, 2012, Parikh, 2002).

The third option for graft materials are xenografts, also known as xenogenic or heterologous grafts. Heterologous grafts come from a different species to humans and are commonly sourced from porcine and bovine species (Oryan *et al.*, 2012; Develioglu *et al.*, 2009). The biggest advantage to these heterologous grafts is that they can be considered an unlimited supply. On the other hand, the major downsides are the possibility that zoonotic diseases can be transmitted to the host and there is also a risk of prion infections. In addition, there is also a lack of osteogenic characteristics which results in a poor clinical outcome (Oryan *et al.*, 2012).

The final option is to use bone graft substitutes when managing bone defects. These substitutes are usually formed of natural tissue scaffolds such as collagen, alginate, elastin, chitosan and cellulose. Synthetic materials such as mono, bi- and tricalcium phosphate including hydroxyapatite (HA), bi-tricalcium phosphate (b-TCP) and calcium-phosphate cements as well as glass ceramics (Finkemeier, 2002, Dimitriou *et al.*, 2005). These materials

are advantageous since they are able to trigger proliferation, migration and differentiation of bone cells that are crucial for bone regeneration.

However, more research into the mechanisms behind these advantages are still being researched and more synthetic materials are being researched every year.

1.7 45S5 bioglass

In 1971, Hench *et al.* began investigating silicate bioglass glasses as 3-D bone tissue scaffolds. Since then the field has been growing and today has expanded into tissue engineering and cellular biology (Baino and Vitale-Brovarone, 2011). Bioglasses are inorganic materials are able to react to physiological tissues and form bonds to bone through the formation of bone-like hydroxyapatite layers. This leads to effective biological interaction and fixation of bone tissue with the material surface (Hench, 1998). Looking specifically at 45S5 bioglass, the reactions on the material surface include the release and exchange of critical concentrations of Si, Ca, P and Na ions. This in turn encourages favourable intracellular and extracellular responses that promote rapid bone formation (Gerhardt and Boccaccini, 2010). These biogl can not only act as scaffolds but also serve as carriers for the delivery of metal ions to mediate cellular functions.

When Hench *et al.* found that certain silicate-based glass compositions could be bonded chemically to rat bone, they termed these glasses as “bioactive”. Bioglasses were classified as materials that elicited a specific biological response at the surface of the material which resulted in the formation of a bond between the tissues and the materials (Hench *et al.*, 1972). One of the oldest compositions of bioglass is the famous 45S5 Bioglass which has multiple successful clinical applications in tissue engineering. The meaning behind the name is that the composition is 45% wt SiO₂, incorporating 25% wt Na₂O, 25% wt CaO, 5% wt P₂O₅. The 5 in 45S5 represents the 5:1 ratio of CaO to P₂O₅ and this high ratio, coupled with the high

amounts of Na_2O , is why the glass surface is highly reactive in physiological environments (Hench, 1993).

After much research, it is now widely believed and accepted that to create a bond with bone a biologically active apatite surface layer must form at the biomaterial-bone interface (Hench, 2006). Therefore, the fundamental necessity of bone bonding property of bioglasses is the chemical reactivity in physiological body fluids resulting in the formation of hydroxycarbonate apatite (HCA) layer to which bone can bond and collagen fibres (CF). It was further found that the products that reacted with the bioglass upregulate the genes that control osteogenesis (Xynos *et al.*, 2000, Xynos *et al.*, 2001). Briefly, ion leaching/exchange and dissolution of the bioglass network and precipitation/growth of the calcium-deficient HCA layer, encourages the colonisation, proliferation and differentiation of osteoblasts (Hench, 1993). Figure 1.9 displays SEM images of HCA binding to collagen fibrils.

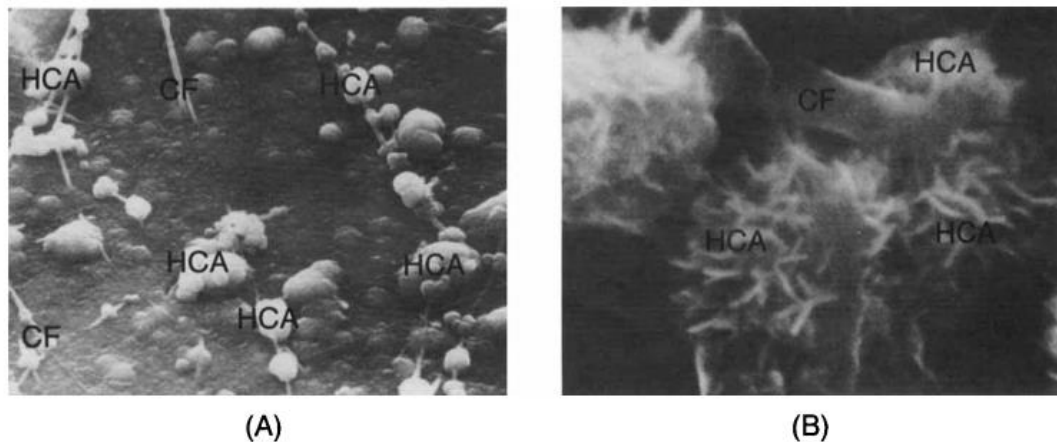


Figure 1.9: **SEM images of the HCA layer bonding to bone.** (A) SEM micrograph of collagen fibrils incorporated within the HCA layer growing on a 4585 Bioglass substrate in vitro (B) Close-up (11300x) of the HCA crystals bonding to a collagen fibril. Adapted from Hench *et al.* 1993.

In parallel to the chemical reactions on the material surface, recent studies have shown that ion dissolution and release from bioglass activate gene expression in osteogenitor cells that give rise to enhanced bone regeneration (Xynos *et al.*, 2000).

This study aims to investigate the differences in the physical characteristics of collagen scaffolds, which have been crosslinked using transglutaminases with and without bioglass particles. Alongside this characterisation of physical characteristics, the validation of inhibitors on TG2 and mTG will be assessed. And the determination of the amount of crosslink per mole of collagen in crosslinked collagen scaffolds will also be determined. Following this, the differences in integrin expression (if any) of human osteoblasts seeded on native, crosslinked collagen and scaffolds with bioglass will be investigated. In addition to this the rates of mineralisation between the scaffolds will also be assessed using von Kossa staining. The main objectives of the thesis are listed below:

1. The micro and macro structural differences between native, crosslinked collagen and collagen scaffolds with 45S5 bioglass using sedimentation assays as well as SEM.
2. The mineralisation rates of HOBs on the various collagen scaffolds
3. Plausible mechanism/pathway that explain the observed rates of mineralisation.

Chapter 2: Materials and Methods

2.1 Materials

2.1.1 General chemicals

All water used was deionised using Purelab Option-S 7/15 system purchased from ELGA. Sterilisation of disposable pipette tips, chemical and stock solutions was autoclaved at 121°C for 1 hour or by filtration through a 0.45µm Millex syringe filter purchased from Merck Millipore, Watford, UK. All general chemicals were purchased from Sigma-Aldrich, Poole, UK unless otherwise stated.

Recombinant human tissue transglutaminase 2 (rhTG2) and mTG were purchased from Zedira GmbH, Germany with the activity between 14-17U/mg as stated in certificate of analysis. Biotin-Cadaverine was purchased from Zedira GmbH, Germany. Silver (I) nitrate was purchased from Fisher Scientific UK Ltd, Leicestershire UK. Collagenase from *Clostridium histolyticum*, subtilisin, pronase, leucine aminopeptidase (LAP), prolidase and carboxypeptidase Y were all purchased from Sigma-Aldrich, Poole, UK. Inhibitors 1-155 and R281 were kindly provided by Dr Vivian Wang. 45S5 bioglass particles (between 40-60 µm) with the composition of: 5 wt% SiO₂, 24.5 wt% CaO, 24.5 wt% Na₂O, and 6.0 wt% P₂O₅) and cobalt bioglass (53 wt% SiO₂, 6 wt % Na₂O, 12 wt % K₂O, 5 wt % MgO, 20 wt % CaO, and 4 wt % P₂O₅) were both kindly provided by Dr Richard Martin.

2.1.2 Cell culture

Dulbecco's Modified Eagle Medium (DMEM) with glucose (4.5 g/l), L-glutamine (200mM), non-essential amino acid (NEAA) concentrate (100x) and penicillin/streptomycin (100x) solution were all purchased from Corning, U.K. Fetal bovine serum (FBS) was purchased from Labtech Sussex, UK.

2.1.3 Immunochemicals

All monoclonal and polyclonal mouse α 1, α 2, α 5, α V, β 1, β 3 and rabbit LRP5 and β -catenin antibodies as well as secondary anti mouse and anti rabbit antibodies were purchased from Santa Cruz, California USA.

2.1.4 Western blot chemicals

Tris-glycine-SDS buffer (10X) and 30% (w/v) solution containing methylene bis acrylamide (in a 29:1 mix) were purchased from Melford Biolaboratories Ltd, Suffolk, UK. Pure nitrocellulose blotting membranes were purchased from Pall Corporation, UK. Blotting pads were purchased from VWR, UK. Enhanced chemiluminescence ECL reagents were purchased from Cynagen Bologna, Italy.

2.1.5 Mineralisation and collagen staining kits

Silver Quest staining kit was purchased from Invitrogen Ltd, Paisley UK. Silver nitrate and sodium thiosulfate were both purchased from Sigma Aldrich Poole, UK.

2.1.6 Sub cellular fractionation

A subcellular Protein Fractionation Kit was purchased from Thermo Scientific Massachusetts, USA.

2.2 Methods

2.2.1 Cell culture

Human osteoblasts (HOBs, passage 18) which were spontaneously immortalized were kindly gifted from Prof Sandra Downes and Dr S Anderson, University of Nottingham).

HOBs were cultured in Dulbecco's Modified Eagle medium with L-glutamine (DMEM) containing 10% (v/v) heat-inactivated foetal bovine serum (FBS), 1% NEAA (v/v) and 1% penicillin/streptomycin (v/v), hereafter described as complete medium (CM). All flasks were kept in a humidified incubator at 37°C the CO₂ concentration was set at 5% (v/v).

2.2.2 Passaging cells

Passaging of cells took place regularly in order to ensure that HOBs were healthy and were not allowed to reach over 90% confluence. After the removal of all medium, the monolayers in flasks were washed once with PBS (pH 7.4) to remove any residual complete medium. Following this, the cells were treated with 0.25% trypsin in 2mM EDTA solution for 5 minutes. Once cells had been observed to have detached from the flask (using a light microscope) double the volume of complete medium (to that of trypsin) was added to inactivate trypsin. The suspension was then centrifuged at 300g for 5 minutes, from which a cell pellet was formed. This pellet was either re-suspended in serum free medium (DMEM) for use in investigations or seeded into the appropriate cell culture flask or vessel and then kept in a humidified incubator at 37°C in 5% CO₂ (v/v).

2.2.3 Cryopreservation

Healthy cell cultures were grown to approximately 90% confluence before trypsinisation. After centrifugation the cell pellet was then suspended in 1ml of "freezing mixture" consisting of 10% (v/v) DMSO in FBS. This solution was aliquoted into cryogenic tubes before being stored in a -20°C freezer for 1 hour, after which time it was stored in a -80°C freezer. Following this the cryogenic tubes were then transferred in vapour phase liquid nitrogen freezer tanks for long term storage.

2.2.4 Retrieving cells from storage

Cells were kept at room temperature (19°C) until completely thawed and were then transferred to a sterile centrifuge tube. Complete medium was then added drop-wise whilst mixing the solution regularly to allow for slow dilution. The suspension was then centrifuged (300g for 5 minutes) to remove the freezing mixture. Using the appropriate growth medium, cells were then re-suspended and transferred into the appropriate tissue culture flask and incubated in a humidified-atmosphere incubator at 37°C (with 5% CO₂ v/v). The respective medium was then changed no more than 8 hours thereafter to remove the remaining DMSO.

2.2.5 Differentiation of HOBs

Cells (passage 20-25) were seeded into either 96-well plates (100 µl) or in 35mm tissue culture plates at a density of 8x10⁴/cm² in 2 ml complete medium (10% FBS in DMEM) for 16 hours. Following this the differentiation treatment began by replacing the complete medium with 50µg/ml ascorbic acid and 10 mM β-glycerophosphate in complete medium. This is differentiation medium (henceforth referred to as DM). Differentiation medium was replaced every 48 hours for 10 days to carry out both mineralisation assays.

2.3 Protein expression assays

2.3.1 Protein concentration

Lowry protein assay was performed (using the Bio-Rad RC kit purchased from Life Sciences, Hemel Hempstead UK). As per the manufacturer's instructions, a set of bovine serum albumin (BSA) standards ranging from 0.2-1 mg/ml were created and 5 µl of these samples were added in triplicate to a 96-well plate. 25 µl of "reagent A" and 200 µl of "reagent B" were then added to the BSA standards. The plate was incubated at room temperature (19°C) for 15 minutes to allow full colour development, the plate was then read at 750nm using

a Spectrafluor plate reader. The concentrations of the proteins in cell lysates were determined against the linear standard curve produced by the BSA protein standards.

2.3.2 Lysing and collecting whole cell lysates

HOBs were seeded in either 35mm (2 ml complete medium) or 60mm petri dishes (4 ml complete medium) at a density of $8 \times 10^4/\text{cm}^2$. Once the cell media had been discarded, the cells were then removed using lysis buffer (0.025M Tris, 0.15M NaCl, 0.001M EDTA, 1% Nonidet P-40 (NP-40), 5% glycerol; pH 7.4) that was supplemented with 0.2mM PMSF and 1% protease inhibitor cocktail (P8340) (purchased from Sigma-Aldrich Dorset, UK). After 5 minutes of incubation at room temperature (19°C) the cell lysates were transferred to Eppendorf tubes and centrifuged at 13,000g for 5 minutes at 4°C to pellet the cell debris.

For the removal of cells bound to the collagen matrix, 75 μl of cell lysis buffer of the following composition was added to each 35mm plate: 1% (v/v) NP-40, 0.5% (w/v) sodium deoxycholate, 0.1% (w/v) SDS, 1mM sodium fluoride, 1mM sodium orthovanadate, 2mM in EDTA in Tris-HCl (pH 7.4) with freshly added 0.1mM of PMSF and 1% (v/v) protease inhibitor complex (PIC).

To lyse cells, the culture medium was removed from the HOBs seeded on collagen matrices before being washed with PBS (pH 7.4). 70 μl of the cell lysis buffer outlined above was then added to the plates for approximately 5 minutes before collection and then left on ice for 30 minutes. The protein concentration was measured using a DC Protein Assay kit (Bio-Rad, UK) (see 2.3.1). The samples were solubilised in 2x Laemmli buffer (60 mM Tris-Cl pH 6.8, 2% SDS, 10% glycerol, 5% β -mercaptoethanol, 0.01% bromophenol blue) then boiled for 5 minutes before being loaded onto a gel or frozen at -80°C for storage.

2.3.3 Transglutaminase activity assay

5 µg/ml microbial transglutaminase (Zedira, Germany) was dissolved in 50 mM Tris-HCl (pH 7.4) buffer before immediate use. The synthetic CBZ-glutaminyl-glycine peptidic analogue R281 was used as an irreversible site-directed microbial transglutaminase inhibitor at a concentration of 250 µM. To inhibit the enzyme, R281 was incubated with mTG for an hour at room temperature (19°C).

5 µg/ml recombinant human TG2 (Zedira, Germany) was solubilised in 50 mM Tris-HCl (pH 7.4) before being used. 1-155 is a cell permeable irreversible inhibitor of TG2 that targets the active site cysteine.

The activity assay was based on a modified technique first used by Slaughter *et al.* (Slaughter *et al.*, 1992). First 96-well plates were coated overnight with 50 µl N,N'-dimethylcasein purchased from Sigma-Aldrich Poole, UK (10 mg/ml) per well at 4°C overnight or 37°C for 1 hour. The plate was washed three times with 50 mM Tris-HCl, pH 7.4 and then blocked with 3% BSA in PBS pH 7.4 (heat inactivated at 78°C), at room temperature (19°C) for 30 minutes. The reaction was started by the addition of 100 µl of solution containing mTG/TG2, 100 µM biotin-cadaverine, 10 mM DTT in Tris-HCl for 1 hour. This is also supplemented with 500 µM R281/ 25 µM 1-155 inhibitor for the negative control. After this incubation the samples were washed three times with TBS-Tween 20 then blocked with BSA blocking buffer at 37°C for 30 minutes in a humidified incubator. Blocking buffer was made up of 3% BSA in Tris-HCl (w/v) pH 7.4 which was heat inactivated (78°C for 3 minutes). Afterwards 100 µl of ExtrAvidin® peroxidase conjugate [diluted 1:1000 in blocking buffer (3% w/v BSA in Tris-HCl pH 7.4)] was added to the samples for 1 hour. After a further three washes with TBS-Tween 20, the reaction was developed using 100 µl per well SIGMAFAST o-phenylenediamine dihydrochloride (OPD) tablets (Sigma-Aldrich, UK) dissolved in 20 ml dH₂O, with a final concentration of 0.4mg/ml. The colour development was terminated by addition of 50 µl of 3M HCl and the absorbance was read at 490 nm using a plate reader.

2.4 Collagen purification and assays

2.4.1 Isolation and purification

Type I collagen was sourced in house by dissecting tendons from rat tails and dissolving them in 0.02M acetic acid, which was then left to stir constantly at 4°C overnight. The solution was centrifuged at 4000g for 3 hours at 4°C to remove insoluble non-collagenous material before the pH of the solution was neutralised to pH 7 by adding 1M NaOH to the solution with gentle stirring. This adjusted solution was stirred for 2 hours at 4°C which allowed for the collagen to precipitate. The final step was to centrifuge the suspension at 4000g for 40 minutes at 4°C. The resulting collagen samples were solubilised in 0.2M acetic acid and the suspension was stirred at 4°C overnight.

2.4.2 Collagen concentration assay

Sircol™ soluble collagen assay (purchased from Biocolor life science assays) was used to calculate the concentration of collagen from the neutralised collagen solution. Following the instructions, a reagent blank was first made up using 0.2M acetic acid. Aliquots of 5, 10 and 15 µg were created for the collagen reference standard curve also made up in 0.2M acetic acid. 1:10, 1:50, 1:100 and 1:1000 dilutions of purified collagen were then made up to individual 100 µl samples to be tested. To each sample 1 ml of Sircol dye reagent was added to fully saturate the collagen within the 100 µl samples (including reagent blanks and standards).

Samples were incubated on a vertical shaker platform for 30 minutes so that a collagen-dye complex could form and precipitate. Samples were then spun in a micro centrifuge at 12,000 rpm for 10 minutes. Supernatants were then removed by inverting the sample tubes. Following this 750 µl of ice-cold acid-salt wash reagent was gently layered onto the collagen-dye pellet in order to remove unbound excess dye. The samples were once again centrifuged at 12,000 rpm for 10 minutes before the acid-salt wash was removed. To release the collagen bound dye, 250µl alkali reagent was added to all samples and vortexed to dissolve all the

bound dye. The colour of the sample is light stable and following the manufacturer's instructions all samples were read within 2 to 3 hours. Measurement of absorbance was carried out by transferring 200 µl of each sample to individual wells of a 96-well plate. A SpectraFluor plate reader was used to measure absorbances from all the samples at 550 nm. From the 3 collagen concentration standards, a standard curve was obtained for collagen samples to be measured against.

2.4.3 Modification of collagen by transglutaminase

Neutralised collagen was treated with mTG, TG2, 40-60 µm 45S5 bioglass (10 mg/ml) in various combinations for the investigations. For collagen scaffolds that contained TG2, 5mM DTT and 10mM CaCl₂ in 10 mM Tris buffer (pH 7.4) were directly added to the neutralised collagen along with 10X PBS and dH₂O in order to make up a final of volume 2 ml (in a 35 mm plate). Stock solutions of 1 mg/ml TG2, 13.1 mg/ml mTG, 1M DTT and 1M CaCl₂ were used to minimise total volume changes. Both mTG and TG2 were always added to the collagen mixture last before being placed in a humidified-atmosphere incubator at 37°C and 5% CO₂ overnight.

2.4.4 Coomassie blue staining of collagen

Native and cross-linked collagen scaffolds were crosslinked overnight on non-treated 35mm petri dishes before 3x10⁵ HOBs were seeded onto them in complete medium. Following the necessary incubation period (humidified incubator at 37°C and 5% CO₂) the media was discarded and washed once with PBS. Afterwards the collagen scaffolds were stained with 0.1% Coomassie blue stain solution (G-250) (50% (v/v) methanol; 10% acetic acid; 40% (v/v) dH₂O). Samples were gently shaken for 5 minutes at room temperature (19°C) before the Coomassie blue stain was discarded and the scaffolds were washed three times with distilled water.

2.4.5 Coomassie blue degradation assay

Native and cross-linked collagen samples were allowed to polymerise/crosslink overnight on non-treated 35mm plates before HOBs were seeded in complete medium. Plates were stored in a humidified incubator at 37°C at 5% CO₂ for 3 days. 2 ml complete medium replaced every 24 hours to ensure the survival of HOBs. After 3 days the media from each plate was discarded and sodium-deoxycholate (0.5%) (w/v) in 10mM Tris-HCl pH 7.4 was added to the plates to remove the cells from the collagen matrix. After two washes with distilled water, the samples were stained with 0.1% (w/v) Coomassie blue stain solution (50% (v/v) methanol; 10% (v/v) acetic acid; 40% (v/v) dH₂O). The samples were left for 5 minutes on shaker before a final rinse with distilled water.

To analyse the stained collagen samples, a GeneBox was used to capture images with the UV light setting activated. Processing of images took place using imageJ (Schneider *et al.* 2012) by converting the images to 8-bit and carrying out densitometry analyses to generate the mean pixel densitometry count.

2.4.6 Collagen sedimentation

To study the effects of crosslinking collagen, changes in deamidation and addition of bioglass nanoparticles on a macromolecular level, scaffolds were centrifuged as follows: Collagen scaffold solutions (10X PBS, distilled water, collagen, Transglutaminase and/or 45S5 bioglass between 2- 4 ml) were crosslinked in 35mm petri dishes overnight before being transferred into 7ml clear screw cap tube (purchased from Falcon, USA). Samples were then centrifuged for 15 minutes at 2500rpm. Images were then captured on Nikon Coolpix 5400 camera.

2.5 Analysis of cell proteins

2.5.1 Sodium dodecyl sulphate polyacrylamide gel electrophoresis (SDS-PAGE)

The gels used consisted of two layers; a separating gel with a final acrylamide concentration of 5.5-10% (w/v) and a 4% (w/v) stacking gel. These were made from a 30% stock solution of acrylamide (w/v) and 0.8% (w/v) N-N'-methylene bisacrylamide. For the stacking gels, Tris-SDS (pH 6.8) was used (0.5M Tris HCl containing 0.4% SDS), whereas the separating gels consisted of a Tris-SDS solution where the pH was 8.8 (1.5M Tris HCl containing 4% SDS). 10% ammonium persulfate and TEMED were also added to the solutions last before being loaded onto the glass loading plate. Table 2.1 below describes the volumes used:

Table 2.1: The recipes for different concentrations of acrylamide in separating gels

Stock Solutions	Final acrylamide concentration in the separating gel (%) ml									
	5	6	7	7.5	8	9	10	12	13	15
30% acrylamide/ 0.8 bisacrylamide	2.5	3.00	3.50	3.75	4.00	4.50	5.00	6.00	6.50	7.50
4X Tri-HCl SDS (pH 8.8)	3.75	3.75	3.75	3.75	3.75	3.75	3.75	3.75	3.75	3.75
dH2O	8.75	8.25	7.75	7.50	7.25	6.75	6.25	5.25	4.75	3.75

10% ammonium persulphate	0.05	0.05	0.05	0.05	0.05	0.05	0.05	0.05	0.05	0.05
TEMED	0.01	0.01	0.01	0.01	0.01	0.01	0.01	0.01	0.01	0.01

To ensure that the gel's top surface was flat and even, 1ml of propan-2-ol was overlaid on top of the separating gel which was then allowed to crosslink for approximately 1 hour at room temperature (19°C). Following crosslinking the iso-propan-2-ol was removed and the surface of the separating gel washed with distilled water before the stacking gel was added. The stacking gel consisted of 325µl 30% (w/v) acrylamide and 0.8% (w/v) N-N'-biscacrylamide solution, 62.5µl of Tris-SDS pH 6.8 and 1.5ml of distilled water, 25µl 10% (w/v) ammonium persulphate and 5µl of TEMED. After mixing the stacking gel solution it was quickly added on top of the separating gel and the appropriate comb was inserted to form the sample wells. Approximately 45 minutes was required before the stacking gel had crosslinked at room temperature (19°C). To run the samples, the gel combs were removed and washed with "1X Running Buffer" which consisted of Tris-glycine (pH 8.5) 0.025M Tris and 0.1% (w/v) SDS. Sample volumes were normalised against protein concentration (between 50-60µg) and added to the same respective volume of 2X Laemmli loading buffer before being loaded onto the wells. 5µl of rainbow marker (New England Bio labs) was loaded into each gel also. Electrophoresis was carried out at 120V for approximately 75 minutes and terminated when the blue marker dye from the Laemmli buffer nearly reached the bottom of the gel.

2.5.2 Western blotting

First nitrocellulose transfer membranes, blotting pads and absorbent filter paper were first pre-soaked with transfer buffer (48.8mM Tris-HCl, 39mM glycine and 20% (v/v) methanol).

Transfer was carried out using a Biorad tank (purchased from Biorad Hertfordshire, UK) and power supply which was set to 300mA for 75 minutes in an ice box. After transfer, the nitrocellulose membrane was separated from the gel and rinsed gels with water before being incubated in blocking buffer (5% (w/v) dried milk powder in PBS pH 7.4) for one hour at room temperature (19°C). After this, the respective primary antibody (1:1000 dilution) in blocking buffer (outlined above) was added to the nitrocellulose paper and left overnight on a shaker platform at 4°C. Blots were washed with 0.5% (v/v) TBS-Tween, pH 7.4, four times. A species specific secondary HRP conjugated antibody in blocking buffer (1:1000 dilution) was then added to the blot for 2 hours at room temperature (19°C) on a shaker-platform. Subsequently, the blot was washed with 0.5% (v/v) TBS-Tween. Development was carried out using ECL chemiluminescence substrate which reacted to the HRP conjugate of the secondary antibody. Excess ECL was removed before the blot was covered in cling film and the light emission was detected using a SynGene GeneBox.

2.5.3 Membrane stripping

The membranes were then re-probed for β-actin as a loading control. To do this the nitrocellulose blots were washed in TBS Tween 20 and then incubated with stripping buffer (62.5 mM Tris-HCl (pH 6.7), 2% SDS (w/v) and 100 mM 2-mercaptoethanol) at 50°C for 30 minutes. The Western blot method outlined above (2.5.3) was then carried out after the membranes had been incubated for one hour in blocking buffer.

2.6 Determination of cell behaviour

2.6.1 Cell proliferation

The proliferation of 2×10^4 HOBs (either with or without treatment/ crosslinking enzyme) was measured in 96-well plates using XTT reagents which changes colour according to the redox state of the solution. These reagents were mixed prior to being added to the samples

which were then incubated at 37°C in 5% CO₂ for four hours. Following this, 100µl of the culture supernatant from each sample well was transferred to a new 96-well flat bottomed plate and the orange coloured solution was quantified using a plate reader where the absorbance was measured at 490 nm (and the reference wavelength at 750 nm).

2.6.2 Mineralisation of HOB cultures

2 x 10⁴ HOBs in 100 µl DM were cultured in 96-well plates. Either on tissue culture plastic, native collagen, mTG cross-linked, TG2-crosslinked and incubated at 37°C in 5% CO₂ for up to 10 days with regular change of medium every 48 hours. After 10 consecutive days post addition of differentiation medium (10% FBS, 50 µg/ml Ascorbic acid, 10 mM β-glycerophosphate in DMEM) the mineralised bone matrix was then visualised using von Kossa staining. Using this method silver ions replace calcium in the matrix to form a precipitation complex with phosphate groups. Samples were washed with distilled water, fixed in 3.7% paraformaldehyde for 30 minutes and then dehydrated in 70% ethanol for 1 hour. Following this the dehydrated samples were washed with distilled water before 2% silver nitrate (Sigma-Aldrich Poole, UK) was added to them. Samples were then exposed to UV light for 20 minutes, washed with distilled water five times and fixed with 5% sodium thiosulphate (Sigma-Aldrich Poole, UK) for 3 minutes. After a final wash with distilled water the samples were viewed at 10X and 40X magnification using a Nikon CK2 microscope. Images of non-overlapping fields were then photographed before they were converted into negative images. Using these negative images mineralisation areas were then quantified using Image J software (Schneider, *et al.* 2012).

2.7 Using SEM to analyse crosslinked surface topography

Following the overnight crosslinking of collagen scaffolds (method outlined above), complete medium was used to wash each scaffold and it was allowed to air dry. Following this,

the collagen samples were freeze dried for 24 hours. This involved cooling the samples to -20°C at a constant cooling rate of 1°C/min and holding samples at this temperature for 20 minutes to allow the scaffolds to freeze. The temperature was then increased to -10°C and held for 7 hours. The final step was to remove any water crystals by sublimation, the temperature was increased to 0°C for 17 hours at 200 mTorr. Once the collagen scaffolds were completely dried, the samples were then sputter-coated with gold and for SEM observation with the kind help of Prof M Salhawa.

2.8 Collagen staining assay

In order to detect and stain for collagen deposition in the ECM, a Silver Quest collagen staining kit (purchased from Invitrogen) was used. First, 3×10^5 HOB cells were seeded onto 35mm petri dishes for 10 days with differentiation medium (media changes every 48 hours). After 10 days the medium was discarded from each plate and cells were washed with PBS. Cells were then manually scraped with 500 µl PBS before 0.1 mg/ml pepsin (50mM acetic acid) was added to the samples. Samples were left in a shaking incubator at 37°C for 2 hours before the medium was collected in an Eppendorf tube. Neutralising solution (200 mM Tris and 150 mM NaCl in distilled water) was added to each sample and centrifuged at 12,000g for 10 minutes. After the supernatant was discarded, samples were denatured using 6X Laemmli buffer and boiled for 5 minutes. These samples were then analysed by SDS-PAGE using a 5% separating gel.

Following electrophoresis, the gel was removed from the cassette and rinsed briefly in distilled water. Each gel was then fixed using 100 ml of fixative solution (prepared according to the Silver Quest kit instructions) and incubated for an hour at room temperature (19°C) on a shaker overnight at 4°C. The fixative solution was discarded before being washed in 30% ethanol for 10 minutes. Following this wash, 100 ml of “sensitising solution” was added to the gel for 10 minutes (to allow protein bands to bind to silver ions). Once the sensitising solution

was decanted the gel was washed again using 30% ethanol followed by a 10 minute wash with distilled water. The gels were then stained using the kit's "staining solution" for 15 minutes. Once the gels had been sufficiently stained, the solution was decanted and washed with distilled water for 30 seconds. After this, the distilled water was discarded, 100 ml of developing solution was added to each gel for 8-10 minutes until the desired band intensity was achieved.

Once the bands became visible, 10 ml of "stopper solution" was immediately added to the gel which was still immersed in developing solution. Gels were gently agitated until a colour change from pink to colourless appeared. The inactivated developing solution was then decanted and washed with distilled water for a final time for 10 minutes.

Gels were then imaged using a Syngene GeneBox with the UV light setting activated, images that were captured were then analysed using ImageJ densitometry analysis software.

2.9 Sub cellular fractionation protocol

3×10^5 HOBs were seeded onto 35 mm petri dishes and grown using differentiation medium for 2, 3, 4, or 6 days with media changes every 24 hours. At the appropriate time point, media was discarded from the petri dish and cells were washed with PBS. Using 1 ml of ice cold PBS, cells were gently scraped off using a cell scraper. If HOBs were grown on collagen scaffolds then 0.125% collagenase (from type III from *Clostridium histolyticum*, purchased from Invitrogen Paisley, UK) was used to degrade collagen. Cells were centrifuged for 5 minutes at 300g and the pellet was discarded.

A whole lysate sample (of 20 μ l) of cell/PBS solution was aliquoted and added to an equal volume of cell lysis buffer and a protein concentration assay was carried out on the sample as outlined above. A protein concentration assay was also carried out on the remaining cell/PBS solution. Using the sub-cellular fractionation kit (Thermo Scientific Massachusetts,

USA) cytoplasmic extraction buffer (CEB) was then prepared using 0.1mM PMSF and 1% protease inhibitor cocktail according to the kit's instructions.

Cell/PBS solution was added to the CEB solution and mixed for 7 minutes at 4°C. Following this the samples were centrifuged at 500g for 3 minutes at 4°C. The supernatant was removed and stored on ice before each pellet was washed three times with ice cold PBS.

The pellets were then vortexed and suspended in ice cold "membrane extraction buffer" (MEB) which was prepared with 0.1mM PMSF and 1% PIC according to the kit's instructions. The samples were then gently mixed for 10 minutes at 4°C before the samples were centrifuged at 3000g for 5 minutes at 4°C. After this the supernatants were removed and stored on ice.

Pellets were washed three times with ice cold PBS before being re-suspended in "nuclear extraction buffer" (NEB) with 0.1 mM PMSF and 1% PIC as per the kit's instructions. The samples were then incubated with gentle shaking at 4°C for 30 minutes before being centrifuged at 5000g for 5 minutes. The final supernatant was then removed and stored on ice. The concentrations of the three sets of sub-cellular fractions: cytoplasmic, membrane-bound and nuclear were then measured using the Lowry method as described in section 2.3.1.

2.10 Amino acid analysis of crosslink proteolytic digestion for crosslink analysis

Collagen samples were crosslinked overnight in 35mm untreated petri dishes before being transferred to 2 ml screw cap Eppendorf tubes and boiled for 10 minutes. Afterwards the samples were cooled before 0.01 mg/ml collagenase sourced from *Clostridium histolyticum* in 0.1M ammonium hydrogen carbonate pH 8 for 24 hours at 37°C with gentle shaking. Following this, 3 consecutive additions of subtilisin (0.01 mg/ml in ammonium hydrogen carbonate) were added once every 24 hours. 0.015 mg/ml pronase (in ammonium hydrogen carbonate, pH 8)

was then added to the samples for 24 hours before being boiled for 15 minutes. Following this there were two consecutive leucine aminopeptidase and prolidase additions, every 24 hours. The final step was to add 0.01 mg/ml carboxy peptidase Y (in ammonium hydrogen carbonate) for 24 hours at 30°C with gentle shaking.

Samples (10-100 µl) were mixed with an equal volume of loading buffer (0.2M lithium citrate, 0.1% phenol pH 2.2) and loaded onto a Biochrom 30 amino acid analyser physiological system using lithium buffers (Biochrom, UK). Buffers 1-6 were obtained from Biochrom. A modified separation method was used (Table 2.2) and detection was by ninhydrin. Dipeptide was determined by addition of known amounts of ϵ (γ -glutamyl)lysine to the sample and comparing peak areas.

Table 2.2: A series of lithium buffers used during the amino acid separation phase

TIME (min)	BUFFER	COLUMN TEMPERATURE
0-9	1	25°C
9-32	2	25°C
32-67	3	25°C
67-107	3	25°C
107-123	6	75°C
123-135	1	75°C
135-147	1	65°C
147-159	1	35°C
159-171	1	25°C

2.10.1 Ammonia analysis

Using ammonium hydroxide standards, collagen samples were allowed to crosslink for 2 hours before being centrifuged for 15 minutes at 2500rpm. The collagen pellet was then discarded and the 50 µl of the supernatant was loaded at a concentration of 1:1 with loading

buffer and run on the Biochrom 30 amino acid analyser using the standard method. A set of ammonia standards were created from a stock solution of ammonia bicarbonate and used to quantify the amount of ammonia released.

2.11 Statistical analysis

For normally distributed multiple data comparisons, one-way and two-way ANOVA tests were used followed by Bonferroni post-hoc test. Results were expressed as mean \pm SD. Where the statistical significance between control and treated samples were evaluated at a 95% confidence level ($p<0.05$), the data set would be considered to be statistically significant and represented with a *, ** or *** above the bars. The calculations were performed using Graphpad Prism 5 statistical package (Graphpad Software, La Jolla California USA).

**Chapter 3: Characterisation of novel type I
collagen scaffolds generated using
transglutaminases**

3.1 Introduction

Due to the ubiquitous expression of TG2 throughout the body and its involvement in various tissue developmental and wound healing processes, it is possible that TG2 modified biomaterials could be beneficial for wound healing. Furthermore, the crosslinking effects of mTG, has still not been fully explored for its potential in enhancing bone tissue mineralisation.

Organic bone matrix is mostly comprised of type I collagen (~90%) and, as stated previously, is a well-known TG2 substrate in mineralised tissue. Regarding extracellular collagen, polymerisation could take place via intermolecular crosslinking (Chau *et al.*, 2005) or between non-collagenous bone matrix proteins and collagen (Mosher *et al.*, 1979). A well-organised fibrillar collagen network forms the foundation of mineralisation, and transglutaminases are suggested to play a role in fibre organisation through their crosslinking ability (Collighan and Griffin, 2009). Evidence has also shown that transglutaminases can promote collagen synthesis and assembly, which leads to the promotion of cell differentiation (Al-Jallad *et al.*, 2006). On the whole, TG2 promotes mineralisation in osteoblasts, promotes matrix protein secretion, deposition and maturation through crosslinking-mediated modification of the ECM, which further enhances cell attachment. By incorporating transglutaminases as well as 45S5 bioglass it may be possible to create a novel collagen scaffold that allows for an increased rate of bone regeneration. Along with 45S5 bioglass, bioglass incorporating cobalt ions was also tested. Cobalt ions are released in certain glass scaffolds in order cause a decrease in oxygen in the wound defective bone site. When hypoxia occurs, a cascade of processes is initiated that results in the production of new blood vessels (Jones, 2015).

The aim of this chapter was to evaluate whether any crosslink bonds could be detected in the “in house prepared type I collagen” and assess the micro and macromolecular differences of crosslinked collagen scaffolds. In addition to test whether the R281 and 1-155 inhibitors are effective at the inhibiting ability of transglutaminases to form crosslinks between collagen strands. This is so that the inhibitors can be used as controls to separate the effects

of transglutaminase protein from transglutaminase activity. Secondly, to observe the effects of crosslinking collagen with TG2 and mTG on a macro and micromolecular level using sedimentation (via centrifugation) and scanning electron microscopy. Finally to investigate how human osteoblast cells interact with the native, crosslinked and collagen scaffolds mixed with 45S5 bioglass.

3.2 Characterisation of transglutaminase inhibitors, type 1 collagen and optimisation of collagen crosslinking

3.2.1 Assessment of type I collagen purity

In order to test the purity of the collagen that is sourced and purified in house, SDS polyacrylamide gel electrophoresis (PAGE) was carried out (Figure 3.1). Using a 5% acrylamide gel (see Materials and Methods), the α_1 and α_2 chains (with N and C terminal sites cleaved) are present at the expected sizes of 130 and 115kDa. Type I collagen is a heterotrimer of two α_1 and one α_2 chain, where there is double the number of α_1 chains compared to α_2 chains which is why the band at 130kDa is double the size of the 115kDa band.

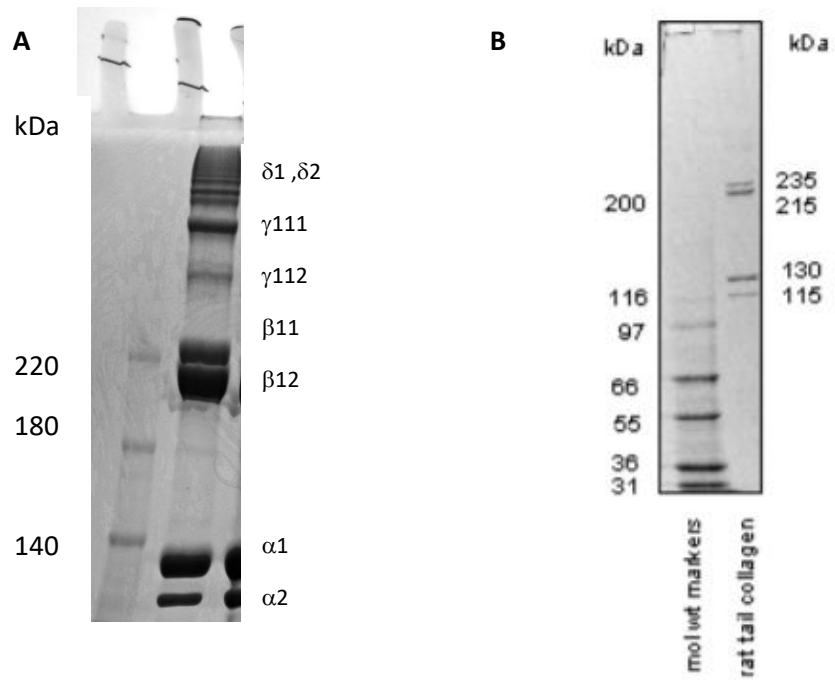


Figure 3.1: Coomassie blue stain for type 1 collagen following separation by SDS PAGE: **A)** Here the denatured α_1 and α_2 chains are visible close together. 0.19 mg of collagen was loaded onto the well before PAGE was carried out as stated in the Materials and Methods. **B)** Western blot for type I collagen that is purified and sold by Sigma Aldrich which has the same corresponding α bands.

3.2.2 Assessing the concentration of 1-155 required to inhibit TG2

1-155 is a cell permeable, irreversible inhibitor that is a substrate analogue that binds at the active site to selectively inhibit TG2 activity (Zonca *et al.*, 2017) and has been reported by Moro *et al.* to selectively inhibit TG2 activity. In Figure 3.2 it is been shown to inhibit almost all TG2 activity at a concentration of 25 μ M, which is similar to what has been reported in the literature (Zonca *et al.*, 2017).

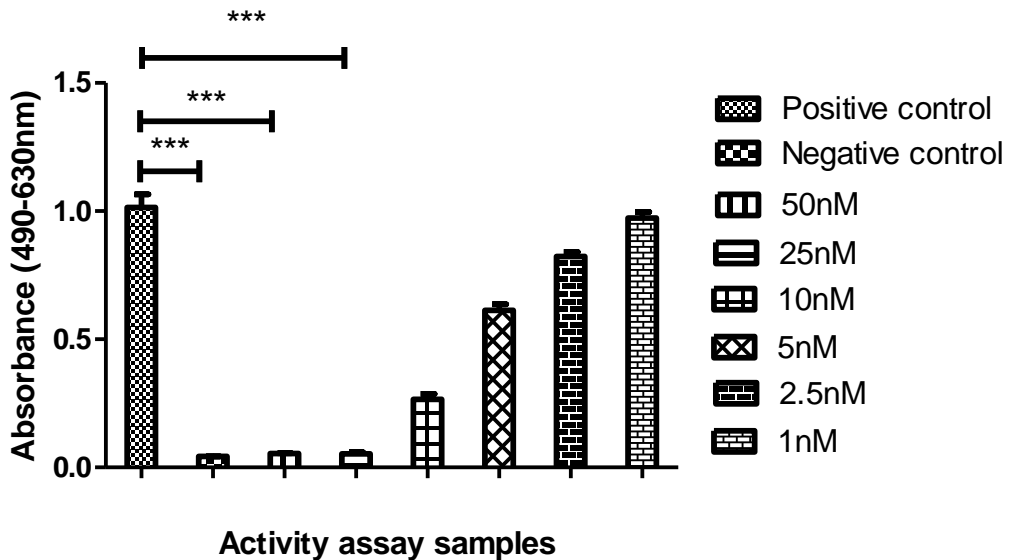


Figure 3.2: **TG2 inhibition activity assay.** TG2 activity with varying concentrations of 1-155 was measured through biotin cadaverine incorporation assay as described in the materials and methods chapter. 5 µg/ml TG2 treated without 1-155 was used as a positive control and a sample without any TG2 was used as a negative control. The data represents mean values +/- SD where n=3. Statistical analysis was carried out using a one way ANOVA test where the inhibition of TG2 samples was compared against a negative control. P-values corresponding to P< 0.001 are represented with a ***.

3.2.3 Assessing the concentration of R281 required to inhibit mTG

R281 is a non-cell-permeable inhibitor that has been reported by Zonca *et al.* to inhibit both TG2 and mTG. In Figure 3.3 it is shown that R281 can inhibit mTG activity when incubated with the enzyme between 250-500 µM.

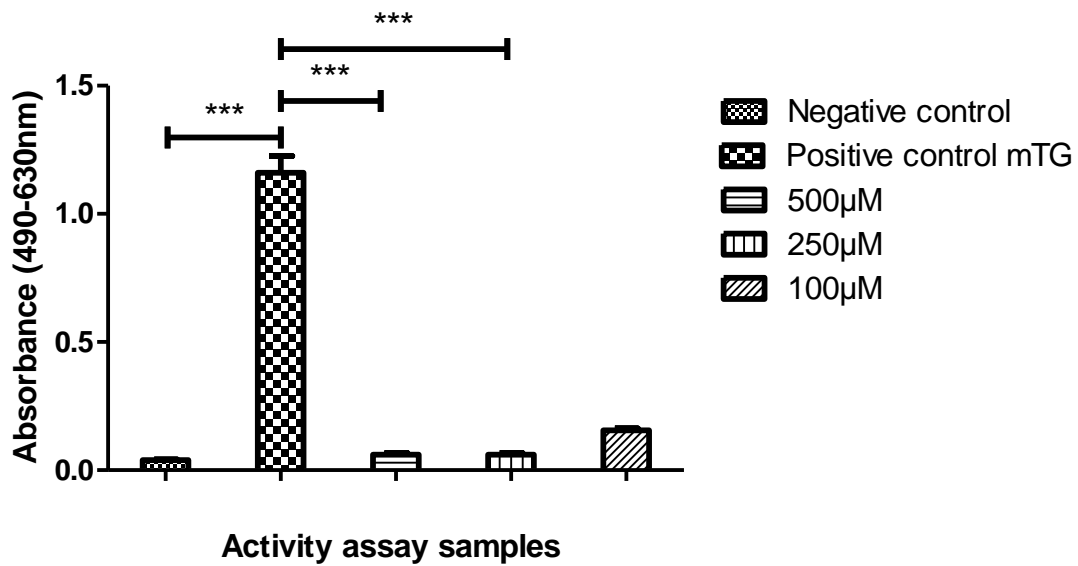


Figure 3.3: R281 inhibition activity assay. mTG activity with varying concentrations of R281 was measured through biotin cadaverine incorporation assay as described in the materials and methods chapter. 5 μ g/ml of mTG treated without R281 was used as a positive control and a sample without any mTG was used as a negative control. The data represents mean values +/- SD where n=3. Statistical analysis was carried out using a one way ANOVA test where the inhibition of mTG samples was compared against a negative control. P-values corresponding to P< 0.001 are represented with a ***.

3.2.4 Dependence of TG2 activity on reduction by DTT

For TG2 to actively form crosslinks, it must be activated by Ca^{2+} ions and be reduced by a reagent such as 1-4, dithiothreitol (DTT). However in high concentrations of DTT can be toxic to cells and therefore it should be used at low concentrations. As expected, the higher the concentration of DTT in a sample, the higher the observed absorption. Since high concentrations of DTT are toxic, 5mM DTT was chosen to reduce TG2 in collagen scaffolds.

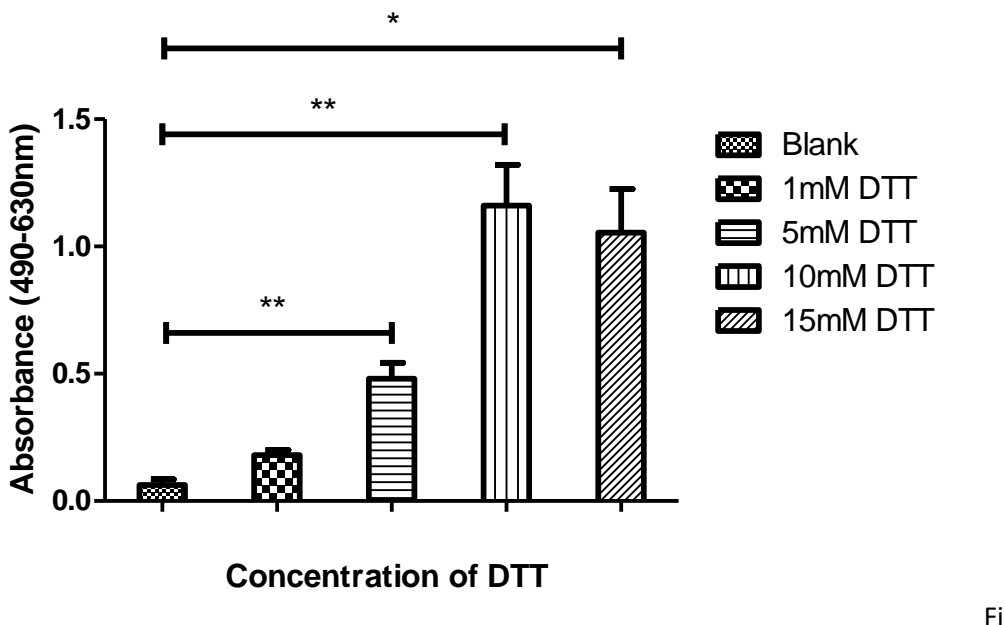


Figure 3.4: DTT activity assay. TG2 activity with varying concentrations of R281 was measured through biotin cadaverine incorporation assay as described in the materials and methods chapter. 5 μ g/ml of mTG treated without R281 was used as a positive control and a sample without any mTG was used as a negative control. The data represents mean values +/- SD where n=3. Statistical analysis was carried out using a one way ANOVA test where the absorbance of samples were compared against a blank control. P-values corresponding to p< 0.05 are represented with a * and where p<0.01 are represented with a **.

3.2.5 The effect of collagen pH on TG2 activity

Due to the collagen solution being solubilised in 0.2 M acetic acid, the pH must be neutralised from 5 to 7 in order for enzymes such as TG2 to be stable and functional. To determine the effect of pH on TG2, a biotin cadaverine activity assay was carried out to ascertain the optimum pH that yields the highest level of TG2 activity. Figure 3.5 shows that collagen neutralised to pH 7 gave the highest activity, which is also reported in the literature (Fleckenstein *et al.*, 2002)

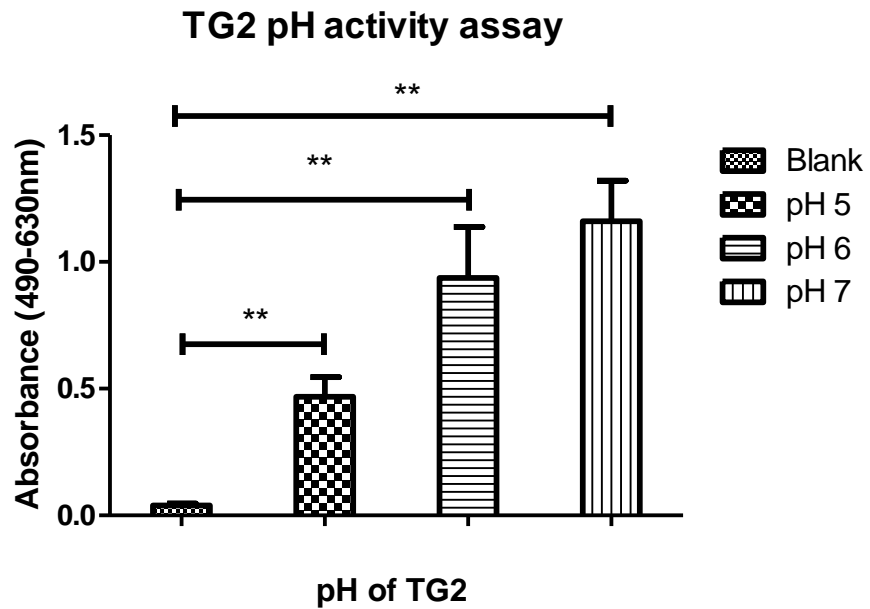


Figure 3.5: **TG2 pH activity assay.** After 5 μ g/ml of TG2 was added to collagen solutions of varying pHs a biotin cadaverine incorporation assay was carried out as described in the materials and methods chapter. A sample without any TG2 was used as a negative control. The data represents mean values +/- SD where n=3. Statistical analysis was carried out using a one way ANOVA test where the absorbance of samples were compared against a blank control. P-values corresponding to p<0.01 are represented with a **.

3.3 Effect of transglutaminase cross-linking on collagen properties

3.3.1 Observing the macromolecular effects of mTG and TG2 crosslinked collagen

To observe the effects of crosslinking collagen on a macromolecular scale, 2.5 mg/ml collagen was allowed to crosslink overnight in untreated 35 mm plastic plates and then collected into individual 7 ml bijou tubes and centrifuged for 15 minutes at 1500 g. Figure 3.6 shows the difference in the overall structure that is seen between cross-linked and non-cross linked collagen. The native collagen sample shows that the collagen had not been sedimented and floated even after the centrifugation process. The second sample from the left contained an R281 inactivated form of mTG which is why it looks similar to the native collagen sample. The third sample is of the activated mTG and the crosslinked collagen is much more compact and sedimented, which sits at the base of the bijou tube. Likewise, the TG2 crosslinked collagen is also more compact and dense than the non-crosslinked samples.

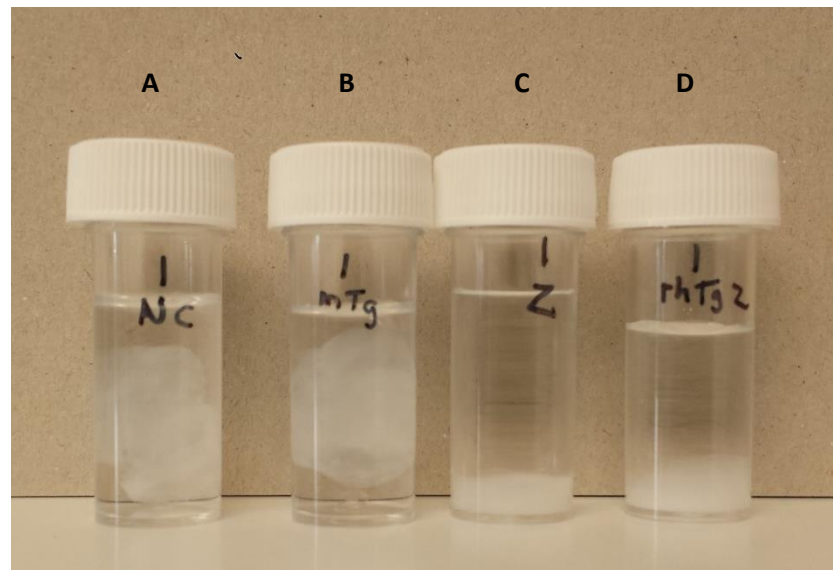


Figure 3.6: **Image of centrifuged collagen samples.** 4 ml collagen samples were crosslinked overnight before being collected and centrifuged for 10 minutes at 1500g. The concentration of all collagen samples was 1mg/ml, from right to left: **A)** Native collagen, **B)** inactive mTG crosslinked collagen, **C)** mTG crosslinked collagen and **D)** recombinant human TG2. Data are representative of one experiment where n=3.

3.3.2 Observing the macromolecular effects of TG2 crosslinked collagen without calcium and DTT

In Figure 3.7, the effects of subtracting calcium and the reducing agent DTT from the TG2 collagen solution is shown. Both of these are needed for TG2 transamidating activity as discussed in chapter 4. The collagen solution was allowed to crosslink overnight in untreated 35 mm plastic plates and then collected into individual 7 ml bijou tubes before the samples were centrifuged for 15 minutes at 1500g. Once again there is a difference between the native collagen and the TG2 sample. TG2 samples without calcium and DTT show a similar macromolecular structure to the native collagen. Their sediments are less compact than the TG2 sample that contains the calcium and DTT.

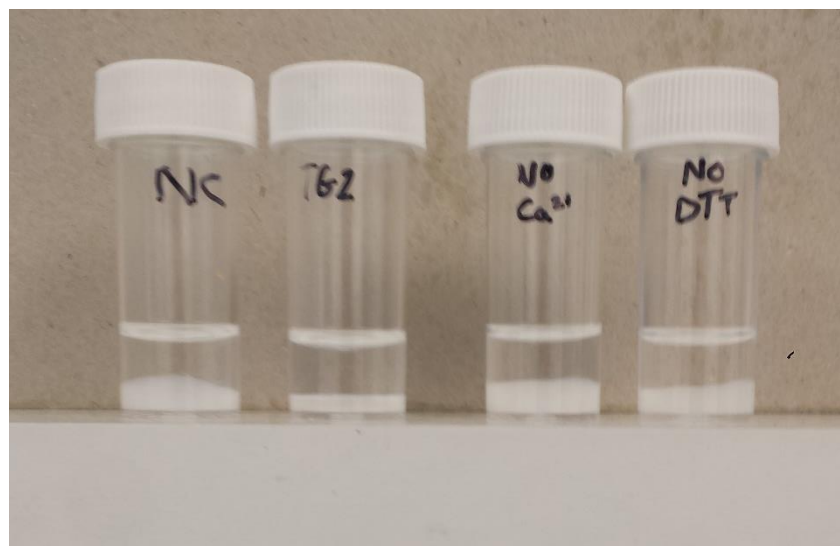


Figure 3.7: **Image of centrifuged collagen samples.** 2.5 mg/ml collagen samples were crosslinked overnight before being collected and centrifuged for 15 minutes at 1500 g. The concentration of all 2 ml collagen samples was 2.5 mg/ml, from left to right: Native collagen, TG2 crosslinked collagen, TG2 crosslinked collagen without calcium and TG2 crosslinked collagen without DTT. Data are representative of one experiment where n=3.

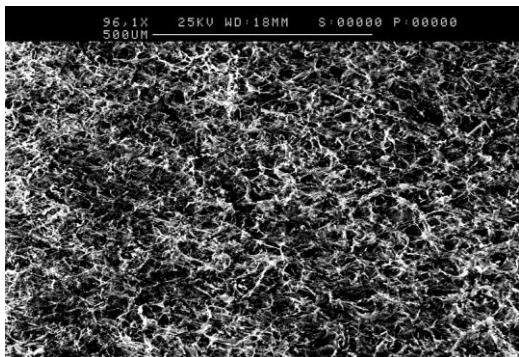
3.3.3 SEM imaging of collagen scaffolds

SEM images shown in Figure 3.8A and 3.8B are of a 2.5 mg/ml sample of native collagen which were taken at 96X and 390X magnification, respectively. Figures 3.8C and 3.8D are SEM images of mTG crosslinked collagen (at 96X and 390X respectively) and 3.8E and 3.8F are images of TG2 crosslinked collagen (at 96X and 390X respectively). The difference in morphology between all three collagen samples is striking in respect to the gaps (in black) between collagen fibres (white). Between Figure 3.8A, 3.8C and 3.8E the gaps between the strands become narrower due to the crosslinking effect. Interestingly Figures 3.8E and 3.8F show a different structure altogether as the collagen fibrils have lost their definition and pores are no longer visible between fibrils.

By using ImageJ software, the space between collagen fibres in each image taken at 96X magnification was measured and averaged. By quantifying the mean pore size, it was possible to quantify which collagen samples had the shortest and longest average space between their respective collagen strands (Figure 3.8G).

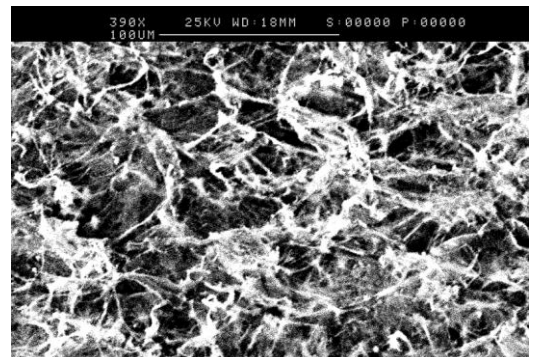
96X

A) NC

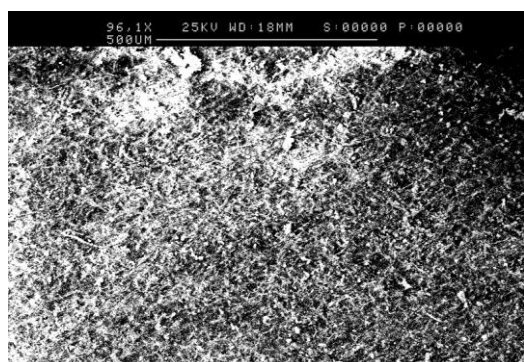


390X

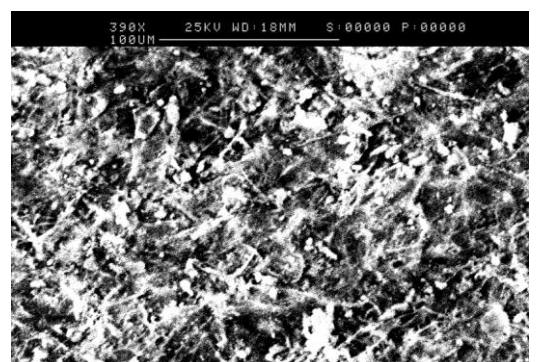
B) NC



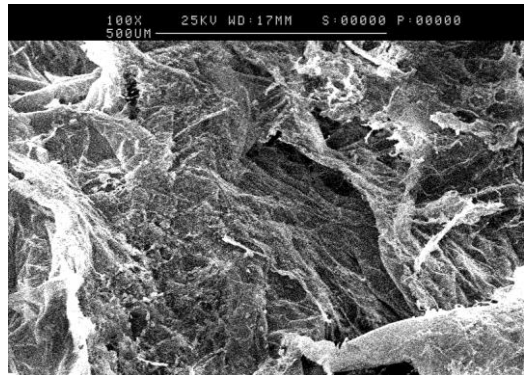
C) mTG



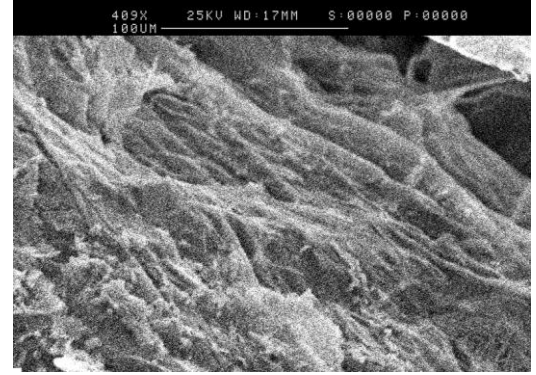
D) mTG



E) TG2



F) TG2



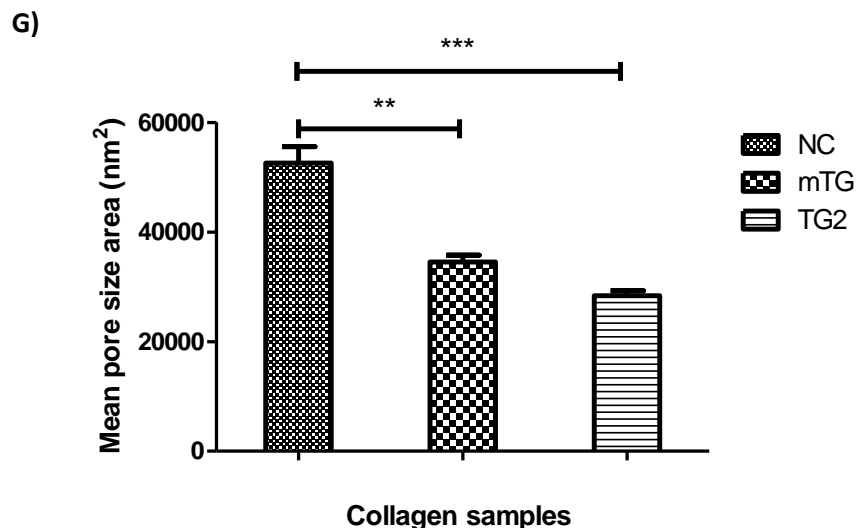


Figure 3.8: SEM images of native and crosslinked collagen: **A)** Collagen samples were crosslinked overnight before being collected and centrifuged for 15 minutes at 1500g. The concentration of all collagen samples was 2.5 mg/ml, from left to right: native collagen, TG2 crosslinked collagen, TG2 crosslinked collagen without calcium and TG2 crosslinked collagen without DTT. **B)** SEM image of 2.5 mg/ml native collagen at 96X magnification **C)** SEM image of 2.5mg/ml native collagen at 390X magnification **D)** SEM image of 2.5 mg/ml mTG crosslinked collagen at 96X magnification **E)** SEM image of 2.5mg/ml mTG crosslinked collagen at 390X magnification **F)** SEM image of 2.5 mg/ml TG2 crosslinked collagen at 96X magnification **G)** SEM image of 2.5 mg/ml TG2 crosslinked collagen at 390X magnification. **H)** SEM images were analysed using ImageJ and the average pore size was measured and plotted. The data represents mean values +/- SD where n=3. Statistical analysis was carried out using a one way ANOVA test where the size of collagen pores were compared against those of the native collagen sample. P-values corresponding to $p < 0.01$ are represented with a ** and where $p < 0.001$ are represented with a ***.

3.3.4 SDS PAGE of native mTG and TG2 crosslinked collagen

In order to further show crosslinking is taking place in the collagen scaffolds (2.5 mg/ml), crosslinked samples were allowed to crosslink overnight and separated by SDS PAGE then stained using Coomassie brilliant blue dye to identify the presence of the bands. In Figure 3.9 there is a significant difference in the bands between the crosslinked collagen and the native collagen bands. Due to the crosslinking effect, the bands in the crosslinked samples are thicker and therefore remain in the loading gel. Furthermore, the γ bands in the crosslinked collagen samples are less visible compared to those in the native and transglutaminase inhibited bands.

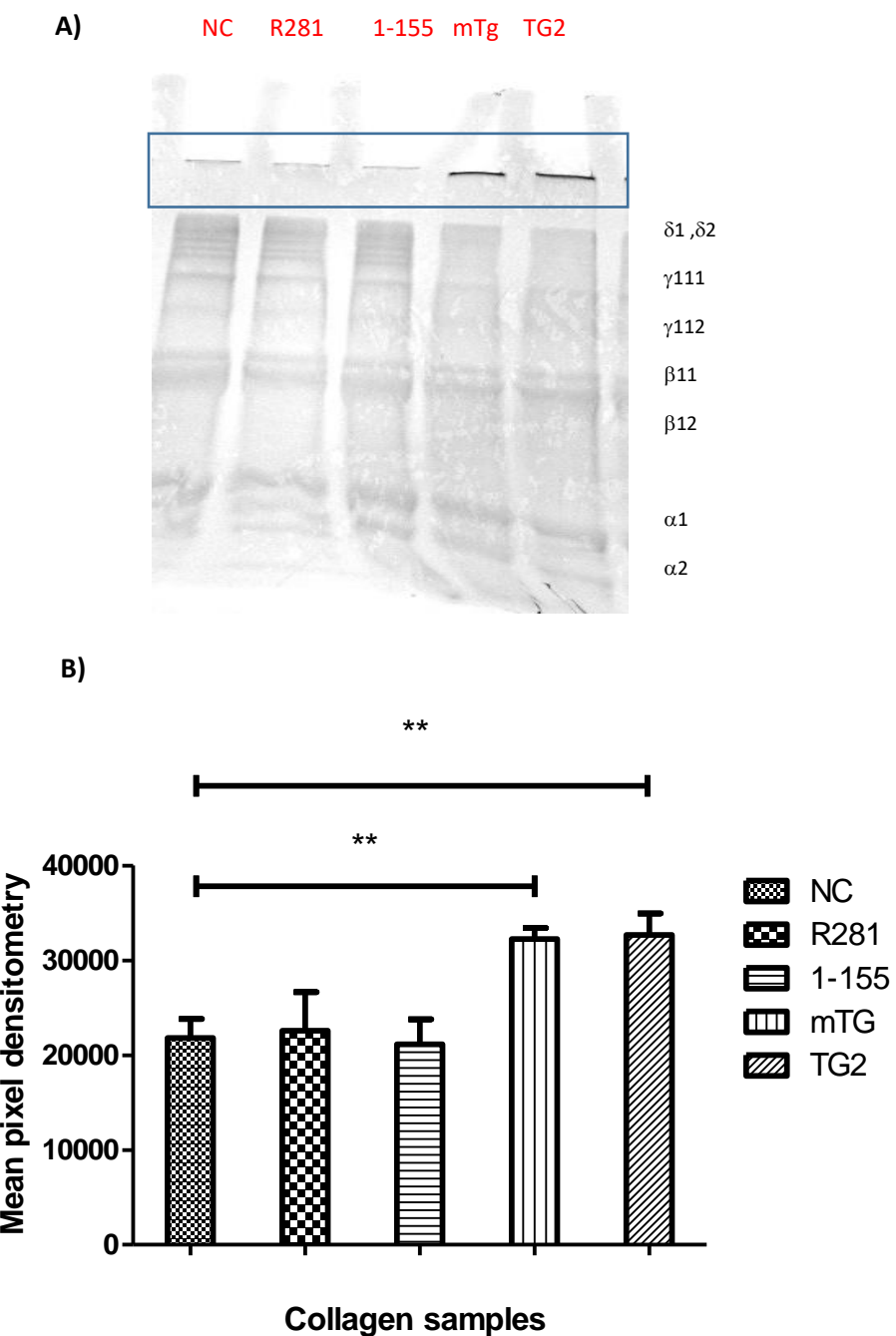


Figure 3.9: Observation and quantification of native and crosslinked collagen bands **A)** Native and cross linked collagen samples (2.5mg/ml) were allowed to crosslink overnight in 96well plates. A 5.5% bis-acrylamide gel was used to carry out a western blot then stained with Coomassie blue dye. The image was taken from a GeneBox using GeneSys software. **B)** Using ImageJ software, the image was converted and bands were analysed. The data represents mean values +/- SD where n=3. Statistical analysis was carried out using a one way ANOVA test where the mean pixel densitometry values of crosslinked collagen scaffolds were compared with those given by native collagen scaffolds. P-values corresponding to $P<0.01$ are represented with a **.

3.3.5 Determination of the $\epsilon(\gamma\text{-glutamyl})$ lysine content of TG cross-linked collagen

In order to prove that the $\epsilon(\gamma\text{-glutamyl})$ lysine isopeptide bond or “crosslink” is being formed, samples of collagen scaffold were digested and analysed. To measure the presence of crosslink various samples of collagen including: native collagen, 10 µg and 50 µg of TG2, 5 µg of mTG that were added to collagen, R281 inactivated mTG and 1-155 inactivated TG2 were exhaustively proteolytically digested. The digestion process is outlined in the Materials and methods chapter and the analysed results using a Biochrom 30 amino acid analyser are shown in Figure 3.10. The collagen sample that contained 5 µg of mTG gave the highest amount of crosslink per nmol of collagen. Followed by the samples of collagen that contained 50 µg and 10 µg of TG2 respectively. The inactivated mTG and TG2 samples contained almost no crosslink, as did the native collagen sample.

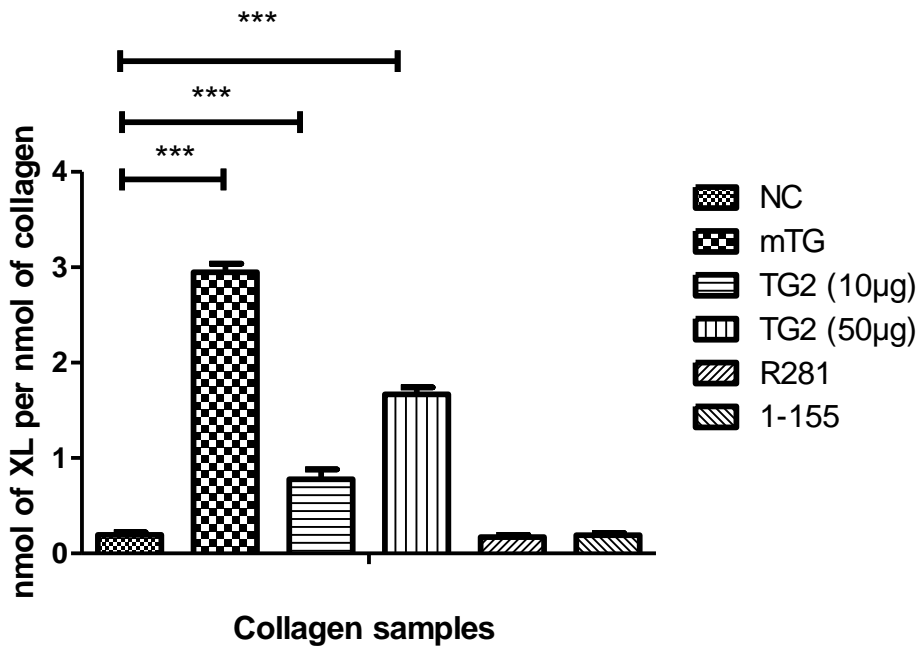


Figure 3.10: Amino acid analyser crosslink assay. 100 μ l of digested collagen (per sample) was loaded in a 1:1 ratio with lithium loading buffer and loaded onto the amino acid analyser. Hydroxyproline and $\epsilon(\gamma\text{-glutamyl})$ isopeptide bond standards were also ran on the analyser so that standard curves could be created for the respective samples. From the standard curves the amount of crosslink per nmol of collagen was then calculated. The data represents mean values +/- SD where n=3. Statistical analysis was carried out using a one way ANOVA test where the nmol of crosslink per nmol of collagen present in crosslinked scaffolds is compared to the base amount of crosslink found in native collagen. The p-values corresponding to P<0.001 are represented with a ***.

3.3.6 Effect of pH on the deamidation activity of TG2

TG2 has been described as a Swiss army knife given its many functions, including crosslinking and deamidation. To measure how much deamidation is occurring at different pH levels, three collagen scaffolds that contained 5 μ g/ml TG2 were crosslink at pH 5, 6 and 7. To measure the amount of deamidation, samples were analysed through the amino acid analyser to detect the amount of ammonia released. Figure 3.11 shows that the negative control of native collagen gave the least amount of ammonia and the sample of collagen containing TG2 at pH 6 gave the highest concentration of ammonia. Due to the acidic conditions at pH 5, the enzyme is likely to denature which may explain the reduction of ammonia released.

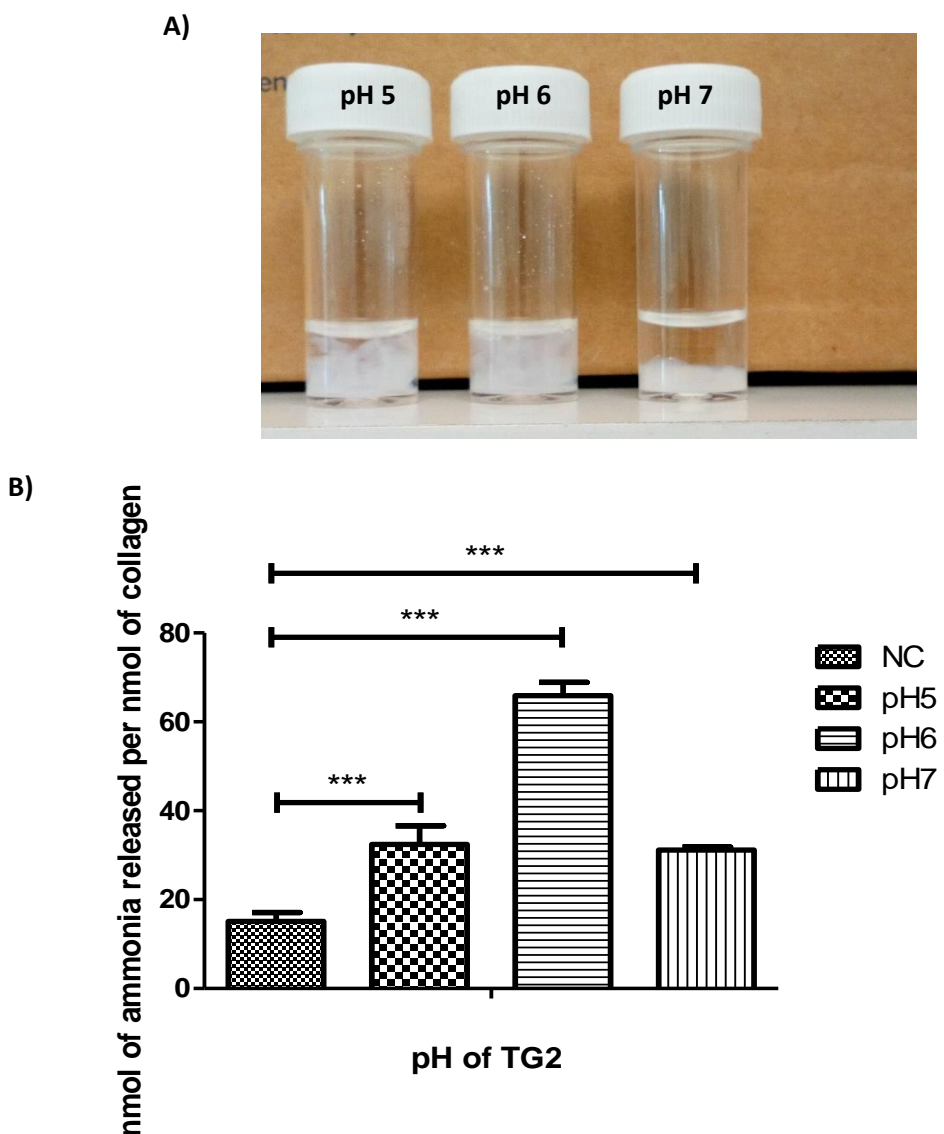


Figure 3.11: Observation of different pH level collagen scaffolds and deamidation assay for collagen scaffolds: A) Image of centrifuged collagen samples. 2.5 mg/ml collagen samples were crosslinked overnight before being collected and centrifuged for 15 minutes at 1500g. The concentration of TG2 in all collagen samples was 5 µg/ml. From right to left: pH 5, pH 6 and pH 7. B) After the collagen samples were crosslinked overnight. Samples were centrifuged and 100 µl of supernatant (per sample) was loaded in a 1:1 ratio with lithium loading buffer and loaded onto the amino acid analyser. A set of ammonia standards were also run on the analyser so that a standard curve could be created for the respective samples. From the standard curve the nmol of ammonia released per nmol of collagen loaded per sample was then calculated. The data represents mean values +/- SD where n=2. Statistical analysis was carried out using a one way ANOVA test where the p-values corresponding to P< 0.001 are represented with a ***.

3.4 Cellular response of HOB cells to native and crosslinked collagen

3.4.1 Proliferation of human osteoblasts on native and crosslinked collagen

An XTT proliferation assay was carried out to observe the difference between the viable cell number of HOBs after growth on native collagen, mTG crosslinked collagen and TG2 crosslinked collagen. 20×10^4 HOBs cultured in 100 μl complete medium (CM, 10% foetal bovine serum in Dulbecco's Modified Eagle Medium) were seeded onto native collagen coated wells (2.5mg/ml), mTG crosslinked collagen wells and TG2-crosslinked collagen. Samples proliferated over the course of 6 days and the absorbances were measured at 490 nm and 630 nm. In Figure 3.12 the day 2 samples all showed relatively similar proliferation rates, however after 4 days osteoblasts grown on mTG and TG2 crosslinked collagen had a far higher rate of proliferation than cells on native collagen. Three days post seeding the proliferation of HOBs grown on TG2 on average still remained higher than the other samples. This suggests that HOBs mitochondrial/metabolic activity can increase over time on collagen scaffolds.

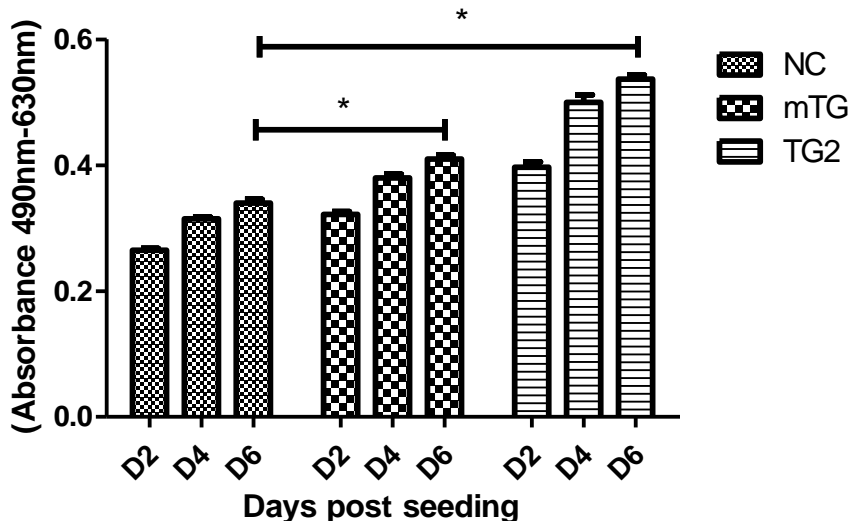


Figure 3.12: XTT proliferation assay for native and crosslinked collagen. HOBs seeded onto the different collagen matrices were monitored between day 2 and day 6 (post seeding) after they had been seeded onto a 96-well plate. The three conditions in which HOBs were seeded (from left to right) are: Native collagen, mTG crosslinked collagen and TG2 cross-linked collagen. A Biotek plate reader was used to measure the absorbances of each sample at 490nm and 630nm. The absorbance values for these respective wavelengths were subtracted and averaged to give the mean absorbance values shown in the graph. The data represent mean values +/- SD where n=3. Statistical analysis was carried out using a one way ANOVA test where the absorbance of samples from crosslinked collagen samples were compared to those from native collagen samples. P-values corresponding to P<0.05 are represented with a *.

3.4.2 Observing the macromolecular effects of mTG and TG2 crosslinked collagen with 45S5 bioglass particles

To observe the effects of crosslinking collagen with 45S5 bioglass on a macromolecular scale, 2.5 mg/ml collagen was mixed with 10 mg/ml 45S5 bioglass and allowed to crosslink overnight in untreated 35 mm plastic plates and then collected into individual 7 ml bijou tubes and centrifuged for 15 minutes at 1500g. Figure 3.13 shows the difference in the sedimentation that is seen between cross-linked collagen with 45S5 bioglass and non-cross linked collagen. The native collagen sample shows that the collagen had not been sedimented and floated after the centrifugation process. The second sample from the left contained uncrosslinked collagen with bioglass and sedimented more densely than native collagen. The third sample contains mTG crosslinked collagen with 45S5 bioglass which was much more compact and sedimented than native collagen. Likewise TG2 crosslinked collagen with 45S5 bioglass is also more compact and appears denser than the non-crosslinked sample.

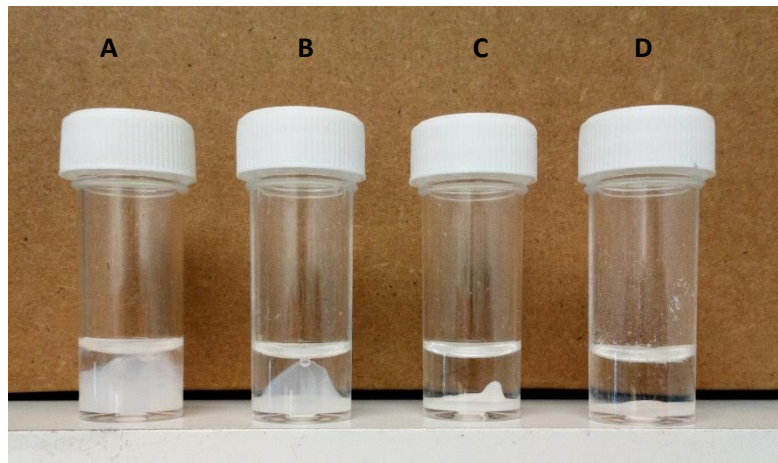


Figure 3.13: Image of centrifuged collagen samples with 45S5 bioglass. Collagen samples (2 ml) were crosslinked overnight before being collected and centrifuged for 10 minutes at 1500g. The concentration of all collagen samples was 2.5 mg/ml, from left to right: **A)** Native collagen, **B)** native collagen mixed with 45S5 bioglass, **C)** mTG crosslinked collagen+ 45S5 bioglass, and **D)** TG2 crosslinked collagen + bioglass. Data are representative of one experiment where n=3.

3.4.3 Proliferation of human osteoblasts on native and crosslinked collagen containing 45S5 bioglass particles

An XTT proliferation assay was carried out to observe the difference between the viable cell numbers of HOBs after growth on native collagen, native collagen mixed with (10 mg/ml) 45S5 bioglass, mTG crosslinked collagen mixed with (10 mg/ml) 45S5 bioglass and TG2 crosslinked collagen mixed with (10mg/ml) 45S5 bioglass. HOBs cultured in complete medium (CM, 10% foetal bovine serum in Dulbecco's Modified Eagle Medium) were seeded onto the scaffolds with medium changes every 48 hours. Samples were measured over the course of 6 days and the absorbances were measured at 490 nm and 630 nm. In Figure 3.14 both the native collagen and native collagen with bioglass showed relatively similar absorbances for all three time points. However, after 4 days, TG2 and mTG crosslinked collagen with bioglass absorbances were greater than that of native collagen. This suggests that crosslinked collagen mixed with 45S5 bioglass is not impairing HOB proliferation.

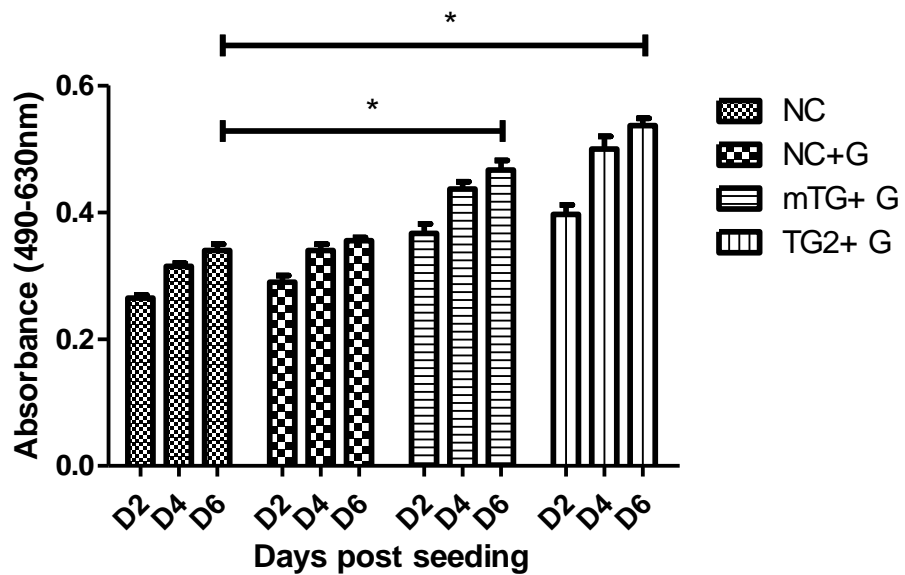


Figure 3.14: XTT proliferation assay for native and crosslinked collagen mixed with 45S5 bioglass. HOBs seeded onto the different collagen matrices were monitored between day 2 and day 6 (post seeding) after they had been seeded onto a 96-well plate. The four conditions in which HOBs were seeded (from left to right) are: Native collagen, native collagen+ 45S5 bioglass, mTG crosslinked collagen+ 45S5 bioglass and TG2 cross-linked collagen+ 45S5 bioglass. A Biotek plate reader was used to measure the absorbances of each sample at 490 nm and 630 nm. The absorbance values for these respective wavelengths were subtracted and averaged to give the mean absorbance values shown in the graph. The data represents mean values +/- SD where n=3. Statistical analysis was carried out using a one way ANOVA test where the absorbance of samples from crosslinked collagen samples were compared to those from native collagen samples. P-values corresponding to P<0.05 are represented with a *.

3.4.4 Stability of crosslinked collagen matrices

Over time, collagen scaffolds are degraded by cells seeded onto it via interactions with the extracellular matrix and the secretion of MMP 8 and MMP 13 (Lu *et al.*, 2011). After seeding collagen with HOBs for 3 days, the effects of collagen degradation can be quantified. Once cells were removed from the collagen scaffold, the scaffold was stained as outlined in the Materials and Methods section. The stained collagen scaffolds were then imaged using the GeneBox.

Representative collagen plates are shown in Figure 3.15. In each case, the mean pixel densitometry value of the collagen plates was higher than in those of both the NC plates and the inactivated mTG and TG2 plates, indicating that crosslinking of collagen by mTG and TG2 stabilises the collagen to cell protease degradation.

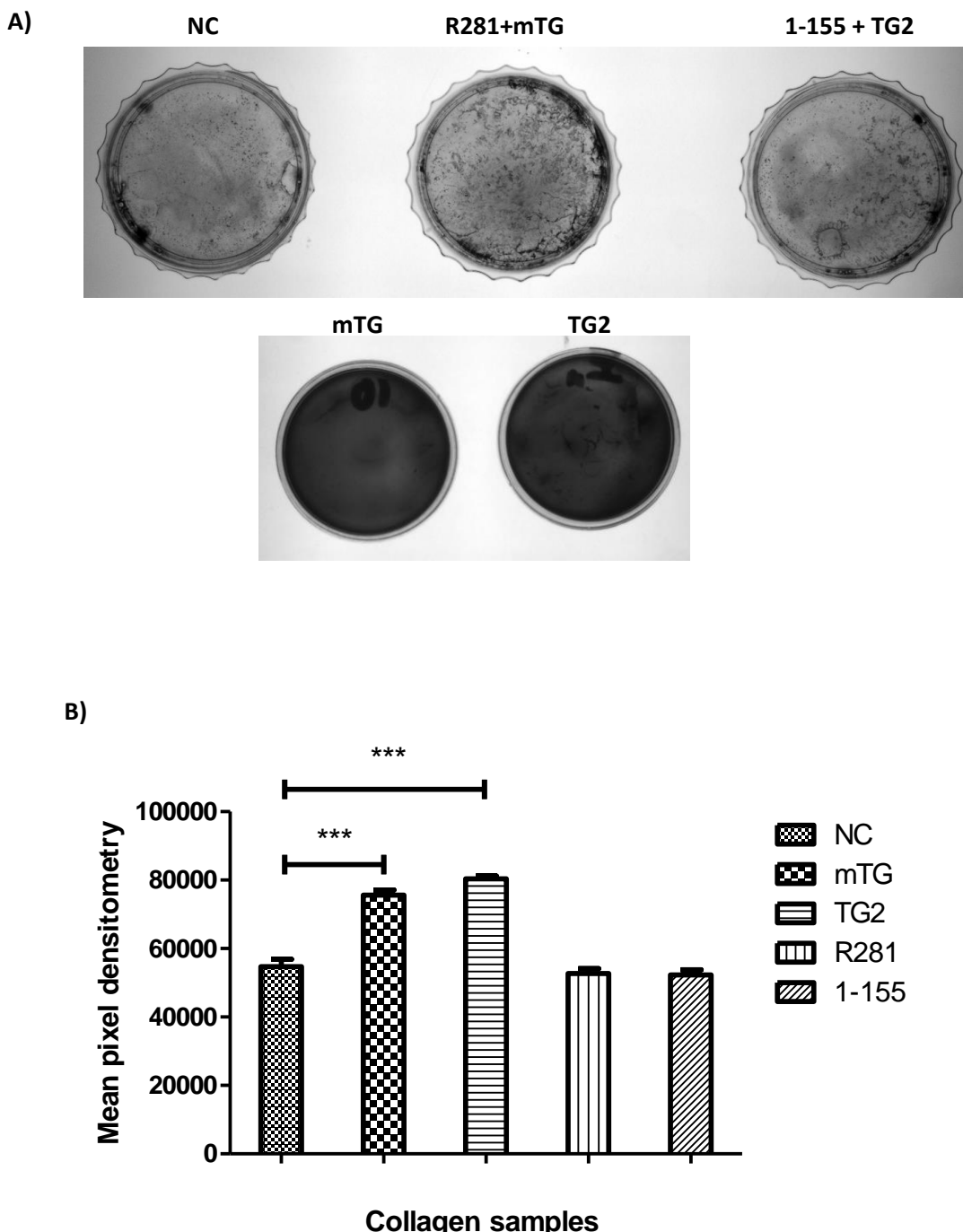


Figure 3.15: Collagen digestion assay. A) 35 mm non-treated plastic tissue culture plates coated with five different types of collagen mixture. From left to right: 1) Native collagen, 2) R281 inactivated mTG collagen, 3) 1-155 inactivated TG2, 4) mTG crosslinked collagen (5 µg/ml) and 5) TG2 crosslinked collagen (5 µg/ml). The samples were sustained using complete medium for 3 days and following HOBs removal with sodium deoxycholate, were stained with Coomassie brilliant blue stain. Samples were captured using the Syngene GeneBox and analysed using ImageJ as described in the Materials and Methods. B) Using ImageJ software, the image was converted, and scaffolds were analysed. The data represents mean values +/- SD where n=3. Statistical analysis was carried out using a one way ANOVA test where the p-values corresponding to P<0.001 are represented with ***.

3.4.5 Proliferation of human osteoblasts on native and crosslinked collagen containing cobalt bioglass

An XTT proliferation assay was carried out to observe the difference between the viable cell number of HOBs after growth on native collagen mixed with 10 mg/ml cobalt bioglass. HOBs cultured in complete medium (CM, 10% foetal bovine serum in Dulbecco's Modified Eagle Medium) were seeded onto native collagen coated wells (2.5 mg/ml), with and without 2% and 4% 10 mg/ml cobalt bioglass. Samples were measured over the course of 6 days and the absorbances were measured at 490 nm and 630 nm. In Figure 3.16 all the samples 2 days post seeding showed relatively similar proliferation rates; however, after 4 days absorbances for the cobalt glass samples began to drop below that of the native collagen samples. By 6 days post seeding, the proliferation rate for 4% cobalt on average still remained lower than the other samples. This shows that cobalt glass particles are not viable for HOB proliferation.

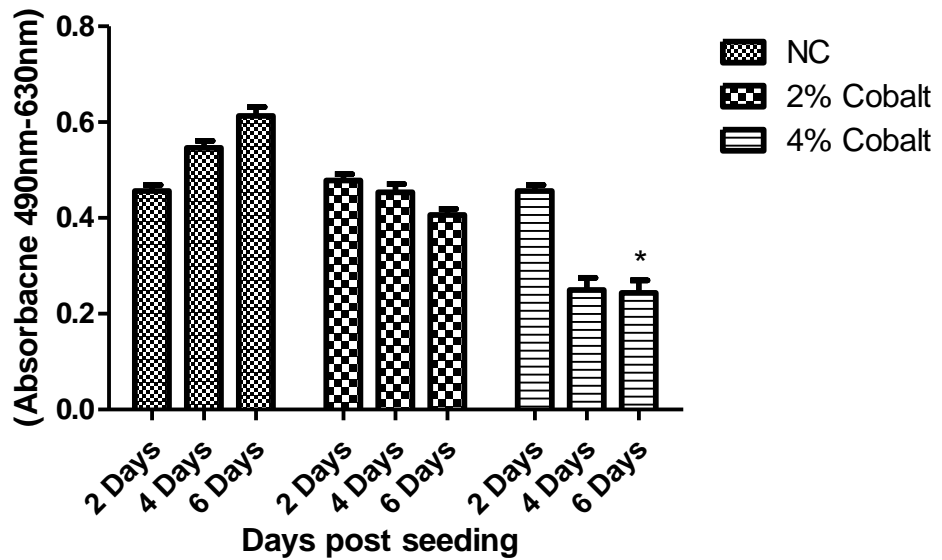


Figure 3.16: XTT proliferation assay for native and collagen mixed with cobalt bioglass. HOBs seeded onto the different collagen matrices were monitored between day 2 and day 6 (post seeding) after they had been seeded onto a 96-well plate. The three conditions in which HOBs were seeded (from left to right) are: Native collagen, collagen with 2% cobalt bioactive glass and collagen with 4% cobalt bioglass. A Biotek plate reader was used to measure the absorbances of each sample at 490nm and 630nm. The absorbance values for these respective wavelengths were subtracted and averaged to give the mean absorbance values shown in the graph. The data represents mean values +/- SD where n=3. Statistical analysis was carried out using a one way ANOVA test where the absorbance of samples from crosslinked collagen samples were compared to those from native collagen samples. P-values corresponding to P<0.05 are represented with a *.

3.5 Discussion

One of the first investigations carried out was the confirmation that the type 1 collagen which was produced in house was pure using SDS PAGE. The gels were stained with Coomassie brilliant blue dye and indicated the presence of bands observed at 130 kDa and 115 kDa showing the denatured α_1 and α_2 chains respectively that make up type 1 human collagen.

Activity assays revealed that a concentration of 25 μM and above was enough to inactivate 5 $\mu\text{g/ml}$ TG2 in a biotin cadaverine incorporation activity assay. In order to inactivate mTG, 1-155 had no effect, and so R281 was used at the concentration reported in the literature (Zonca *et al.*, 2017). The effects of omitting calcium and dithiothreitol (DTT) from the TG2 collagen solution was observed in Chapter 3. Ca^{2+} is required to activate TG2, while DTT is needed to maintain the enzyme in a reduced active form. Studies in Chinese Hamster V79 cells showed that concentrations of DTT in low doses were not toxic to cells (Held and Melder, 1987). Using a biotin cadaverine assay, it was found that 10 mM DTT was sufficient to reach the same level of activity as 100 mM DTT. The activity of TG2 has long been established to be optimal at pH7 (or physiological pH) (Fleckenstein *et al.*, 2002, Gundemir *et al.*, 2012) and this was supported by data in this chapter.

Amino acid analysis indicated there was a low level of $\epsilon(\gamma\text{-glutamyl})$ crosslinking in the proteolytically digested native collagen sample when compared to the 1 nmol crosslinked standard sample alone. As expected, there was a significant peak representing $\epsilon(\gamma\text{-glutamyl})$ crosslink in the mTG sample, and when spiked with the $\epsilon(\gamma\text{-glutamyl})$ standard, it was clear that the two peaks had the same retention time, confirming the presence of the crosslink in the mTG crosslinked collagen. There was roughly half the amount of nmol crosslink per nmol of collagen present in TG2 crosslinked collagen than there was in mTG crosslinked collagen.

Likewise, there also seemed to be significant differences in the SEM images taken of the native, mTG and TG2 crosslinked images. The mean pore size area between collagen fibrils were also different, even between mTG and TG2 crosslinked collagen. This difference in structure could be due to the difference in the nmol of crosslink per nmol of hydroxyproline present in the two crosslinked collagen scaffolds.

In order to observe the visible effects of TG crosslinking on collagen, samples were crosslinked overnight in untreated 35 mm plastic plates and centrifuged. The difference in the overall structure between cross-linked and non-crosslinked collagen was shown to be substantial. The native collagen sample was far less sedimented and floated in the water and PBS. The inactive form of mTG appeared very similar to the native collagen sample. The active mTG and TG2 samples showed a far more sedimented and compact scaffold that was found at the base of the bijou tube. This was confirmed that both TG2 and mTG had having a physical effect on collagen, which affected its macromolecular structure. This is confirmed by a previous study on collagen fibril modification by atomic force microscopy showing that the rigidity of TG2 crosslinked collagen is three fold higher than compared to native collagen (Wang & Martin, 2013).

The native collagen in Figure 3.7 was shown to be more sedimented than in Figure 3.6 most likely due to the concentration of collagen to be 2.5mg/ml instead of 1mg/ml, but there is a clear difference between the structure seen between it and the TG2 sample. Centrifuged crosslinked collagen samples with 45S5 bioglass were seen to be more sedimented than native collagen samples with and without 45S5 bioglass. Similar to the native collagen sample, the TG2 samples without calcium and DTT showed a similar macromolecular structure to native collagen.

This confirms that both Calcium (upon which TG2 is dependent upon to be active) and the reducing agent DTT which maintains activity are both needed for the modification of collagen fibril structure by TG2. It is well-known that TG2 is calcium dependent with regards to its transamidase activity (Verderio *et al.* 2004) and thus the enzyme alone will have had little

crosslinking effect on the collagen without calcium, explaining why it had a similar morphology to the native collagen sample. The sample that contained calcium but not the reducing reagent DTT also had a similar morphology when centrifuged to the native collagen sample. Thus transamidating activity is likely to only be transient until TG2 becomes oxidised, which is why it resembles the structure of native collagen (Pinka *et al.* 2007).

When observing the deamidation limits of TG2, there was no clear relationship between lowering the pH and the amount of ammonia released. In the literature, it was first reported that deamination was only favoured by certain conditions like pH conditions under 7 (Fleckenstein *et al.*, 2002). Recently though, a study has been published that shows that a glutamine residue in Hsp20 was specifically deminimated while other glutamine residues are transamidated (Boros *et al.*, 2006). We have shown that deamidation is low at pH 7, peaks at pH 6 and drops at pH 5, likely due to enzyme denaturation.

The cell proliferation data indicate a clear trend for all samples, showing that as time increased so did the number of viable HOBs in each group. This indicates that the inclusion of 45S5 glass nanoparticles may not be toxic to the cell. However this needs to be confirmed by more tests such as an LDH assay and other proliferation assays. Moreover, it can be seen that the inclusion of glass into the mixture had little effect on the cells grown on native collagen since the proliferation rates did not vary. When the glass particles were added to the TG2 collagen mixture, there was a decrease in proliferation by day 6; up until then, it had been higher than the average absorbance for each day for samples without bioglass particles. One hypothesis for this is that the HOBs are differentiating and mineralising quicker on this collagen scaffold than they are on mTG and native collagen scaffolds. Investigations into the underlying mechanisms will be discussed in chapter 5.

As shown by Akhouayri *et al.* (2010), Chau *et al.* (2005) and Ignatius *et al.* (2005), cells that are seeded onto collagen will adhere and interact in the matrix, but also degrade it to some degree. Since crosslinking collagen with TG2 is known to improve not only mechanical strength

but also its resistance to proteolytic digestion the same was to be expected from mTG crosslinked collagen.

The mean pixel value, which indicates the amount of collagen still present, was repeatedly higher for the mTG crosslinked collagen than that of native collagen and the R281 inactivated mTG treated collagen. Likewise TG2 samples on average showed 0.25 fold less digestion compared to native collagen and 1-155 inactivated TG2 collagen.

Finally, a cell proliferation assay was carried out on HOBs that were grown on native collagen mixed with 2% and 4% 10 mg/ml cobalt bioglass. After 4 days, a decrease in cell proliferation was shown in HOBs seeded on 2% cobalt collagen and an even greater decrease was shown in HOBs seeded on 4% cobalt collagen. The decrease in cell viability is likely due to the cells becoming hypoxic, leading to the cell death (Jones, 2015). To summarise, there is a clear difference in micro and overall structure between native, mTG and TG2 crosslinked collagen. As well as a difference in the nmol of crosslink per nmol collagen between mTG and TG2 crosslinked collagen samples.

Chapter 4: Mineralisation of human osteoblasts in novel collagen scaffolds

4.1 Introduction

Throughout the human life span, bone undergoes continuous remodelling, which is a response to physiological and mechanical environmental stressors. Essentially bone remodelling is made up of two reciprocal activities: the resorption of bone matrix by osteoclasts and bone formation by osteoblasts. As stated previously, osteoblasts derive from mesenchymal stem cells and orchestrate bone formation under the strict regulation of hormones, cytokines and the extracellular environment.

It has been well-established in recent decades that transglutaminases play a role in matrix maturation, calcification and mineralisation (Yin *et al.*, 2012b). TG2 expression has now been found in cartilage, specifically in hypertrophic chondrocytes (Aeschlimann *et al.*, 1993, Aeschlimann *et al.*, 1996, Nurminskaya *et al.*, 1998, Johnson and Terkeltaub, 2005), as well as in MCT3 pre-osteoblasts (Al-Jallad *et al.* 2006), primary osteoblasts and human and rat osteosarcoma cells. However, the mechanism behind transglutaminase-mediated mineral deposition has not been well-established. Nai *et al.* hypothesised that ECM protein assemblies, in the presence of TG2, could participate in matrix stabilisation and in cell adhesion processes (Chau *et al.* 2005, Verderio *et al.* 1998 & Yeh *et al.* 2014).

Furthermore, the importance of transglutaminase activity in mineralisation was demonstrated by Al-Jallad *et al.* (2006) who showed that, by using transamidase inhibitors, it was possible to block mineralisation in mouse pre-osteoblasts *in vitro*, even though TG2/FXIIia double knockouts mice show no abnormality in bone formation. Therefore, it is hypothesised that transglutaminase, mediated differentiation could be transamidase dependent, as several bone matrix proteins are also transglutaminase substrates, including type I collagen, osteocalcin, osteonectin and vitronectin (Mosher and Schad, 1979, Kaartinen *et al.* 1997). These ECM protein assemblies, in the presence of TG2, could contribute to matrix stabilisation and cell adhesion processes (Verderio *et al.* 1998, Chau *et al.* 2005, Telci *et al.* 2008). Nurminskaya and Kaartinen (2006) suggested that mineralisation induced by transglutaminase

crosslinking activity may involve a complex interplay between extracellular matrix proteins and the local calcium concentration in mineralised tissue.

How human osteoblasts react to being seeded onto TG2 and mTG crosslinked collagen is assessed in this chapter. Importantly, it has been shown that HOBs are able to differentiate small changes in the distance between collagen fibres (Boccaccini *et al.*, 2010). These distances in collagen pore size act as signalling cues, which in turn influence cell behaviour and induce migration and matrix production, in this case mineralisation.

Changes in the extracellular matrix such as the concentration of calcium or pH will change how HOBs mineralise, as does crosslinking collagen. This was shown by Chau *et al.* (2005), who showed that TG2 crosslinked collagen matrices allowed more HOBs to attach to the scaffold compared to native collagen, suggesting that either more RGD sites (Arg-Gly-Asp triplicate repeating amino acids on collagen helices) are available on crosslinked collagen or that cells are exploiting alternative binding sites via upregulation or alternative compensatory mediated binding sites.

The inclusion of bioglass particles could also yield interesting data in terms of whether there is a change in mineralisation rates and if so, how this comes about. This aspect will be investigated when cells are seeded onto collagen mixed with bioglass particles; one hypothesis is that the leaching of calcium from the glass particles into the ECM could affect mineralisation rates. This could lead to an increase in mineralisation as HOBs are stimulated further by contact with the HCA layer which has been shown by Hench's group (Hench *et al.*, 1991) to form between the bioglass and cells.

4.2 Characterising the mineralisation of collagen scaffolds with mTG and TG2

4.2.1 Mineralisation of HOBs

HOBs cultured in differentiation medium (10% foetal bovine serum in DMEM supplemented with 50 µg/ml ascorbic acid and 10 mM β-glycerophosphate) for 0, 6, 8 and 10 days (represented in graph figures as D0, D6, D8 etc). As shown in Figure 4.1, HOBs cultured with this medium began to show mineralisation taking place by day 6 and much more positive von Kossa staining by day 10. This suggested that a 10-day differentiation treatment course was an appropriate time frame to observe osteoblast mineralisation *in vitro* and this would be a suitable model for assessing the effect of mTG and TG2 treatments on mineralisation (Nai *et al.* 2014).

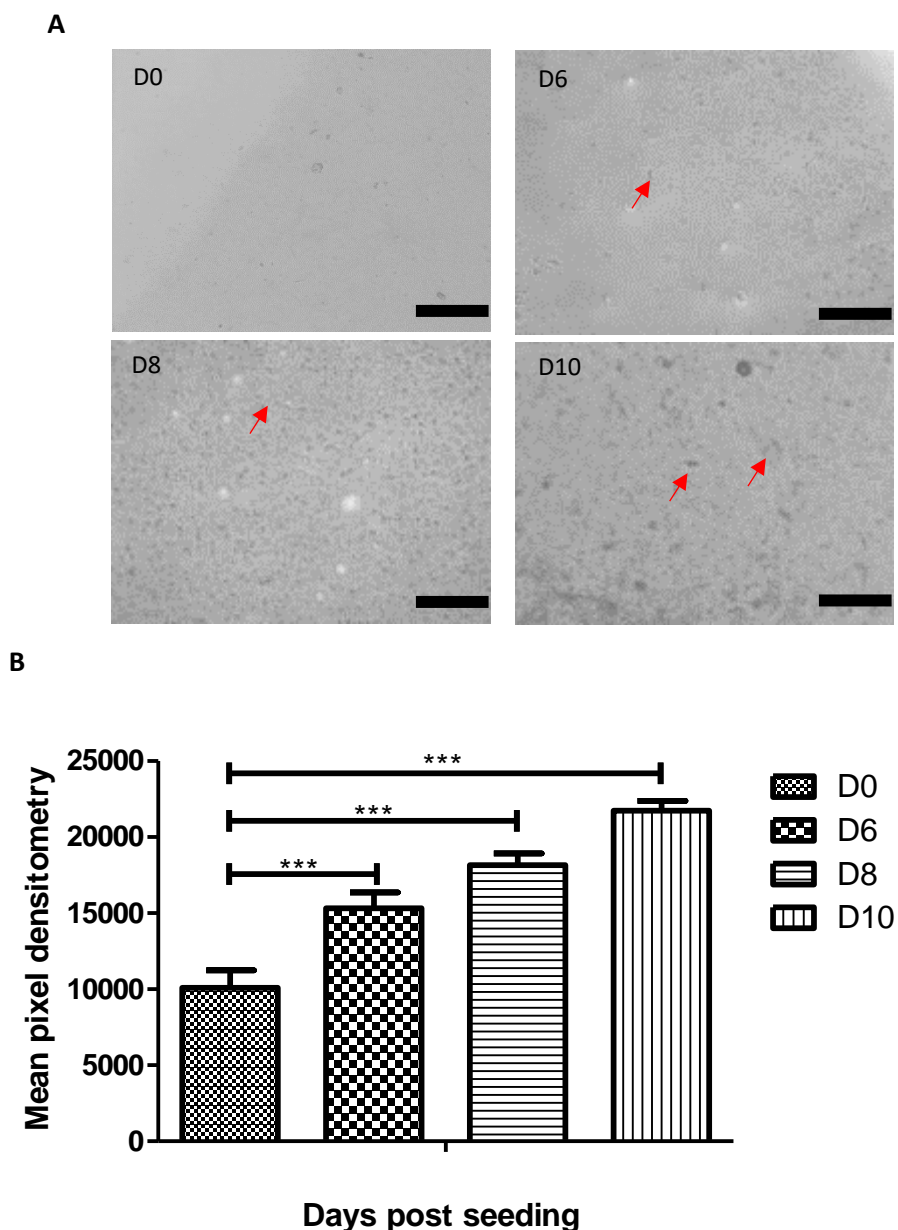


Figure 4.1: Mineralisation of HOBs cultured over 10 days on tissue culture plastic. A) HOBs were cultured in differentiation medium for 0-10 days. Calcium deposition in extracellular matrix was stained black using Von Kossa staining and highlighted by red arrows. Scale bars= 200 µm. (as described in the Materials and Methods). **B)** The results represent the mean values of pixel density for images that were taken on a Nikon digital camera and inverted on ImageJ. Analysis involved each pixel of the image being graded a value of how black it was on a scale of 0-255. The results represent mean values +/- S.D, where n=3. Statistical analysis was carried out using a one-way ANOVA test where mean pixel densitometry of HOBs was compared to the day 0 sample. The p-values corresponding to P< 0.001 are represented with a ***.

4.2.2 Effect of mTG and TG2 on mineralisation in HOBs

HOBs were cultured in differentiation medium (10% fetal bovine serum in DMEM supplied with 50 µg/ml ascorbic acid and 10 mM β-glycerophosphate) for 6, 8 and 10 days (Figure 4.2). Here, HOBs were cultured with this medium along with 5 µg/ml recombinant human TG2 or mTG, which was added every 48 hours. This is because media is replaced every 48 hours. Mineralisation rates were significantly higher from D6 onwards for the mTG and TG2 samples. By day 10, there was a statistical significance in the difference between mineralisation of cells grown with just differentiation medium and those grown with transglutaminases added with media changes.

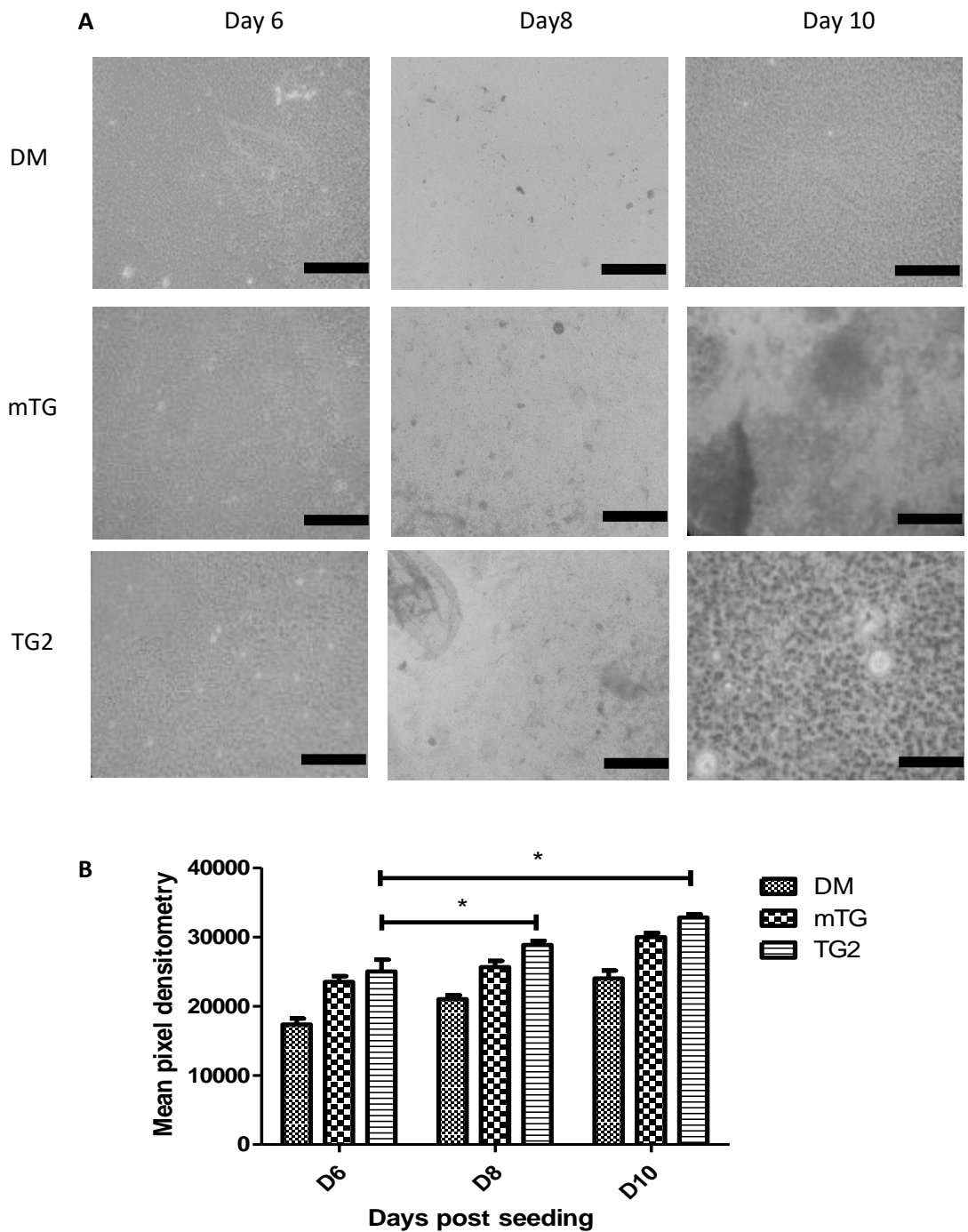


Figure 4.2: Mineralisation of HOBs with mTG and TG2 added. (A) HOBs cultured with DM, 5 µg/ml mTG and 5 µg/ml TG2 were subjected to von Kossa staining on day 6, 8 and 10. The mineral depositions were stained in black and for all groups increased from day 6 to 10. By Day 10 HOBs with 5 µg/ml TG2 added with each media change gave the most mineralisation. Samples were viewed at x10 magnification using a Nikon CK2 and photographed with an Olympus DP10 digital camera. Scale bars= 200 µm. (B) The mineralised area was visualised by von Kossa staining and positive staining was quantified by ImageJ. The results represent mean values +/- S.D, where n=3. Statistical analysis was carried out using a one-way ANOVA test where the mean pixel densitometry of cells grown without TGs were compared to those with TGs added. The p-values corresponding to P< 0.05 are represented with a *.

4.2.3 Mineralisation of HOBs when seeded on mTG and TG2 crosslinked collagen

HOBs were grown on 2.5 mg/ml collagen scaffolds where 5 µg/ml TG2 and mTG were added to the collagen scaffolds before they were crosslinked overnight (see Materials and Methods) with differentiation medium changes every 48 hours (DM, CM supplied with 50 µg/ml ascorbic acid and 10 mM β-glycerophosphate) for 6, 8 and 10 days (Figure 4.3). Mineralisation was determined using von Kossa staining. HOBs grown on crosslinked collagen scaffolds were shown to have a statistically significantly higher rate of mineralisation.

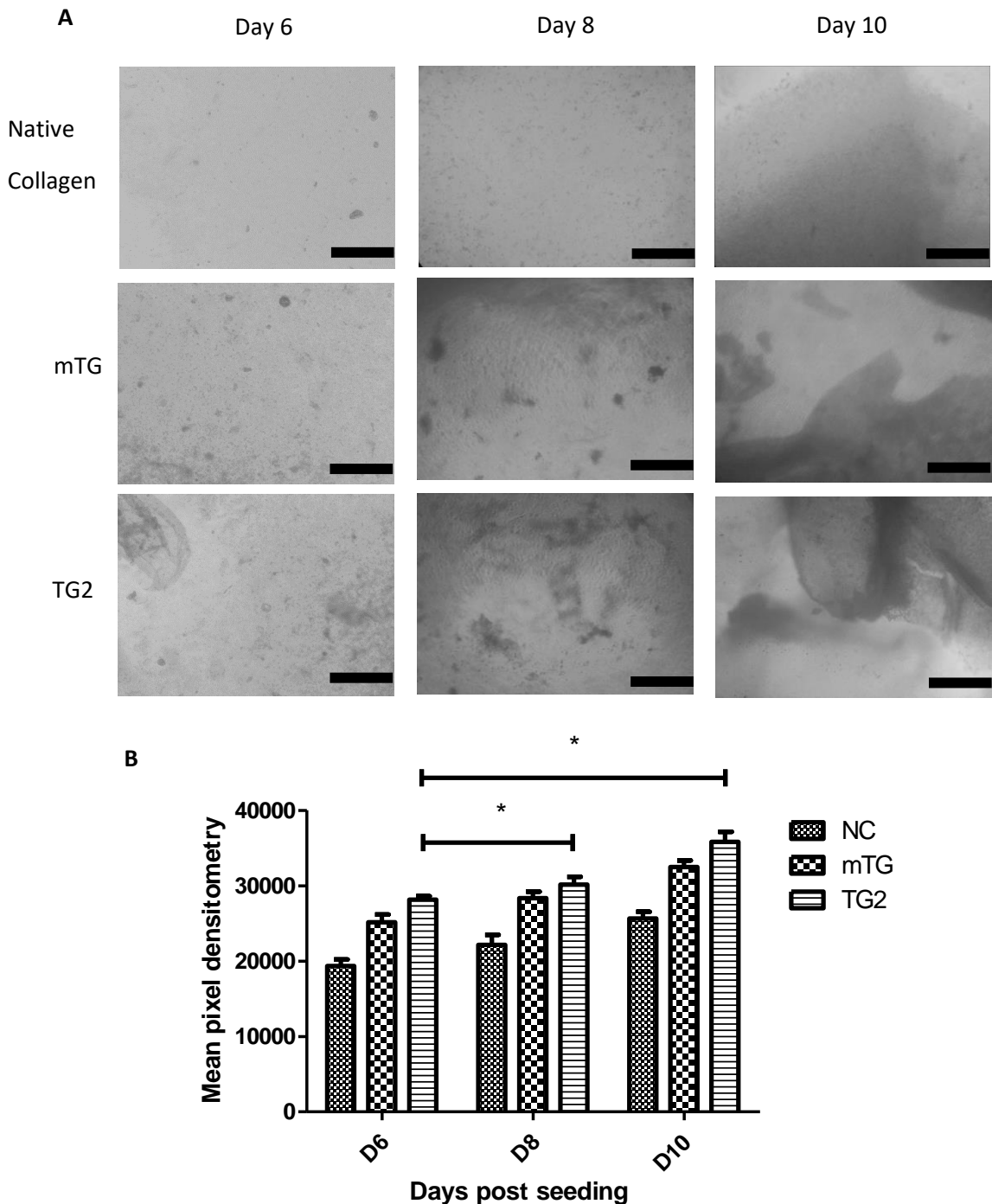


Figure 4.3: Mineralisation of HOBs when seeded onto mTG and TG2 crosslinked collagen. (A) HOBs were seeded onto native, 5 µg/ml mTG and 5 µg/ml TG2 crosslinked collagen (2.5 mg/ml) and subjected to von Kossa staining on day 6, 8 and 10. The mineral depositions were stained in black and for all groups increased from day 6 to 10. Samples were viewed at x10 magnification using a Nikon CK2 and photographed with an Olympus DP10 digital camera. Scale bars= 200 µm. **(B)** The mineralised area was visualised by von Kossa staining and positive staining was quantified by ImageJ. The results represent mean values +/- S.D, where n=3. Statistical analysis was carried out using a one-way ANOVA test where the mean pixel densitometry of HOBs on native collagen scaffolds were compared to those seeded on crosslinked scaffolds. P-values corresponding to P< 0.05 are represented with a *.

4.2.4 Mineralisation of HOBs when seeded onto TG2 crosslinked collagen without DTT

The effects of omitting calcium and the reducing agent DTT from the TG2 collagen solution was observed in Chapter 3. Both of these are needed for TG2 transamidating activity. TG2 in collagen samples without DTT show a similar macromolecular structure to native collagen. They are not as sedimented or dense as the TG2 sample that contains the calcium and DTT. Here, the ability for HOBs to mineralise when seeded onto TG2 crosslinked collagen (without DTT) is shown in Figure 4.4. There was a clear difference as HOBs seeded onto TG2 collagen scaffolds with DTT included, showing a greater mineralisation compared to its counterpart without DTT.

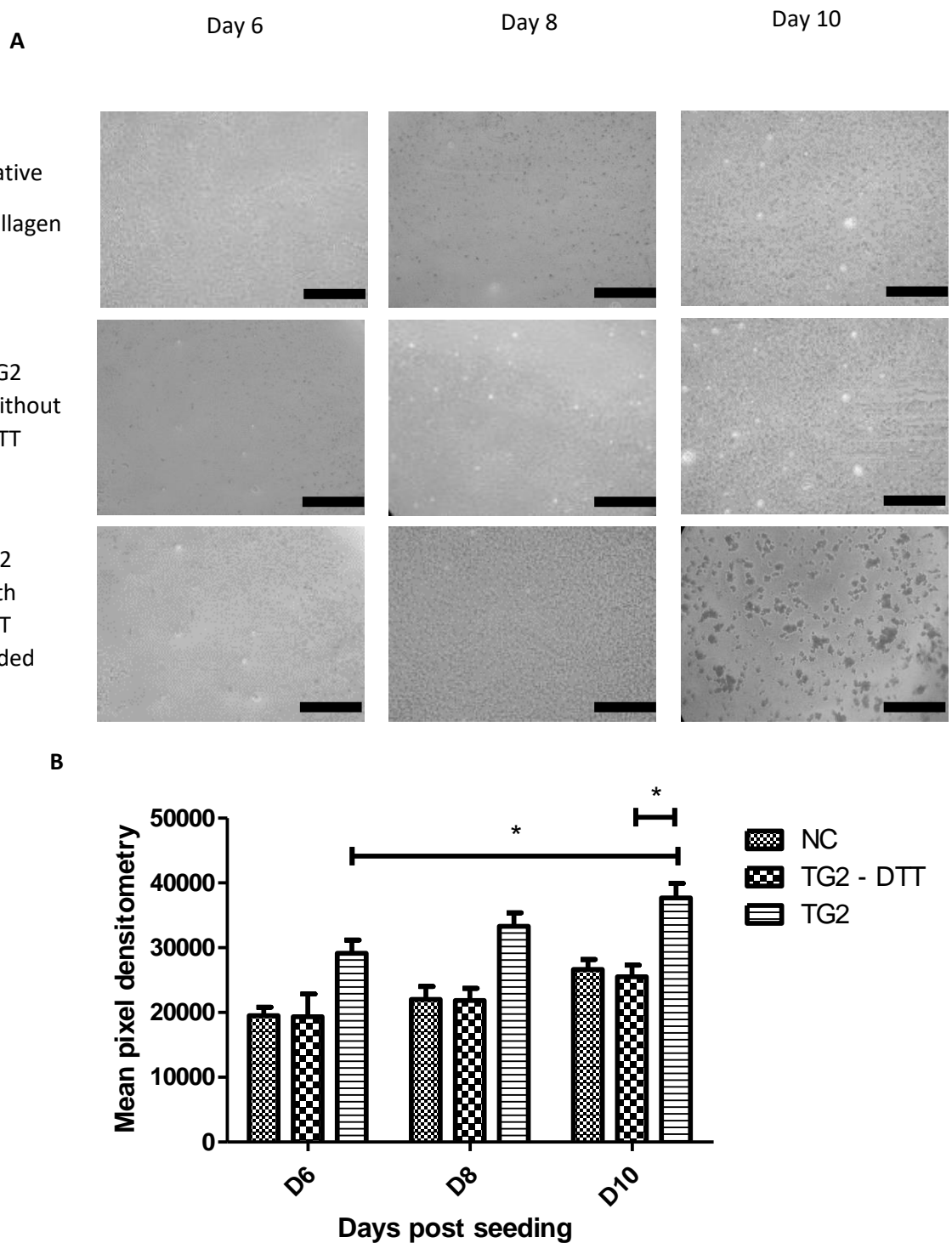


Figure 4.4: Mineralisation when HOBs were seeded onto TG2 crosslinked collagen without DTT. (A) HOBs were seeded onto native, 5 µg/ml TG2 and 5 µg/ml TG2 without 10 mM DTT crosslinked collagen (2.5mg/ml) and subjected to von Kossa staining on day 6, 8 and 10. The mineral depositions were stained in black and for all groups increased from day 6 to 10. Samples were viewed at x10 magnification using a Nikon CK2 and photographed with an Olympus DP10 digital camera. Scale bars= 200 µm. **(B)** The mineralised area was visualised by von Kossa staining and positive staining was quantified by ImageJ. The results represent mean values +/- S.D, where n=3. Statistical analysis was carried out using a one-way ANOVA test where the mean pixel densitometry of HOBs on native collagen scaffolds were compared to those seeded on crosslinked scaffolds. The p-values corresponding to P< 0.05 are represented with a *.

4.2.5 Mineralisation of HOBs when seeded onto TG2 crosslinked collagen without Calcium

In Figure 1.8 the effects of subtracting calcium and/or DTT from the TG2 collagen solution was observed. These samples show a similar macromolecular structure to native collagen due to the lack of crosslinks between collagen fibres. Calcium is needed for TG2 to become activated but to show that inactive TG2 does not affect mineralisation rates, a collagen scaffold that contained TG2 and DTT but no calcium was measured against one with TG2 and calcium but no DTT (Figure 4.5). There was a clear difference in HOBs seeded onto TG2 collagen scaffolds with calcium versus the samples without calcium. When HOBs were seeded onto collagen scaffolds with TG2 and calcium, there was a significantly higher amount of mineralisation taking place to that of HOBs seeded onto collagen with TG2 and no calcium by day 10, suggesting that TG2 in the active state is required for increased mineralisation to occur, most likely due to the enzyme catalysing crosslink bonds between collagen fibres.

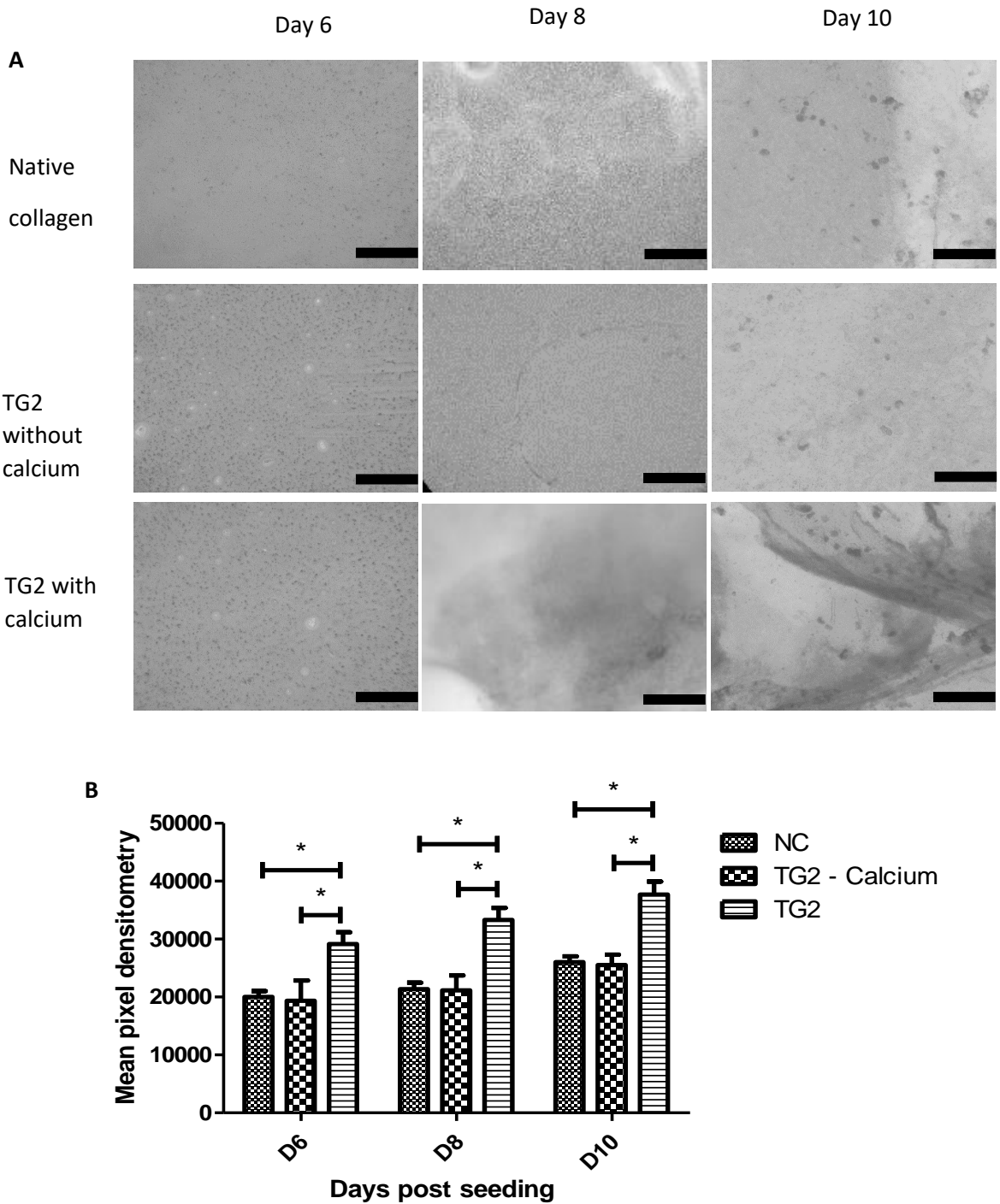


Figure 4.5: Mineralisation of HOBs when HOBs were seeded onto TG2 crosslinked collagen without calcium. (A) HOBs were seeded onto native, 5 µg/ml TG2 and 5 µg/ml TG2 without 20 mM Ca²⁺ crosslinked collagen (2.5 mg/ml) and subjected to von Kossa staining on day 6, 8 and 10. The mineral deposits were stained in black and for all groups increased from day 6 to 10. Samples were viewed at x10 magnification using a Nikon CK2 and photographed with an Olympus DP10 digital camera. Scale bars= 200 µm. **(B)** The mineralised area was visualised by von Kossa staining and positive staining was quantified by ImageJ. The results represent mean values +/- S.D, where n=3. Statistical analysis was carried out using a one-way ANOVA test where the mean pixel densitometry of HOBs on native collagen scaffolds were compared to those seeded on crosslinked scaffolds. The p-values corresponding to P<0.05 are represented with a *.

4.2.6 Mineralisation of HOBs when seeded onto TG2 crosslinked collagen without calcium and DTT

Having shown that both DTT and calcium are required for TG2 to crosslink collagen and an increase in mineralisation, samples of collagen alone (without DTT and calcium) were tested to see if TG2 alone would affect mineralisation. These scaffolds have already shown a similar macromolecular structure to native collagen due to the lack of crosslinks between collagen fibres. It was found that TG2 alone was not as effective at mineralising HOBs (when seeded on the scaffold for 10 days) and was comparable with cells grown on collagen.

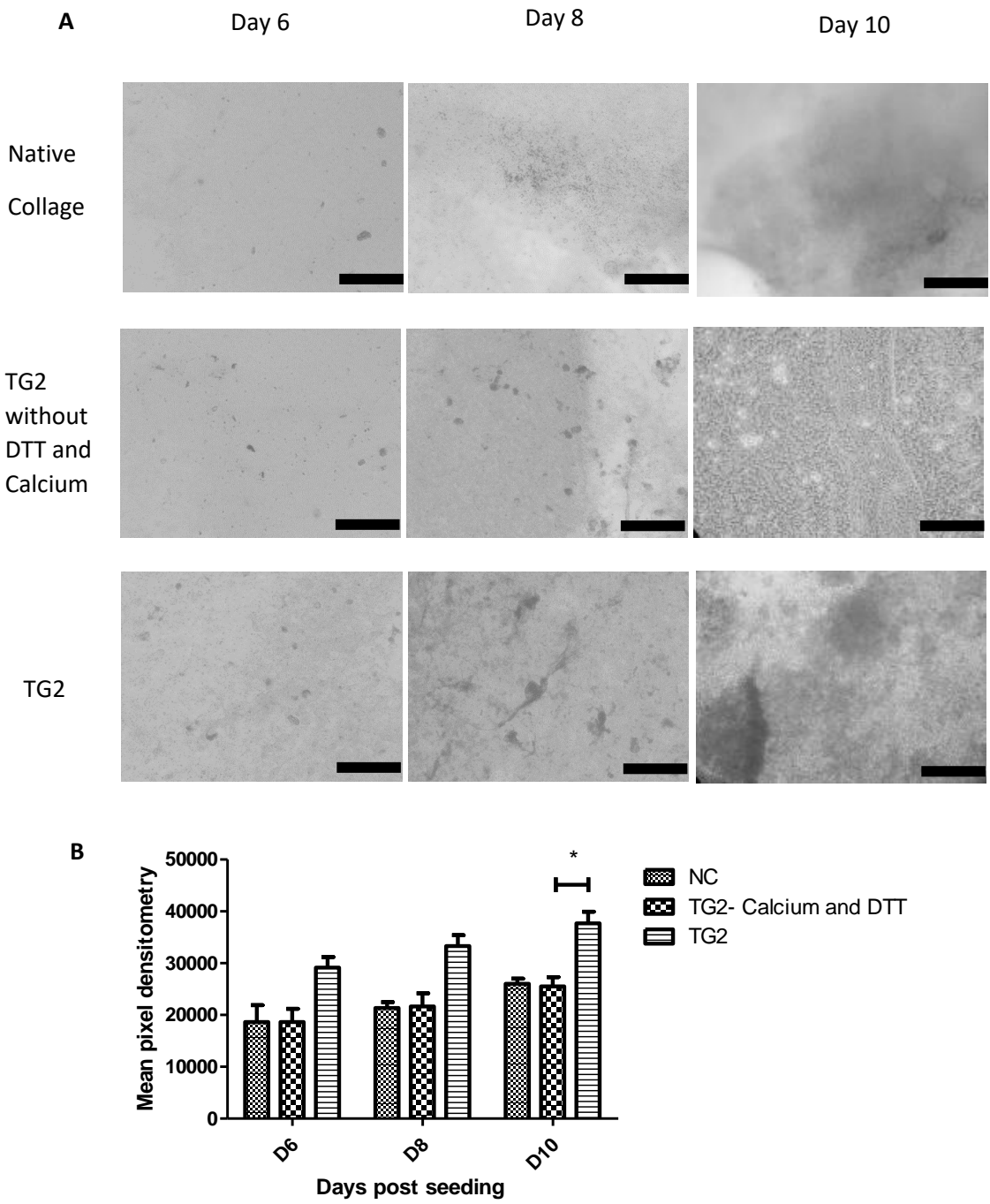


Figure 4.6: Mineralisation when HOBs were seeded onto TG2 crosslinked collagen without calcium and DTT. (A) HOBs were seeded onto native, 5 µg/ml, 5 µg/ml TG2 without DTT and Ca²⁺ and TG2 crosslinked collagen (2.5 mg/ml) and subjected to von Kossa staining on day 6, 8 and 10. The mineral deposits were stained in black and for all groups increased from day 6 to 10. Samples were viewed at x10 magnification using a Nikon CK2 and photographed with an Olympus DP10 digital camera. Scale bars= 200 µm. **(B)** The mineralised area was visualised by von Kossa staining and positive staining was quantified by ImageJ. The results represent mean values +/- S.D, where n=3. Statistical analysis was carried out using a one-way ANOVA test where the mean pixel densitometry of HOBs on native collagen scaffolds were compared to those seeded on crosslinked scaffolds. The p-values corresponding to P<0.05 are represented with a *.

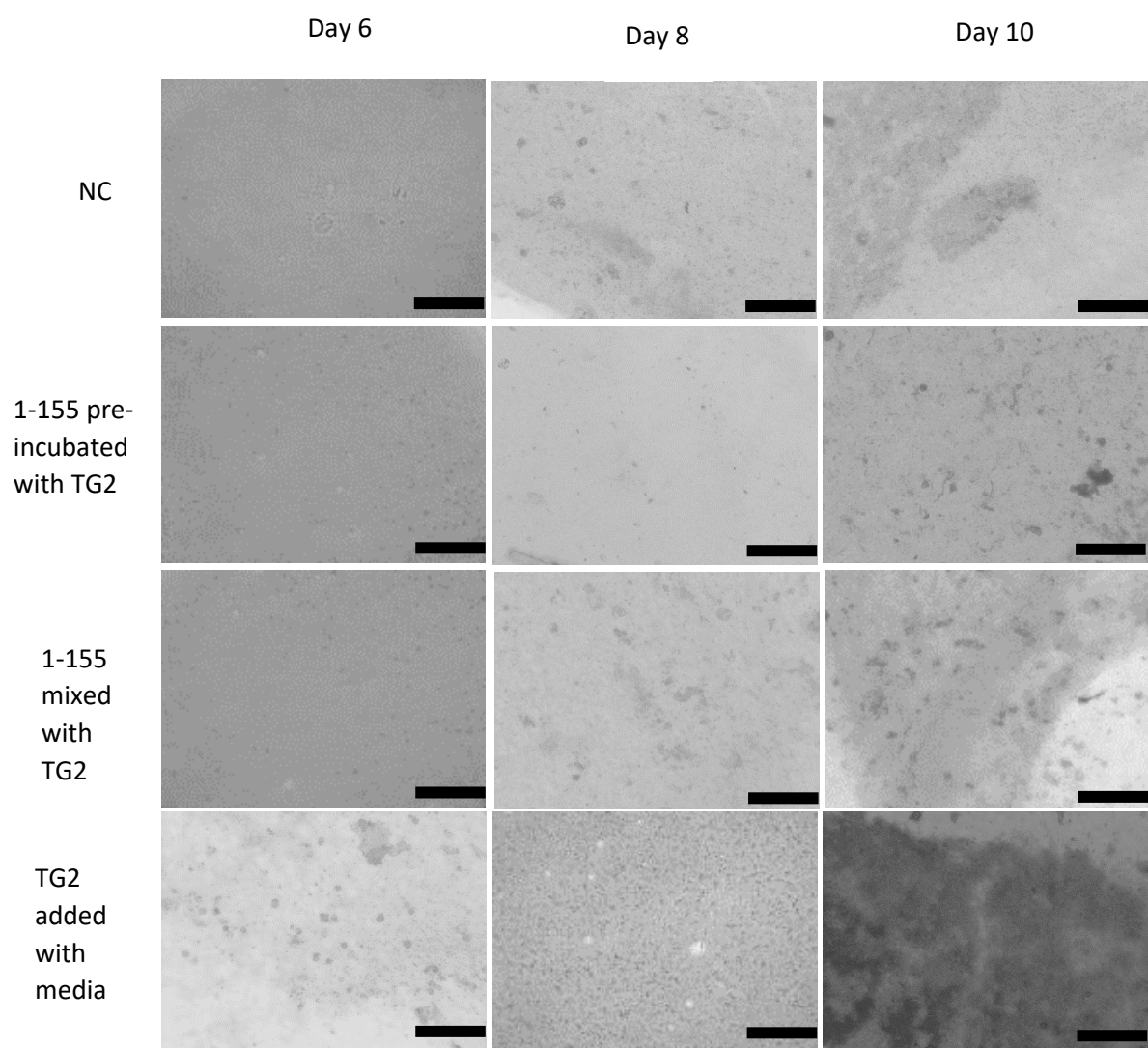
4.3 Characterising the mineralisation of collagen scaffolds with transglutaminases and transglutaminase inhibitors

4.3.1 Optimising the use of 1-155 inhibitor when cells are seeded onto TG2 crosslinked collagen

1-155 is described as a cell permeable, irreversible inhibitor that is a substrate analogue which binds at the active site to selectively inhibit TG2 activity (Zonca *et al.*, 2017). At a concentration of 25 μ M, it was shown to reduce activity of almost all of the 5 μ g/ml concentration of TG2. First, the method in which 1-155 was added to TG2 and collagen needed to be optimised. Three ways of adding the inhibitor to collagen and TG2 were assessed to establish the most efficient method to inhibit TG2 crosslinking ability.

- 1- 1-155 (25 μ M) was pre-incubated with active 5 μ g/ml TG2 for one hour on ice before this solution was added to collagen, 10X PBS and water and allowed to crosslink overnight (as described in materials and methods)
- 2- 1-155 (25 μ M) was added to the collagen mixture containing 5 μ g/ml TG2 and allowed to crosslink overnight (as described in materials and methods)
- 3- 1-155 (25 μ M) was added to cells seeded onto 2.5 mg/ml TG2 crosslinked collagen with media changes every 48 hours

The cells that were seeded onto crosslinked collagen where 1-155 was pre-incubated with TG2 showed a rate of mineralisation that was similar to cells seeded onto native collagen. There was more mineralisation shown in samples where 1-155 and TG2 was added to collagen mixture at the same time. This means that some of the TG2 was likely to have been inhibited but some remained active and therefore increased the amount of mineralisation in those samples compared to that seen in native collagen. However, adding 1-155 to the cells seeded onto TG2 crosslinked collagen had almost no effect.

A

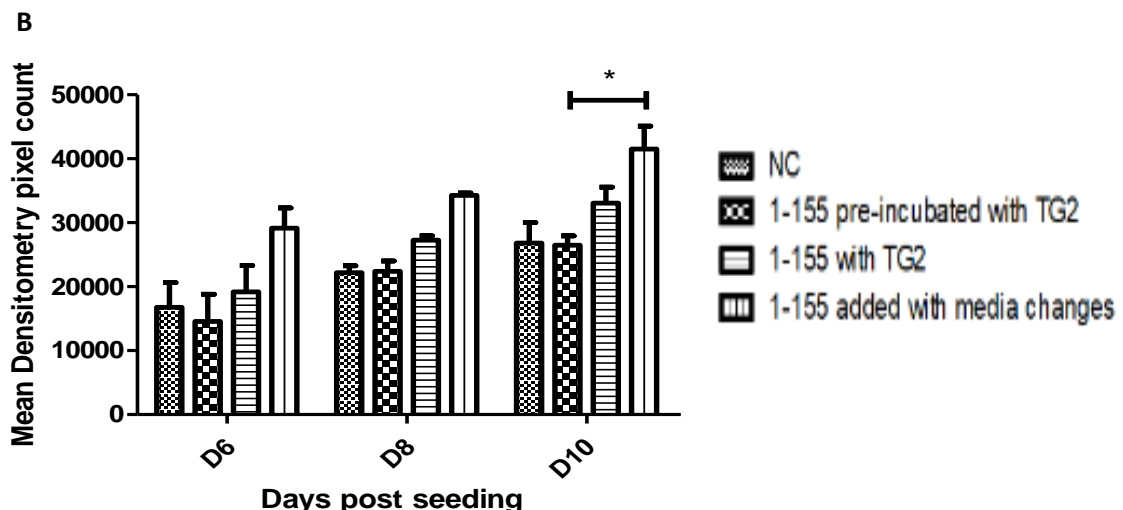


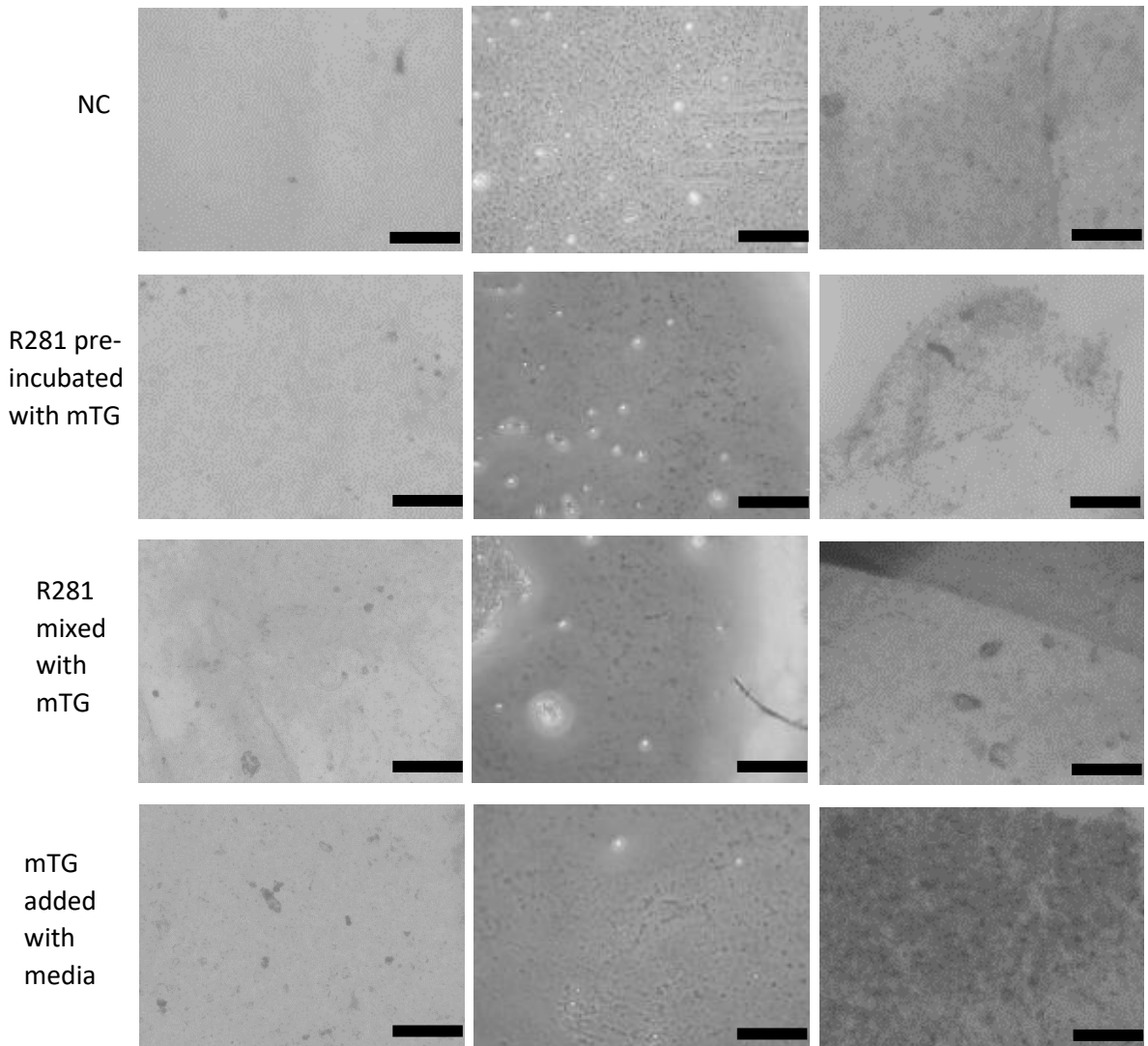
Figure 4.7: Mineralisation of HOBs when 1-155 was added to collagen. **(A)** HOBs seeded onto various collagen scaffolds were grown using differentiation medium. The mineral depositions were stained in black and for all groups increased from day 6 to 10. Samples were viewed at x10 magnification using a Nikon CK2 and photographed with an Olympus DP10 digital camera. Scale bars= 200 μ m. **(B)** The mineralised area was visualised by von Kossa staining and positive staining was quantified by ImageJ. The results represent mean values +/- S.D, where n=3. Statistical analysis was carried out using a one-way ANOVA test where the mean pixel densitometry of HOBs on native collagen scaffolds were compared to those seeded on inhibited crosslinked scaffolds the p-values corresponding to P< 0.05 are represented with a *.

4.3.2 Optimising the use of R281 inhibitor when cells are seeded onto mTG crosslinked collagen

In the previous chapter, R281 was described as a non-cell-permeable inhibitor which has been reported by Zonca (Zonca *et al.* 2017) to inhibit both TG2 and mTG. It was shown that R281 can almost completely inhibit mTG activity when incubated with the enzyme at 250 μ M. As with 1-155 and TG2, the method in which R281 was added to mTG and collagen needed to be optimised. Three ways of adding the inhibitor to collagen and mTG were investigated.

- 1- R281 (250 μ M) was pre-incubated with active 5 μ g/ml mTG for one hour on ice before this solution was added to collagen, 10X PBS and water and allowed to crosslink overnight (as described in methods in materials)
- 2- R281 (250 μ M) was added to the collagen mixture containing 5 μ g/ml mTG and allowed to crosslink overnight (as described in methods in materials)
- 3- R281 (250 μ M) was added to cells seeded onto 2.5 mg/ml mTG crosslinked collagen with media changes every 48 hours

A Day 6 Day 8 Day 10



B

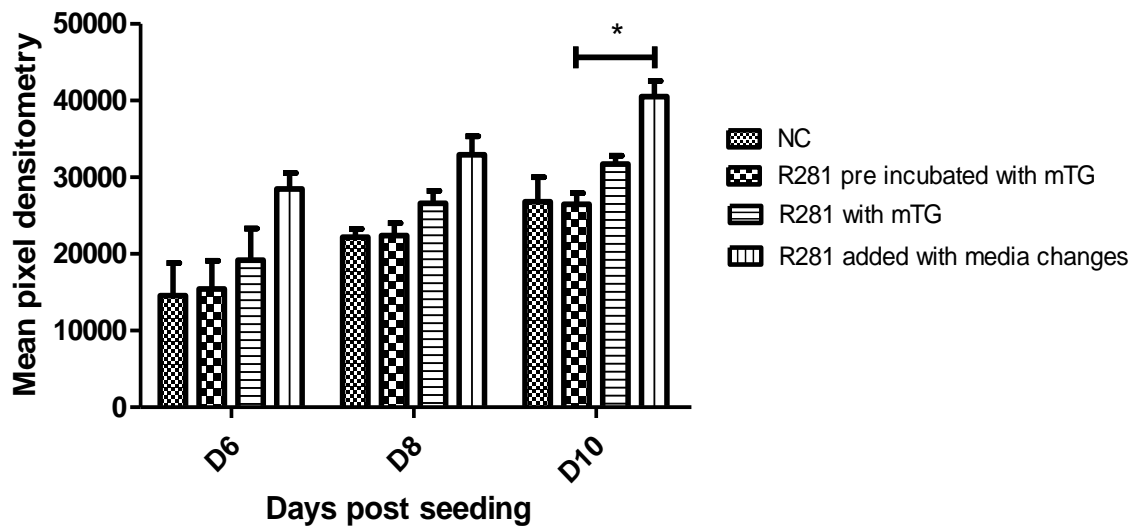
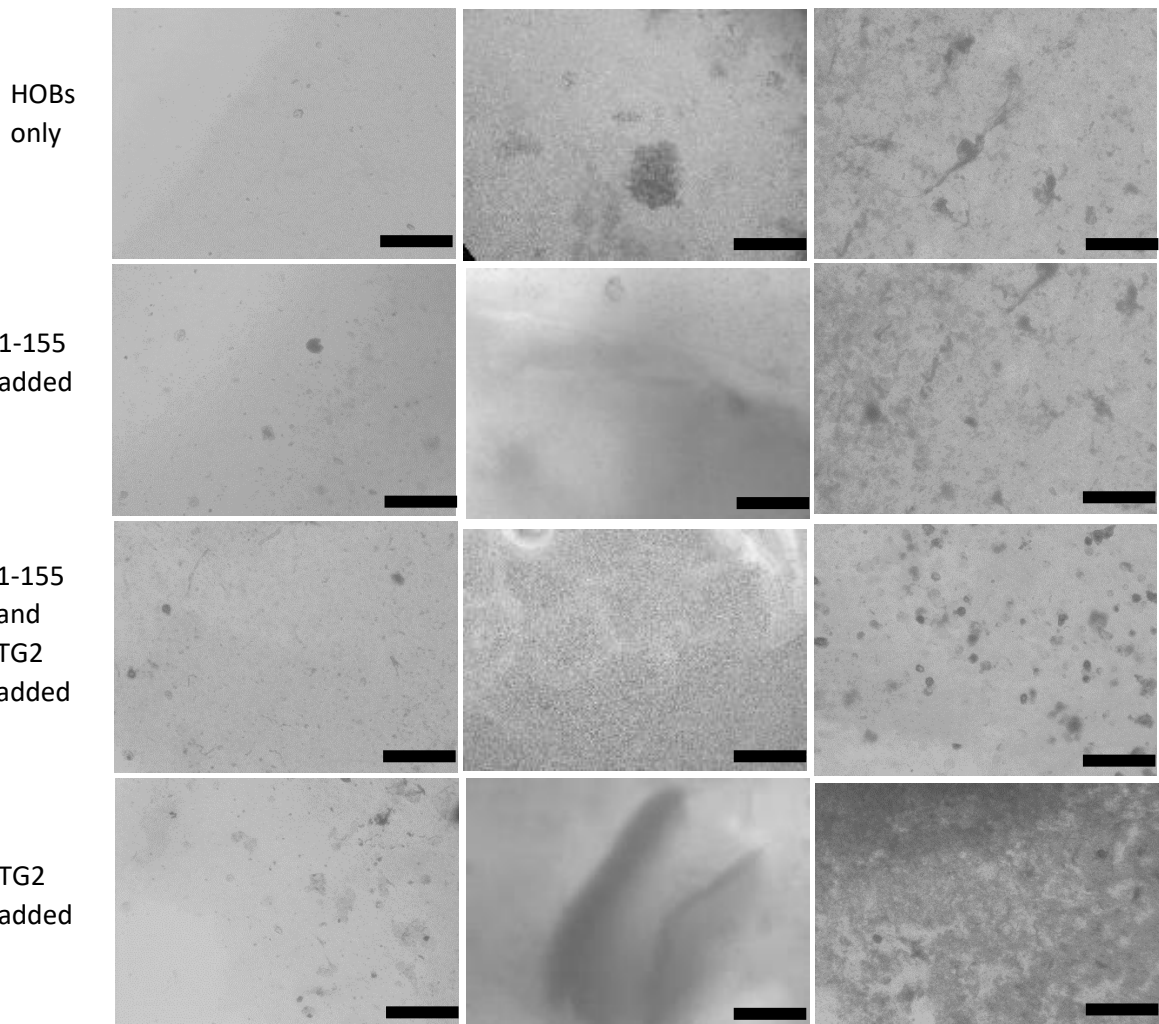


Figure 4.8: Mineralisation of HOBs when R281 was added to collagen. (A) HOBs seeded onto various collagen scaffolds were grown using differentiation medium. The mineral depositions were stained in black and for all groups increased from day 6 to 10. Samples were viewed at x10 magnification using a Nikon CK2 and photographed with an Olympus DP10 digital camera. Scale bars= 200 μ m. **(B)** The mineralised area was visualised by von Kossa staining and positive staining was quantified by ImageJ. The results represent mean values +/- S.D, where n=3. Statistical analysis was carried out using a one-way ANOVA test where the mean pixel densitometry of HOBs on native collagen scaffolds were compared to those seeded on inhibited crosslinked scaffolds the p-values corresponding to P< 0.05 are represented with a *.

4.3.3 Assessing the mineralisation effect of 1-155 on HOBs

In this experiment, 1-155 was added to HOBs alone in order to determine whether its presence alone had any effect on the mineralisation rates of HOBs after 6, 8 and 10 days (Figure 4.9). It was clear that there was no statistically significant difference between mineralisation rates between cells and cells with 25 µM 1-155 added. When comparing samples where cells had TG2 added versus both TG2 and 1-155 added there was a clear difference. Cells where 1-155 and TG2 were added showed similar rates of mineralisation to that of cells alone and the cells where 1-155 was added.

A Day 6 Day 8 Day 10



B

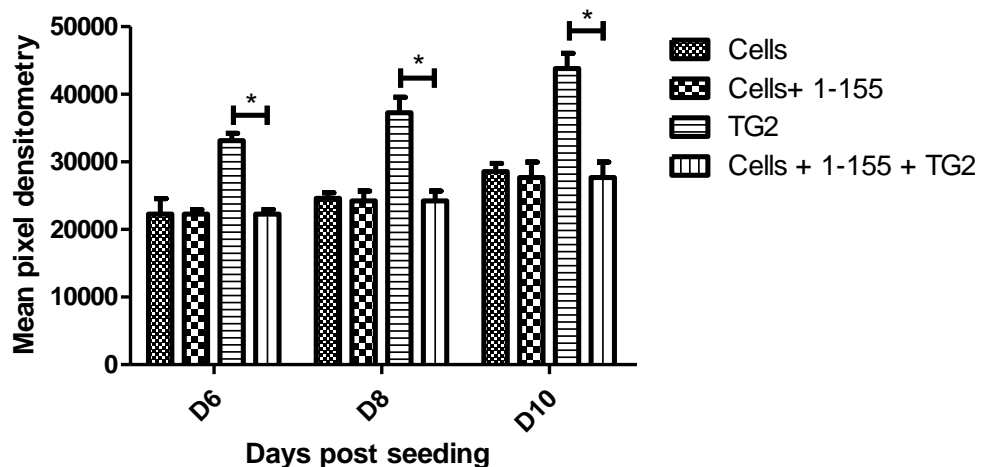
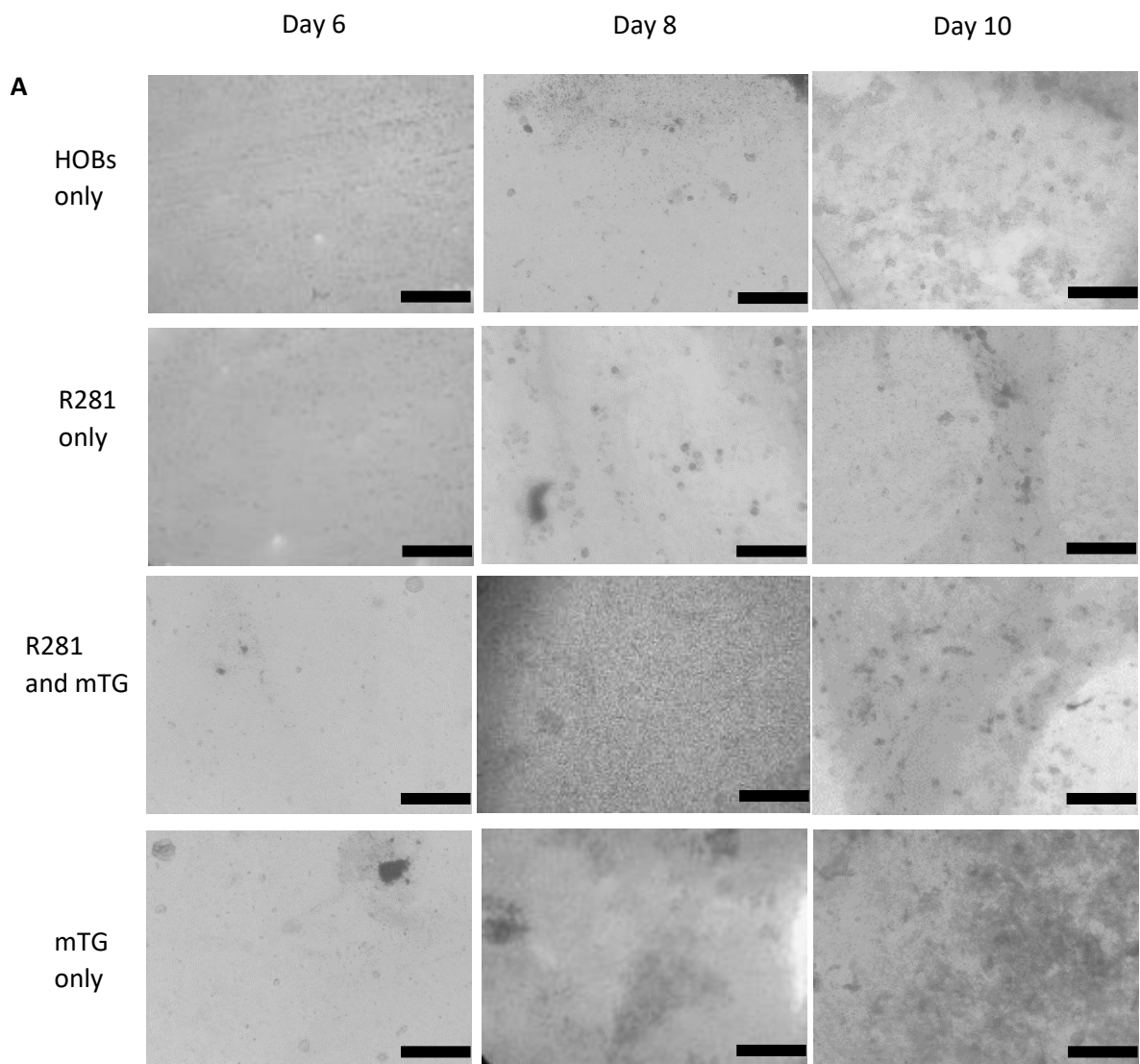


Figure 4.9: Mineralisation of HOBs when 1-155 was added. (A) HOBs, HOBs with 25 μM 1-155, HOBs with 5 $\mu\text{g/ml}$ TG2 and HOBs with 25 μM 1-155 and 5 $\mu\text{g/ml}$ TG2 were subjected to von Kossa staining on day 6, 8 and 10. The mineral depositions were stained in black and for all groups increased from day 6 to 10. Samples were viewed at $\times 10$ magnification using a Nikon CK2 and photographed with an Olympus DP10 digital camera. Scale bars= 200 μm . **(B)** The mineralised area was visualised by von Kossa staining and positive staining was quantified by ImageJ. The results represent mean values +/- S.D, where n=3. Statistical analysis was carried out using a one-way ANOVA test where the mean pixel densitometry of HOBs on native collagen scaffolds were compared to those seeded on inhibited crosslinked scaffolds p-values corresponding to $P < 0.05$ are represented with a *.

4.3.4 Assessing the effect of R281 on mineralisation of HOBs

In this experiment, R281 was added to HOBs in order to determine whether its presence alone had any effect on the mineralisation rates of HOBs after 6, 8 and 10 days. It was clear from Figure 4.10 that there were no statistically significant changes between mineralisation rates between cells and cells with 250 µM R281 added. When comparing samples where cells had mTG added versus both mTG and R281 added there was a clear difference. Cells where R281 and mTG added showed similar rates of mineralisation to that of cells alone and the cells where R281 was added.



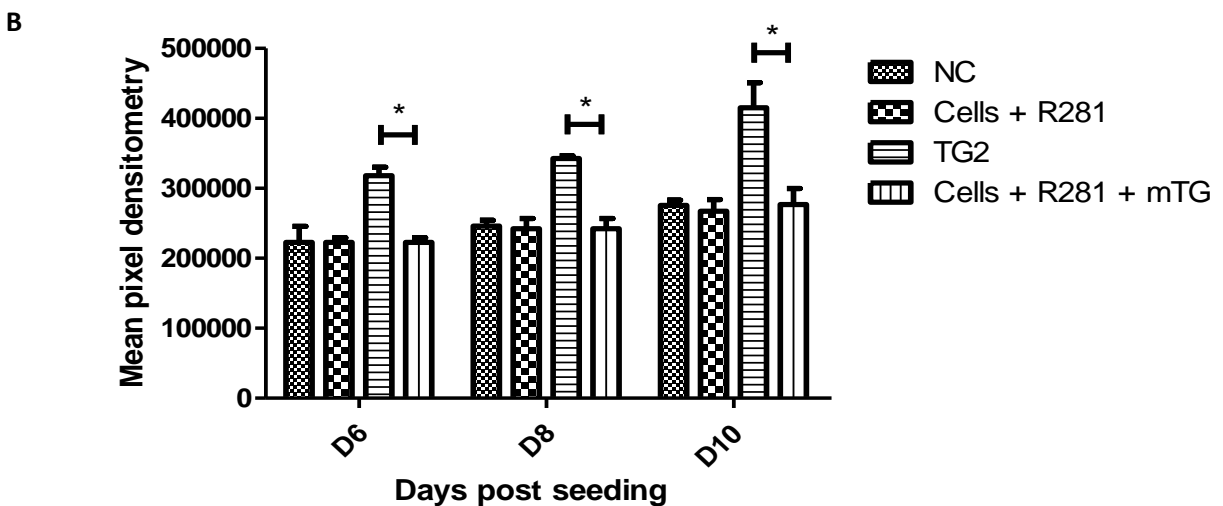


Figure 4.10: Mineralisation of HOBs when R281 was added. (A) HOBs, HOBs with 250 µM R281, HOBs with 5 µg/ml mTG and HOBs with 250 µM R281 and 5 µg/ml mTG were subjected to von Kossa staining on day 6, 8 and 10. The mineral depositions were stained in black and for all groups increased from day 6 to 10. Samples were viewed at x10 magnification using a Nikon CK2 and photographed with an Olympus DP10 digital camera. Scale bars= 200 µm (B) The mineralised area was visualised by von Kossa staining and positive staining was quantified by ImageJ. The results represent mean values +/- S.D, where n=3. Statistical analysis was carried out using a one-way ANOVA test where the mean pixel densitometry of HOBs on native collagen scaffolds were compared to those seeded on inhibited crosslinked scaffolds. The p-values corresponding to P< 0.05 are represented with a *.

4.3.5 Mineralisation of HOBs on mTG crosslinked collagen with 1-155

It has already been shown that R281 can inhibit both mTG and TG2 (Zonca *et al.*, 2017) but it is unknown if 1-155, which inhibits TG2, can also inhibit mTG activity. In order to determine whether 1-155 inhibits or decreases mineralisation by cells seeded onto mTG crosslinked collagen, mineralisation rates of HOBs after 6, 8 and 10 days were assessed. It was clear that there was a statistically significant change in the mineralisation rates of HOBs seeded on native collagen and cells with 1-155 (25 µM) and mTG added to the collagen. When comparing samples where HOBs were seeded onto active mTG crosslinked collagen versus HOBs seeded onto mTG with 1-155 in collagen, there was no clear difference.

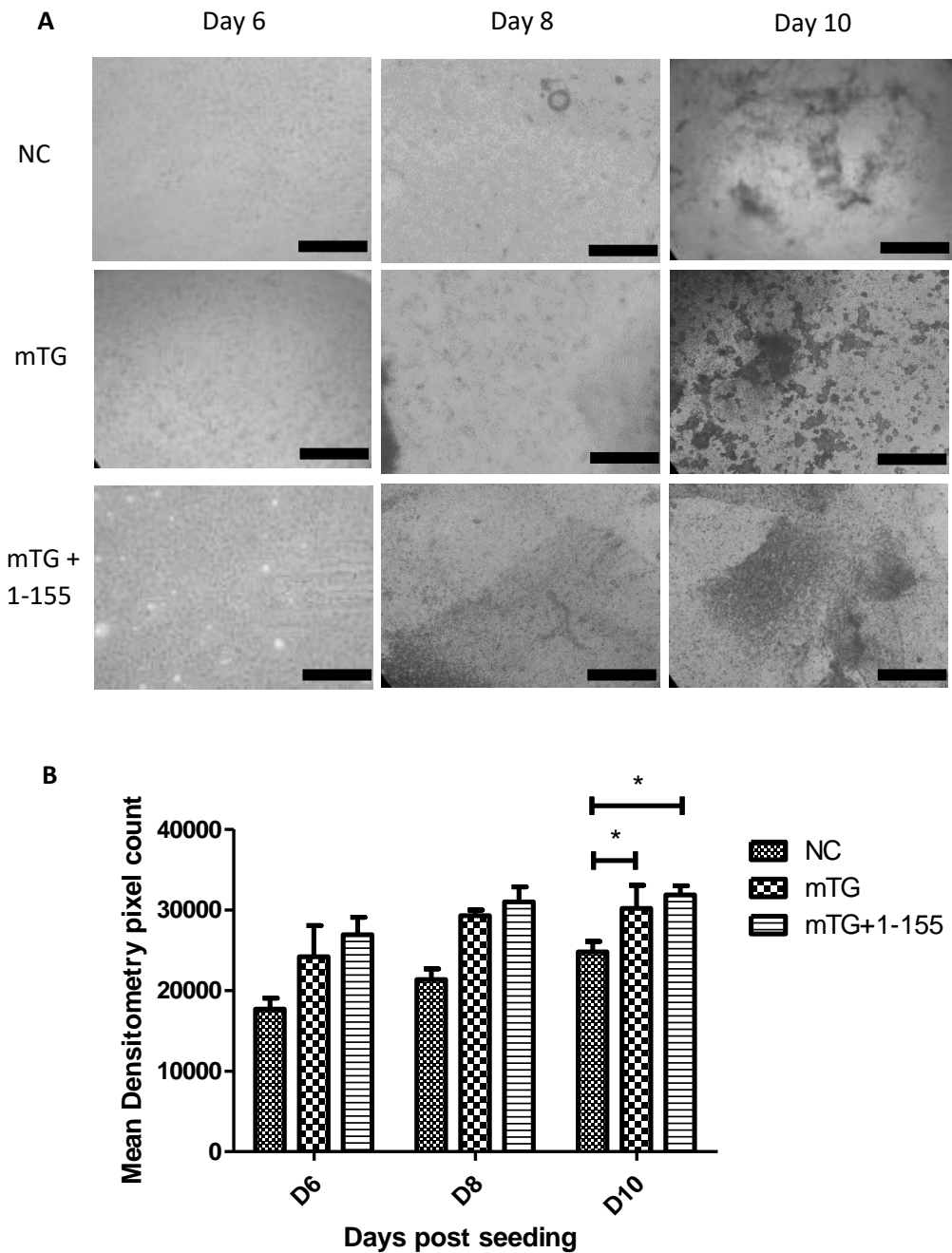


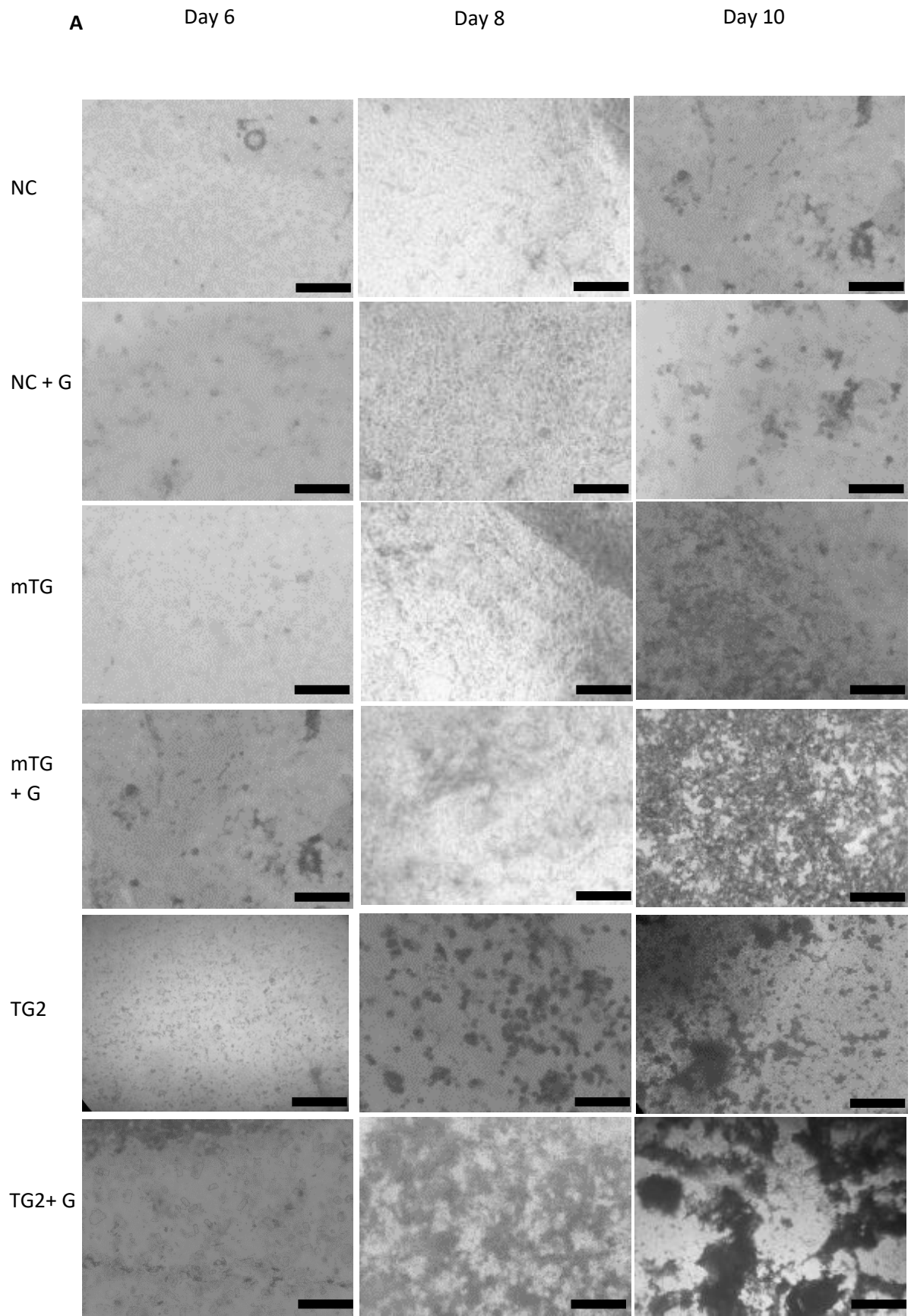
Figure 4.11: Mineralisation of HOBs when 1-155 was added to mTG crosslinked collagen. **(A)** HOBs seeded onto collagen scaffolds with mTG and mTG with 1-155 were grown using differentiation medium. The mineral depositions were stained in black and for all groups increased from day 6 to 10. Samples were viewed at x10 magnification using a Nikon CK2 and photographed with an Olympus DP10 digital camera. Scale bars= 200 μ m. **(B)** The mineralised area was visualised by von Kossa staining and positive staining was quantified by ImageJ. The results represent mean values +/- S.D, where n=3. Statistical analysis was carried out using a one-way ANOVA test where the mean pixel densitometry of HOBs on native collagen scaffolds were compared to those seeded on crosslinked scaffolds. The p-values corresponding to $P < 0.05$ are represented with a *

4.4 Assessing the mineralisation of HOBs on crosslinked collagen and crosslinked collagen mixed with glass

4.4.1 Comparing the mineralisation rates between collagen scaffolds with transglutaminases and 45S5 bioglass particles

Now that the mineralisation rates for HOBs seeded onto crosslinked collagen has been established the next variable to be assessed was how they might mineralise differently if seeded onto native and crosslinked scaffolds with 10 mg/ml 45S5 bioglass particles.

When the mineralisation assay was carried out it was shown that when TG2 and mTG were mixed with collagen and bioglass particles a statistically significant higher amount of mineralisation took place when compared to the native collagen scaffold. However, there was no significance when comparing mineralisation between native collagen and native collagen mixed with bioglass particles.



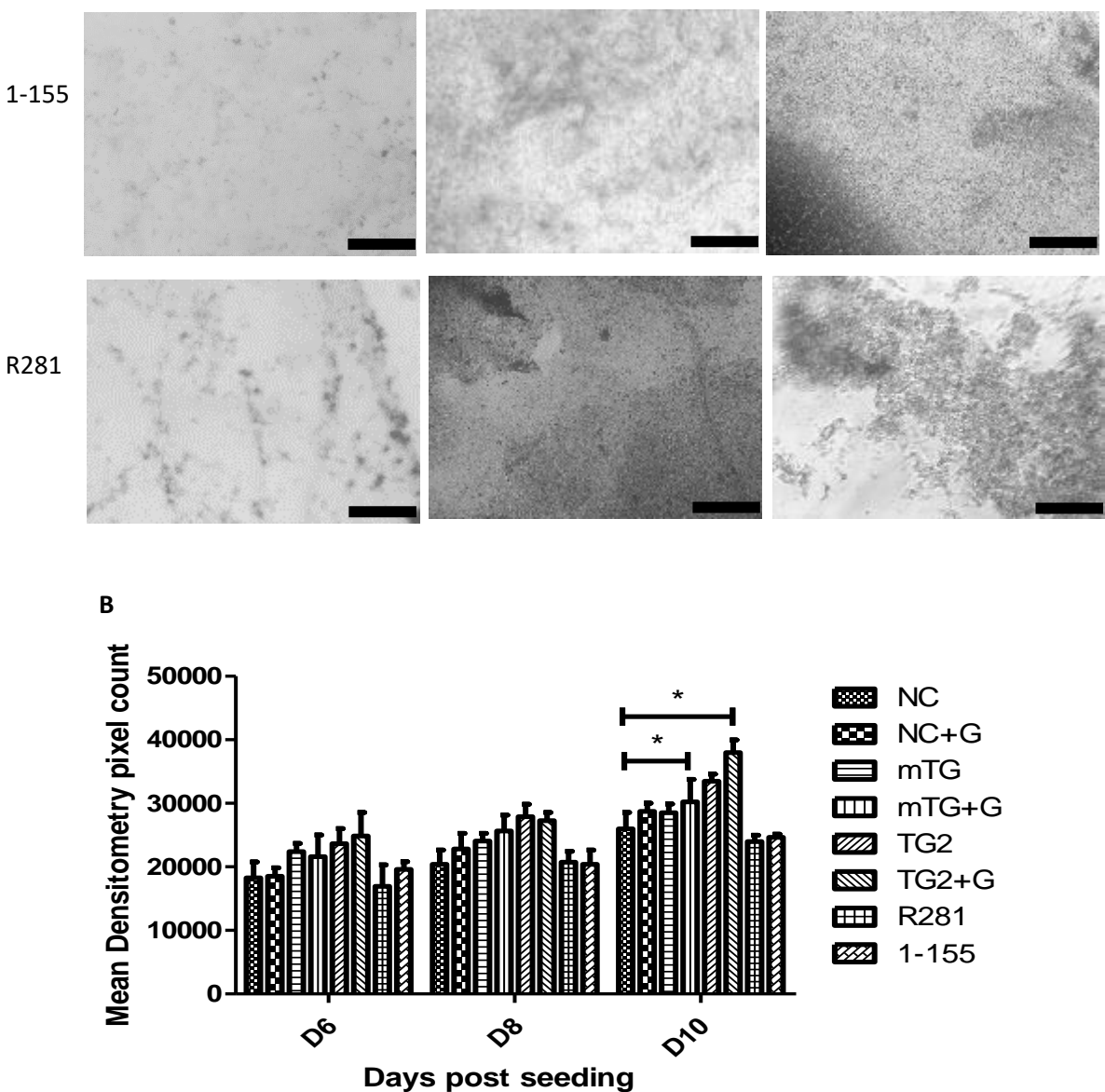
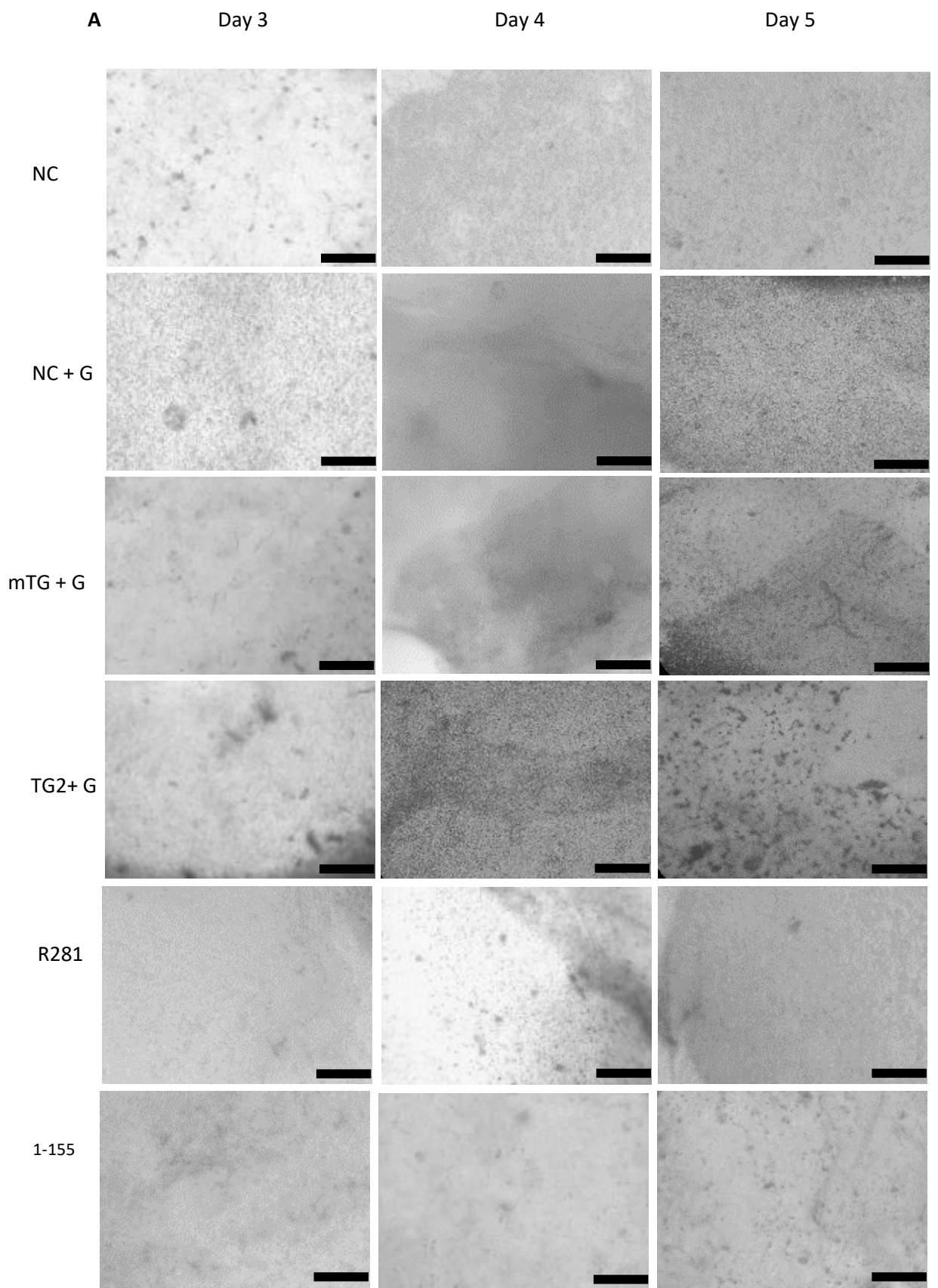


Figure 4.12: Mineralisation of HOBs when seeded onto native and crosslinked collagen with 45S5 bioglass particles. (A) HOBs seeded onto native and crosslinked collagen scaffolds which were grown using differentiation medium. The mineral deposits were stained in black and for all groups increased from day 6 to 10. Samples were viewed at x10 magnification using a Nikon CK2 and photographed with an Olympus DP10 digital camera. Scale bars= 200 µm. (B) The mineralised area was visualised by von Kossa staining and positive staining was quantified by ImageJ. From left to right: Native collagen, native collagen mixed with bioglass, mTG crosslinked scaffold, mTG crosslinked scaffold mixed with bioglass, TG2 crosslinked scaffold, TG2 crosslinked scaffold mixed with bioglass, R281 inactivated mTG scaffold and 1-155 inactivated TG2 scaffold. The results represent mean values +/- S.D, where n=3. Statistical analysis was carried out using a one-way ANOVA test where the mean pixel densitometry of HOBs on native collagen scaffolds were compared to those seeded on crosslinked scaffolds with and without bioglass. The p-values corresponding to P< 0.05 are represented with a *.

4.4.2 Assessing the mineralisation rates between collagen scaffolds with transglutaminases and 45S5 bioglass particles at earlier time points

In the previous chapter, the XTT cell proliferation analysis of cells grown on TG2 crosslinked collagen showed a slight fall in absorbance by day 6. We hypothesise that this is not a sign that the cells find the ECM to be toxic, since absorbance was increasing up until the last day it was measured. Instead, it may have decreased because cells seeded onto the crosslinked collagen have mineralised and differentiated quicker than on native collagen. To test this theory, the mineralisation rate of cells on native collagen and on crosslinked collagen with glass were measured before the normal 6 day starting point. As shown below, there was a clear statistical difference between the mineralisation rate between native collagen and crosslinked collagen with bioglass particles.



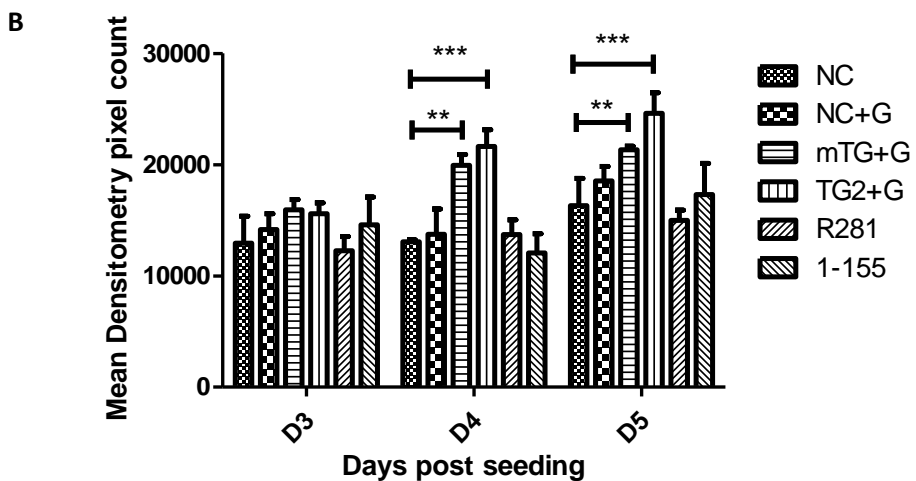


Figure 4.13: Mineralisation of HOBs when seeded onto native and crosslinked collagen with 45S5 bioglass particles over 5 days. (A) HOBs seeded onto native and crosslinked collagen scaffolds which were grown using differentiation medium. The mineral deposits were stained in black and for all groups increased from day 3 to 5. Samples were viewed at x10 magnification using a Nikon CK2 and photographed with an Olympus DP10 digital camera. Scale bars= 200 μ m. **(B)** The mineralised area was visualised by von Kossa staining and positive staining was quantified by ImageJ. The results represent mean values +/- S.D, where n=3. Statistical analysis was carried out using a one-way ANOVA test where the mean pixel densitometry of HOBs on native collagen scaffolds were compared to those seeded on crosslinked scaffolds with and without bioglass. The p-values corresponding to P< 0.01 are represented with a ** and where p< 0.001 is represented with ***.

4.5 Crosslinked collagen deposition by human osteoblasts

4.5.1 Quantification of crosslinked collagen when transglutaminases are added to HOBs on plastic tissue

To assess collagen deposition by HOBs, cells were allowed to grow on tissue culture plastic for 10 days in differentiation medium before being discarded. From the remaining matrix bound to the plastic wells, the proteins were digested with pepsin. Samples were then loaded onto a 5% acrylamide gel. Using the Silver Quest staining kit (see Materials and Methods) the collagen was then stained and imaged using G-box.

Figure 4.14 shows that there was a difference in the collagen deposited in the ECM between the control samples and samples where 5 µg/ml of TG2 and mTG was added to the samples every 48 hours.

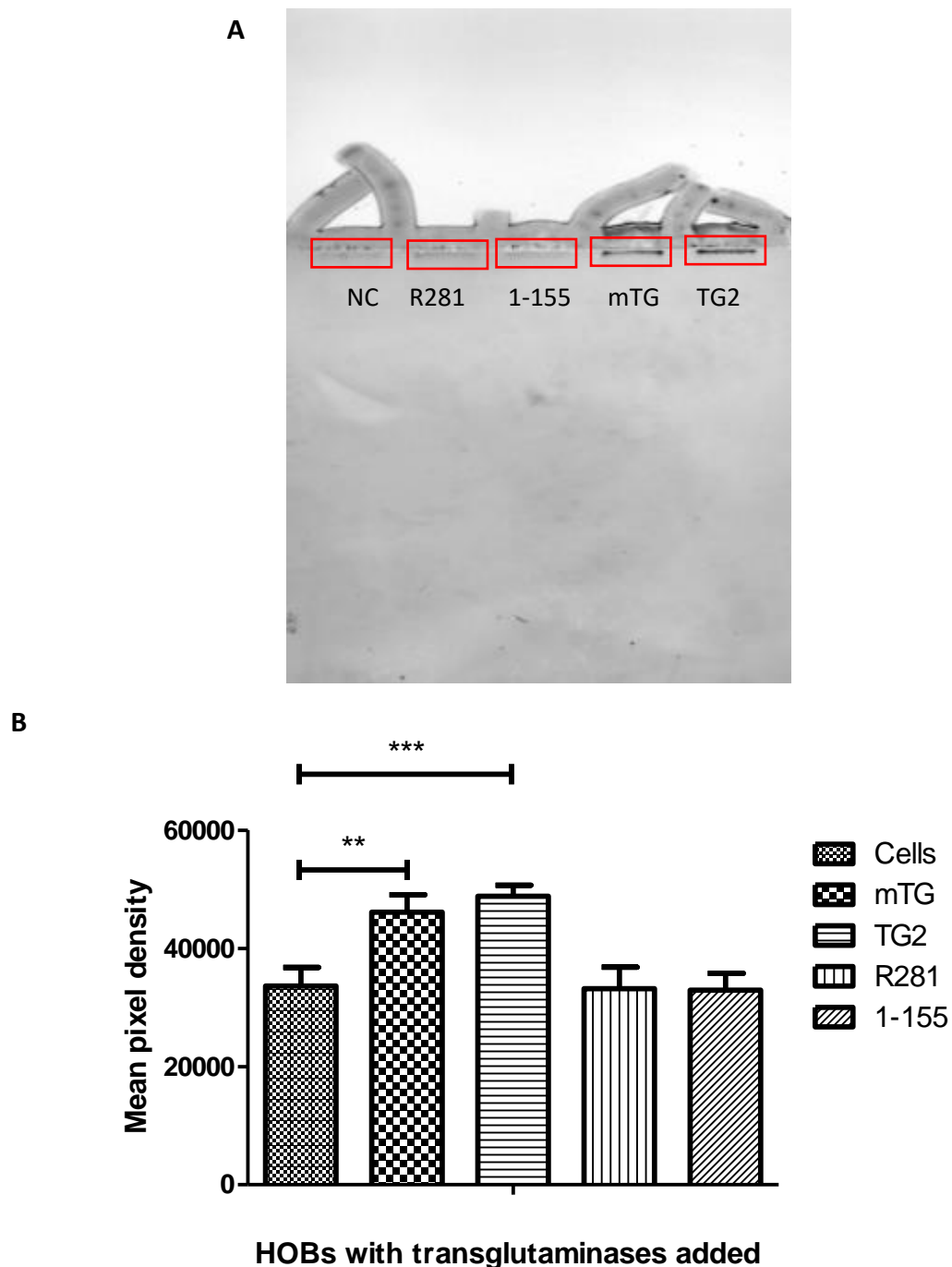


Figure 4.14: HOB production of collagen in the Extracellular matrix. (A) Cells were removed from the wells 10 days post seeding. Resulting ECM was digested and samples and ran on 5% bis-acrylamide gel before being stained for collagen using Silver Quest staining kit. A representative gel is shown where the red boxes indicated the bands analysed. (B) Normalised collagen expression was plotted where the results represent mean values +/- S.D, where n=3. Statistical analysis was carried out using a one-way ANOVA test where the mean pixel densitometry of bands representing collagen deposition by HOBs were compared to those seeded with TGs. The p-values corresponding to P< 0.001 are represented with *** and p-values corresponding to P<0.01 are represented with **.

4.6 Discussion

The bone formation process is carried out by osteoblasts under the control of hormones and cytokines in the extracellular matrix of bone. The bone matrix itself is mostly made up of type 1 collagen, which is secreted from osteoblasts and assembled into macromolecular structures to give bone its tensile strength and to act as a scaffold for mineralisation and cell adhesion (Al-Jallad *et al.* 2006). One of the many non-collagenous proteins shown to reside within bone matrix are transglutaminases (which, as stated previously, are capable of linking primary amines to specific glutamine residues of its protein substrates). In this case TG2 and mTG are used to crosslink collagen to non-collagenous matrix components such as fibronectin and osteopontin *in vitro* (Kaartinen *et al.* 1999). It has been suggested, that by stabilising the matrix further (via crosslinking in this manner) mineralisation and cell adhesion are increased (Lorand and Graham, 2003; Nurminskaya *et al.* 2003; Akimov *et al.* 2000; Fortunati *et al.* 2014). We have shown in this chapter how mineralisation on tissue culture plastic begins around 6 days post seeding and increases until a plateau is reached approximately after 10 days.

We have shown that when mTG and TG2 are added to HOBs on tissue culture plastic, there is a significant increase in mineralisation compared to HOBs alone. It has also been thought that TG2 in the extracellular environment could trigger a signal from the outside to the cell to begin mineralisation (Nurminskaya *et al.* 2003). This was later backed up by studies carried out by Faverman *et al.* who showed that LRP5 binds to TG2, triggering the Wnt non-canonical pathway. Once activated, this pathway leads to the release of β -catenin from the cytoplasm into the nucleus. This translocation of β -catenin causes TCF/LEF transcription factors to be released from the DNA and triggers HOB mineralisation (Faverman *et al.*, 2008). We hypothesise that TG2 binds to LRP5 on HOBs as well as crosslinking the matrix laid down in the ECM over time by HOBs. In contrast, mTG only crosslinks the ECM matrix and does not bind to LRP5 and therefore has less of an effect on mineralisation than TG2.

The data strongly suggests that the crosslinking of collagen has had a positive effect on mineralisation. This could be due to an increase in the expression of $\alpha V\beta 3$ integrins that regulate cell proliferation and maturation. Also further stabilisation of the collagen matrix allows for greater cell adherence and proliferation. The crosslinking of collagen has already been shown to increase the mechanical strength of the overall scaffold compared to native collagen scaffolds (Chau, 2005; Fortunati *et al.* 2014). Moreover, investigations have shown mesenchymal stem cells (MSCs) will change their differentiation fate depending on the elasticity of the surface they are seeded on (Discher *et al.*, 2007). Discher *et al.* found that native MSCs would commit to osteogenic cell pathways if seeded on collagen that was crosslinked on relatively stiff matrices. This would explain why HOBs seeded on stiffer, crosslinked collagen show higher levels of mineralisation.

As expected, removing calcium from TG2 collagen scaffolds led to a mineralisation that was similar to that of native collagen mineralisation. Interestingly, the absence of DTT from the TG2 samples led to a decrease in mineralisation. This suggests that TG2 must be active in order to allow for a statistically significant increase in mineralisation. This implies that TG2 protein alone cannot be responsible for increased mineralisation.

The data in this chapter show that either R281 or 1-155, when added to cells will not have any effect on HOB mineralisation. When added along with mTG or TG2, there is sufficient inactivation taking place to reduce the mineralisation rates of those samples to that seen in the control HOB sample. It has been shown in the literature that R281 can inhibit both TG2 and mTG activity (Zonca *et al.*, 2017), whereas our data show that only TG2 is inhibited by 1-155.

Although HOBs on both mTG and TG2 crosslinked collagen mineralised more than those on native collagen, there was still a difference in mineralisation rates. This could be explained by the differences seen in the stiffness between the two crosslinked collagen scaffolds (Lee *et al.*, 2013, Grover *et al.*, 2012, Chau *et al.*, 2005). These differences may lead to HOBs reacting differently to the differences in stiffness (Pawelec *et al.*, 2015), causing different rates of mineralisation (Discher *et al.*, 2007). It has been reported that epithelial cells

seeded on stiffer matrices also upregulate expression of LRP5/6, which could explain the upregulation seen on HOBs seeded on crosslinked collagen (Han *et al.*, 2016).

Another reason for this difference in mineralisation rate could be explained by differences in the mean collagen pore size as observed in Chapter 3. Given that HOBs on average are 20-30µm in length (Wheless *et al.* 2016) and the gaps between collagen fibres are nanometres apart, the amount of contact that each HOB has on collagen fibres is different between the scaffolds. The changes in distance between collagen fibres or pore alignment is known in the literature to be a signalling cue to osteoblasts (Ashworth *et al.*, 2016, Pawelec *et al.*, 2015). These signalling cues in turn influence cell behaviour and induce migration and matrix production. Given the increased contact that HOBs on crosslinked collagen have this could contribute to the increased integrin expression seen in Chapter 5 (Grover *et al.*, 2012).

If increased surface area seen on crosslinked collagen increase mineralisation of HOBs, then adding 45S5 bioglass would also give more surface area for HOBs to adhere to in the overall ECM. Furthermore, from multiple studies it is established that 45S5 bioglass will bond to soft tissues as well as bone (Hench *et al.*, 1972, Hench, 1993). Once implanted, the surface of the 45S5 bioglass forms a biologically active hydroxycarbonate apatite (HCA layer) this is crucial to providing the bonding interface with tissues. The HCA phase that is formed on the bioglass is the chemical and structural equivalent of the mineral phase in bone, which in turn induces cells to mineralise (Hench, 1993).

Finally, when mTG and TG2 were added to collagen mixed with bioglass, there was an early (day 5) and significant increase in mineralisation this increased rate is shown to start as early as day 4-5. Briefly, ion/leaching/exchange and dissolution of the bioglass network and precipitation/growth of the calcium deficient HCA layer encourages the colonisation and proliferation of osteoblasts (Hench, 1993). These findings by Hench and Xynos could explain why increased mineralisation was found in the collagen samples with 45S5 bioglass. One interesting observation is that when bioglass is added to native collagen alone, there was an increase in mineralisation but this was not shown to be statistically significant. It should also be noted that when TGs are added to HOBs grown on culture that after 10 days there seems

to be more exogenous type 1 collagen found in the ECM. This could possibly be leading to a positive feedback cycle, since HOBs are able to make more contact (via cell surface and integrins) to collagen which stimulates further proliferation and mineralisation.

To summarise, the effect of TG2 increasing mineralisation of HOBs is only seen when the enzyme is active and reduced (by calcium and DTT respectively). Similarly, when mTG is active there is a significant increase in mineralisation seen in collagen scaffolds too. The addition of bioglass particles further increases mineralisation of HOBs on crosslinked collagen scaffolds and this is likely due to HOBs interacting with the HCA layer that is formed between bioglass particles and HOBs.

**Chapter 5: Intracellular effects of seeding
HOBs on novel crosslinked collagen scaffolds**

5.1 Introduction

In the ECM, there are a variety of cues that are interpreted by cells that lead to different integrins being expressed. Integrin ligands are recognised by integrins via their conserved amino acid sequences. One of the most studied conserved amino acid sequences on these ligands is the RGD sequence (arginine, glycine, aspartate). Many proteins in the ECM, including collagen, contain the RGD sequence, which only become, accessible after processing (such as crosslinking) or degradation (Barczyk et al., 2010). Thus, collagen only reveals these RGD sequence, following crosslinking or denaturation and can recognise integrins such as $\alpha V\beta 3$ and $\alpha V\beta 5$ (Pawelec et al., 2016).

A variety of integrins have been shown to be expressed by osteoblasts, including $\alpha V\beta 3$, $\alpha V\beta 5$ and $\alpha 2\beta 1$ (Lai and Cheng, 2005). These integrins are expressed on the cell surface and modulate cell adhesion, cell spreading, differentiation and mineralisation.

In addition to these integrins, another important transmembrane protein is involved: low density lipoprotein receptor-related protein 5 or LRP5 is an important protein that is involved in the Wnt- β -catenin pathway. Once a ligand has bound to LRP5, a cascade of reactions leading to the dissociation of β -catenin from glycogen synthase kinase 3 β or GSK3 (He et al., 2004). Once dissociated, β -catenin accumulates in the nucleus, where it can form a complex and displace TCF/ LEF transcription factors from the cell's DNA. This displacement leads to cell differentiation (Chau et al., 2009). It has been shown by Faverman et al, (2008) that TG2 binds to LRP5 to activate the Wnt- β -catenin pathway in vascular smooth muscle cells.

The synthesis and release of collagen from HOBs is seen during mineralisation and differentiation (Rutkovskiy et al., 2016). The collagen produced is an important ECM protein as it further adds to the scaffold and in turn becomes mineralised to form bone (Pawelec et al., 2016)

Native collagen are only able to recognise integrins such as $\alpha 1$ and $\alpha 2$ via the RGD site GFOGER (a 30 amino acid sequence) (Pawelec et al., 2016). TG2 crosslinked collagen

expresses “cryptic” RGD peptides in such a way that HOBs perceive the scaffold to be more like gelatin than collagen. As seen by the decrease of α 1 and α 2 integrins seen on HOBs seeded on TG2 crosslinked collagen.

5.2 Integrin expression of HOBs on collagen scaffolds

5.2.1 Expression of β 3 integrin on human osteoblasts over 3 days

By monitoring β 3 integrin expression in whole lysates, it was found that β 3 integrin expression steadily increased after 3 days (post seeding) when grown on un-treated 96-well plates. It was seen that, by day 3, the expression of β 3 integrin was approximately 1.6 fold higher than it was at day 1.

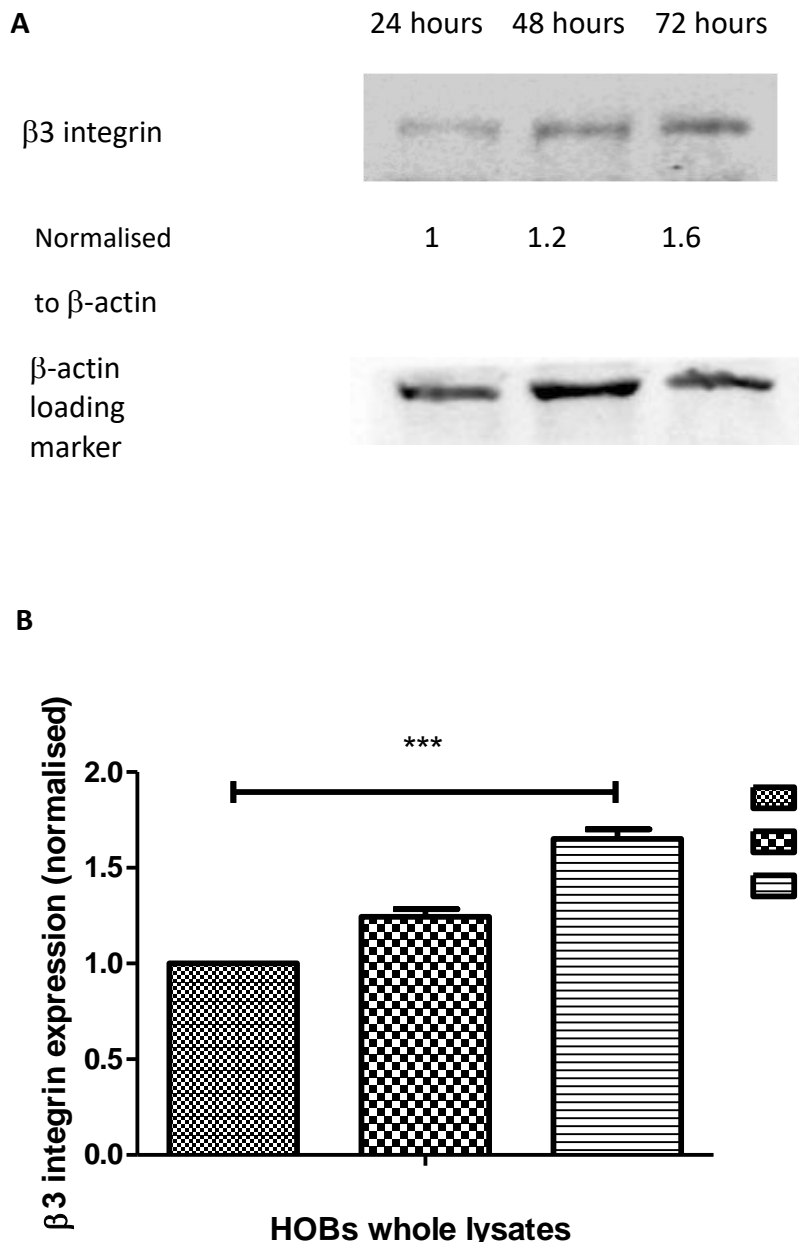


Figure 5.1: Expression of $\beta 3$ integrin in whole cell lysate. Cell lysates were collected after 1, 2 and 3 days post seeding and Western blotting was performed to analyse $\beta 3$ integrin expression. A representative Western blot result is shown in **(A)**. β -actin was used as loading control and normalised data are shown in the graph. **(B)**. Normalised integrin expression was plotted where the results represent mean values \pm S.D, where n=3. Statistical analysis was carried out using a one-way ANOVA test where the p-values corresponding to P< 0.001 are represented with ***.

5.2.2 Expression of αV integrin on human osteoblasts over 3 days

By monitoring αV integrin expression in whole lysates, it was found that αV integrin expression was approximately 1.64 fold higher than it was at day 1, as shown in Figure 5.2. Since $\beta 3$ is paired with αV on the cell surface it could be expected that the expression of αV would also increase, although αV can be paired with other β integrins.

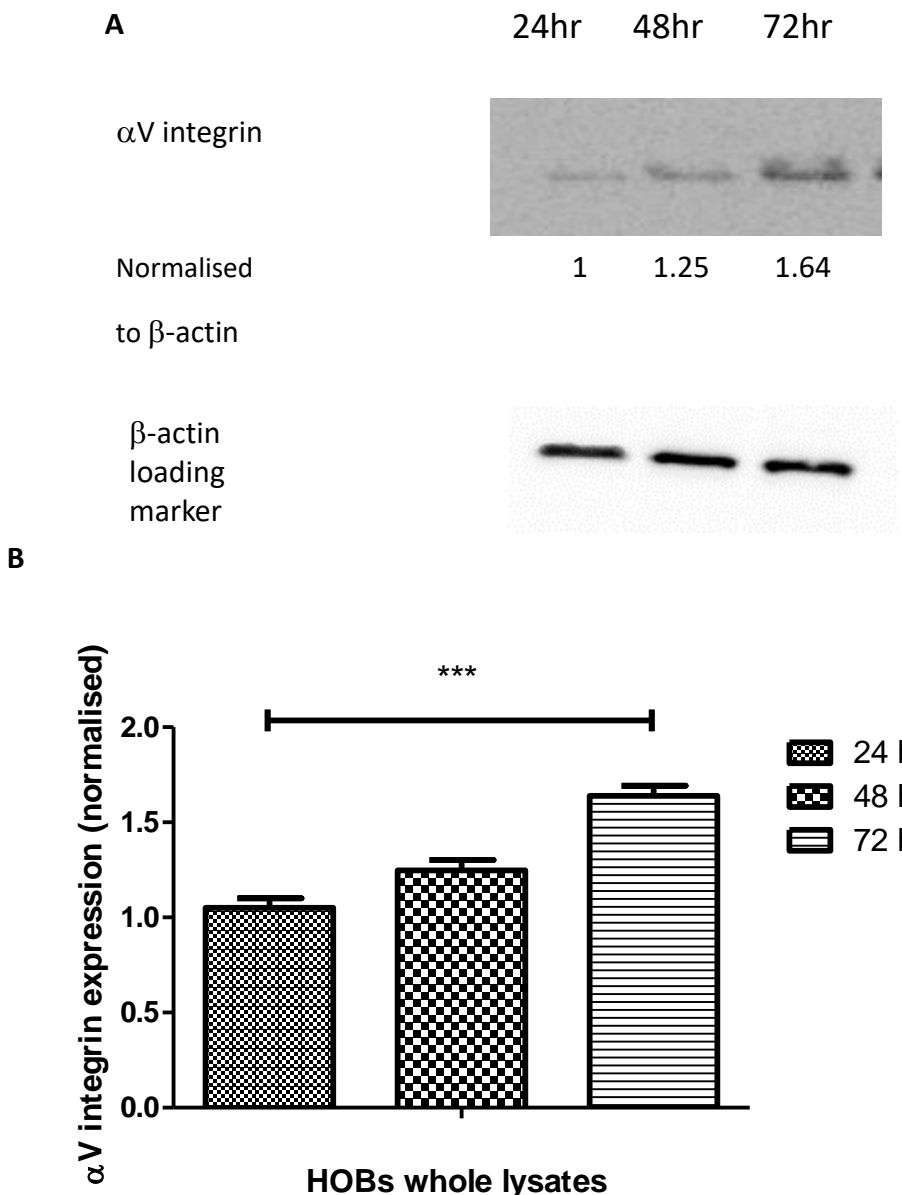


Figure 5.2: Expression of αV integrin in whole cell lysate. Cell lysates were collected after 1, 2 and 3 days post seeding and Western blotting was performed to analyse αV integrin expression. A representative Western blot result is shown in **(A)** β -actin was used as loading control and normalised data are shown in the graph. **(B)** Normalised integrin expression was plotted where the results represent mean values +/- S.D, where n=3. Statistical analysis was carried out using a one-way ANOVA test where the p-values corresponding to P< 0.001 are represented with ***.

5.2.3 Expression of LRP5 on human osteoblasts with transglutaminases added

Cell lysates were measured for LRP5 using Western blotting, as shown in Figure 5.3. It shows that HOBs grown with mTG and TG2 added to express LRP5 1.25 and 1.64 fold higher compared to native collagen. This suggests that, as in vascular smooth muscle cells, TG2 might be binding to LRP5 in HOBs. However, to conclusively show the binding of TG2 to LRP5 further investigation is needed.

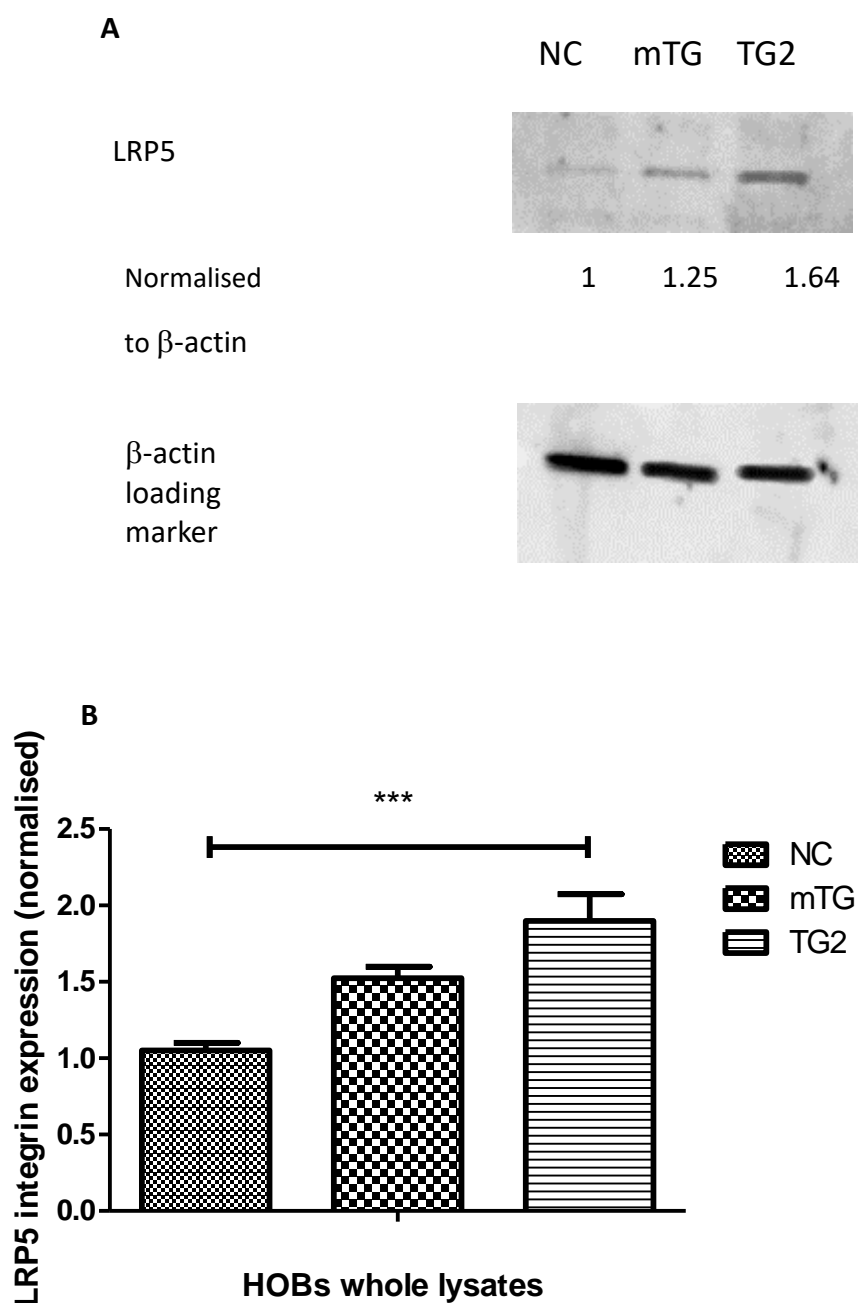


Figure 5.3: Expression of LRP5 integrin in whole cell lysate. Cell lysates were collected 3 days post seeding and Western blotting was performed to analyse LRP5 integrin expression. A representative Western blot result is shown in **(A)** β -actin was used as loading control and normalised data are shown in the graph. **(B)** Normalised integrin expression was plotted where the results represent mean values \pm S.D, where $n=3$. Statistical analysis was carried out using a one-way ANOVA test where the p-values corresponding to $P < 0.001$ are represented with ***.

5.3 Characterisation of integrin expression on human osteoblasts when seeded onto collagen scaffolds with transglutaminase

5.3.1 $\beta 3$ integrin expression in HOBs grown on collagen scaffolds

To contrast the differences in integrin expression, HOBs were grown on collagen scaffolds with and without modification by transglutaminases. In figure 5.4, the expression of $\beta 3$ was measured via Western blotting. After 3 days post seeding, HOBs grown on TG2 crosslinked collagen were seen to express $\beta 3$ integrin 2.1 fold more than on cells grown on native collagen as seen below. Furthermore, the cells grown on mTG crosslinked collagen expressed $\beta 3$ 1.62 fold more than HOBs seeded on native collagen.

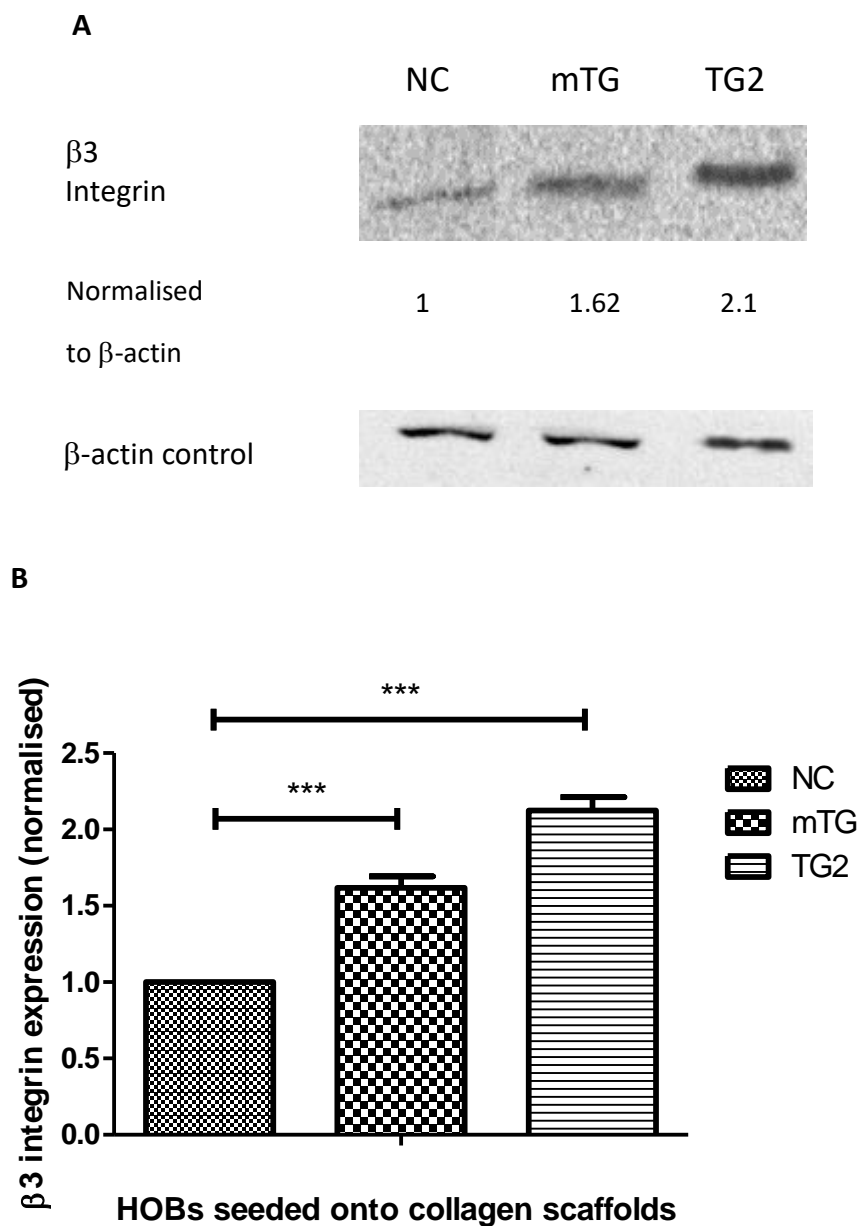


Figure 5.4: Expression of $\beta 3$ integrin in HOBs seeded onto collagen scaffolds. Cells were lysed after 3 days post seeding and Western blotting was performed to analyse $\beta 3$ integrin expression. A representative Western blot result is shown in **(A)**. β -actin was used as loading control and normalised data are shown in the graph. **(B)** Normalised integrin expression was plotted where the results represent mean values \pm S.D., where $n=3$. Statistical analysis was carried out using a one-way ANOVA test where the p-values corresponding to $P < 0.001$ are represented with ***.

5.3.2 α V integrin expression for HOBs grown on collagen scaffolds

Given the changes in β 3 integrin expression on HOBs seeded on crosslinked collagen, it was necessary to investigate the expression of α V integrin since it forms the other half of the α V β 3 signalling complex. HOBs were grown on collagen scaffolds with and without modification by transglutaminases. Figure 5.5 shows the expression of α V measured via Western blotting. There was a 1.71 fold increase in expression of α V integrins found in cells grown on mTG. In addition a similar increase of 1.78 fold expression of α V in HOBs seeded on TG2 crosslinked collagen compared to native collagen. This further demonstrates that cellular pathways are being affected by being grown on modified collagen scaffolds.

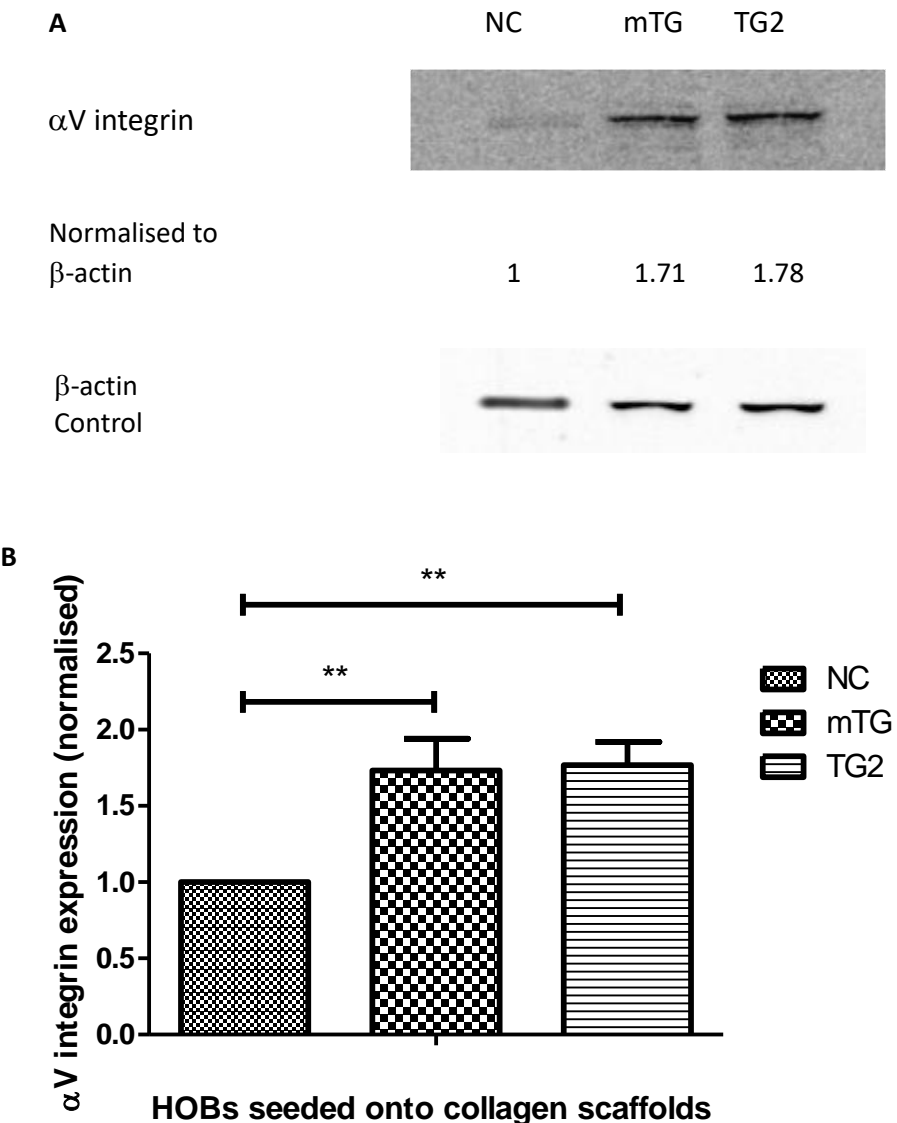


Figure 5.5: Expression of αV integrin in HOBs seeded onto collagen scaffolds. Cells were lysed after 3 days post seeding and Western blotting was performed to analyse αV integrin expression. A representative Western blot result is shown in **(A)**. β -actin was used as loading control and normalised data are shown in the graph. **(B)** Normalised integrin expression was plotted where the results represent mean values \pm S.D, where n=3. Statistical analysis was carried out using a one-way ANOVA test where the p-values corresponding to P<0.01 are represented with **.

5.3.3 β 1 integrin expression for HOBs grown on collagen scaffolds

Having observed the expression of the integrin pair α V β 3 (individually), the next step was to look at α 5 and β 1. α 5 β 1 is expressed on the surface of osteoblasts and, along with α V β 3, binds to ligands such as BMPs in the ECM to influence the fate of osteoblasts, including proliferation, attachment and mineralisation (Fortunati et al., 2014, Orban et al., 2004). Figure 5.6 shows that HOBs seeded onto mTG and TG2 collagen were shown to express β 1 integrin 1.5 and 1.79 fold more than HOBs seeded onto native collagen.

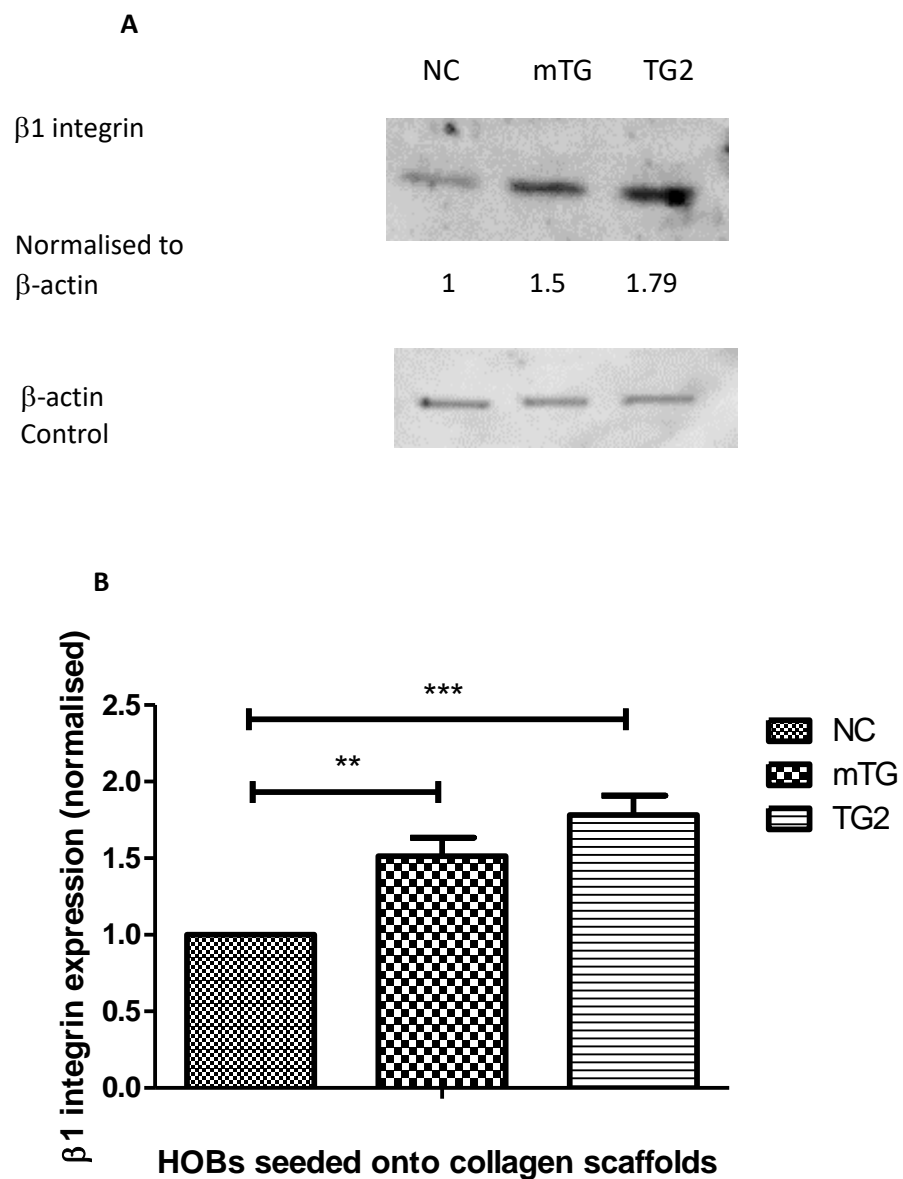


Figure 5.6: Expression of $\beta 1$ integrin in HOBs seeded onto collagen scaffolds. Cell lysates were lysed after 3 days post seeding and Western blotting was performed to analyse $\beta 1$ integrin expression. A representative Western blot result is shown in (A). β -actin was used as loading control and normalised data were shown in the graph. (B) Normalised integrin expression was plotted where the results represent mean values +/- S.D, where n=3. Statistical analysis was carried out using a one-way ANOVA test where the p-values corresponding to P< 0.001 are represented with *** and p-values corresponding to P<0.01 are represented with **.

5.3.4 α 5 integrin expression for HOBs grown on collagen scaffolds

Having shown the differences in β 1 integrin expression on HOBs seeded on crosslinked collagen in Figure 5.6, it was necessary to investigate the expression of α 5 integrin since it forms the other half of the β 1 α 5 signalling complex. HOBs were grown on collagen scaffolds with and without modification by transglutaminases. Figure 5.7 shows the expression of α 5 was measured via Western blotting. There was a 1.65 fold increase in expression of α 5 integrins found in cells grown on mTG. Furthermore a 2.13 fold increase in α 5 integrin was seen in HOBs seeded on TG2 crosslinked collagen compared to native collagen.

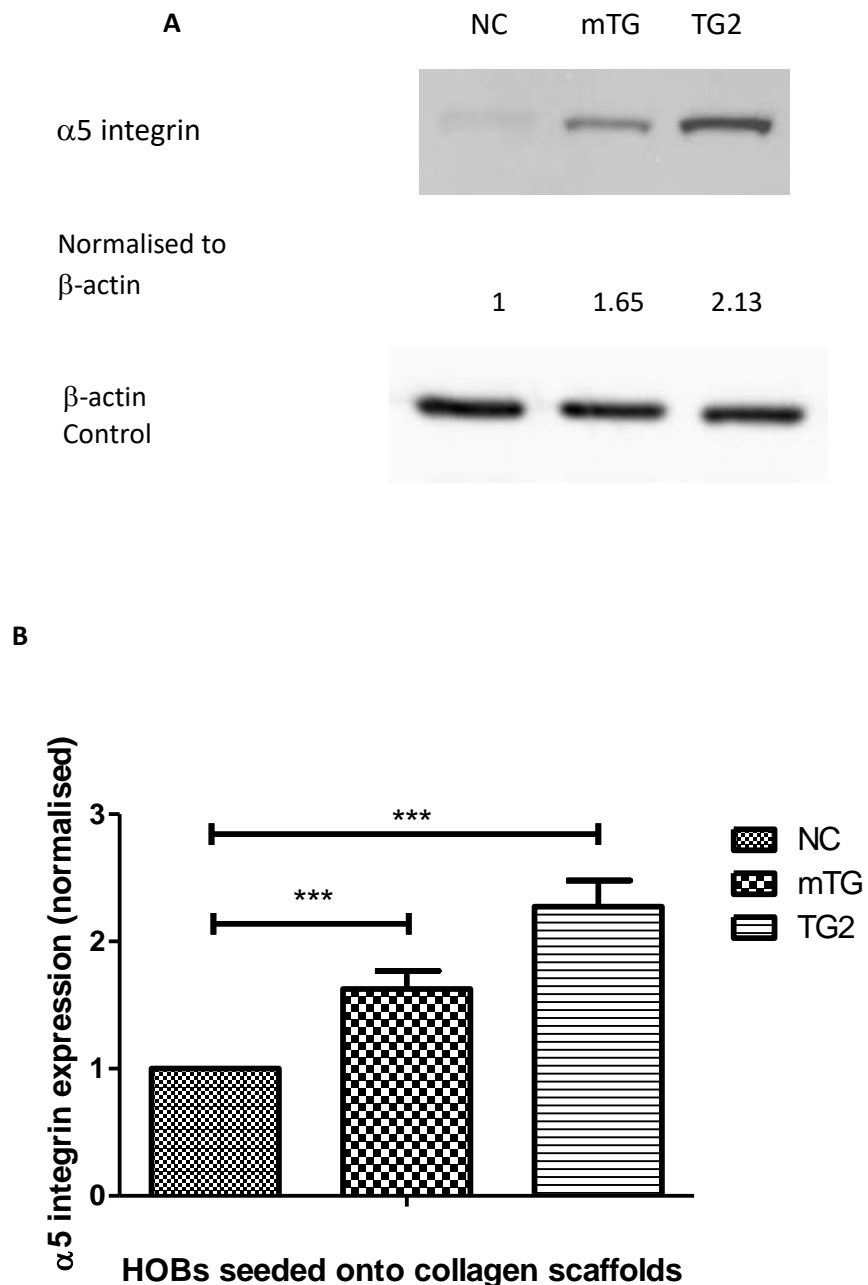


Figure 5.7: Expression of $\alpha 5$ integrin in HOBs seeded onto collagen scaffolds. Cells were lysed after 3 days post seeding and Western blotting was performed to analyse $\alpha 5$ integrin expression. A representative Western blot result is shown in **(A)**. β -actin was used as loading control and normalised data are showed in chart. **(B)** Normalised integrin expression was plotted where the results represent mean values +/- S.D, where n=3. Statistical analysis was carried out using a one-way ANOVA test where the p-values corresponding to P< 0.001 are represented with ***.

5.3.5 α 1 integrin expression for HOBs grown on collagen scaffolds

HOBs were grown on collagen scaffolds with and without modification by transglutaminases. Expression of α 1 was measured via Western blotting in figure 5.8. There was nearly a 0.5 fold decrease in expression of α 1 integrins found in cells grown on TG2 crosslinked collagen compared to native collagen. However HOBs on mTG crosslinked collaged did not show a decrease in α 1 or α 2 integrins. α 1 integrin is often observed on the HOBs surface when they bind to a collagen scaffold (Barczyk et al., 2010).

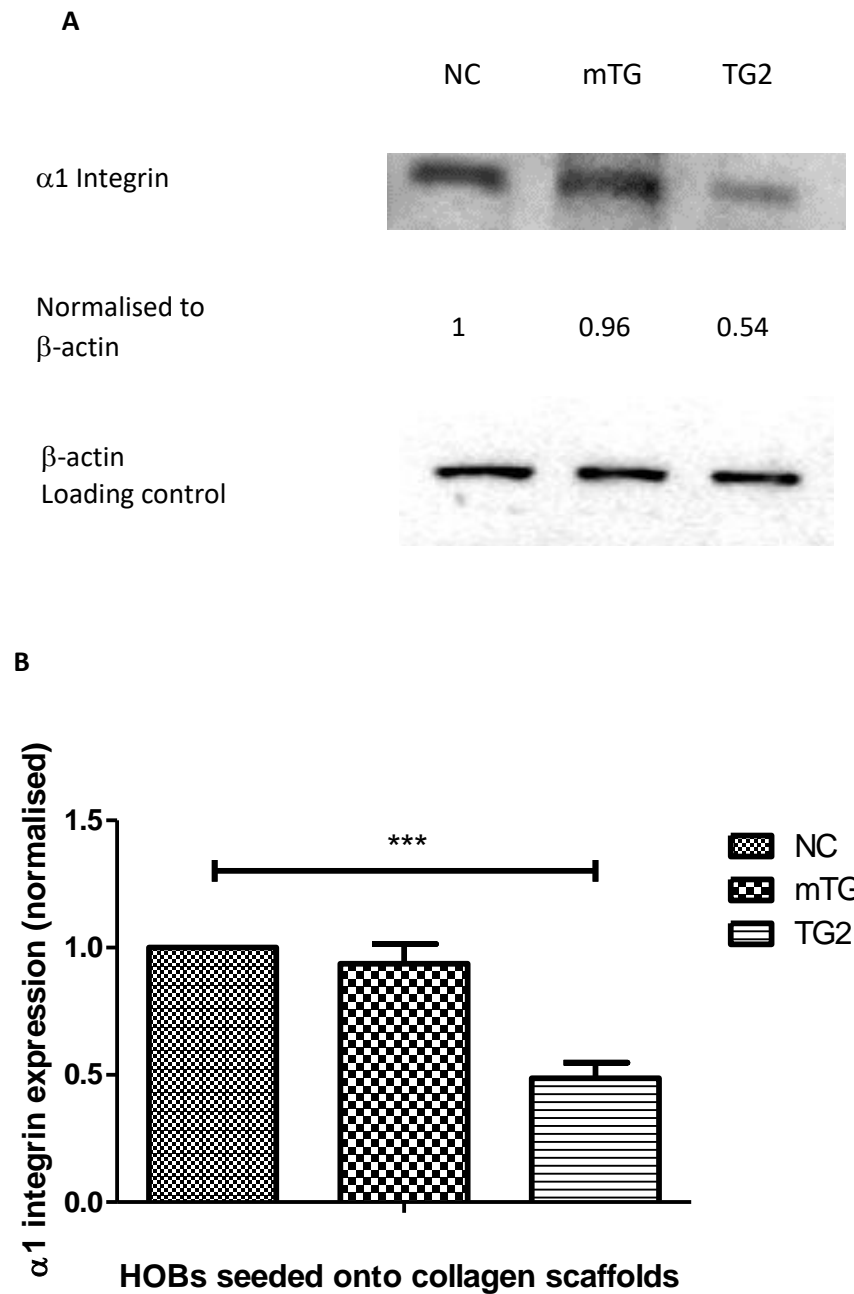


Figure 5.8: Expression of $\alpha 1$ integrin in HOBs seeded onto collagen scaffolds. Cells were lysed after 3 days post seeding and Western blotting was performed to analyse $\alpha 1$ integrin expression. A representative Western blot result is shown in **(A)**. β -actin was used as loading control and normalised data are shown in the graph. **(B)** Normalised integrin expression was plotted where the results represent mean values \pm S.D, where n=3. Statistical analysis was carried out using a one-way ANOVA test where the p-values corresponding to P< 0.001 are represented with ***.

5.3.6 α 2 integrin expression for HOBs grown on collagen scaffolds

Given that α 1 expression levels decreased in HOBs grown on TG2 crosslinked collagen, it was necessary to investigate if α 2 expression differed. This is because, along with α 1, α 2 is an integrin that does not recognise denatured collagen (Knight et al., 2000).

HOBs were grown on collagen scaffolds with and without modification by transglutaminases. Expression of α 2 was measured via Western blotting. There was nearly a 0.4 fold decrease in expression of α 2 integrins found in cells grown on TG2 crosslinked collagen compared to native collagen.

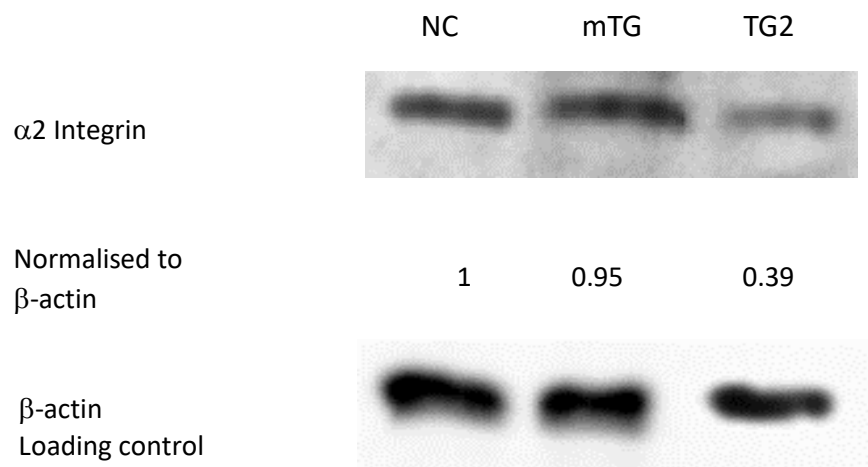
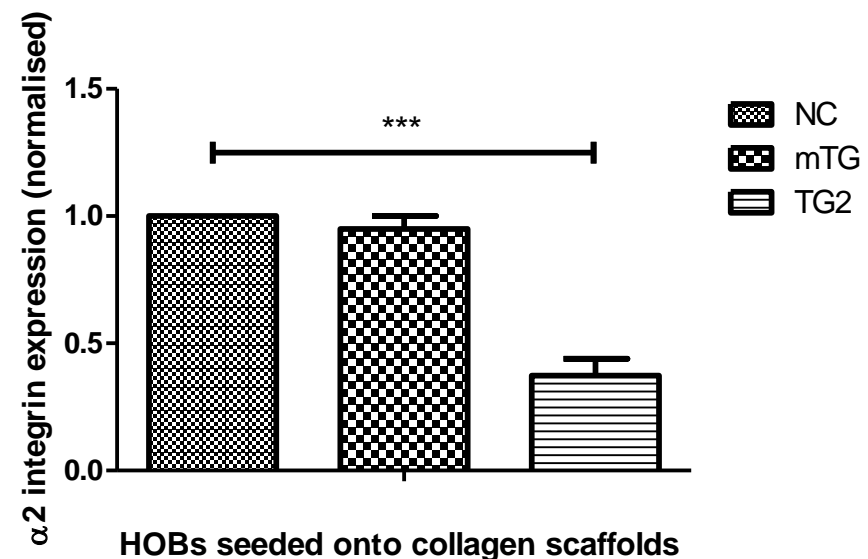
A**B**

Figure 5.9: Expression of $\alpha 2$ integrin in HOBs seeded onto collagen scaffolds. Cells were lysed after 3 days post seeding and Western blotting was performed to analyse $\alpha 2$ integrin expression. A representative Western blot result is shown in (A). β -actin was used as loading control and normalised data are shown in the graph. (B) Normalised integrin expression was plotted where the results represent mean values +/- S.D, where $n=3$. Statistical analysis was carried out using a one-way ANOVA test where the p-values corresponding to $P < 0.001$ are represented with ***.

5.3.7 LRP5 integrin expression for HOBs grown on collagen scaffolds

Since Figure 5.3 showed that HOBs increase their expression of LRP5 when transglutaminases are present. To see if LRP5 expression changed in HOBs grown on collagen scaffolds with and without modification by transglutaminases, Western blotting on cell lysates was carried out as shown in Figure 5.10. There was a 2.96 fold increase in expression of LRP5 found in cells grown on TG2 crosslinked collagen compared to native collagen. Similarly a 1.49 increase in fold expression was found in HOBs grown on mTG crosslinked collagen.

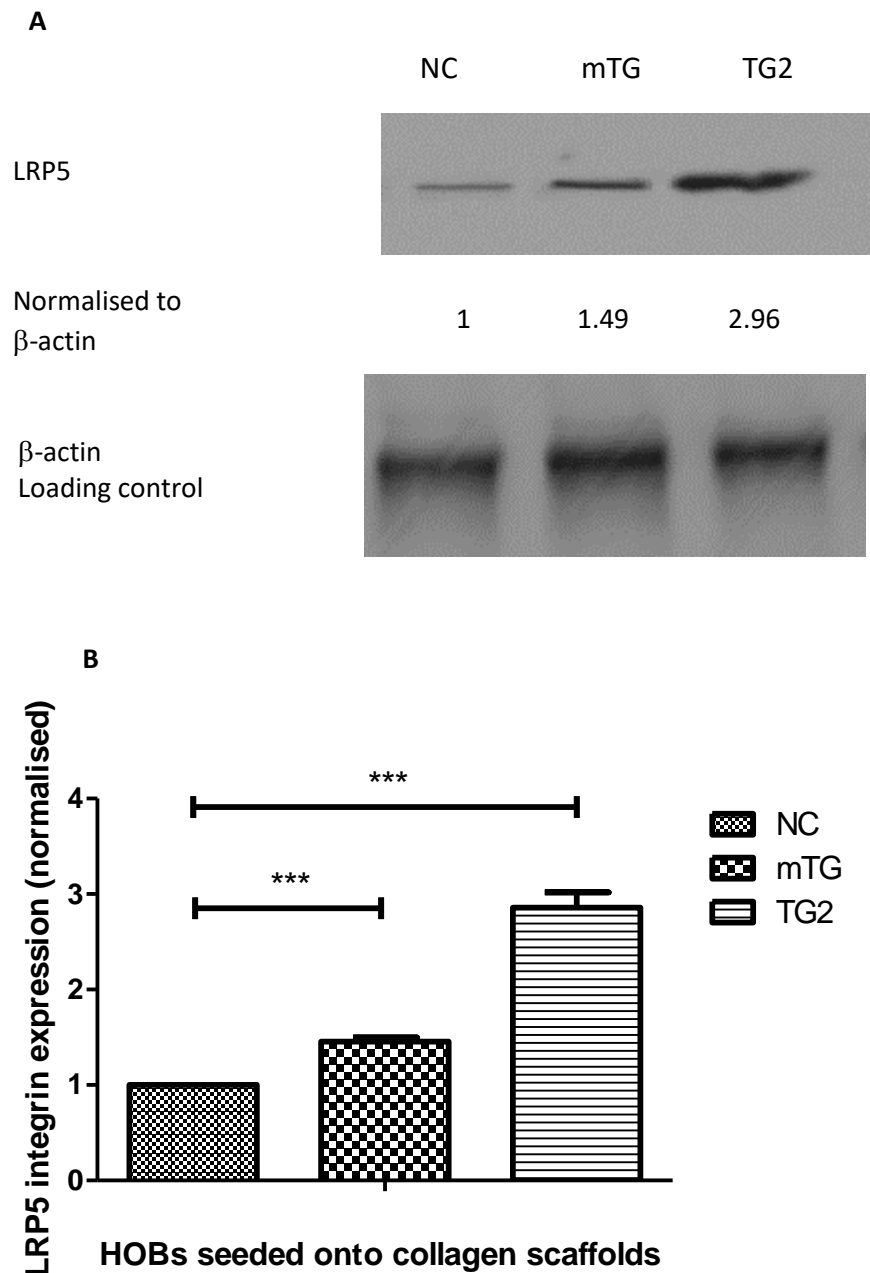


Figure 5.10: Expression of LRP5 integrin in HOBs seeded onto collagen scaffolds. Cells were lysed after 3 days post seeding and Western blotting was performed to analyse LRP5 integrin expression. A representative Western blot result is shown in (A). β -actin was used as loading control and normalised data are shown in the graph. (B) Normalised integrin expression was plotted where the results represent mean values \pm S.D, where $n=3$. Statistical analysis was carried out using a one-way ANOVA test where the p-values corresponding to $P < 0.001$ are represented with ***.

5.4 Characterisation of integrin expression on human osteoblasts when seeded onto collagen scaffolds with transglutaminase and 45S5 bioglass

5.4.1 β 3 integrin expression for HOBs grown on collagen scaffolds mixed with 45S5 bioglass

Having shown that β 3 integrin expression on HOBs increases over time in Figure 5.1 and when seeded onto crosslinked collagen in Figure 5.4. It was necessary to investigate the impact that 45S5 bioglass might have on cells. β 3 integrin expression was measured on HOBs seeded on native collagen and crosslinked collagen with 10 mg/ml 45S5 bioglass particles was then measured. After seeding HOBs on the collagen scaffolds, cell lysates were collected and the expression of β 3 integrins was measured using Western blotting. The results are shown in Figure 5.11.

β 3 integrin expression increased in HOBs on all collagen scaffolds that had 45S5 bioglass mixed with them. The lowest increase was seen in native collagen mixed with bioglass (by 1.25 fold) and the highest increase was found in HOBs seeded on TG2 crosslinked with 45S5 bioglass (2.25 fold). The β 3 integrin expression was found to be significantly higher on HOBs grown on native collagen with glass than without (0.25 fold higher). Similarly, HOBs grown on TG2 and mTG crosslinked collagen with glass showed significantly higher expression of β 3 integrins than their respective scaffolds without glass.

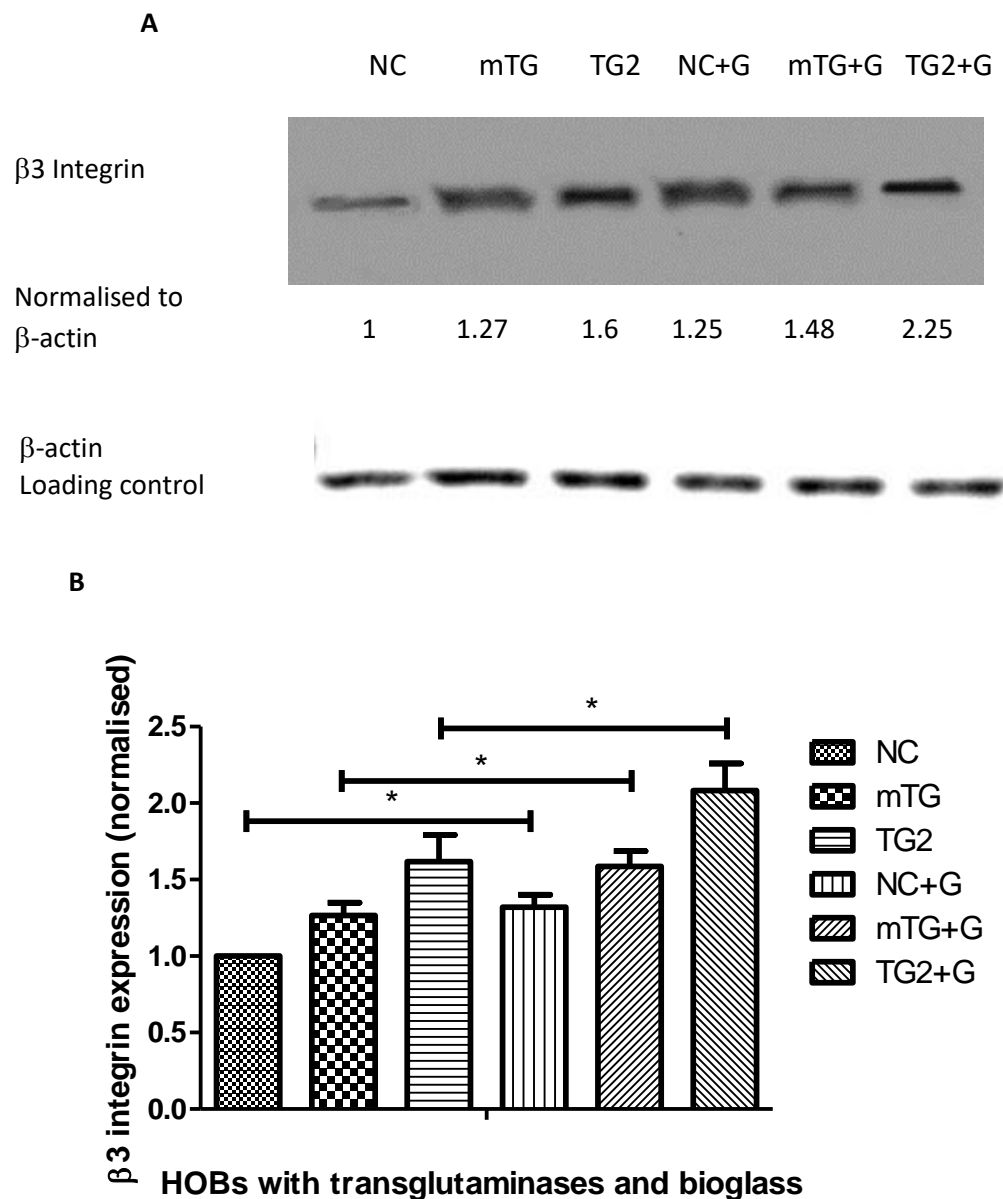


Figure 5.11: Expression of $\beta 3$ integrin in HOBs seeded onto collagen scaffolds with 45S5 bioglass. Cells were lysed after 3 days post seeding and Western blotting was performed to analyse $\beta 3$ integrin expression. A representative Western blot result is shown in **(A)**. β -actin was used as loading control and normalised data are showed in the graph. **(B)** Normalised integrin expression was plotted where the results represent mean values \pm S.D, where n=3. Statistical analysis was carried out using a one-way ANOVA test where the p-values corresponding to P< 0.05 are represented with *.

5.4.2 α V integrin expression for HOBs grown on collagen scaffolds mixed with 45S5 bioglass

Having shown that α V integrin expression on HOBs increases over time in Figure 5.2 and when seeded onto crosslinked collagen in Figure 5.5. It was necessary to investigate the influence of bioglass on cells. The expression of α V integrin expression on HOBs when seeded on native collagen and crosslinked collagen with 10 μ g/ml 45S5 bioglass particles was then measured. After seeding HOBs on the collagen scaffolds cell lysates were collected and using Western blotting the expression of α V integrins was measured. The results are shown in Figure 5.12

α V integrin expression increased in HOBs on all collagen scaffolds that had 45S5 bioglass mixed with them. The lowest increase was seen in native collagen mixed with bioglass (by 1.52 fold) and the highest increase was found in HOBs seeded on mTG crosslinked with 45S5 bioglass (2.76 fold). As with β 3, HOBs grown on TG2 and mTG crosslinked collagen with glass showed significantly higher expression of α V integrins than their respective scaffolds without glass.

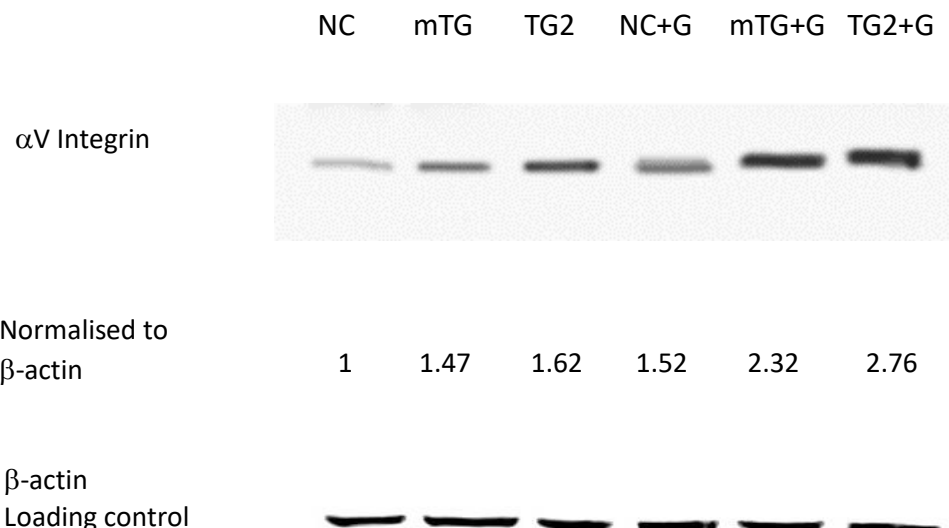
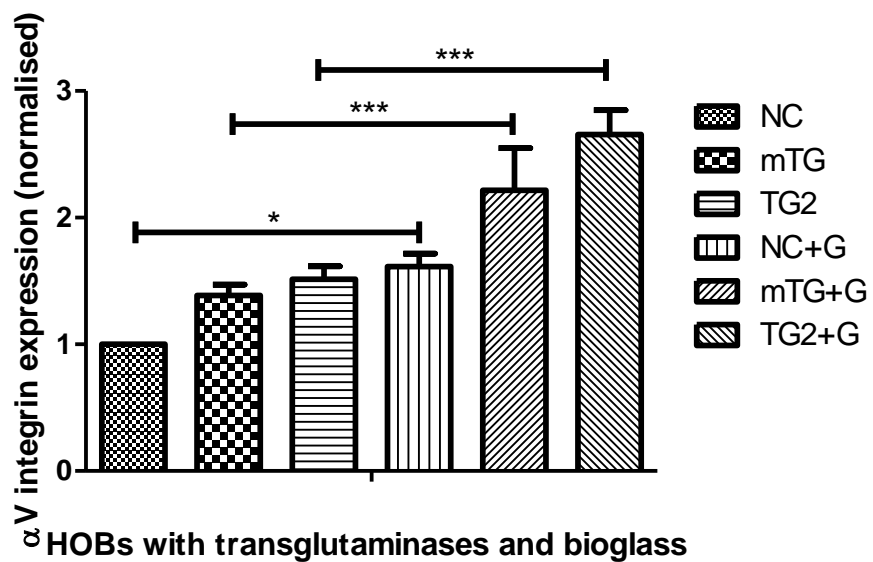
A**B**

Figure 5.12: Expression of αV integrin in HOBs seeded onto collagen scaffolds with 45S5 bioglass. Cells were lysed after 3 days post seeding and Western blotting was performed to analyse αV integrin expression. A representative Western blot result is shown in (A). β -actin was used as loading control and normalised data are shown in the graph. (B) Normalised integrin expression was plotted where the results represent mean values \pm S.D, where n=3. Statistical analysis was carried out using a one-way ANOVA test where the p-values corresponding to P< 0.05 are represented with * and P< 0.001 are represented with ***.

5.4.3 β 1 integrin expression for HOBs grown on collagen scaffolds mixed with 45S5 bioglass

Figure 5.13 shows that the β 1 integrin expression increased in HOBs on all crosslinked collagen scaffolds that had 45S5 bioglass mixed with them. A decrease in expression was seen in native collagen which was mixed with bioglass (by 1.2 fold) the highest increase was found in HOBs seeded on TG2 crosslinked with 45S5 bioglass (2.3 fold).

β 1 integrin expression was significantly higher on mTG and TG2 crosslinked collagen with bioglass than when grown on their respective collagen scaffolds without bioglass.

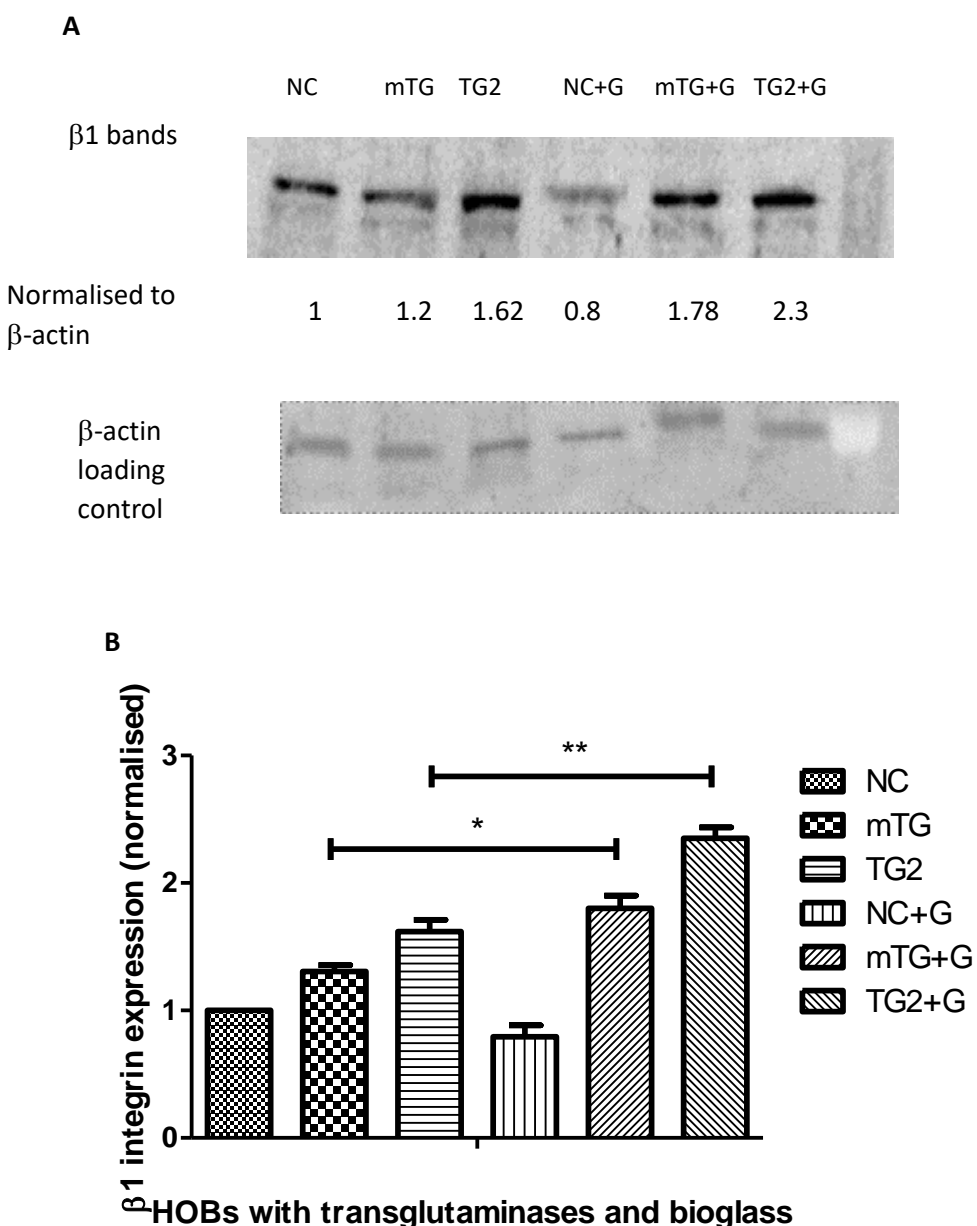


Figure 5.13: Expression of $\beta 1$ integrin in HOBs seeded onto collagen scaffolds with 45S5 bioglass. Cell lysates were lysed after 3 days post seeding and Western blotting was performed to analyse $\beta 1$ integrin expression. A representative western blot result is shown in (A). β -actin was used as loading control and normalised data are shown in the graph. (B) Normalised integrin expression was plotted where the results represent mean values \pm S.D, where n=3. Statistical analysis was carried out using a one-way ANOVA test where the p-values corresponding to P< 0.05 are represented with * and p-values corresponding to P<0.01 are represented with **.

5.4.4 $\alpha 5$ integrin expression for HOBs grown on collagen scaffolds mixed with 45S5 bioglass

Having shown that $\alpha 5$ integrin increases when seeded onto crosslinked collagen in Figure 5.7, it was appropriate to investigate the influence of bioglass on the cells. The expression of $\alpha 5$ integrin expression on HOBs when seeded on native collagen and crosslinked collagen with 10 $\mu\text{g/ml}$ 45S5 bioglass particles was then measured. After seeding HOBs on the collagen scaffolds cell lysates were collected and using western blotting the expression of $\alpha 5$ integrins was measured. The results are shown in Figure 5.14.

$\alpha 5$ integrin expression increased in HOBs on all collagen scaffolds that had 45S5 bioglass mixed with them. The lowest increase was seen in native collagen which was mixed with bioglass (by 1.24 fold) and the highest increase was found in HOBs seeded on TG2 crosslinked with 45S5 bioglass (2.51 fold). $\alpha 5$ integrin expression was significantly higher on mTG and TG2 crosslinked collagen with bioglass than their respective collagen scaffolds without bioglass.

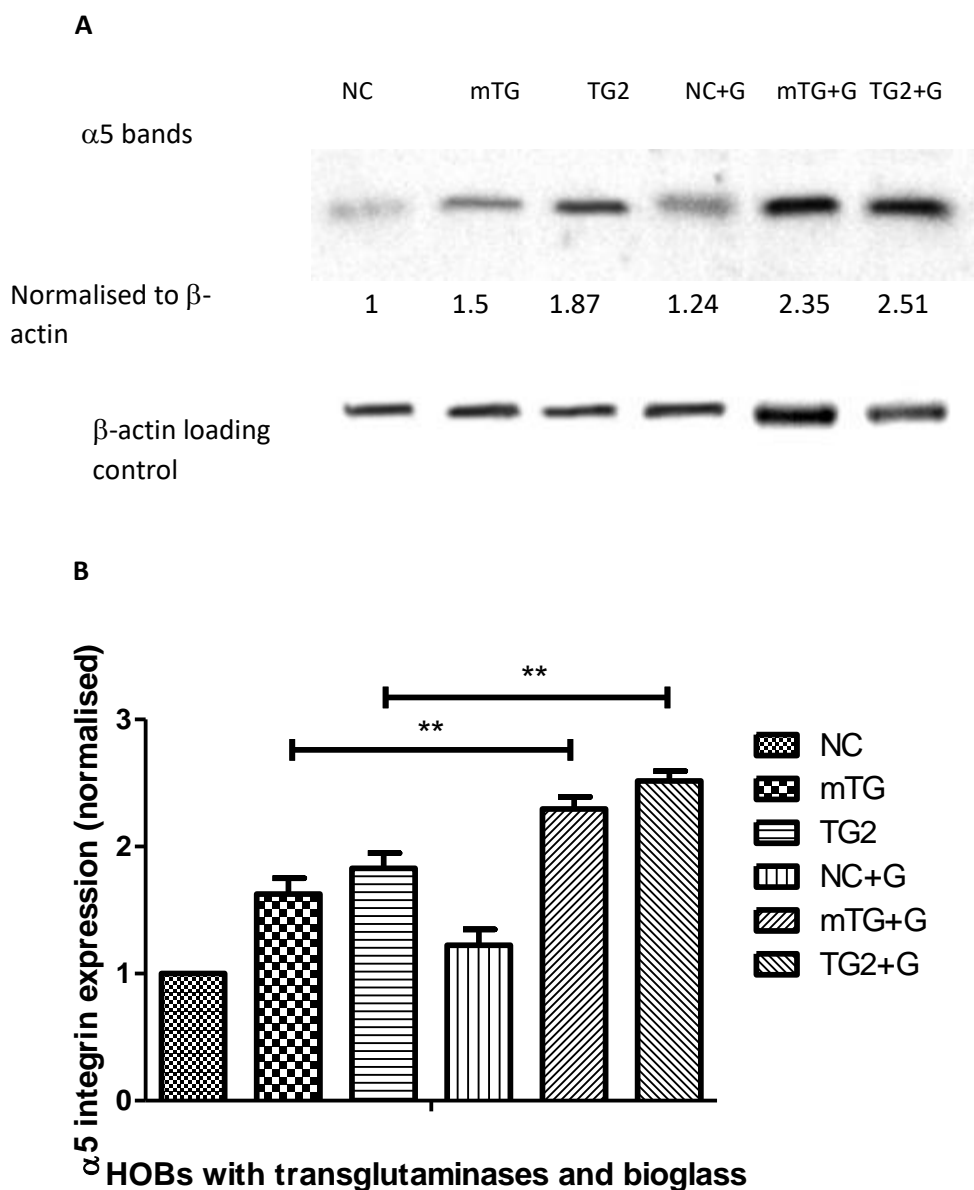


Figure 5.14: Expression of $\alpha 5$ integrin in HOBs seeded onto collagen scaffolds with 45S5 bioglass. Cell lysates were lysed after 3 days post seeding and Western blotting was performed to analyse $\alpha 5$ integrin expression. A representative western blot result is shown in (A). β -actin was used as loading control and normalised data are shown in the graph. (B) Normalised integrin expression was plotted where the results represent mean values +/- S.D, where n=3. Statistical analysis was carried out using a one-way ANOVA test where the p-values corresponding to P< 0.01 are represented with **.

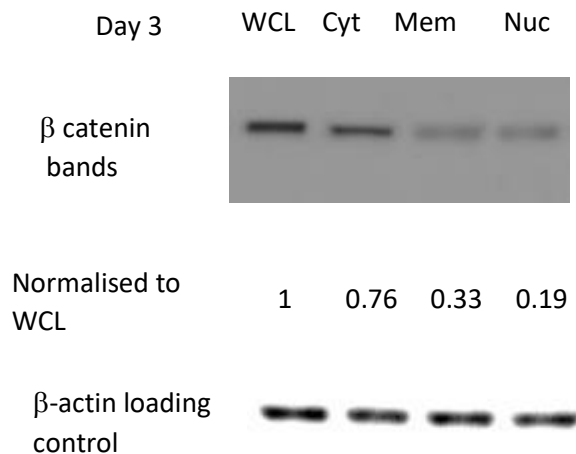
Table 5.1: A summary of integrin expression seen on HOBs when seeded on various collagen scaffolds

Collagen scaffolds	Expression of integrin relative to that seen on HOBs seeded on native collagen. Green = increase in expression and Red = decrease in expression						
	α1	α2	α5	αV	β1	β3	LRP5
mTG	0.96	0.95	1.5	1.47	1.2	1.27	1.49
TG2	0.54	0.35	1.87	1.62	1.62	1.6	2.56
NC+G			1.24	1.52	0.8	1.25	
mTG+G			2.35	2.32	1.78	1.48	
TG2+G			2.51	2.76	2.3	2.25	

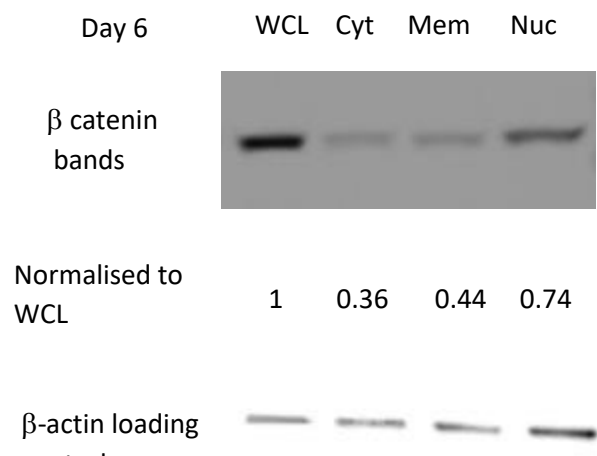
5.4.5 β -catenin expression in HOBs

The expression of β -catenin in HOBs grown on tissue culture plastic was observed between 3 and 6 days post seeding the results are shown in Figure 5.15. The Western blots show a decrease in the amount of β -catenin present in the cytoplasm and a simultaneous increase amount found in the nucleus fraction as time passed.

A



B



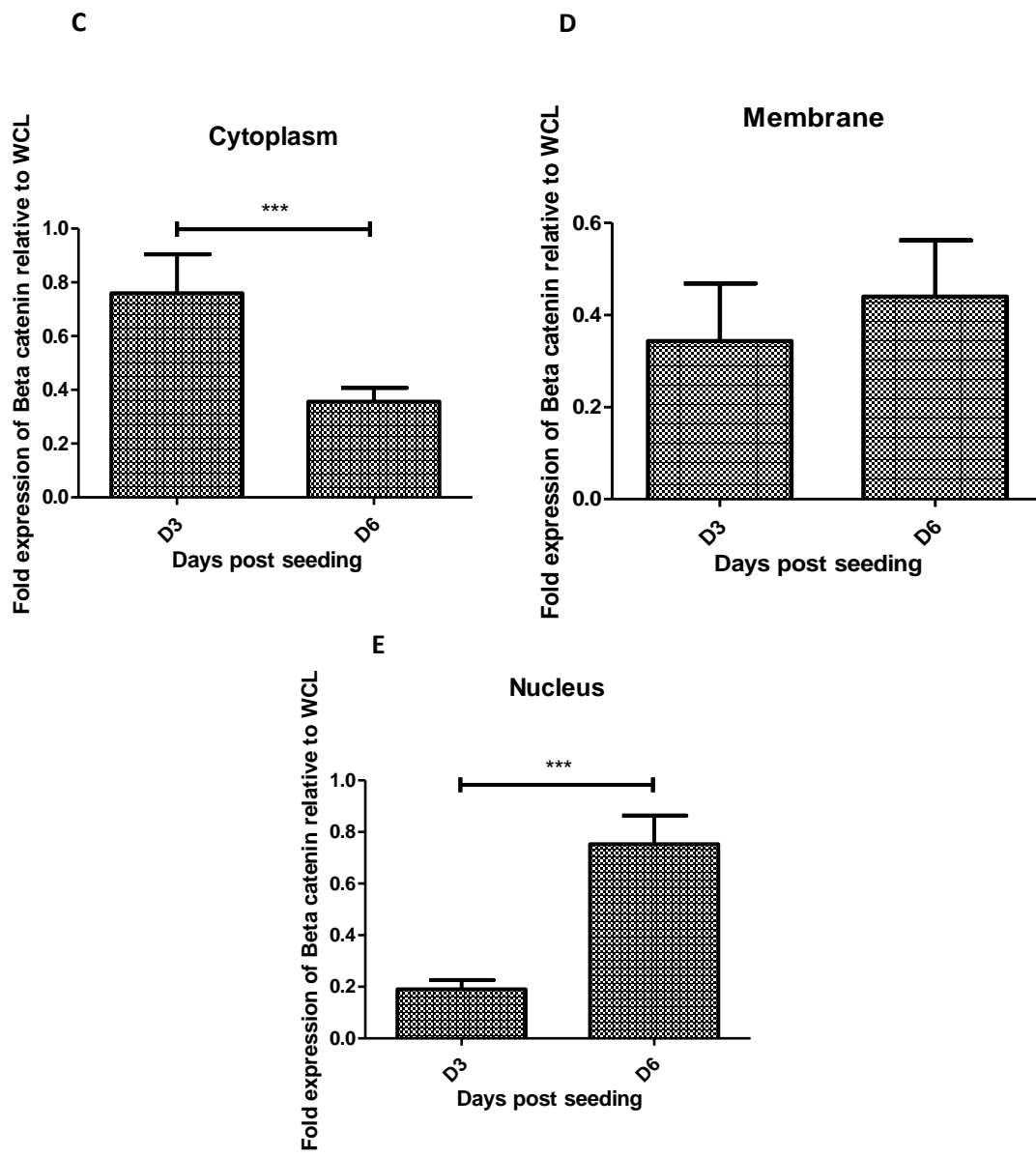
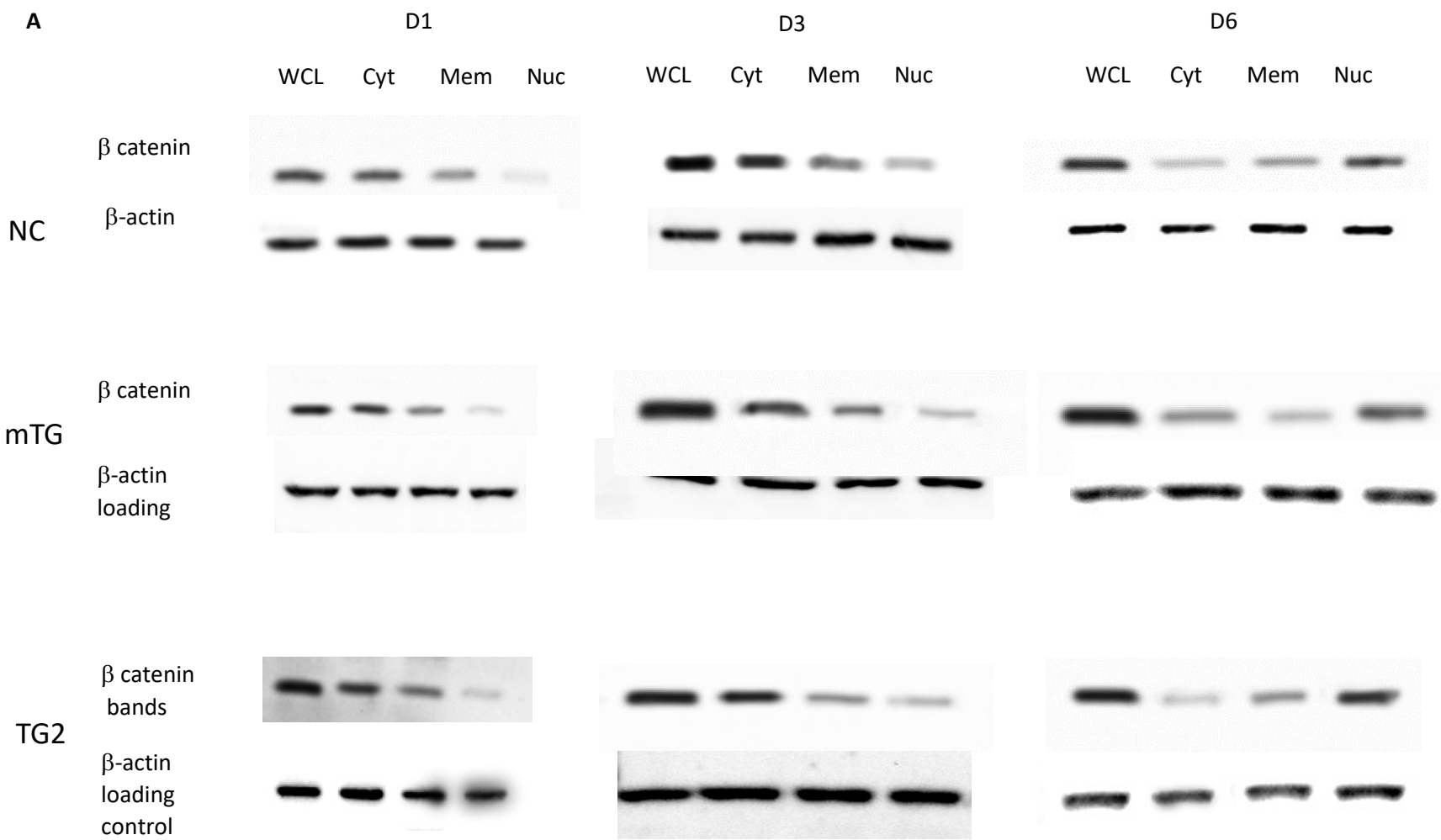
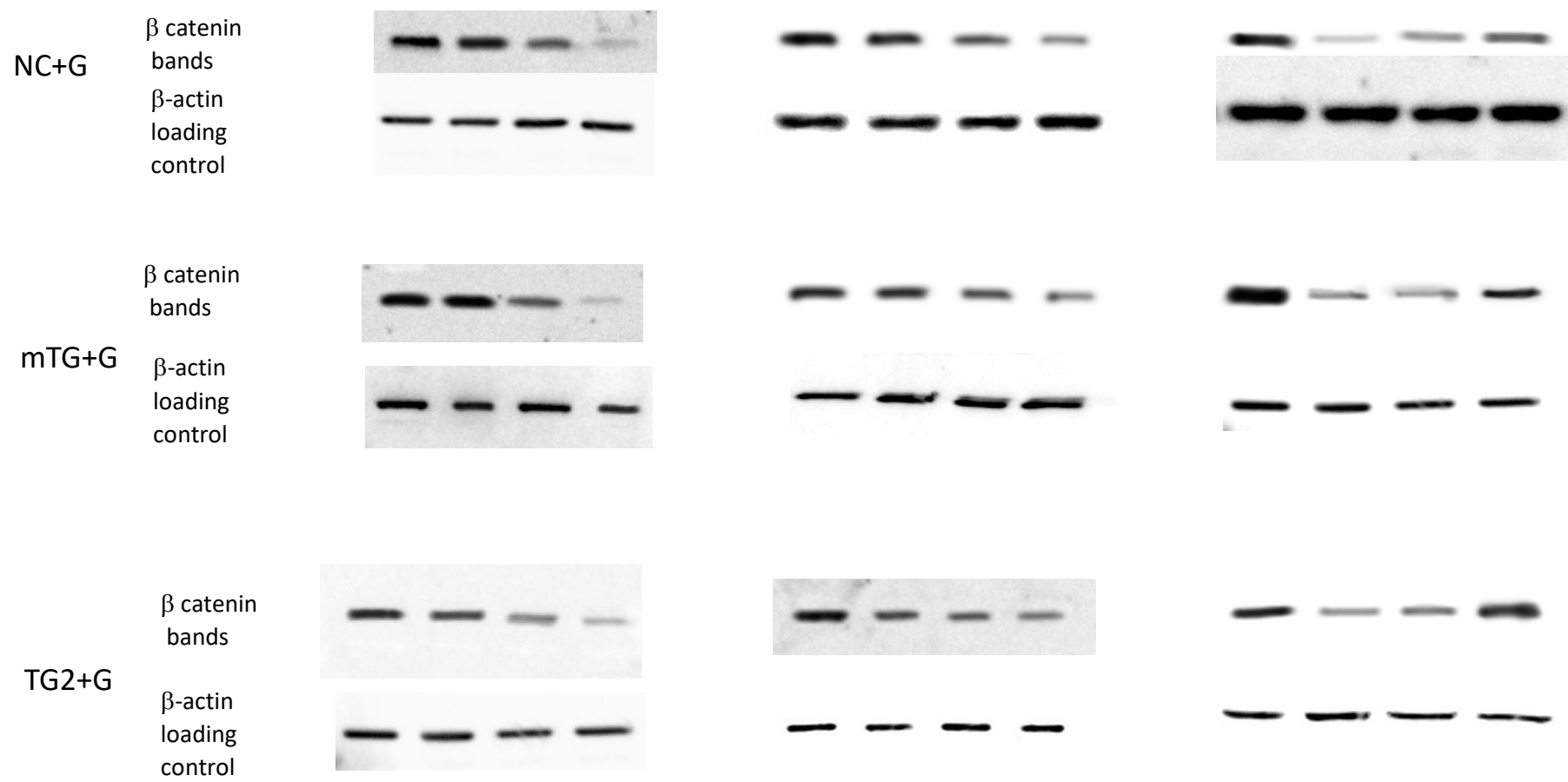


Figure 5.15: Expression of β -catenin in HOB cell fractions. Cellular fractions were separated through centrifugation (see materials and methods) after 3 and 6 days post seeding and Western blotting was performed to analyse β -catenin expression. A representative western blot result for day 3 is shown in (A). A representative western blot result for day 3 is shown in (B) β -actin was used as loading control and fractions were normalised to the total β -catenin expression found in the whole lysate. (C-E) Normalised β -catenin expression was plotted where the results represent mean values +/- S.D, where n=3 for cytoplasmic, membrane bound and nuclear fractions. Statistical analysis was carried out using a one-way ANOVA test where the p-values corresponding to P< 0.001 are represented with ***.

5.4.6 β -catenin expression in HOBs grown on collagen scaffolds

Having shown that β -catenin is translocated from the cytoplasm to the nucleus in Figure 5.16, the differences in translocation of β -catenin in HOBs seeded on various collagen scaffolds were measured. HOBs were seeded on various collagen scaffolds with mTG, TG2 (5 μ g/ml) and 45S5 bioglass, and the results for the translocation of β -catenin from cell lysates are shown in Figure 5.17. Western blot analysis shows that there was a significant increase in the expression of β -catenin in the nuclear fraction in HOBs seeded on TG2, mTG+G and TG2+G by day 6 compared to the amount seen in cells on HOBs seeded on native collagen. Interestingly a significant decrease in fold β -catenin expression is also seen in day 3 HOBs lysates between those seeded on native collagen and TG2 with bioglass.





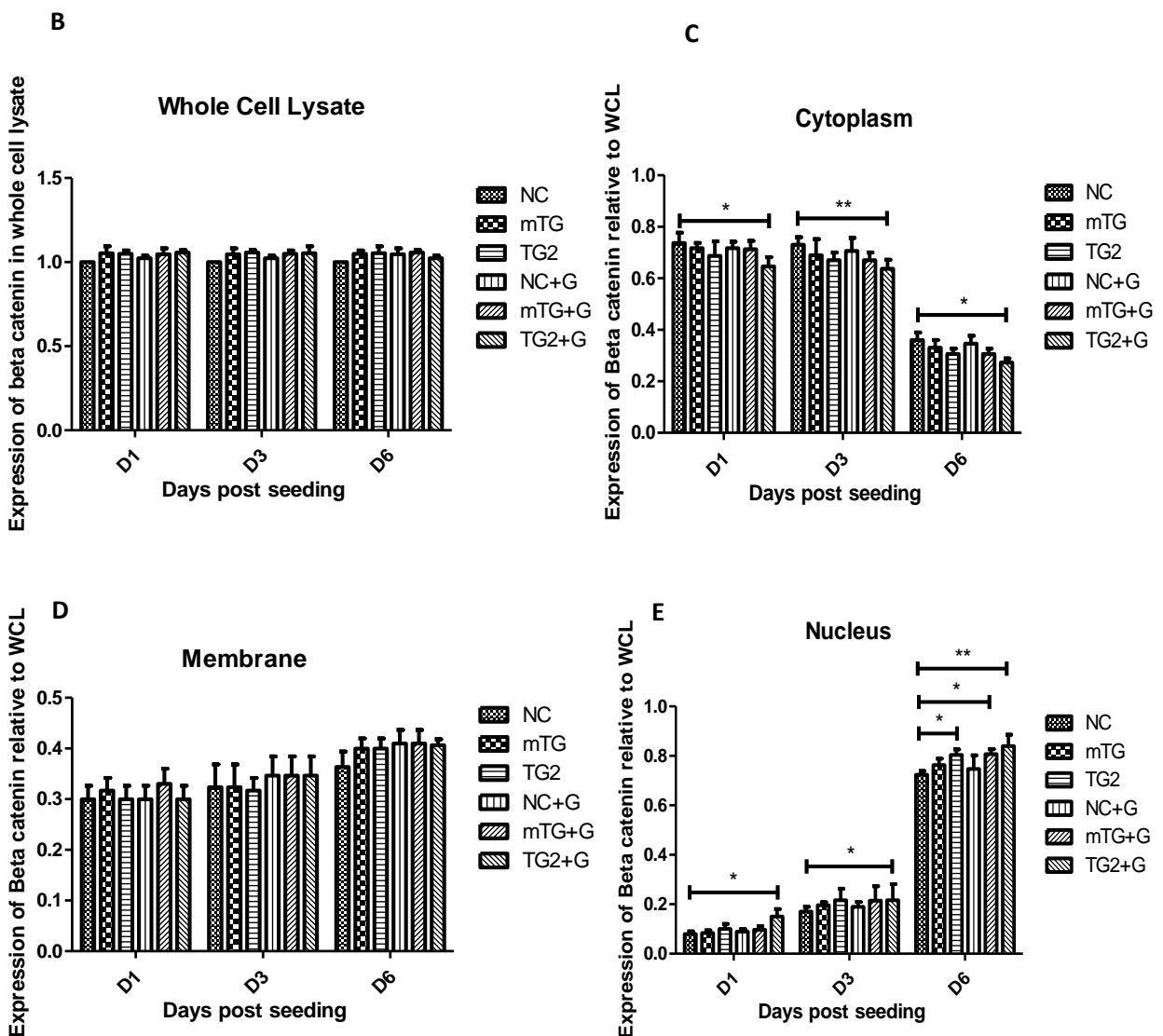


Figure 5.16: Expression of β -catenin in HOB cell fractions seeded on collagen scaffolds.

(A) Cellular fractions were separated through centrifugation (see materials and methods) after 3 and 6 days post seeding and Western blotting was performed to analyse β -catenin expression. A representative western blot result for day 3 and 6 is shown whereby β -actin was used as loading control and fractions were normalised to the total β -catenin expression found in the whole lysate. **(B-E)** Normalised β -catenin expression was plotted for each cell fraction where the results represent mean values +/- S.D, where n=3 for cytoplasmic, membrane bound and nuclear fractions. Statistical analysis was carried out using a two-way ANOVA test where the p-values corresponding to P< 0.05 are represented with * and p< 0.01 are represented with **.

5.5 Discussion

The integrins αV and $\beta 3$ are found paired on osteoblasts cell surface and work to facilitate cell spreading and differentiation. Fourel *et al.* showed that once the integrin receptors bind to cell matrix proteins such as collagen/fibronectin a multistep process is set into motion. The destruction of the GSK3- β -catenin complex, through the Wnt pathway, also results in the translocation of β -catenin from the cytoplasm into the nucleus resulting in HOB differentiation and mineralisation. It can also lead to the C-terminal phosphorylation of Smad and second to inhibit GSK3 activity via the Srk-FAK-ILK pathway. This leads to both cell spreading and fate commitment (Fourel *et al.* 2014).

The findings in this chapter show that HOBs grown *in vitro* will express αV and $\beta 3$ integrins increasingly as time passes (when seeded in DM). This is to be expected since previous studies have shown in osteoblasts that mineralisation occurs roughly 5-6 days post seeding upon which the “ECM maturation and mineralisation” stage begins within osteoblasts (Lian & Stein, 1995). Similarly, there is a rise in the integrin LRP5 could explain the reason why the β -catenin expression in cells from day 3 and day 6 change. Typically, in the Wnt pathway, the release of β -catenin from the GSK3 complex within the cell cytoplasm leads to β -catenin leaving the cytoplasm and entering the nucleus and displacing Groucho protein to bind to TCF1 in order to set cell differentiation in motion and mineralisation (Holmen *et al.* 2005).

We have shown that even over the course of 3 days there is an increase in the expression of αV , $\alpha 5$, $\beta 1$ and $\beta 3$ integrins when cells are grown on mTG or TG2 crosslinked collagen compared to those grown on native collagen. There are several reasons for this. Cellular functions and growth are driven by the ECM and its characteristics; mechanical and chemical (Marklein and Burdick, 2010, Brown *et al.*, 2010).

One mechanical reason for this increase in integrin expression so early on could be seen in chapter 3. The gaps between collagen fibres are significantly smaller in TG2 crosslinked collagen than in native collagen as seen by the smaller space between fibres. Pore alignment and size has been shown to influence cell behaviour including migration and matrix production (Pawelec et al., 2015, Ashworth et al., 2016). There is also growing evidence that shows cells to be sensitive enough to detect and respond to differences on the nano-scale in changes to the environment (Boccaccini et al., 2010). Since HOBs will have more collagen fibres to bind and interact with, this could be the reason why αV , $\alpha 5$, $\beta 3$ and $\beta 1$ integrins are expressed more so in crosslinked collagen scaffolds than in native ones.

Another mechanical cue which could be driving cell migration and differentiation is the difference in collagen stiffness between native and crosslinked collagen. Chau *et al.* have shown rheological differences and an increased mechanical stiffness in crosslinked collagen, this substrate stiffness can act as a cellular signal and lead to differences in cell behaviour (Roskelley et al., 1995, Discher et al., 2007). This is hypothetical however, since the stiffness of these collagen scaffolds were not assessed in this thesis.

Finally, one of the chemical characteristics that is likely to increase the expression of integrins is the increase of RGD peptides. RGD peptides are ligands that have conserved amino acid sequences (Barczyk et al., 2010). These peptides are revealed by crosslinked collagen (Barczyk et al., 2010) and when collagen is denatured into gelatin (Pawelec et al., 2016). Importantly, RGD acts as a primary mediator of the response in HOBs and bind to αV , $\alpha 5$ and $\beta 1$ subunits which is why they increase in fold expression on cells grown on crosslinked collagen (Orban et al., 2004).

$\beta 3$ has been shown to be upregulated in the literature (Orban et al., 2004, Fortunati et al., 2014). A paper by Wozniak *et al.* showed that differences in mechanical stiffness of the collagen and vitronectin substrates can affect the clustering and expression of $\alpha V\beta 3$ (Wozniak et al., 2000).

Native collagen, on the other hand, does not reveal these RGD peptides. Collagen recognition is via a different binding site, i.e GFOGER, which is dependent on collagen's

helical structure (Knight et al., 2000). Here, $\alpha 1$ and $\alpha 2$ integrins have been reported to bind to collagen (Orban et al., 2004), and this is likely to be why expression of these integrins drops by around 0.5 fold in HOBs on TG2 crosslinked collagen. The HOBs are no longer able to bind to GFOGER sites on crosslinked collagen and are expressed less on the HOBs surface.

Interestingly, there was even greater expression of the integrin $\alpha V\beta 3$ pair when HOBs had been seeded on collagen scaffolds with 45S5 bioglass nanoparticles incorporated into them. Here, the expression of $\beta 3$ in mTG and TG2 crosslinked collagen was 1.65 and 1.24 times higher than in native collagen. Xynos *et al.* (2001) showed that these bioglass nanoparticles are capable of stimulating osteogenesis and have an impact on gene regulation regarding differentiation.

While $\beta 1$ integrin expression decreased when HOBs were seeded on native collagen with bioglass, $\alpha 5$ integrin expression did increase. $\alpha 5\beta 1$ are a pair of integrins that have been shown in the literature to bind to RGD peptides to mediate cell adhesion and promote osteogenic differentiation in MSCs (Saidak et al., 2015). Specifically, this pair of integrin receptors link the ECM to intracellular bundles of actin filaments. Once transduced, extracellular signals cross the plasma membrane resulting in the activation of various intracellular signalling cascades, including the Wnt pathway (Schneider et al., 2001). The literature also shows how important the $\alpha 5\beta 1$ integrins are to osteoblast mineralisation by exposing them to antibodies directed at the integrins and showing significant decrease in osteoblast mineralisation (Schneider et al., 2001).

The synthesis and release of collagen from HOBs is seen during mineralisation and differentiation (Rutkovskiy et al., 2016). The collagen produced is an important ECM protein as it further adds to the scaffold and in turn becomes mineralised to form bone (Fortunati et al., 2014). What has been seen is an increase of collagen type 1 being secreted in the ECM when mTG and TG2 are added with media changes. This is explained in the literature, as TG2 has been shown to be a Wnt ligand that binds to LRP5, which leads to the translocation of β -catenin from the cytoplasm and into the nucleus (Faverman et al., 2008).

As stated already, the translocation of β -catenin from the cytoplasm and into the nucleus is crucial in the mineralisation process. It has been shown in the data that this translocation occurs between day 3 and 6 and the total amount of β -catenin does not change within the cell. Curiously, the amount of β -catenin in the cytoplasm and nucleus between HOBs on all collagen scaffolds was different. It has been shown in the data that translocation of β -catenin is occurring earlier than in day 3 on collagen with bioglass, with and without transglutaminase.

The reason for these differences in translocation and activation of the Wnt pathway is likely to be due to the HOBs reacting differently to the mechanical and chemical cues. As stated previously, these include the differences in collagen stiffness, mean collagen pore size, RGD peptides availability and osteogenic stimulation when bioglass is added.

A slight decrease in proliferation seen at day 6 in HOBs seeded on TG2 crosslinked collagen with bioglass (see Chapter 1) might be explained by the increased and more rapid translocation of β -catenin seen in the data here. Since there seems to be a more rapid translocation, there is a possibility that cells on TG2 crosslinked collagen with glass are mineralising and differentiating more quickly than HOBs on native collagen. The increased mineralisation and differentiation leads osteoblasts to mature and become trapped. These cells are then known as osteocytes (Dallas and Bonewald, 2010).

Chapter 6- General discussion

6.1 Background

When biomaterials were first used, they were designed to be inert and elicit no response from the immune system (Hench and Polak, 2002). However, as our understanding of molecular and cellular biology increased a new standard was set: to create materials which could stimulate native tissue regeneration and restore the original functionality. Scaffolds and constructs of this kind would not only support the overall function of the tissue but also communicate with the body at the cellular level (Hench and Polak, 2002). These scaffolds are made from a variety of materials and more natural biological polymers are being introduced every year.

One of the first biological polymers used widely in medical applications was collagen (Ehrmann and Gey, 1956). Since the initial investigations carried out by Ehrman and Gey in 1956, collagen has been used to grow and differentiate many cell types (Lynch et al., 1995, Ivarsson et al., 1998, Reznikoff et al., 1987). There are many diverse applications that have been found for collagen scaffolds by tailoring their structures. These include osteochondral defects, connective tissues, adipose tissues and mammary glands (Tuan-Mu et al., 2016, Shepherd et al., 2013, Davidenko et al., 2010). When processed, however, native collagen is inherently mechanically weak, thermally unstable and susceptible to proteolytic breakdown. In order to overcome this, different techniques have been utilised to crosslink collagen to overcome these deficiencies. Even so, these techniques have impractical drawbacks or leave residual chemical agents at the large scale production level. Thus, many investigations into safer alternatives have been carried out including UVA light and Riboflavin/glucose.

With this in mind, the aim of this thesis was to use TG2 and mTG to achieve the desired crosslinking. Crosslinked collagen with and without 45S5 bioglass was then used as a scaffold for human osteoblasts to be seeded on. From this point, the differences in HOB mineralisation between native and crosslinked collagen with 45S5 bioglass were investigated. The differences in mineralisation rates between the collagen scaffolds were then investigated on

the intracellular level, focussing specifically at the integrins expressed, LRP5 expression and translocation of β -catenin within the cell.

6.2 How novel collagen scaffolds effect the behaviour of human osteoblasts

Figure 6.1 is a summary of how both mechanical and chemical cues contribute to the increased mineralisation compared to native collagen.

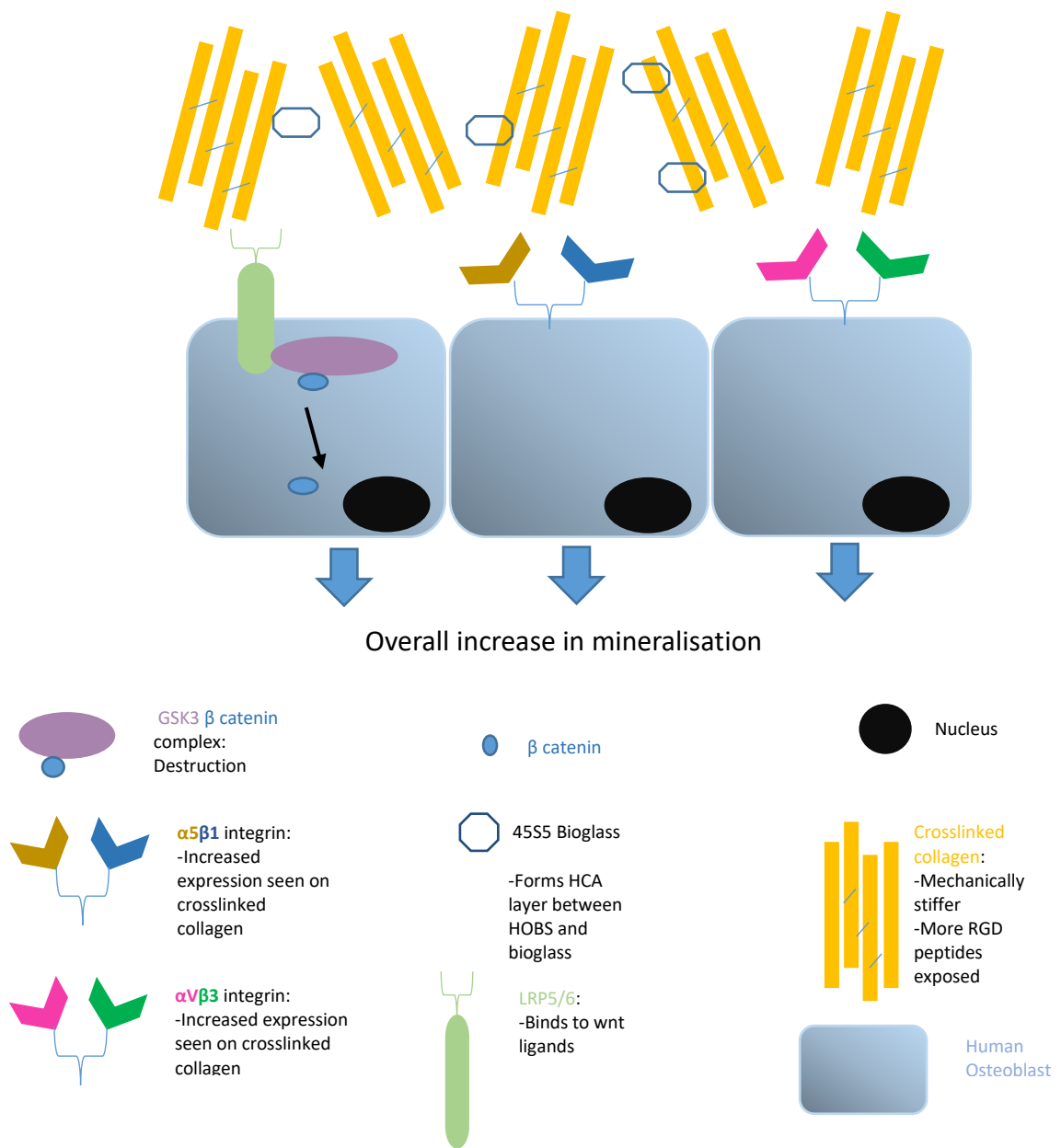


Figure 6.1: A graphic depicting the proposed intracellular process of mineralisation when HOBs are seeded on crosslinked collagen. Here the increased mechanical stiffness, smaller pore size and increased exposure of RGD peptides exposed all contribute to increased expression of $\alpha V\beta 3$ and $\alpha 5\beta 1$ integrins on the cell surface. Coupled with this is the HCA layer formed between the calcium rich 45S5 bioglass and the osteogenic inducing properties of the bioglass (Hench, 1993, Hench et al., 1972, Xynos et al., 2000). The LRP5/6 integrin is also expressed more likely due to HOBs being seeded on a stiffer collagen matrix (Han et al., 2016). All these mechanical and chemical cues lead to the activation of the Wnt pathway and increased mineralisation.

We have shown that over 3 days there is an increase in the expression of αV , $\alpha 5$, $\beta 1$ and $\beta 3$ integrins when cells are grown on mTG or TG2 crosslinked collagen compared to those grown on native collagen. Moreover, there was a decrease in $\alpha 1$ and $\alpha 2$ integrins, which are the integrins that HOBs express when they are exposed to collagen in the ECM. There are several reasons for this.

The gaps between collagen fibres are shown to be significantly smaller in TG2 crosslinked collagen than in native collagen as shown by the SEM images. Pore alignment and size have been shown to influence cell behaviour including migration and matrix production (Pawelec et al., 2015, Ashworth et al., 2016). There is also evidence that shows cells to be sensitive enough to detect and respond to differences on the nano-scale in changes to the environment (Boccaccini et al., 2010). Since HOBs will have more collagen fibres to bind and interact with, this could be a reason why αV , $\alpha 5$, $\beta 3$ and $\beta 1$ integrins are expressed more so in crosslinked collagen scaffolds than in native ones.

As mentioned before another mechanical cue which is likely to be driving cell migration and differentiation is the difference in the stiffness between native and crosslinked collagen. While mechanical stiffness has not been measured in this thesis, Chau *et al.* have shown rheological differences and an increased mechanical stiffness in crosslinked collagen; this substrate stiffness can act as a cellular signal and lead to differences in cell behaviour (Discher et al., 2007). This increased stiffness of the matrix upon which HOBs are seeded on could also be a plausible reason why increase in LRP5 is being observed. Investigations into cells grown on matrices of varying stiffness show there are differences in cell behaviour. When grown on stiffer matrices, epithelial cells have been shown to upregulate LRP5/6 for example (Han et al., 2016). $\beta 3$ integrin has been shown to also be upregulated in the literature (Orban et al., 2004, Fortunati et al., 2014). A paper by Wozniak *et al.* showed that differences in mechanical stiffness of the collagen and vitronectin substrates can affect the clustering and expression of $\alpha V\beta 3$ (Wozniak et al., 2000).

Finally, one of the chemical characteristics that is likely to increase the expression of integrins is the increase of RGD binding sites. These peptides are revealed by crosslinked

collagen (Davidenko et al., 2018) when collagen is denatured into gelatin (Pawelec et al., 2016). αV , $\alpha 5$ and $\beta 1$ subunits all bind to RGD motifs which is why they increase in fold expression on HOBs grown on crosslinked collagen (Orban et al., 2004).

Native collagen does not reveal these RGD binding sites. Collagen recognition by HOBs is via a different binding site: GFOGER, which is dependent on collagen's helical structure (Knight et al., 2000). $\alpha 1$ and $\alpha 2$ integrins are reported to bind to collagen (Orban et al., 2004) and this is likely to be why expression of these integrins drops by around 0.5 fold in HOBs on TG2 crosslinked collagen. The HOBs are less able to bind to GFOGER sites on crosslinked collagen and are expressed less on HOBs surface. It is still uncertain as to why cells seeded on mTG crosslinked collagen did not show a fold decrease in expression of $\alpha 1$ and $\alpha 2$ integrins, although it is clear that the two transglutaminases crosslink collagen differently (Chau et al., 2005). It is clear that there is a difference in the micro-molecular structures between TG2 and mTG crosslinked collagen such as the mean pore size of collagen fibres and this may explain the observed behaviour of HOBs seeded on the respective scaffolds.

An even greater expression of the $\alpha V\beta 3$ and $\alpha 5\beta 1$ integrin pairs were shown when HOBs had been seeded onto crosslinked collagen scaffolds with 45S5 bioglass particles incorporated into them. Xynos *et al.* 2001 have shown that these bioglass nanoparticles are capable of stimulating osteogenesis and have an impact on the upregulation of many genes. Hench *et al.* have also shown that the HCA layer formed between cells and collagen fibres which we hypothesise could also be leading to the HOBs behaving differently (increasing integrin expression) when seeded on these scaffolds.

Whilst $\beta 1$ expression did not increase in HOBs seeded on native collagen with bioglass, we have shown that both $\alpha 5$ and $\beta 1$ integrins are increased on cells seeded on crosslinked collagen with bioglass. This leads to integrins sending extracellular signals across the plasma membrane, resulting in the activation of various intracellular signalling cascades including the Wnt pathway (Schneider et al., 2001). Increased osteoblast mineralisation would be explained by this activation of the Wnt pathway and is also shown in the literature; it has been shown

that by exposing $\alpha 5$ and $\beta 1$ integrins to function blocking antibodies directed at the integrins, there is a significant decrease in osteoblast mineralisation (Schneider et al., 2001).

The collective increase in expression of integrins direct the behaviour of the cells to proliferate and spread and ultimately differentiation and mineralisation (Lai and Cheng, 2005). The increased mineralisation also comes from the exposure to either TG2 itself or cells upregulating LRP5/6 on the cell surface and triggering the destruction of the GSK3 complex. The β -catenin released from this complex is then able to displace Groucho protein to bind to TCF1 in order to set cell differentiation in motion and mineralisation (Holmen et al. 2005).

6.3 Conclusions

In summary, data presented here suggests that treating native collagen with transglutaminases alters it in such a way that it is perceived differently by HOBs during culture. It is theorised that this modified collagen presents itself as being almost gelatin-like with stiffer mechanical properties and a smaller pore size. This behaviour is inferred by the altered integrin expression profile on HOBs. Consequently, this leads to greater expression of LRP5 protein, resulting in the downstream processing required for the observed increased mineralisation.

In this thesis, we have shown that crosslinked collagen mixed with 45S5 bioglass could potentially be used as a biomaterial that enhances mineralisation in bone scaffolds for non-union bone breaks. These crosslinked collagen scaffolds with 45S5 bioglass are more biocompatible than native collagen and also show increased rates of mineralisation. The scaffolds would have low immunogenicity and could grow with the host. This would be a distinct advantage over the titanium plates currently used.

As stated in the introduction, 10% of all bone breaks are non-union and require metal plates and screws in order for the bone to heal. Here we have characterised a base scaffold upon which future development and research can take place.

An immune response against collagen mainly targets epitopes in the telopeptide region at each end of the tropocollagen molecule (Scmitt *et al.* 1964; Davison *et al.*, 1967) However, the conformation of the helical part and the amino acid sequence on the surface of the polymerized collagen fibril, also influence the immunologic profile of the collagen molecule (Michaeli *et al.*, 1969). Thus, the difference of immunogenicity between polymerized collagen and their smaller counterpart lies on the accessibility of the antigenic determinants that decrease during the polymerisation process. This is certainly something to consider when creating a collagen scaffold to be used as an implant in an animal model. Despite this type I collagen is still considered a suitable material for implantation since only a small amount of people possess humoral immunity against it and a simple serologic test can verify if a patient is susceptible to an allergic reaction in response to this collagen-based biomaterial (Charriere *et al.* 1989).

Further rheological studies as well as characterisation and optimisation of the crosslinked scaffold, could one day lead to a low immunogenic, simple and effective implant that can be transplanted into humans.

References

- Aeschlimann, D. & V. Thomazy (2000) Protein crosslinking in assembly and remodelling of extracellular matrices: The role of transglutaminases. *Connective Tissue Research*, 41, 111-121.
- Aeschlimann, D., A. Wetterwald, H. Fleisch & M. Paulsson (1993) Expression of tissue transglutaminase in skeletal tissues correlates with events of terminal differentiation of chondrocytes. *Journal of Cell Biology*, 120, 1461-1470.
- Akimov, S. S. & A. M. Belkin (2000) Integrin-associated cell surface tissue transglutaminase promotes fibronectin matrix assembly. *Molecular Biology of the Cell*, 11, 266A-266A.
- Akimov, S. S. (2001) Cell-surface transglutaminase promotes fibronectin assembly via interaction with the gelatin-binding domain of fibronectin: a role in TGF beta-dependent matrix deposition. *Journal of Cell Science*, 114, 2989-3000.
- Akimov, S. S., D. Krylov, L. F. Fleischman & A. M. Belkin (2000) Tissue transglutaminase is an integrin-binding adhesion coreceptor for fibronectin. *Journal of Cell Biology*, 148, 825-838.
- Al-Jallad, H. F., Y. Nakano, J. L. Y. Chen, E. McMillan, C. Lefebvre & M. T. Kaartinen (2006) Transglutaminase activity regulates osteoblast differentiation and matrix mineralization in MOT3-E1 osteoblast cultures. *Matrix Biology*, 25, 135-148.
- Ando, H., M. Adachi, K. Umeda, A. Matsuura, M. Nonaka, R. Uchio, H. Tanaka & M. Motoki (1989) Purification and characteristics of a novel transglutaminase derived from microorganisms. *Agricultural and Biological Chemistry*, 53, 2613-2617.
- Auld, G. C., H. Ritchie, L. A. Robbie & N. A. Booth (2001) Thrombin upregulates tissue transglutaminase in endothelial cells - A potential role for tissue transglutaminase in stability of atherosclerotic plaque. *Arteriosclerosis Thrombosis and Vascular Biology*, 21, 1689-1694.
- Baino, F. & C. Vitale-Brovarone (2011) Three-dimensional glass-derived scaffolds for bone tissue engineering: Current trends and forecasts for the future. *Journal of Biomedical Materials Research Part A*, 97A, 514-535.
- Barczyk, M., S. Carracedo & D. Gullberg (2010) Integrins. *Cell and Tissue Research*, 339, 269-280.
- Barrere, F., T. A. Mahmood, K. de Groot & C. A. van Blitterswijk (2008) Advanced biomaterials for skeletal tissue regeneration: Instructive and smart functions. *Materials Science & Engineering R-Reports*, 59, 38-71.
- Barsigian, C., A. M. Stern & J. Martinez (1991) Tissue (type-II) transglutaminase covalently incorporates itself, fibrinogen, or fibronectin into high-molecular-weight complexes on the extracellular surface of isolated hepatocytes - use of 2-(2-oxopropyl)thio imidazolium derivatives as cellular transglutaminase inactivators. *Journal of Biological Chemistry*, 266, 22501-22509.
- Bauer, T. W. & G. F. Muschler (2000) Bone graft materials - An overview of the basic science. *Clinical Orthopaedics and Related Research*, 10-27.
- Beazley, K. E., S. Deasey, F. Lima & M. V. Nurminskaya (2012) Transglutaminase 2-mediated activation of beta-catenin signaling has a critical role in warfarin-induced vascular Calcification. *Arteriosclerosis Thrombosis and Vascular Biology*, 32, 123-U302.
- Begg, G. E., L. Carrington, P. H. Stokes, J. M. Matthews, M. A. Wouters, A. Husain, L. Lorand, S. E. Iismaa & R. M. Graham (2006) Mechanism of allosteric regulation of transglutaminase 2 by GTP. *Proceedings of the National Academy of Sciences of the United States of America*, 103, 19683-19688.

- Belkin, A. M. (2011) Extracellular TG2: emerging functions and regulation. *Febs Journal*, 278, 4704-4716.
- Benilova, I., E. Karan & B. De Strooper (2012) The toxic A beta oligomer and Alzheimer's disease: an emperor in need of clothes. *Nature Neuroscience*, 15, 349-357.
- Beninati, S. (1995) Posttranslational modification of protein in cancer-cells - the transglutaminase-catalyzed reactions. *Cancer Journal*, 8, 234-236.
- Beninati, S. & M. Piacentini (2004) The transglutaminase family: an overview: Minireview article. *Amino Acids*, 26, 367-372.
- Boccaccini, A. R., M. Erol, W. J. Stark, D. Mohn, Z. Hong & J. F. Mano (2010) Polymer/bioactive glass nanocomposites for biomedical applications: A review. *Composites Science and Technology*, 70, 1764-1776.
- Boros, S., E. Ahrman, L. Wunderink, B. Kamps, W. W. de Jong, W. C. Boelens & C. S. Emanuelsson (2006) Site-specific transamidation and deamidation of the small heat-shock protein Hsp20 by tissue transglutaminase. *Proteins-Structure Function and Bioinformatics*, 62, 1044-1052.
- Bowness, J. M., A. H. Tarr & T. Wong (1988) Increased transglutaminase activity during skin wound-healing in rats. *Biochimica Et Biophysica Acta*, 967, 234-240.
- Boyce, B. F. & L. P. Xing (2007) Biology of RANK, RANKL, and osteoprotegerin. *Arthritis Research & Therapy*, 9.
- Boyden, L. M., J. H. Mao, J. Belsky, L. Mitzner, A. Farhi, M. A. Mitnick, D. Q. Wu, K. Insogna & R. P. Lifton (2002) High bone density due to a mutation in LDL-receptor-related protein 5. *New England Journal of Medicine*, 346, 1513-1521.
- Bruce, S. E. & T. J. Peters (1983) The subcellular-localization of transglutaminase in normal liver and in glucagon-treated and partial hepatectomized rats. *Bioscience Reports*, 3, 1085-1090.
- Brydone, A. S., D. Meek & S. MacLaine (2010) Bone grafting, orthopaedic biomaterials, and the clinical need for bone engineering. *Proceedings of the Institution of Mechanical Engineers Part H-Journal of Engineering in Medicine*, 224, 1329-1343.
- Chau, D. Y. S., R. J. Collighan, E. A. M. Verderio, V. L. Addy & M. Griffin (2005) The cellular response to transglutaminase-cross-linked collagen. *Biomaterials*, 26, 6518-6529.
- Chau, J. F. L., W. F. Leong & B. Li (2009) Signaling pathways governing osteoblast proliferation, differentiation and function. *Histology and Histopathology*, 24, 1593-1606.
- Charriere, G., Bejot, M., Schnitzler, L., Ville, G., & Hartmann, D. J. (1989). Reactions to a bovine collagen implant: Clinical and immunologic study in 705 patients. *Journal of the American Academy of Dermatology*, 21(6), 1203-120
- Chen, J. S. K. & K. Mehta (1999) Tissue transglutaminase: an enzyme with a split personality. *International Journal of Biochemistry & Cell Biology*, 31, 817-836.
- Cho, T. J., L. C. Gerstenfeld & T. A. Einhorn (2002) Differential temporal expression of members of the transforming growth factor beta superfamily during murine fracture healing. *Journal of Bone and Mineral Research*, 17, 513-520.
- Cooper, D. M. L., J. R. Matyas, M. A. Katzenberg & B. Hallgrímsson (2004) Comparison of microcomputed tomographic and microradiographic measurements of cortical bone porosity. *Calcified Tissue International*, 74, 437-447.

- Davidenko, N., J. J. Campbell, E. S. Thian, C. J. Watson & R. E. Cameron (2010) Collagen-hyaluronic acid scaffolds for adipose tissue engineering. *Acta Biomaterialia*, 6, 3957-3968.
- Develioglu, H., S. U. Saraydin & U. Kartal (2009) The bone-healing effect of a xenograft in a rat calvarial defect model. *Dental Materials Journal*, 28, 396-400.
- DiGirolamo, D. J., T. L. Clemens & S. Kousteni (2012) The skeleton as an endocrine organ. *Nature Reviews Rheumatology*, 8, 674-683.
- Dimitriou, R., E. Jones, D. McGonagle & P. V. Giannoudis (2011) Bone regeneration: current concepts and future directions. *Bmc Medicine*, 9.
- Dimitriou, R., E. Tsiridis & P. V. Giannoudis (2005) Current concepts of molecular aspects of bone healing. *Injury-International Journal of the Care of the Injured*, 36, 1392-1404.
- Discher, D. E., L. Sweeney, S. Sen & A. Engler (2007) Matrix elasticity directs stem cell lineage specification. *Biophysical Journal*, 32A-32A.
- Doherty, M., R. P. Boot-Handford, M. E. Grant & A. E. Canfield (1998) Identification of genes expressed during the osteogenic differentiation of vascular pericytes in vitro. *Biochemical Society Transactions*, 26, S4-S4.
- Duran, R., M. Junqua, J. M. Schmitter, C. Gancet & P. Goulas (1998) Purification, characterisation, and gene cloning of transglutaminase from *Streptoverticillium cinnamoneum* CBS 683.68. *Biochimie*, 80, 313-319.
- Dy, C. J., K. E. McCollister, D. A. Lubarsky & J. M. Lane (2011) An economic evaluation of a systems-based strategy to expedite surgical treatment of hip fractures. *Journal of Bone and Joint Surgery-American Volume*, 93A, 1326-1334.
- Eckert, R. L., M. T. Sturniolo, A. M. Broome, M. Ruse & E. A. Rorke (2005) Transglutaminase function in epidermis. *Journal of Investigative Dermatology*, 124, 481-492.
- Ehrler, D. M. & A. R. Vaccaro (2000) The use of allograft bone in lumbar spine surgery. *Clinical Orthopaedics and Related Research*, 38-45.
- Ehrmann, R. L. & G. O. Gey (1956) The growth of cells on a transparent gel of reconstituted rat-tail collagen. *Journal of the National Cancer Institute*, 16, 1375-403.
- Esposito, C. & I. Caputo (2005) Mammalian transglutaminases - Identification of substrates as a key to physiological function and physiopathological relevance. *Febs Journal*, 272, 615-631.
- Faverman, L., L. Mikhaylova, J. Malmquist & M. Nurminskaya (2008) Extracellular transglutaminase 2 activates beta-catenin signaling in calcifying vascular smooth muscle cells. *Febs Letters*, 582, 1552-1557.
- Fayaz, H. C., P. V. Giannoudis, M. S. Vrahas, R. M. Smith, C. Moran, H. C. Pape, C. Krettek & J. B. Jupiter (2011) The role of stem cells in fracture healing and nonunion. *International Orthopaedics*, 35, 1587-1597.
- Fazzalari, N. L. (2011) Bone fracture and bone fracture repair. *Osteoporosis International*, 22, 2003-2006.
- Fesus, L. & M. Piacentini (2002) Transglutaminase 2: an enigmatic enzyme with diverse functions. *Trends in Biochemical Sciences*, 27, 534-539.
- Fesus, L. & Z. Szondy (2005) Transglutaminase 2 in the balance of cell survival and death. *Febs Journal*, 272, 409-409.

- Fesus, L., V. Thomazy & A. Falus (1987) Induction and activation of tissue transglutaminase during programmed cell-death. *Febs Letters*, 224, 104-108.
- Finkemeier, C. G. (2002) Bone-grafting and bone-graft substitutes. *Journal of Bone and Joint Surgery-American Volume*, 84A, 454-464.
- Fleckenstein, B., Y. Molberg, S. W. Qiao, D. G. Schmid, F. von der Mullbe, K. Elgstoer, G. Jung & L. M. Sollid (2002) Gliadin T cell epitope selection by tissue transglutaminase in Celiac disease - Role of enzyme specificity and pH influence on the transamidation versus deamidation reactions. *Journal of Biological Chemistry*, 277, 34109-34116.
- Folk, J. E. (1983) Mechanism and basis for specificity of transglutaminase-catalyzed -epsilon-(gamma-glutamyl) lysine bond formation. *Advances in Enzymology and Related Areas of Molecular Biology*, 54, 1-56.
- Forsprecher, J., Z. M. Wang, H. A. Goldberg & M. T. Kaartinen (2011) Transglutaminase-mediated oligomerization promotes osteoblast adhesive properties of osteopontin and bone sialoprotein. *Cell Adhesion & Migration*, 5, 65-72.
- Fortunati, D., D. Y. S. Chau, Z. Wang, R. J. Collighan & M. Griffin (2014) Cross-linking of collagen I by tissue transglutaminase provides a promising biomaterial for promoting bone healing. *Amino Acids*, 46, 1751-1761.
- Fratzl, P. (2008). Collagen: structure and mechanics, an introduction. In *Collagen* (pp. 1-13). Springer, Boston, MA
- Friess, W. (1998). Collagen–biomaterial for drug delivery. *European journal of pharmaceutics and biopharmaceutics*, 45(2), 113-136
- Gentile, V., M. Saydak, E. A. Chiocca, O. Akande, P. J. Birckbichler, K. N. Lee, J. P. Stein & P. J. A. Davies (1991) Isolation and characterization of cdna clones to mouse macrophage and human endothelial-cell tissue transglutaminases. *Journal of Biological Chemistry*, 266, 478-483.
- Gerhardt, L.-C. & A. R. Boccaccini (2010) Bioactive glass and glass-ceramic scaffolds for bone tissue engineering. *Materials*, 3, 3867-3910.
- Gerstenfeld, L. C., D. M. Cullinane, G. L. Barnes, D. T. Graves & T. A. Einhorn (2003) Fracture healing as a post-natal developmental process: Molecular, spatial, and temporal aspects of its regulation. *Journal of Cellular Biochemistry*, 88, 873-884.
- Gomes, K. U., J. L. Carlini, C. Biron, A. Rapoport & R. A. Dedivitis (2008) Use of Allogeneic Bone Graft in Maxillary Reconstruction for Installation of Dental implants. *Journal of Oral and Maxillofacial Surgery*, 66, 2335-2338.
- Gong, Y. Q., R. B. Slee, N. Fukai, G. Rawadi, S. Roman-Roman, A. M. Reginato, H. W. Wang, T. Cundy, F. H. Glorieux, D. Lev, M. Zacharin, K. Oexle, J. Marcelino, W. Suwairi, S. Heeger, G. Sabatakos, S. Apte, W. N. Adkins, J. Allgrove, M. Arslan-Kirchner, J. A. Batch, P. Beighton, G. C. M. Black, R. G. Boles, L. M. Boon, C. Borrone, H. G. Brunner, G. F. Carle, B. Dallapiccola, A. De Paepe, B. Floege, M. L. Halfhide, B. Hall, R. C. Hennekam, T. Hirose, A. Jans, H. Juppner, C. A. Kim, K. Keppler-Noreuil, A. Kohlschuetter, D. LaCombe, M. Lambert, E. Lemyre, T. Letteboer, L. Peltonen, R. S. Ramesar, M. Romanengo, H. Somer, E. Steichen-Gersdorf, B. Steinmann, B. Sullivan, A. Superti-Furga, W. Swoboda, M. J. van den Boogaard, W. Van Hul, M. Vikkula, M. Votruba, B. Zabel, T. Garcia, R. Baron, B. R. Olsen, M. L. Warman & S. Osteoporosis Pseudoglioma (2001) LDL receptor-related protein 5 (LRP5) affects bone accrual and eye development. *Cell*, 107, 513-523.

- Greenwald, A. S., S. D. Boden, V. M. Goldberg, Y. Khan, C. T. Laurencin, R. N. Rosier & I. Comm Biological (2001) Bone-graft substitutes: Facts, fictions, and applications. *Journal of Bone and Joint Surgery-American Volume*, 83A, 98-103.
- Griffin, M., R. Casadio & C. M. Bergamini (2002) Transglutaminases: Nature's biological glues. *Biochemical Journal*, 368, 377-396.
- Grover, C. N., Cameron, R. E., & Best, S. M. (2012). Investigating the morphological, mechanical and degradation properties of scaffolds comprising collagen, gelatin and elastin for use in soft tissue engineering. *Journal of the mechanical behavior of biomedical materials*, 10, 62-74
- Gundemir, S., G. Colak, J. Tucholski & G. V. W. Johnson (2012) Transglutaminase 2: A molecular Swiss army knife. *Biochimica Et Biophysica Acta-Molecular Cell Research*, 1823, 406-419.
- Hall, B. K. & T. Miyake (2000) All for one and one for all: condensations and the initiation of skeletal development. *Bioessays*, 22, 138-147.
- Han, B. G., J. W. Cho, Y. D. Cho, K. C. Jeong, S. Y. Kim & B. I. Lee (2010) Crystal structure of human transglutaminase 2 in complex with adenosine triphosphate. *International Journal of Biological Macromolecules*, 47, 190-195.
- Hasegawa, G., M. Suwa, Y. Ichikawa, T. Ohtsuka, S. Kumagai, M. Kikuchi, Y. Sato & Y. Saito (2003) A novel function of tissue-type transglutaminase: protein disulphide isomerase. *Biochemical Journal*, 373, 793-803.
- He, X., M. Semenov, K. Tamai & X. Zeng (2004) LDL receptor-related proteins 5 and 6 in Wnt/beta-catenin signaling: Arrows point the way. *Development*, 131, 1663-1677.
- Hench, L. L. (1993) Bioceramics - from concept to clinic. *American Ceramic Society Bulletin*, 72, 93-98.
- Hench, L. L. (1998) Bioceramics. *Journal of the American Ceramic Society*, 81, 1705-1728.
- Hench, L. L. (2006) The story of Bioglass (R). *Journal of Materials Science-Materials in Medicine*, 17, 967-978.
- Hench, L. L. & Polak, J. M. (2002) Third-generation biomaterials. *Science*, 295, 1014-1017.
- Hench, L. L., R. J. Splinter, W. C. Allen & T. K. Greenlee (1972) Bonding mechanisms at the interface of ceramic prosthetic materials. Hall, C. W., S. F. Hulbert, S. N. Levine and F. A. Young. *Journal of Biomedical materials research*. Biomedical Materials symposium, no. 2. bioceramics-engineering in medicine. Henniker, New Hampshire, August 3-7, 1970. Illus. Interscience publishers, A division of John Wiley and sons: New York, U.S.A.; London, England, 117-141.
- Ho, M. L., S. Z. Leu, J. F. Hsieh & S. T. Jiang (2000) Technical approach to simplify the purification method and characterization of microbial transglutaminase produced from *Streptomyces* ladakanum. *Journal of Food Science*, 65, 76-80.
- Horch, R. E. (2006) Future perspectives in tissue engineering. *Journal of Cellular and Molecular Medicine*, 10, 4-6.
- Huebsch, N., Arany, P. R., Mao, A. S., Shvartsman, D., Ali, O. A., Bencherif, S. A. & Mooney, D. J. (2010). Harnessing traction-mediated manipulation of the cell/matrix interface to control stem-cell fate. *Nature materials*, 9(6), 518
- Hutmacher, D. (2013) Bone regeneration based on tissue engineering conceptions - A 21st century perspective. *Human Gene Therapy*, 24, A27-A27.

- Iismaa, S. E. (2016) The prostate-specific protein, transglutaminase 4 (TG4), is an autoantigen associated with male subfertility. *Annals of Translational Medicine*, 4.
- Ikura, K., T. Nasu, H. Yokota, Y. Tsuchiya, R. Sasaki & H. Chiba (1988) Amino-acid sequence of guinea-pig liver transglutaminase from its cdna sequence. *Biochemistry*, 27, 2898-2905.
- Jang, T. H., D. S. Lee, K. Choi, E. M. Jeong, I. G. Kim, Y. W. Kim, J. N. Chun, J. H. Jeon & H. H. Park (2014) Crystal structure of transglutaminase 2 with GTP complex and amino acid sequence evidence of evolution of GTP binding site. *Plos One*, 9.
- Janiak, A., E. A. Zemskov & A. M. Belkin (2006) Cell surface transglutaminase promotes RhoA activation via integrin clustering and suppression of the Src-p190RhoGAP signaling pathway. *Molecular Biology of the Cell*, 17, 1606-1619.
- Janicki, P. & G. Schmidmaier (2011) What should be the characteristics of the ideal bone graft substitute? Combining scaffolds with growth factors and/or stem cells. *Injury-International Journal of the Care of the Injured*, 42, S77-S81.
- Johnson, K. A. & R. A. Terkeltaub (2005) External GTP-bound transglutaminase 2 is a molecular switch for chondrocyte hypertrophic differentiation and calcification. *Journal of Biological Chemistry*, 280, 15004-15012.
- Johnson, T. S., M. Fisher, J. L. Haylor, Z. Hau, N. J. Skill, R. Jones, R. Saint, I. Coutts, M. E. Vickers, A. M. El Nahas & M. Griffini (2007) Transglutaminase inhibition reduces fibrosis and preserves function in experimental chronic kidney disease. *Journal of the American Society of Nephrology*, 18, 3078-3088.
- Johnson, T. S., M. Griffin, G. L. Thomas, J. Skill, A. Cox, B. Yang, B. Nicholas, P. J. Birckbichler, C. MuchanetaKubara & A. M. ElNahas (1997) The role of transglutaminase in the rat subtotal nephrectomy model of renal fibrosis. *Journal of Clinical Investigation*, 99, 2950-2960.
- Johnson, T. S., N. J. Skill, A. M. El Nahas, S. D. Oldroyd, G. L. Thomas, J. A. Douthwaite, J. L. Haylor & M. Griffin (1999) Transglutaminase transcription and antigen translocation in experimental renal scarring. *Journal of the American Society of Nephrology*, 10, 2146-2157.
- Jones, R. A., P. Kotsakis, T. S. Johnson, D. Chau, E. Verderio, S. Ali & M. Griffin (2005) Extracellular matrix changes induced by transglutaminase 2 block angiogenesis and tumor growth. *Febs Journal*, 272, 411-411.
- Jones, R. A., B. Nicholas, S. Mian, P. J. A. Davies & M. Griffin (1997) Reduced expression of tissue transglutaminase in a human endothelial cell line leads to changes in cell spreading, cell adhesion and reduced polymerisation of fibronectin. *Journal of Cell Science*, 110, 2461-2472.
- Kaartinen, M. T., A. Pirhonen, A. Linnala-Kankkunen & P. H. Maenpaa (1999) Cross-linking of osteopontin by tissue transglutaminase increases its collagen binding properties. *Journal of Biological Chemistry*, 274, 1729-1735.
- Kaartinen, M. T., A. Pirhonen, A. LinnalaKankkunen & P. H. Maenpaa (1997) Transglutaminase-catalyzed cross-linking of osteopontin is inhibited by osteocalcin. *Journal of Biological Chemistry*, 272, 22736-22741.
- Kalinin, A. E., A. V. Kajava & P. M. Steinert (2002) Epithelial barrier function: assembly and structural features of the cornified cell envelope. *Bioessays*, 24, 789-800.

- Kanaji, T., H. Ozaki, T. Takao, H. Kawajiri, H. Ide, M. Motoki & Y. Shimonishi (1993) Primary structure of microbial transglutaminase from streptoverticillium sp strain-s-8112. *Journal of Biological Chemistry*, 268, 11565-11572.
- Kashiwagi, T., K. Yokoyama, K. Ishikawa, K. Ono, D. Ejima, H. Matsui & E. Suzuki (2002) Crystal structure of microbial transglutaminase from Streptoverticillium mobaraense. *Journal of Biological Chemistry*, 277, 44252-44260.
- Kawano, Y. & R. Kypta (2003) Secreted antagonists of the Wnt signalling pathway. *Journal of Cell Science*, 116, 2627-2634.
- Klingberg, F., B. Hinz & E. S. White (2013) The myofibroblast matrix: implications for tissue repair and fibrosis. *Journal of Pathology*, 229, 298-309.
- Knight, C. G., L. F. Morton, A. R. Peachey, D. S. Tuckwell, R. W. Farndale & M. J. Barnes (2000) The collagen-binding A-domains of integrins alpha(1)beta(1) and alpha(2)beta(1) recognize the same specific amino acid sequence, GFOGER, in native (triple-helical) collagens. *Journal of Biological Chemistry*, 275, 35-40.
- Kothari, A. N., Mi, Z., Zapf, M., & Kuo, P. C. (2014). Novel clinical therapeutics targeting the epithelial to mesenchymal transition. *Clinical and translational medicine*, 3(1), 35
- Kronenberg, H. M. (2003) Developmental regulation of the growth plate. *Nature*, 423, 332-336.
- Lai, C. F. & S. L. Cheng (2005) alpha v beta integrins play an essential role in BMP-2 induction of osteoblast differentiation. *Journal of Bone and Mineral Research*, 20, 330-340.
- Lai, T. S., T. F. Slaughter, K. A. Peoples, J. M. Hettasch & C. S. Greenberg (1998) Regulation of human tissue transglutaminase function by magnesium-nucleotide complexes - Identification of distinct binding sites for Mg-GTP and Mg-ATP. *Journal of Biological Chemistry*, 273, 1776-1781.
- Langer, R. & J. P. Vacanti (1993) Tissue engineering. *Science*, 260, 920-926.
- Lash, N. J., J. A. Feller, L. M. Batty, J. Wasiak & A. K. Richmond (2015) Bone grafts and bone substitutes for opening-wedge osteotomies of the Knee: A Systematic Review. *Arthroscopy-the Journal of Arthroscopic and Related Surgery*, 31, 720-730.
- Lee, P. F., Y. Bai, R. L. Smith, K. J. Bayless & A. T. Yeh (2013) Angiogenic responses are enhanced in mechanically and microscopically characterized, microbial transglutaminase crosslinked collagen matrices with increased stiffness. *Acta Biomaterialia*, 9, 7178-7190.
- Leighton, R., J. T. Watson, P. Giannoudis, C. Papakostidis, A. Harrison & R. G. Steen (2017) Healing of fracture nonunions treated with low-intensity pulsed ultrasound (LIPUS): A systematic review and meta-analysis. *Injury-International Journal of the Care of the Injured*, 48, 1339-1347.
- Lesort, M., K. Attanavanich, J. W. Zhang & G. V. W. Johnson (1998) Distinct nuclear localization and activity of tissue transglutaminase. *Journal of Biological Chemistry*, 273, 11991-11994.
- Lieberman, J. R., A. Daluisi & T. A. Einhorn (2002) The role of growth factors in the repair of bone - Biology and clinical applications. *Journal of Bone and Joint Surgery-American Volume*, 84A, 1032-1044.
- Lindfors, K., T. Rauhavirta, R. Kivistö, P. T. Mannisto, A. G. Horsman, M. Griffin, M. Maki & K. Kaukinen (2011) Are TG2 inhibitors able to decrease gliadin-induced toxicity related to celiac disease - A proof-of-concept study. *Gastroenterology*, 140, S644-S644.

- Liu, S. P., R. A. Cerione & J. Clardy (2002) Structural basis for the guanine nucleotide-binding activity of tissue transglutaminase and its regulation of transamidation activity. *Proceedings of the National Academy of Sciences of the United States of America*, 99, 2743-2747.
- Logan, C. Y. & R. Nusse (2004) The Wnt signaling pathway in development and disease. *Annual Review of Cell and Developmental Biology*, 20, 781-810.
- Lorand, L. & S. M. Conrad (1984) Transglutaminases. *Molecular and Cellular Biochemistry*, 58, 9-35.
- Lynch, M. P., J. L. Stein, G. S. Stein & J. B. Lian (1995) The influence of type-i collagen on the development and maintenance of the osteoblast phenotype in primary and passaged rat calvarial osteoblasts - modification of expression of genes supporting cell-growth, adhesion, and extracellular-matrix mineralization. *Experimental Cell Research*, 216, 35-45.
- Majidinia, M., A. Sadeghpour & B. Yousefi (2018) The roles of signaling pathways in bone repair and regeneration. *Journal of Cellular Physiology*, 233, 2937-2948.
- Makarova, K. S., L. Aravind & E. V. Koonin (1999) A superfamily of archaeal, bacterial, and eukaryotic proteins homologous to animal transglutaminases. *Protein Science*, 8, 1714-1719.
- Mariani, P., F. Carsughi, F. Spinozzi, S. Romanzetti, G. Meier, R. Casadio & C. M. Bergamini (2000) Ligand-induced conformational changes in tissue transglutaminase: Monte Carlo analysis of small-angle scattering data. *Biophysical Journal*, 78, 3240-3251.
- Marks, S. C. & S. N. Popoff (1988) Bone cell biology - the regulation of development, structure, and function in the skeleton. *American Journal of Anatomy*, 183, 1-44.
- Marsell, R. & T. A. Einhorn (2011) The biology of fracture healing. *Injury-International Journal of the Care of the Injured*, 42, 551-555.
- Martin, R. B. (1991) Determinants of the mechanical-properties of bones. *Journal of Biomechanics*, 24, 79-88.
- Martínez, A., Blanco, M. D., Davidenko, N., & Cameron, R. E. (2015). Tailoring chitosan/collagen scaffolds for tissue engineering: Effect of composition and different crosslinking agents on scaffold properties. *Carbohydrate polymers*, 132, 606-619
- Melino, G., & Piacentini, M. (1998). Tissue transglutaminase in cell death: a downstream or a multifunctional upstream effector?. *FEBS letters*, 430(1-2), 59-63.
- Miller, S. C., L. Saintgeorges, B. M. Bowman & W. S. S. Jee (1989) Bone lining cells - structure and function. *Scanning Microscopy*, 3, 953-961.
- Mills, S. J., Cowin, A. J., & Kaur, P. (2013). Pericytes, mesenchymal stem cells and the wound healing process. *Cells*, 2(3), 621-634
- Mishra, S. & L. J. Murphy (2004) Tissue transglutaminase has intrinsic kinase activity - Identification of transglutaminase 2 as an insulin-like growth factor-binding protein-3 kinase. *Journal of Biological Chemistry*, 279, 23863-23868.
- Mosher, D. F., P. E. Schad & H. K. Kleinman (1979) Cross-linking of fibronectin to collagen by blood-coagulation factor-xiiia. *Journal of Clinical Investigation*, 64, 781-787.
- Mountziaris, P. M. & A. G. Mikos (2008) Modulation of the inflammatory response for enhanced bone tissue regeneration. *Tissue Engineering Part B-Reviews*, 14, 179-186.

- Mullen, L. M., Best, S. M., Brooks, R. A., Ghose, S., Gwynne, J. H., Wardale, J. & Cameron, R. E. (2010). Binding and release characteristics of insulin-like growth factor-1 from a collagen–glycosaminoglycan scaffold. *Tissue Engineering Part C: Methods*, 16(6), 1439-1448.
- Murthy, S. N. P., S. Iismaa, G. Begg, D. M. Freymann, R. M. Graham & L. Lorand (2002) Conserved tryptophan in the core domain of transglutaminase is essential for catalytic activity. *Proceedings of the National Academy of Sciences of the United States of America*, 99, 2738-2742.
- Murthy, S. N. P., J. Wilson, S. L. Guy & L. Lorand (1991) Intramolecular cross-linking of monomeric fibrinogen by tissue transglutaminase. *Proceedings of the National Academy of Sciences of the United States of America*, 88, 10601-10604.
- Nadalutti, C., K. M. Viiri, K. Kaukinen, M. Maki & K. Lindfors (2011) Extracellular transglutaminase 2 has a role in cell adhesion, whereas intracellular transglutaminase 2 is involved in regulation of endothelial cell proliferation and apoptosis. *Cell Proliferation*, 44, 49-58.
- Naderi, H., M. M. Matin & A. R. Bahrami (2011) Review paper: Critical issues in tissue engineering: Biomaterials, cell sources, angiogenesis, and drug delivery systems. *Journal of Biomaterials Applications*, 26, 383-417.
- Nagy, L., M. Saydak, N. Shipley, S. Lu, J. P. Basilion, Z. H. Yan, P. Syka, R. A. S. Chandraratna, J. P. Stein, R. A. Heyman & P. J. A. Davies (1996) Identification and characterization of a versatile retinoid response element (retinoic acid receptor response element-retinoid X receptor response element) in the mouse tissue transglutaminase gene promoter. *Journal of Biological Chemistry*, 271, 4355-4365.
- Nakajima, A., N. Shimoji, K. Shiomi, S. Shimizu, H. Moriya, T. A. Einhorn & M. Yamazaki (2002) Mechanisms for the enhancement of fracture healing in rats treated with intermittent low-dose human parathyroid hormone (1-34). *Journal of Bone and Mineral Research*, 17, 2038-2047.
- Nakanishi, K., K. Nara, H. Hagiwara, Y. Aoyama, H. Ueno & S. Hirose (1991) Cloning and sequence-analysis of cdna clones for bovine aortic-endothelial-cell transglutaminase. *European Journal of Biochemistry*, 202, 15-21.
- Nakano, Y., W. N. Addison & M. T. Kaartinen (2007) ATP-mediated mineralization of MOT3-E1 osteoblast cultures. *Bone*, 41, 549-561.
- Nakano, Y., J. Forsprecher & M. T. Kaartinen (2010) Regulation of ATPase activity of transglutaminase 2 by MT1-MMP: Implications for mineralization of MC3T3-E1 osteoblast cultures. *Journal of Cellular Physiology*, 223, 260-269.
- Nijweide, P. J., E. H. Burger & J. H. M. Feyen (1986) Cells of bone - proliferation, differentiation, and hormonal-regulation. *Physiological Reviews*, 66, 855-886.
- Nonaka, M., Y. Matsuura, K. Nakano & M. Motoki (1997) Improvement of the pH-solubility profile of sodium caseinate by using Ca²⁺-independent microbial transglutaminase with gelatin. *Food Hydrocolloids*, 11, 347-349.
- Nonaka, M., H. Sakamoto, S. Toiguchi, H. Kawajiri, T. Soeda & M. Motoki (1992) Sodium caseinate and skim milk gels formed by incubation with microbial transglutaminase. *Journal of Food Science*, 57, 1214-8.
- Nurminskaya, M. & M. T. Kaartinen (2006) Transglutaminases in mineralized tissues. *Frontiers in Bioscience*, 11, 1591-1606.

- Nurminskaya, M. & T. F. Linsenmayer (1996) Identification and characterization of up-regulated genes during chondrocyte hypertrophy. *Developmental Dynamics*, 206, 260-271.
- Nurminskaya, M., C. Magee, L. Faverman & T. F. Linsenmayer (2003) Chondrocyte-derived transglutaminase promotes maturation of preosteoblasts in periosteal bone. *Developmental Biology*, 263, 139-152.
- Opperman, L. A. (2000) Cranial sutures as intramembranous bone growth sites. *Developmental Dynamics*, 219, 472-485.
- Orban, J. M., L. B. Wilson, J. A. Kofroth, M. S. El-Kurdi, T. M. Maul & D. A. Vorp (2004) Crosslinking of collagen gels by transglutaminase. *Journal of Biomedical Materials Research Part A*, 68A, 756-762.
- Oryan, A., A. M. Parizi, Z. Shafiei-Sarvestani & A. S. Bigham (2012) Effects of combined hydroxyapatite and human platelet rich plasma on bone healing in rabbit model: radiological, macroscopical, histopathological and biomechanical evaluation. *Cell and Tissue Banking*, 13, 639-651.
- Ou, H. S., J. Haendeler, M. R. Aeby, L. A. Kelly, B. C. Cholewa, G. Koike, A. Kwitek-Black, H. J. Jacob, B. C. Berk & J. M. Miano (2000) Retinoic acid-induced tissue transglutaminase and apoptosis in vascular smooth muscle cells. *Circulation Research*, 87, 881-887.
- Parikh, S. N. (2002) Bone graft substitutes in modern orthopedics. *Orthopedics*, 25, 1301-1309.
- Pasternack, R., S. Dorsch, J. T. Otterbach, I. R. Robenek, S. Wolf & H. L. Fuchsbauer (1998) Bacterial pro-transglutaminase from *Streptoverticillium moharaense* - Purification, characterisation and sequence of the zymogen. *European Journal of Biochemistry*, 257, 570-576.
- Pawelec, K. M., Husmann, A., Best, S. M., & Cameron, R. E. (2014). Understanding anisotropy and architecture in ice-templated biopolymer scaffolds. *Materials Science and Engineering: C*, 37, 141-14.
- Pawelec, K. M., S. M. Best & R. E. Cameron (2016) Collagen: a network for regenerative medicine. *Journal of Materials Chemistry B*, 4, 6484-6496.
- Pawelec, K. M., R. J. Wardale, S. M. Best & R. E. Cameron (2015) The effects of scaffold architecture and fibrin gel addition on tendon cell phenotype. *Journal of Materials Science-Materials in Medicine*, 26.
- Pechak, D. G., M. J. Kujawa & A. I. Caplan (1986) Morphological and histochemical events during 1st bone-formation in embryonic chick limbs. *Bone*, 7, 441-458.
- Phinney, D. G., & Prockop, D. J. (2007). Concise review: mesenchymal stem/multipotent stromal cells: the state of transdifferentiation and modes of tissue repair—current views. *Stem cells*, 25(11), 2896-2902.
- Pinkas, D. M., P. Strop, A. T. Brunger & C. Khosla (2007) Transglutaminase 2 undergoes a large conformational change upon activation. *Plos Biology*, 5, 2788-2796.
- Pittenger, M. F., A. M. Mackay, S. C. Beck, R. K. Jaiswal, R. Douglas, J. D. Mosca, M. A. Moorman, D. W. Simonetti, S. Craig & D. R. Marshak (1999) Multilineage potential of adult human mesenchymal stem cells. *Science*, 284, 143-147.
- Png, E. & L. Tong (2013) Transglutaminase-2 in cell adhesion All roads lead to paxillin? *Cell Adhesion & Migration*, 7, 412-417.

- Rachel, N. M. & J. N. Pelletier (2013) Biotechnological applications of transglutaminases. *Biomolecules*, 3, 870-88.
- Reznikoff, C. A., L. J. Loretz, D. M. Pesciotta, T. D. Oberley & M. M. Ignjatovic (1987) Growth-kinetics and differentiation invitro of normal human uroepithelial cells on collagen gel substrates in defined medium. *Journal of Cellular Physiology*, 131, 285-301.
- Rho, J. Y., L. Kuhn-Spearing & P. Ziopoulos (1998) Mechanical properties and the hierarchical structure of bone. *Medical Engineering & Physics*, 20, 92-102.
- Richards, R. J., L. C. Masek & R. F. R. Brown (1991) Biochemical and cellular mechanisms of pulmonary fibrosis. *Toxicologic Pathology*, 19, 526-539.
- Rodolfo, C., E. Mormone, P. Matarrese, F. Ciccosanti, M. G. Farrace, E. Garofano, L. Piredda, G. M. Fimia, W. Malorni & M. Piacentini (2004) Tissue transglutaminase is a multifunctional BH3-only protein. *Journal of Biological Chemistry*, 279, 54783-54792.
- Ruberti, J. W. & J. D. Zieske (2008) Prelude to corneal tissue engineering - Gaining control of collagen organization. *Progress in Retinal and Eye Research*, 27, 549-577.
- Rundle, C. H., H. L. Wang, H. R. Yu, R. B. Chadwick, E. I. Davis, J. E. Wergedal, K. H. W. Lau, S. Mohan, J. T. Ryaby & D. J. Baylink (2006) Microarray analysis of gene expression during the inflammation and endochondral bone formation stages of rat femur fracture repair. *Bone*, 38, 521-529.
- Rutkovskiy, A., K.-O. Stenslokken & I. J. Vaage (2016) Osteoblast differentiation at a glance. *Medical Science Monitor Basic Research*, 22, 95-106.
- Saidak, Z., C. Le Henaff, S. Azzi, C. Marty, S. Da Nascimento, P. Sonnet & P. J. Marie (2015) Wnt/beta-catenin signaling mediates osteoblast differentiation triggered by peptide-induced alpha 5 beta 1 Integrin priming in mesenchymal skeletal cells. *Journal of Biological Chemistry*, 290, 6903-6912.
- Salis, B., G. Spinetti, S. Scaramuzza, M. Bossi, G. S. Jotti, G. Tonon, D. Crobu & R. Schrepfer (2015) High-level expression of a recombinant active microbial transglutaminase in Escherichia coli. *Bmc Biotechnology*, 15.
- Sayah, D. N., C. Soo, W. W. Shaw, J. Watson, D. Messadi, M. T. Longaker, X. L. Zhang & K. Ting (1999) Downregulation of apoptosis-related genes in keloid tissues. *Journal of Surgical Research*, 87, 209-216.
- Schaffler, M. B., W.-Y. Cheung, R. Majeska & O. Kennedy (2014) Osteocytes: Master orchestrators of bone. *Calcified Tissue International*, 94, 5-24.
- Schett, G. (2011) Effects of inflammatory and anti-inflammatory cytokines on the bone. *European Journal of Clinical Investigation*, 41, 1361-1366.
- Schnabel, C., I. Sawitza, C. G. Tag, B. Lahme, A. M. Gressner & K. Breitkopf (2004) Expression of cytosolic and membrane associated tissue transglutaminase in rat hepatic stellate cells and its upregulation during transdifferentiation to myofibroblasts in culture. *Hepatology Research*, 28, 140-145.
- Schneider, G. B., R. Zaharias & C. Stanford (2001) Osteoblast integrin adhesion and signaling regulate mineralization. *Journal of Dental Research*, 80, 1540-1544.
- Scotti, C., E. Piccinini, H. Takizawa, A. Todorov, P. Bourgine, A. Papadimitropoulos, A. Barbero, M. G. Manz & I. Martin (2013) Engineering of a functional bone organ through endochondral ossification. *Proceedings of the National Academy of Sciences of the United States of America*, 110, 3997-4002.

- Sheikh, Z., C. Sima & M. Glogauer (2015) Bone replacement materials and techniques used for achieving vertical alveolar bone augmentation. *Materials*, 8, 2953-2993.
- Shepherd, J. H., S. Ghose, S. J. Kew, A. Moavenian, S. M. Best & R. E. Cameron (2013) Effect of fiber crosslinking on collagen-fiber reinforced collagen-chondroitin-6-sulfate materials for regenerating load-bearing soft tissues. *Journal of Biomedical Materials Research Part A*, 101, 176-184.
- Schiller, H. B., & Fässler, R. (2013). Mechanosensitivity and compositional dynamics of cell-matrix adhesions. *EMBO reports*, 14(6), 509-519
- Shweke, N., N. Boulos, C. Jouanneau, S. Vandermeersch, G. Melino, J. C. Dussaule, C. Chatziantoniou, P. Ronco & J. J. Boffa (2008) Tissue transglutaminase contributes to interstitial renal fibrosis by favoring accumulation of fibrillar collagen through TGF-beta activation and cell infiltration. *American Journal of Pathology*, 173, 631-642.
- Skill, N. J., M. Griffin, A. M. El Nahas, T. Sanai, J. L. Haylor, M. Fisher, M. F. Jamie, N. N. Mould & T. S. Johnson (2001) Increases in renal epsilon-(gamma-glutamyl)-lysine crosslinks result from compartment-specific changes in tissue transglutaminase in early experimental diabetic nephropathy: Pathologic implications. *Laboratory Investigation*, 81, 705-716.
- Smethurst, P. A. & M. Griffin (1996) Measurement of tissue transglutaminase activity in a permeabilized cell system: Its regulation by Ca²⁺ and nucleotides. *Biochemical Journal*, 313, 803-808.
- Stammaes, J., B. Fleckenstein & L. M. Sollid (2008) The propensity for deamidation and transamidation of peptides by transglutaminase 2 is dependent on substrate affinity and reaction conditions. *Biochimica Et Biophysica Acta-Proteins and Proteomics*, 1784, 1804-1811.
- Steffen, W., F. C. Ko, J. Patel, V. Lyamichev, T. J. Albert, J. Benz, M. G. Rudolph, F. Bergmann, T. Streidl, P. Kratzsch, M. Boenitz-Dulat, T. Oelschlaegel & M. Schraerm (2017) Discovery of a microbial transglutaminase enabling highly site-specific labeling of proteins. *Journal of Biological Chemistry*, 292, 15622-15635.
- Stein, G. S., J. B. Lian & T. A. Owen (1990) Relationship of cell-growth to the regulation of tissue-specific gene-expression during osteoblast differentiation. *Faseb Journal*, 4, 3111-3123.
- Strop, P. (2014) Versatility of microbial transglutaminase. *Bioconjugate Chemistry*, 25, 855-862.
- Teitelbaum, S. L. & F. P. Ross (2003) Genetic regulation of osteoclast development and function. *Nature Reviews Genetics*, 4, 638-649.
- Telci, D., Z. Wang, X. Li, E. A. M. Verderio, M. J. Humphries, M. Baccarini, H. Basaga & M. Griffin (2008) Fibronectin-tissue transglutaminase matrix rescues RGD-impaired cell adhesion through syndecan-4 and beta(1) integrin co-signaling. *Journal of Biological Chemistry*, 283, 20937-20947.
- Telci, D., Wang, Z., Li, X., Verderio, E.A., Humphries, M.J., Baccarini, M., Basaga, H. and Griffin, M. Fibronectin-tissue transglutaminase matrix rescues RGD-impaired cell adhesion through syndecan-4 and β 1 integrin co-signaling." *Journal of biological chemistry*283.30 (2008): 20937-20947.
- Tuan-Mu, H. Y., P. C. Lu, P. Y. Lee, C. C. Lin, C. J. Chen, L. L. H. Huang, J. H. Lin & J. J. Hu (2016) Rapid fabrication of a cell-seeded collagen gel-based tubular construct that withstands arterial pressure. *Annals of Biomedical Engineering*, 44, 3384-3397.

- Upchurch, H. F., E. Conway, M. K. Patterson & M. D. Maxwell (1991) Localization of cellular transglutaminase on the extracellular-matrix after wounding - characteristics of the matrix bound enzyme. *Journal of Cellular Physiology*, 149, 375-382.
- Verderio, E. A., Telci, D., Okoye, A., Melino, G., & Griffin, M. (2003). A novel RGD-independent cell adhesion pathway mediated by fibronectin-bound tissue transglutaminase rescues cells from anoikis. *Journal of Biological Chemistry*.
- Wang, J. L., X. Yang, K. Xia, Z. M. Hu, L. Weng, X. Jin, H. Jiang, P. Zhang, L. Shen, J. F. Guo, N. Li, Y. R. Li, L. F. Lei, J. Zhou, J. A. Du, Y. F. Zhou, Q. A. Pan, J. A. Wang, J. Wang, R. Q. Li & B. S. Tang (2010a) TGM6 identified as a novel causative gene of spinocerebellar ataxias using exome sequencing. *Brain*, 133, 3510-3518.
- Wang, W. & K. W. K. Yeung (2017) Bone grafts and biomaterials substitutes for bone defect repair: A review. *Bioactive materials*, 2, 224-247.
- Wang, X., Y. Wang, W. L. Gou, Q. Lu, J. Peng & S. B. Lu (2013) Role of mesenchymal stem cells in bone regeneration and fracture repair: a review. *International Orthopaedics*, 37, 2491-2498.
- Wang, Z., R. J. Collighan, S. R. Gross, E. H. J. Danen, G. Orend, D. Telci & M. Griffin (2010b) RGD-independent cell adhesion via a tissue transglutaminase-fibronectin matrix promotes fibronectin fibril deposition and requires syndecan-4/2 and alpha 5 beta 1 integrin co-signaling. *Journal of Biological Chemistry*, 285, 40212-40229.
- Wang, Z. & M. Griffin (2013) The Role of TG2 in Regulating S100A4-Mediated Mammary Tumour Cell Migration. *Plos One*, 8 57017.
- Wang, Z., Stuckey, D. J., Murdoch, C. E., Camelliti, P., Lip, G. Y., & Griffin, M. (2018). Cardiac fibrosis can be attenuated by blocking the activity of transglutaminase 2 using a selective small-molecule inhibitor. *Cell Death & Disease*, 9(6), 613.
- Wang, Z., D. Telci & M. Griffin (2011) Importance of syndecan-4 and syndecan-2 in osteoblast cell adhesion and survival mediated by a tissue transglutaminase-fibronectin complex. *Experimental Cell Research*, 317, 367-381.
- Webster, T. J. & E. S. Ahn (2007) Nanostructured biomaterials for tissue engineering bone. *Tissue Engineering II: Basics of Tissue Engineering and Tissue Applications*, 103, 275-308.
- Weraarchakulboonmark, N., J. M. Jeong, S. N. P. Murthy, J. D. Engel & L. Lorand (1992) Cloning and expression of chicken erythrocyte transglutaminase. *Proceedings of the National Academy of Sciences of the United States of America*, 89, 9804-9808.
- Wheless, C R, Nunely, J A, Urbaniak, J 2016 *Wheless' textbook of orthopaedics* Data Trace Internet Publishing.
- Xynos, I. D., A. J. Edgar, L. D. K. Buttery, L. L. Hench & J. M. Polak (2001) Gene-expression profiling of human osteoblasts following treatment with the ionic products of Bioglass (R) 45S5 dissolution. *Journal of Biomedical Materials Research*, 55, 151-157.
- Xynos, I. D., M. V. J. Hukkanen, J. J. Batten, L. D. Buttery, L. L. Hench & J. M. Polak (2000) Bioglass (R) 45S5 stimulates osteoblast turnover and enhances bone formation in vitro: Implications and applications for bone tissue engineering. *Calcified Tissue International*, 67, 321-329.
- Yang, M. T., C. H. Chang, J. M. Wang, T. K. Wu, Y. K. Wang, C. Y. Chang & T. T. Li (2012) Crystal structure and inhibition studies of transglutaminase from *Streptomyces mobaraense* (vol 286, pg 7301, 2011). *Journal of Biological Chemistry*, 287, 23851-23851.

- Yawata, Y. (1994) BAND-4.2 Abnormalities in human red-cells. *American Journal of the Medical Sciences*, 307, 190-203.
- Yin, X., Z. Chen, Z. Liu & C. Song (2012) Tissue transglutaminase (TG2) activity regulates osteoblast differentiation and mineralization in the SAOS-2 cell line. *Brazilian Journal of Medical and Biological Research*, 45, 693-700.
- Yokoyama, K., N. Nio & Y. Kikuchi (2004) Properties and applications of microbial transglutaminase. *Applied Microbiology and Biotechnology*, 64, 447-454.
- Zemskov, E. A., A. Janiak, J. Hang, A. Waghray & A. M. Belkin (2006) The role of tissue transglutaminase in cell-matrix interactions. *Frontiers in Bioscience*, 11, 1057-1076.
- Zimmermann, G. & A. Moghaddam (2011) Allograft bone matrix versus synthetic bone graft substitutes. *Injury-International Journal of the Care of the Injured*, 42, S16-S21.
- Zonca, S., G. Pinton, Z. Wang, M. F. Soluri, D. Tavian, M. Griffin, D. Sblattero & L. Moro (2017) Tissue transglutaminase (TG2) enables survival of human malignant pleural mesothelioma cells in hypoxia. *Cell Death & Disease*, 8.

End of thesis